SELF - VULCANISABLE RUBBER BLENDS BASED ON EPOXIDISED NATURAL RUBBER

THESIS SUBMITTED TO THE INDIAN INSTITUTE OF TECHNOLOGY, KHARAGPUR FOR THE AWARD OF THE DEGREE OF

Doctor of Philosophy

BY
ROSAMMA ALEX

RUBBER TECHNOLOGY CENTRE
INDIAN INSTITUTE OF TECHNOLOGY
KHARAGPUR - 721302, INDIA

1991

Dedicated to my Loving Parents

INDIAN
INSTITUTE OF
TECHNOLOGY
KHARAGPUR-721302

भारतीय
प्रौद्योगिकी
संस्थान
खड़गपुर

RUBBER TECHNOLOGY CENTRE

Dr. (Mrs.) Prajna P. De
Assistant Professor

C E R T I F I C A T E

This is to certify that the thesis entitled "Self-vulcanisable Rubber Blends Based on Epoxidised Natural Rubber", which is being submitted by Mrs. Rosamma Alex, for the award of the degree of `Doctor of Philosophy' to the Indian Institute of Technology, Kharagpur is a record of bonafide research work carried out by her under the joint supervison of myself and Dr. N.M. Mathew, Deputy Director, Rubber Research Institute of India, Kottayam, Kerala.

Mrs. Alex has worked on this research problem for about five years. In my opinion, the thesis has fulfilled all the requirements according to the regulations and has reached the standard necessary for submission. The results embodied in the thesis have not been submitted for award of any other degree or diploma. Mrs. Alex has published eight research papers in International Journals.

Prajna Pde 26.12.91
(PRAJNA P. DE)

DECEMBER 23, 1991

भारतीय रबड़ गवेषण संस्थान

THE RUBBER RESEARCH INSTITUTE OF INDIA

(वाणिज्य एवं पूर्ति मन्त्रालय, भारत सरकार)

(Ministry of Commerce & Supply, Government of India)

Tele { Grams: RUBRBOARD
Phone: 8311 (7 lines)

Telex: 888 285 RRII IN

रबड बोर्ड
RUBBER BOARD
कोट्टयम - ९, केरल
KOTTAYAM-686 009

DR. N.M. MATHEW,
DEPUTY DIRECTOR.

Ref: No.

Date 28--11--1991.

CERTIFICATE

This is to certify that the thesis entitled "SELF VULCANISABLE RUBBER BLENDS BASED ON EPOXIDISED NATURAL RUBBER", which is being submitted by Mrs. Rosamma Alex, for the award of the degree of Doctor of Philosophy to the Indian Institute of Technology, Kharagpur, is a record of bonafide research work carried out by her.

Mrs. Alex has worked on this research problem for about five years (1987-1991) under the joint guidance of Dr (Mrs) Prajna P. De and myself. The results embodied in the thesis have not been submitted earlier for the award of any other degree or diploma. Eight research papers from this thesis have been published/accepted for publication in international journals.

N.M. MATHEW

A C K N O W L E D G E M E N T

I express my sincere gratitude to Professor S.K. De, Head of Rubber Technology Centre and former Dean of Post-graduate Studies, Indian Institute of Technology, Kharagpur, for his personal interest, for kindly suggesting the problem and for the encouragement given during the course of this work.

I am very much grateful to my supervising teachers, Dr. (Mrs.) P.P. De, Assistant Professor, Rubber Technology Centre, Indian Institute of Technology, Kharagpur and Dr. N.M. Mathew, Deputy Director, R.C.P.T. Division, Rubber Research Institute of India, Kottayam, for their inspiring guidance, encouragement and personal interest in this work. Their joint supervision has significantly contributed to the standard of this work. I gratefully acknowledge the authorities of Rubber Board for granting me leave, for providing laboratory and other facilities in carrying out this work.

I acknowledge the help rendered by Dr. Baby Kuriakose of Rubber Research Institute of India in the course of this work.

I very much appreciate teachers and staff and my friends at the Rubber Technology Centre, Kharagpur and at the Rubber Research Institute of India, Kottayam for their good wishes and co-operation.

My indebtedness to my husband is limitless and to be honest without his constant patience and sincerity, this work would never have materialised. I owe a lot to my children Rojimon and Savanmol, who missed me a lot especially in their early childhood, when they required affection and attention of their mother.

I sincerely acknowledge my uppapan, sister and brother for thier encouragement given in carrying out this work.

Rosamma

DECEMBER 23, 1991 (ROSAMMA ALEX)

P R E F A C E

Blending of polymers is of interest due to the versatility in achievable properties. Polymer blends of two phase or multi-phase morphology have been routinely used. However, there are not many examples of miscible polymer blend systems with single phase morphology because of the high molecular weight factor. The combinatorial entropy change is usually too small to result in the necessary free energy of mixing because the enthalpy of mixing is generally positive at least for relatively non-polar polymers. However, the thermodynamic condition that the free energy of mixing must be negative for miscible polymer systems are obtained for polymer blends in which the exchange interaction between the two components becomes negative. This requirement is satisfied by the specific interaction of polymers in the case of homopolymer blends and by the strong segmental repulsion in the case of copolymer based blends.

In rubber blends with appropriate functional groups, chemical interaction between the groups can result in crosslinking at high temperature. A thorough investigation on such self-crosslinkable rubber blends in respect to mechanical behaviour, polymer-filler interaction, dynamic mechanical properties and ageing characteristics have not been made as yet. The present work is aimed at studying some of these rubber blends which crosslink themselves through their functional groups during high temperature moulding, in

absence of external vulcanising agents. The blends studied here include the binary blends of epoxidised natural rubber (ENR) and carboxylated nitrile rubber (XNBR), ENR and polychloroprene rubber (CR) and the ternary blend ENR/XNBR/CR. ENR is a new class of rubber obtained by the epoxidation of natural rubber with a per acid. While the double bonds can be crosslinked by sulphur and peroxide, the epoxide groups provide alternative sites for crosslinking with polyfunctional chemicals. Research studies on ENR is as important as that on natural rubber for promoting the development of natural rubber in natural rubber producing countries.

Since no crosslinking agents are used the problems related to conventinal polymer blending like co-crosslinking and crosslink heterogeniety arising out of unequal distribution of vulcanising agents do not exist.

The contents of the thesis are divided into six chapters with a section on summary and conclusions at the end. The first chapter is a description on background introduction of broad literature survey highlighting the general aspects of polymer miscibility, properties and the background, scope and objectives of the present work. Chapter 2 gives details of the experimental procedures followed in the present investigations.

Chapter 3 deals with studies on the binary blends of epoxidised natural rubber (ENR) and carboxylated nitrile

rubber (XNBR). This chapter is divided into four parts. The first part deals with characterisation of self-vulcanisable blends of epoxidised natural rubber and carboxylated nitrile rubber by Monsanto rheometry, differential scanning calorimetry, thermogravimetry, infrared spectrophotometry and solvent swelling. The second part deals with the effect of fillers and moulding conditions on cure characteristics and processing behaviour. This part also deals with polymer-filler interaction, failure envelope studies and stress relaxation behaviour. The third part deals with dynamic mechanical studies and miscibility of the self-vulcanised blend. The fourth part deals with the ageing studies. Chapter 4 deals with self-vulcanisable rubber blends based on ENR and polychloroprene rubber (CR). Results on cure characteristics, processing characteristics, technical properties and dynamic mechanical properties of the blends are included in this chapter. Chapter 5 deals with self-vulcanisable ternary rubber blends based on ENR, XNBR and CR. This chapter is divided into two parts. The first part deals with the effects of blend ratio, moulding time and fillers on the miscibility of the ternary blend. The second part deals with the effect of blend ratio and fillers on physical properties of the self-vulcanisable ternary rubber blend. Chapter 6 deals with the viscosity measurements from the capillary flow of the tricomponent rubber blends of ENR, XNBR and CR.

The last section of the thesis is summary and conclusions with a view to provide a review on the objectives, abstract and conclusions of the present work.

Eight papers from the results of the present work have been published/accepted for publication in International Journals. A list of publications is given at the end of the thesis.

Rosamma.

DECEMBER 23, 1991 (ROSAMMA ALEX)

B I O - D A T A

1. Name : ROSAMMA ALEX

2. Present address : Technical Consultancy Division,
Department of Processing and
Product Development,
Rubber Research Institute of India
KOTTAYAM - 686 009, Kerala

3. Permanent address : Velinthara House,
P.O. Puthor,
Kottarakara,
Quilon, Kerala

4. Date of birth : 30th March, 1955

5. Educational Qualifications :

1985-1986	Master of Technology in Rubber Technology	Indian Institute of Technology, Kharagpur
1976-1977	Bachelor of Education in Physical Science	Kerala University
1974-1976	Master of Science, in Chemistry	Kerala University
1971-1974	Bachelor of Science, Chemistry main	Kerala University
1971-	All India Higher Secondary Examination	C.B.S.E., New Delhi

6. Professional Experience :

1980 February - till date — Rubber Research Institute of India, Kottayam-9.

Position : Assistant Rubber Technologist

A B S T R A C T

Mill mixed blends of rubbers with appropriate functional groups can undergo self-crosslinking during high temperature moulding. Examples of such binary blends include epoxidised natural rubber (ENR) - carboxylated nitrile rubber (XNBR) and epoxidised natural rubber (ENR) - polychloroprene (CR). Similarly, the tricomponent blend of ENR, XNBR and CR can form self-crosslinkable ternary rubber blend system. The heterogeneity of the crosslinked structure depends on blend composition and mixes containing CR need special mention here in the sense that CR alone undergoes thermovulcanization and ENR undergoes profound structural changes in presence of liberated acid from CR. Accordingly, some of the blends are miscible and some are only partially miscible. In some instances, fillers increase heterogeniety of the phases. In general, these blends behave like conventional rubber vulcanisates in respect to physical properties and reinforcement by fillers. Self-vulcanisable rubber blends open up new area of research in the field of polymer technology in general and in area of blends in particular.

Key Words : epoxidised natural rubber, carboxylated nitrile rubber, polychloroprene rubber, self-vulcanisable rubber blend, miscible rubber blend, polymer-filler interaction, flow behaviour.

C O N T E N T S

PAGE NO.

PAGE NO.

PAGE NO.

PAGE NO.

CHAPTER - 6 RHEOLOGICAL BEHAVIOUR OF THE TERNARY BLEND OF EPOXIDISED NATURAL RUBBER (ENR), CARBOXYLATED NITRILE RUBBER (XNBR) AND POLYCHLOROPRENE RUBBER (CR)

CHAPTER 1

INTRODUCTION

Blending of rubbers is important in view of the wide spectrum of properties that can be achieved by proper manipulation of rubber characteristics, blend composition, choice of additives (like vulcanising agents, fillers and compatibilising agents), blending techniques and vulcanising conditions. These parameters control compatibility of rubbers in the blend and its final properties.

1.1 POLYMER-POLYMER MISCIBILITY

Miscibility refers to the intimate mixing of two or more rubbers. Depending on the degree of miscibility, blends are classified as compatible, incompatible and partially compatible. A compatible blend does not exhibit gross symptoms of phase segregation. Partially phase segregated blends are referred as partially compatible and completely phase segregated are referred as incompatible systems. The aspects of polymer-polymer miscibility and the properties and applications of polymer blends have been reviewed by several authors[1-6].

1.1.A Thermodynamics of Polymer Blends

If polymers are to be made thermodynamically miscible, the Gibbs free energy of mixing must be negative. The expression that governs Gibbs free energy of mixing is given by

$$\Delta G_m = \Delta H_m - T \Delta S_m \qquad ...(1)$$

where ΔH_m and ΔS_m represent the enthalpy and entropy of mixing, respectively. ΔH_m is essentially independent of molecular weight and is a measure of the entropy change associated with intermolecular interactions. ΔS_m reflects the energy change associated with the changes in the molecular arrangement. Because of the high molecular weights of polymers, the number of molecules involved in a mixing process is much smaller in the case of polymers than in the case of equal weights of low molecular weight compounds. The magnitude of entropy change is inversely related to the molecular weight of the polymer being mixed. The higher is the molecular weight, the lower is the number of possible arrangements available to the segments of the covalently linked molecules. Though the combinational entropy change favours mixing as in equation (1), it is usually too small to result in the necessary negative free energy because the enthalpy of mixing (ΔH_m) is generally positive, at least for relatively non-polar systems.

One of the earliest attempts for approximation of equation (1) was done by Koningsveld[7]. Flory-Huggins[8-10] theory of polymer solutions for blends was first applied by Scott[11] and Tompa[12]. Scott obtained the following expression for G_m from a total volume V of two polymers.

$$\Delta G_m = \frac{RTV}{V_r}\left[(\phi_A/X_A)\ln\phi_A + (\phi_B/X_B)\ln\phi_B + \chi_{AB}\phi_A\phi_B\right] \quad \ldots(2)$$

where R is the universal gas constant, T is the temperature, V_r is the reference volume, which is taken as close to the

molar volume of the smallest repeat unit. X_A and X_B are the degree of polymerisation of A and B, ϕ_A and ϕ_B are the volume fractions of A and B. χ_{AB} is related to the enthalpy of interaction of the polymer repeat units. The phase behaviour of a ternary system was calculated by Su and Fried[13]. The free energy of mixing, G_m of the monodisperse homopolymers is expressed in terms of their volume fractions ϕ_A, ϕ_B, and ϕ_C[13] as

$$\Delta G_m = \frac{RTV}{V_r} \left[(\phi_A/X_A)\ln\phi_A + (\phi_B/X_B)\ln\phi_B + (\phi_C/X_C)\ln\phi_C + \chi_{AB}\phi_A\phi_B + \chi_{BC}\phi_B\phi_C + \chi_{CA}\phi_C\phi_A \right] \quad ...(3)$$

where, X_A, X_B and X_C are the degree of polymerisation of the three polymers. χ is assumed to be dependent on temperature but independent of the composition. Morphology of ternary blend is strongly dependent on χ value for any two phases. The interaction parameter between molecules of comparable size can be expressed as[14,15]

$$\chi_{AB} = \frac{V_r}{RT} (\delta_A - \delta_B)^2 \quad ...(4)$$

where δ_A and δ_B are the solubility parameters.

In nonpolar systems where there are only dispersive or van der Waal type bonding between the segments, the heat of mixing can be written as

$$\Delta H_m = V (\delta_A - \delta_B)^2 \phi_A\phi_B \quad ...(5)$$

This equation shows that there cannot be a negative heat of

mixing in nonpolar polymers, and in such cases compatibility of polymers of substantial molecular weights occur only when the solubility parameters are precisely matched[16].

Scott[11] set the first and second derivative with respect to ΔG_m to zero and found that when the two polymers are at their critical solution temperatures,

$$(\chi_{AB})_{Cr} = 1/2 \left(1/X_A^{1/2} + 1/X_B^{1/2}\right)^2 \qquad \ldots(6)$$

$$(\phi_A)_{Cr} = \frac{X_B^{1/2}}{X_A^{1/2} + X_B^{1/2}} \qquad \ldots(7)$$

$$(\phi_B)_{Cr} = \frac{X_A^{1/2}}{X_A^{1/2} + X_B^{1/2}} \qquad \ldots(8)$$

X_A and X_B are the degree of polymerisation of the two components A and B. ϕ_A and ϕ_B are the volume fractions of the components A and B. Scott noted that (χ_{AB}) would be very small for two polymers having appreciable degree of polymerisation and that polymers of infinite molecular weight would be incompatible if there were any positive heat of mixing.

1.1.B Exothermic Heat of Mixing due to Specific Interactions

Many miscible pairs of polymers have chemical structures capable of interaction by mechanisms including hydrogen bonding[17-19], complex formation[20,21], ionic interaction[22,23], dipolar interactions[24] and donor acceptor types of interactions[25-31]. The miscibility of two polymers

can often be enhanced through specific interactions by incorporating suitable functional groups. For instance, polystyrene (PS) modified by hexafluorodimethyl carboxyl groups is miscible with both bis-phenol A, polycarbonate (PC) and poly-n-butyl methacrylate (PnBMA) whereas the unmodified PS is immiscible with both PC and PnBMA[32,33]. Goh et al[34] have shown that interaction between poly(methyl methacrylate) (PMMA) and methyl styrene acrylonitrile (MSAN) is enhanced by the incorporation of chlorine in the pendent methyl group of PMMA.

Miscibility of styrene acrylonitrile (SAN) with polyesters has been ascribed to specific interactions[35].

In blends, it is also possible to have chemical reactions which lead to crosslinking, grafting and copolymerisation. At high temperatures rapid interchange reactions can occur in polyesters, as a result of which they become miscible[36].

1.1.C Exothermic Heat of Mixing due to a Negative Interaction Parameter

In many cases miscibility has been reported to be due to a negative interaction parameter. This type of miscibility is observed in systems in which one or both the components are copolymers. If the repulsion between the groups in copolymers is sufficiently strong, the net interaction parameter between two species become negative.

It has been observed that blends containing homopolymer and copolymer were miscible within certain ranges of copolymer composition even though blends with homopolymers of the monomers comprising the copolymer were immiscible. This miscibility was considered to be due to repulsion between the monomer units of the copolymer[37-39]. For example, miscibility of bis-phenol A polycarbonate (PC) and a random copolymer polystyrene-co-methacrylic acid (PS-MAA) can be ascribed to the repulsion theory. Cowie and Lath[40] determined miscibility ranges of the ternary system polystyrene-co-acrylonitrile (SAN)/ poly methyl methacrylate-co-acrylonitrile (MMA-AN)/polystyrene-co-methyl methacrylate (S-MMA) on the basis of the repulsion theory.

1.1.D Interfacial Tension in Polymer Blends

The interfacial tension arises due to disparity between the polarities of the two phases, as the contribution due to nonpolar interactions do not vary much from system to system. For two polymers to be compatible, the interfacial tension must be zero or negative. The difference between the solubility parameters for the two polymers gives an idea of the interfacial tension. Lower the difference between the solubility parameters of the two phases the greater is the miscibility.

1.1.E Enhancement of Miscibility by Reduction of Interfacial Tension

The interfacial tension between polymers may be

reduced with additives to improve the compatibility and adhesion between the phases. This principle forms the basis of an important aspect in the technology of polymer blends. These additives are referred to as compatibilisers or interfacial agents[41]. A homopolymer or copolymer may act as a compatibiliser for two immiscible polymers, if it is miscible separately with each of the individual polymer. Majority of the commercial ternary blends belongs to this category.

One class of such additives is the block and graft copolymers with blocks or segments having the same chemical composition as those of the polymers to be blended. This will reduce the interfacial tension, ensure finer dispersion of the components and increase compatibility against phase separation.

Block copolymers, due to their ability to migrate into both the phases are considered better than graft polymers and triblock polymers. The poor adhesion between polyethylene (PE) and polyisoprene (PI) was improved by polyethylene-b-polyisoprene diblock copolymer[42]. The first systematic study on ternary miscible blends was made by Kwei and coworkers[43], whereby poly(vinylidene fluoride)(PVF_2) was used as compatibiliser for poly(methyl methacrylate) and poly(ethyl acrylate) (PEA). Paul and coworkers used polyesters[44] to solubilise poly(carbonate)(PC) and poly(styrene-co-acrylonitrile)(SAN) containing acrylonitrile. It was

observed that in this system, the polyesters poly(1,4-butylene adipate) PBA, and poly(1,4-cyclohexane dimethylene succinate)(PCDS) were better than poly caprolactone (PCL) as compatibilising agents. Wang and Chen[45] used nitrile rubber to compatibilise the poly(vinylidine fluoride-co-vinyl chloride)/poly(vinyl chloride) blend. Belaribi et al.[46] have shown that in ternary blends of poly(tetramethyl carbonate) MPC, poly carbonate (PC), polystyrene (PS), MPC has more affinity for PC than polystyrene, whereas binary PS/MPC blends are fully miscible and PC/MPC blends are miscible upto 70 wt.% PC. It was shown by Min et al.[47] that poly(methyl methacrylate, poly(epichlorohydrin) and poly(ethylene oxide) formed a completely miscible ternary blend where all the three binary pairs were miscible.

A compatibiliser can also be formed in situ. Functionalised polymer pairs, polyamide/rubber[48], polyolefin/rubber[49], polystyrene/polyethylene[50] and polystyrene/rubber[51,52] can be made compatible by chemical reaction between the reactive polymers. The resulting graft block or crosslinked polymer imparts compatibility as it behaves like an insitu compatibiliser. For example, binary blends of poly amide (PA) and ethylene propylene copolymer (EPM) modified by grafting of maleic anhydride during melt mixing, form EPM-g-PA graft copolymer, which acts as interfacial agent and improves compatibility with polyamide and EPDM phases[53]. Appropriate dispersion of rubber particles into glassy polymers can lead to significant

toughening by inducing crazing or shear-yielding deformation mechanisms in an otherwise brittle matrix[54].

1.1.F Adhesion between Components in Polymer Blends

Adhesion refers to bonding or joining of dissimilar bodies. If two phases are in perfect molecular contact, Van der Waal's forces alone would be sufficient to give strong adhesive strength. In practice, it is very difficult to achieve perfect molecular contact. From the various theories put forward to explain adhesion, it can be summarised that there is interfacial contact by wetting and if adhesion is strong there is formation of chemical bonds between the two phases[55].

The adhesive strength between some polymers have been shown to decrease with increasing disparity in the solubility parameters of the two phases[56]. Interfacial chemical bonds could be utilised effectively to promote adhesion. Agents based on silanes and titanates have been found to form interfacial chemical bonding[57]. Reactive functional groups such as carboxyl, amide, hydroxyl, epoxide and isocyanates have been forced to promote adhesion to various substrates[58,59]. The adhesive strength tends to increase as the extent of functional group increases.

1.2 CRITERIA FOR MISCIBILITY

1.2.A Optical Clarity

Miscible polymer blends are characterised by good

optical clarity and mechanical integrity[60]. Optical clarity for immiscible blends is observed in rare cases when their refractive indices are equal[61]. Such blends appear to be clear at a particular temperature but may be translucent or opaque at other temperatures if the temperature co-efficient of refractive indices are different. Optical clarity in incompatible blends is also attained in the case of very thin films because light can pass through only one of the phases[62].

1.2.B Existance of a Single Composition Dependent Tg

The most commonly used method for establishing miscibility or phase morphology in polymer-polymer blends is through the determination of the glass transition temperature (Tg). A miscible polymer blend will exhibit a single glass to rubber transition occurring in between the Tg s of the components with a sharpness of transition similar to that of the components. In the case of border line miscibility broadening of the transition zone will occur. In the case of limited miscibility between the blend components 1 and 2, two separate transitions occurring in between the Tg s of the constituent polymers may result, depicting a component 1-rich phase and a component 2-rich phase. Microlevel inhomogeneity in the blend is indicated by a low level broadening of the transition zone.

Tg s of compatible blends generally obey the Fox equation[63],

$$\frac{1}{Tg_{1,2}} = \frac{w_1}{Tg_1} + \frac{w_2}{Tg_2} \qquad \ldots(9)$$

and the Gordon-Taylor equation[64].

$$Tg_{1,2} = W_1 Tg_1 + W_2 Tg_2 \qquad \ldots(10)$$

where $Tg_{1,2}$ is the Tg of the compatible blend, Tg_1 and Tg_2 are the Tg s of the constituent polymers, 1 and 2. w_1 and w_2 are the weight fractions of the polymer 1 and 2 and K is a constant. Several compatible blends exhibit Tg-composition dependencies which could be correlated by Fox equation[65-67] and by Gordon-Taylor[68,69] equation. A more detailed expression used for polymer-miscibility is Kelley-Bueche expression[70,71].

$$Tg_{1,2} = \left[Tg_1 + (K\ Tg_2 - Tg_1)\emptyset_2\right] \Big/ \left[1 + (K-1)\emptyset_2\right] \qquad \ldots(11)$$

where, the parameter K represents the ratio of thermal expansion co-efficient differences above and below the glass transition temperatures for components 1 and 2

$$K = \frac{\Delta\alpha_1}{\Delta\alpha_2}$$

α_1 and α_2 are the thermal expansion co-efficients of the two components and $\emptyset_1$ and $\emptyset_2$ are the volume fractions of the two components.

2.2.C Scattering Methods

Polymer blends which exhibit compatibility at low

temperature may exhibit phase-separation at high temperature. The transition from compatible to incompatible or from transparent to opaque, at high temperatures is named lower critical solution temperature (LCST) behaviour. The LCST behaviour has been reported to be a common phenomenon for several compatible blends[72,73].

Another optical technique used to characterise compatibility of blends is by the determination of cloud point. The cloud point which is the temperature corresponding to the transition point of the incipient phase separation, is usually measured by observing the appearance of the opaqueness of a thin film made from blends, when the film is subjected to heating. The cloud point depends on factors like, blend composition, molecular weight, thermal expansion co-efficient and thermal pressure co-efficient of the components.

The physical structure of polymer mixtures can be characterised by the chain conformation, the local order and the morphology. Scattering methods are quite effectively used for this purpose. Small-angle neutron scattering elucidates the chain conformation[74]. The local order can be studied by means of electron and Rayleigh-Brillouin Scattering[75], whereas the morphology can be studied by means of light scattering, small angle, X-ray scattering and magnetic birefringence method[74,75].

1.2.D Specific Volume

Blends of incompatible polymers generally show no deviation in specific volume, over that calculated by the additivity rule[76,77]. In the case of miscible polymer blends specific volumes are not additive. Generally, miscible blend densities are higher than those calculated from volumetric additivity relationship especially where specific interactions exist. Specific interactions may cause a loss in free volume and increase in density[78-79].

1.2.E Melting Point Depression

A characteristic feature of a crystalline-amorphous blend is the substantial depression of the crystalline melting temperature (Tm) as a result of the diluent effect of the amorphous component. Examples include poly(ε -caprolactone)-poly(vinyl chloride)[80], isotactic polystyrene-poly(2,6-dimethyl 1,4-phenylene oxide)(PPO) and poly (vinylidene fluoride)-poly(methylacrylate)[82,83]. Such a drop in Tm, in part explains the reluctance of blends with a high content of the amorphous component to crystallise. In addition, this drop in Tm is accompanied by an elevation in Tg as the low-Tg components crystallise out from solid state solution and as the content of the amorphous, high-Tg component increases. For these reasons, Tm-Tg interval decreases and this induces a severe kinetic restriction on the crystallisation process. An additional cause for the inability of blends with high amorphous content to

crystallise is the growing isolation of the individual chains of the crystalline polymer with increasing amorphous polymer content. There is random placement of different molecules in the homogeneous compatible state and there is restriction on molecular mobility during the crystallisation process. As a result, at higher amorphous contents, the domain of the crystalline polymer is likely to be smaller than the critical nucleus size for crystallisation.

For polymer mixtures depression of melting point of one polymer by the addition of another is given by the expression,

$$\frac{1}{Tm} - \frac{1}{Tm^{o}} = \frac{-R\ V_2}{\Delta H_2\ V_1} \chi_{1,2}\ (1-\theta_2)^2 \qquad \ldots(12)$$

where $\chi_{1,2}$ is the interaction parameter, Tm is the experimental melting point. Tm^{o} is the equilibrium melting point, ΔH_2 is the heat of fusion of 100% crystalline polymer per mole of repeat unit, V_1 the molar volume of the diluent, V_2 molar volume of the polymer repeat unit and θ_2 the volume fraction of crystalline polymer. Equilibrium melting points can be determined by extrapolation of experimental melting point data obtained at various temperatures of crystallisation to a temperature at which Tm equals the temperature of crystallisation[84,85]. It has been determined in this way by numerous investigators[86-89].

1.2.F Microscopy

Microscopy is a useful technique to determine if a blend is single or multipurpose. Microscopy is best applied to systems where the phases can be differentiated from one another by physical or chemical treatment such as staining or solvent swelling[90]. Transmission electron microscopy (TEM) has been widely used in polymer-polymer blend studies. The necessary step of microtoming can be facilitated by cryogenic or chemical methods. Electron opacity differences are often achieved by selective chemical reaction[91,92] or by annealing in the beam[91,93]. Smith and Andres[91] found that the system, styrene butadiene rubber (SBR)-polybutadiene (PB) was immiscible even with as little as 3% styrene in the SBR, but that the phase size progressively decreased with increase in styrene content. Matsuo et al.[92] observed heterogeniety in the system PVC/NBR containing 40% acrylonitrile, although only one glass transition was observed. MacMaster[93] found that TEM was useful for studying the phase decomposition of the misicble system poly(methyl methacrylate)(PMMA)-styrene acrylonitrile (SAN).

Scanning electron microscopy (SEM) is another useful technique in phase studies[94]. Contrast in this technique depends on differences in surface topography or texture and this can be accomplished by breaking the specimen in its glassy state. Using SEM morphology of the polymer blends can also studied by selectively etching one of the phases[95]. SEM fractography is useful in understanding the mechanism of

failure of rubbers under different test conditions[96-99].

1.3 MEASUREMENT OF GLASS-RUBBER TRANSITION TEMPERATURE

Different methods of determination of Tg[2,60] include dilatometric method, thermo-optical analysis (TOA), dielectric method, radioluminiscence spectroscopy, differential thermal analysis (DTA), thermomechanical analysis (TMA), differential scanning calorimetric method (DSC) and dynamic mechanical thermal analysis (DMTA). The last two methods are most commonly used in the study of compatibility of polymer blends.

1.3.A Measurement of Glass Transition Temperature

(a) Viscoelastometer

The material is subjected to a cyclic tensile strain, so that the sinusoidal tensile strain applied to a polymeric material generates a corresponding sinusoidal tensile stress, with a phase difference, δ. A horizontal specimen, one end of which is connected to the unit of oscillation and the other to a load transducer is provided oscillatory motion. Outputs of the stress and strain transducers are converted to provide direct tanδ readings.

$$E'' = E^* \sin \theta \qquad ...(13)$$

$$E' = E^* \cos \theta \qquad ...(14)$$

$$\tan \delta = E'' / E' \qquad ...(15)$$

At Tg, damping (tan δ) and E" (viscous modulus) are maximum,

while the elastic modulus changes sharply to a much lower value. It detects essentially all changes in the state of molecular motion with temperature. Hence the glass transition temperature Tg, crystalline melting temperature (Tm), β-relaxation due to the motion of side groups, and other factors related to phase morphology can be detected by DMA[74].

(b) Differential Scanning Calorimetry (DSC)

DSC thermograms also provide useful information in regard to Tg, Tm as well as crystallization temperature (Tc) and degree of crystallinity.

1.4 PROPERTIES OF POLYMER BLENDS

1.4.A Mechanical Behaviour

The mechanical properties of a polymer blend may be approximated from those of the components. The typical compositional plots are step, maximum, minimum or linear[5]. The step shaped plot is common for heterogeneous rubber blends used for toughening plastics. For this purpose rubber should not be miscible in the matrix but rather form a dispersed phase. The rubber particles act as stress concentrators, causing localised deformations in the matrix and thus the catastropic failure is prevented[100]. McGarry[101] had shown that fracture energy of epoxy resins could be significantly increased by addition of carboxyl terminated butadiene acrylonitrile rubbers. Pearson and Yee[102] and Sutta et al.[103] have studied the toughening mechanism of

elastomer modified epoxies by scanning electron microscopy, transmission electron microscopy and optical microscopy. A maximum in properties is often observed for miscible blends because the specific interactions that provide miscibility cause increase in cohesive energy density and packing efficiency of molecules[104-106]. Dynamic vulcanisation is a process of vulcanising the rubber phase in a thermoplastic elastomer while it is being mixed at the melt state[107-110]. Dynamically vulcanised rubber-plastic blends can be processed like thermoplastics and show superior mechanical properties over non-vulcanised counter parts.

Flory-Rehner[111,112] network theory of swelling is used to estimate the degree of crosslinking in vulcanised elastomers. Swelling in solvents has been used to assess degree of reinforcement in elastomers[113-115]. Swelling in solvent is restricted due to the chemical crosslinks introduced during vulcanisation and physical crosslinks formed due to polymer-filler interaction[115]. Both particle size and structure of fillers have important effects on the solvent swelling of filled elastomers. Swelling studies of filled and unfilled vulcanisates were reported by Butenuth[116]. Dependence of degree of swelling on the volume concentration of filler has been investigated by Kraus[113,117].

Lorentz and Parks[118] have suggested several relationships for the swelling of the filled vulcanisates.

Additional crosslinks due to reinforcing fillers are manifested from the restriction to swelling. If one measures the volume fraction V_r of the rubber phase in the swollen gel, the ratio of V_{ro}/V_{rf} decreases with increase of filler loading, where V_{ro} is the value of V_r in gum vulcanisate and V_{rf} is the value of V_r in filled vulcanisate. The filler is assumed not to swell. This ratio represents the degree of restriction of the swelling of the rubber matrix due to the presence of filler, provided the filler does not interact with the vulcanising system.

Both the particle size and the structure of fillers have important effects on the swelling data for filled elastomers. In general as the particle size increases, the polymer-filler attachment become less and the restriction on swelling is expected to be less. Assuming that swelling is completely restricted to the surface and that the rubber matrix at some distance away from the surface was swollen isotropically in a manner characteristic of unfilled rubber, it was found by Kraus[113], that

$$\frac{V_{ro}}{V_{rf}} = 1 - \frac{m\emptyset}{1-\emptyset} \qquad \ldots(16)$$

where m is a constant, characteristic of the filler. It has been shown that polymer-filler interaction depended on the filler[119], on the vulcanisation system[120] and vulcanising conditions[121].

1.4.B Processability and Rheology

Miscible blends constitute one phase and are processed like a homopolymer or random copolymer[5]. However, two-phase blends have unique processing characteristics. Multiphase blends can exhibit phase segregation and orientation under high shear processing conditions. The degree of orientation depends upon many factors including relative viscosities to the separate phases, the degree of shear and the degree of which dispersed phase is crosslinked.

Rheological properties are generally studied from measurements of their viscometric flow behaviour. The rheological parameters influencing the processability are viscosity and elasticity as determined by die-swell ratio, principal normal stress difference, recoverable shear strain, shear modulus and extrudate characteristics.

The processability of elastomers which includes the behaviour of the materials during processing operations such as mixing, shaping, moulding, calendering and extrusion is one of the major concerns of rubber industry. The major aspect in the processing step is the flow behaviour of elastomers. The influence of fillers and blending of rubbers on flow properties of elastomers has great industrial importance as elastomers are seldom used without fillers and in most cases a blend of elastomers is preferred to achieve a particular end use. Einhorn and Turetzky[122] showed the use of capillary rheometry to characterise elastomeric flow. A

number of researchers have investigated the rheology of polymer blends[123-126]. A comprehensive review on dependence of rheological properties on blend composition has been given by Plochoki[127]. Generally viscosities of blends vary monotonically with blend composition. Several workers have reported the rheological behaviour of NR with plastics[129,130], epoxidised natural rubber (ENR) with PVC[131], blends of ethylene propylene diene rubber (EPDM) and bromobutyl rubber (BIIR)[132], as well as many other elastomers and elastomer blends[133-135].

Several models for viscosity of blends has been applied to polymer blends, from a knowledge of their composition[136-138]. The different blend additivity rules, logarithmic rule, Hashin's upper control rule, Hashin's lower control rule , Heitmillers inverse additivity rule[124] and sheath-core rule have been used for polymer melts. Agreement between additivity rules and the experimental results varies with the blends[139].

Elasticity of polymer melts respond differently to changes in extrusion conditions like increasing the residence time in the capillary and increasing temperature[140]. The behaviour of elastomers is concerned with three functions, the viscosity co-efficient $\eta(\dot{\gamma})$, principal normal stress co-efficient $\psi_1(\dot{\gamma})$ and secondary stress co-efficient $\psi_2(\dot{\gamma})$[141,142]. The behaviour of an elastomer blend is determined not only by dependence of shear stress on shear rate but also of normal stress on shear stress and shear

rate. The die swell of extrudates depends on fundamental properties of the polymers such as molecular weight and its distribution, as well as on flow conditions such as temperature, shear rate, shear stress and L/D ratio of the capillary. Fillers, depending on their concentration and type, generally reduce die swell in elastomers.

1.5 SOME ASPECTS OF ELASTOMER BLENDING

1.5.A Continuity of Phase and Zone Size

The performance of elastomer blends is composition dependent and in some cases blends can be compounded to perform at a higher level for a particular property than would be anticipated from the relative proportion of individual elastomers. Among the factors contributing to enhanced performance are the continuity of phase and zone size.

Usually the component that is present in small amounts forms a dispersed phase (zone). The relative zone size in an elastomer blend depends directly on the viscosities or the individual polymer components[143-145]. The component that is less viscous forms a continuous phase easily, if it is present in sufficient concentration[146]. The size of the dispersed phase depends on the following factors :

(a) Mooney viscosities of the samples,

(b) Solubility parameters of the components, and

(c) Shear rate of mixing

Tokita[147] has derived an expression from colloidal dispersion system theory for elastomer blends for the zone size R :

$$R = \frac{12\ P\ \sigma\ \phi_d}{\pi\ \eta\ \dot{\gamma}} \left(1 + \frac{4\ P\phi_d\ E_{dk}}{\pi\ \eta\ \dot{\gamma}}\right) \qquad \ldots(17)$$

E_{dk} is the microscopic breakdown energy of component phase, which is proportional to Mooney viscosity; σ is the difference in surface tension between polymers; η is the Mooney viscosity of the blend system; $\dot{\gamma}$ is the shear rate of mixing; P is the probability that coalescence will occur when dispersed particles collide with one another and ϕ_d is the volume fraction of dispersed phase.

In incompatible blends there are regions where some molecules of the two components interdiffuse. This region is termed the boundary surface[148]. If the interfacial tension is low then boundary surfaces will be thicker and when boundary layers of sufficient thickness are formed then it is possible that the two polymers co-crosslink, so that enhanced physical properties can be achieved.

The zone size depends mainly on viscosity of polymer. In some elastomeric blends, it is possible that both components may form continuous phase simultaneously[149,150]. This can be considered to be an interpenetrating network (IPN). Such an interpenetrating network is interesting because immiscible blends with interpenetrating phases show

improved mechanical properties relative to the usual dispersed phase/continous phase mixtures.

1.5.B Distribution of Filler in Rubber Blends

In elastomer blends, it is difficult to distribute fillers uniformly in the two phases, particularly for carbon black. The factors that dominate the partitioning of carbon black are[151] : (i) degree of saturation of polymers, (ii) viscosity of the polymers, (iii) polarities of the polymers, (iv) type and amount of filler, and (v) mixing method.

As a general rule, affinity for carbon black is very high for BR and very low for IIR[148] and it follows the following order :

BR > SBR > CR > NBR > NR > EPDM > IIR

During and after mixing, carbon black in some cases preferentially migrates from one phase to another[152,153]. In blends of chlorobutyl rubber and polybutadiene rubber (Cl-IIR/BR) carbon black that is taken up in the Cl-IIR phase migrates to BR phase on continued milling[152]. In blends of natural rubber and high viscosity polybutadiene rubber (NR/BR), carbon black distributed itself in the low viscosity NR phase in the beginning and then migrates to BR on continued milling[148]. Distribution of carbon black in different phases in blend strongly affects the final properties.

1.5.C Distribution of Curatives in the Blends

It is important that the vulcanisate network structure formed is uniform throughout. Sulphur and accelerators are more soluble in unsaturated elastomers[154,155]. Accelerators have greater affinity for polar elastomers. These curatives have tendency to migrate to low viscosity phase since it tends to occupy the outer regions of flow and usually the low viscosity phase forms the continuous phase[156]. During flow of elastomer blends, curatives have tendency to migrate to the outer regions of flow, since it tends to be occupied by the low viscous phase. If there is great difference in the solubilities of curatives in the two phases, the crosslink density of final vulcanisate will be heterogenous. Rate of vulcanisation varies for different elastomers in the blend, depletion of curatives in the faster curing component also cause curative negative loss and hence cure imbalance[157]. Thus the use of combination of properties is achieved when the two elastomers are similar in respect to polarity, saturation level and Mooney viscosity.

An attempt to improve blend crosslink distribution was made by using special curatives with minimum solubility difference between the phases[158] by some modification of component polymers[159]. Chemical modification of accelerator[160,161] and direct attachment of curatives to polymer chain[162-164] were studied in order to distribute the curatives uniformly in the two phases. The migration of some thiuram based accelerators in rubber is reduced by using

Pb_3O_4 along with ZnO, so that the complex formed by Pb_3O_4 and thiuram based accelerator, makes the solubility in both phases almost same[165,166].

In another method sulphur is chemically bound to the elastomer in which it has the lowest solubility so that migration of curatives is prevented, when blended with other elastomers. This is applied to NR/EPDM system[167,168].

Preblending of curatives into the elastomers has been adopted to improve blend crosslink distribution though scorch problems may arise. Miscibility in elastomers has been shown to be enhanced by co-curing of elastomers which have similar polarity and unsaturation level as in the case of SBR/BR blends[169]. BR/NR blends were immiscible but after curing their miscibility was improved[170].

The extent of co-crosslinking is sensetive to both rate of vulcanisation as well as specific cure systems employed[171-173]. The accumulation of curative at the interface can be brought about by adding a monomeric component soluble in both phases as compatibiliser, which improves co-crosslinking[173,174].

1.6 BACKGROUND, SCOPE AND OBJECTIVES OF THE PRESENT WORK

From the discussion above, it is clear that broadly there are three fundamental aspects of elastomer blending : the first is to create the desired phase morphology through mixing and processing step; the second is to get uniform

crosslink density by control of migration of the compounding ingredients; and the third is improvement of adhesion between the phases by crosslinks formed across the interphase.

It has been shown that compatibility in polymer blends improve by reducing the interfacial tension, which can be achieved by blending rubbers which have close solubility parameters. Compatibility in polymer blends is also improved by co-crosslinking. So, if the blend constituents themselves crosslink then crosslink density homogeniety could be obtained and at the same time use of external curing agents could be avoided.

Functionalisation of elastomers is done to improve and optimise the properties of the existing rubber and to introduce new curing sites in the rubbers. The desired functional groups are introduced into an elastomer by two ways : either by polymerisation of monomers with desirable functional groups or by chemical reactions of the polymer in presence of suitable catalysts and other chemicals.

Addition of a small amount acrylic acid or methacrylic acid during polymerisation of butadiene and acrylonitrile is an appropriate means whereby reactive carboxyl groups can be introduced into the polymer chain of acrylonitrile-butadiene rubber.

On the other hand, the oxidation of diene rubbers like cis-polyisoprene in presence of a catalyst offers a

potentially useful method for improving and optimizing properties like low gas permeability and oil resistance.

Epoxidised natural rubber (ENR) is a new class of rubber obtained by the epoxidation of natural rubber (NR) latex. At the latex stage natural rubber is subjected to a partial and random epoxidation with a peracid[175-178]. Depending on the epoxidation level, the properties of ENR vary and become comparable to those of acrylonitrile-butadiene rubber in oil resistance and butyl rubber in damping[175,178]. While the double bonds of ENR can be crosslinked by the usual sulphur, accelerator or peroxide systems, the epoxide groups provide alternative sites for crosslinking with polyfunctional molecules[179-181]. Epoxy groups react with a variety of reagents such as acids, amines and hydroxides to form stable crosslinks. Compounds with similar structures are also used in curing of epoxy resins.

Fluoroelastomers are modified by intoducing epoxy groups for vulcanisation[182]. In carboxylated nitrile rubber, carboxyl groups can be crosslinked by epoxy compound through esterification[183,184].

It was shown that low molecular weight acrylic rubbers containing both epoxy and carboxylic curing sites underwent self-crosslinking by esterification[185]. Epoxy resins could be used to cure polychloroprene rubbers[186]. These results open up the possibility that blends of several functionally active rubbers can crosslink themselves in the absence of

conventional curing agents, when heated at high temperatures. There has been very little studies on blends of ENR with other elastomers. Ability of ENR to form self-vulcanisable blends with other elastomers has not been reported as yet. ENR is of special interest in natural rubber producing countries like India. It is also important to note that the country does not produce all speciality rubbers. Accordingly, it is worthwhile to undertake investigations on rubber blends based on ENR and other elastomers. It is likely that such blends can provide useful rubbery materials with novel properties.

In the present investigations, it was observed that ENR can form self-crosslinkable binary blend with carboxylated nitrile rubber (XNBR) and also with polychloroprene (CR). It was also observed that ENR can form a self-crosslinkable ternary blend when incorporated into a binary blend of XNBR and CR. The present thesis reports the results of investigations on : (a) binary blend of ENR and XNBR, (b) binary blend of ENR and CR and (c) ternary blend of ENR, XNBR and CR. Emphasis has been put on the characterisation, miscibility, physical and dynamic mechanical properties of the blends with special reference to the effect of fillers commonly used in reinforcement of rubbers.

REFERENCES

1. D.R. Paul and S. Newman, "Polymer Blends", Vol. 1 & 2, Academic Press, New York, 1978.
2. O. Olabisi, L.M. Robeson and M.T. Shaw, "Polymer-polymer Miscibility", Academic Press, New York, 1979.
3. J.A. Manson and L.H. Sperling, "Polymer Blends and Composites", Plenum Press, New York, 1981.
4. J.W. Barlow and D.R. Paul, Polym. Eng. Sci., 21 (1981) 985.
5. D.W. Fox and R.B. Allen, Encyclopedia of Polymer Science and Engineering, J.I. Kroschwitz (Editor-in-Chief) H.F. Mark, N.M. Bikales, C.G. Over.
6. C.M. Roland, Rubber Chem. Technol., 61 (1988) 866.
7. R. Koningsveld, L.A. Kleintjens and H.M. Scholffeleers, Pure Appl. Chem., 39 (1974) 1.
8. P.J. Flory, J. Chem. Phys., 9 (1941) 660.
9. P.J. Flory, J. Chem. Phys., 10 (1942) 51.
10. M.L. Huggins, J. Chem. Phys., 9 (1941) 440.
11. R.L. Scott, J. Chem. Phys., 17 (1949) 279.
12. H. Tompa, Trans. Faraday Soc., 45 (1949) 1142.
13. A.C. Su and J.R. Fried, Polym. Eng. Sci., 27 (1987) 1657.
14. J.H. Hilderbrand and R.L. Scott, "The Solubility of Non-electrolytes", 3rd Ed., Van Nostrand-Reinhold, Princeton, New Jersey, 1950, reprinted Dover, New York, 1964.

15. J.H. Hilderbrand and R.L. Scott, "Regular Solutions", Prentice Hall, Englewood, Cliffs, New Jersey, 1962.

16. D.R. Paul and J.W. Barlow, J. Macromol. Sci. Rev., Macromol. Chem., C18 (1980) 109.

17. O. Olabisi, Macromolecules, 8 (1975) 316.

18. T.K. Kwei, J. Polym. Sci., Polym. Chem. Edn., 19 (1981) 1451.

19. S. Djadoun, R.N. Goldberg and H. Morawetz, Macromolecules, 10 (1975) 1015.

20. T. Sulzberg and R.J. Cotter, J. Polym. Sci., Part A-1, 8 (1970) 2747.

21. N. Ohno and J. Kumanotanu, Polym. J., 11 (1979) 947.

22. A. Eisenberg, P. Smith and Z.L. Zhou, Polym. Eng. Sci., 22 (1982) 1118.

23. R. Murali and A. Eisenberg, J. Polym. Sci., Polym. Phys. Ed., 26 (1988) 1385.

24. M. Aubin, Y. Bedard, M.F. Morisette and R.E. Prud'homme, J. Polym. Sci., Polym. Phys. Edn., 21 (1983) 233.

25. A.G. Margaritis, J.K. Kallitsis and N.K. Kalfoglou, Polymer, 28 (1987) 2122.

26. J.K. Kallitsis and N.K. Kalfoglou, Angew Makromol. Chem., 148 (1987) 103.

27. A.G. Margaritis and N.K. Kalfoglou, Polymer, 28 (1987) 497.

28. A.G. Margaritis and N.K. Kalfoglou, Eur. Polym. J., 24 (1988) 1043.

29. C.K. Sham and D.J. Walsh, Polymer, 28 (1987) 804.

30. M.M. Coleman and J.J. Zaryan, J. Polym. Sci., Polym. Phys., Edn., 17 (1979) 873.

31. M.E. Fowler, J.W. Barlow and D.R. Paul, Polymer, 28 (1987) 1177.

32. S.P. Ting, E.M. Pearce and T.K. Kwei, J. Polym. Sci., Polym. Lett. Ed., 18 (1980) 201.

33. E.M. Pearce, T.K. Kwei and B.Y. Min, J. Macromol Sci., Chem. A(21) (1984) 1181.

34. S.H. Goh and S.Y. Lee, Polym. Commun., 31 (1990) 463.

35. H. Tamai, M. Hasegawa and T. Suzawa, J. Appl. Polym. Sci., 37 (1989) 403.

36. L.M. Robeson and E.B. Furtek, J. Appl. Polym. Sci., 23 (1979) 645.

37. G. ten Brinke, F.E. Karasz and W.J. Macknight, Macromolecules., 16 (1983) 1827.

38. S. Akiyama, W.J. Macknight, F.E. Karasz and J. Nambu, Polym. Commun., 28 (1987) 236.

39. D.R. Paul and J.W. Barlow, Polymer, 25 (1984) 487.

40. J.M.G. Cowie and D. Lath, Polym. Commun., 28 (1987) 300.

41. J. Noolandi, Polym. Eng. Sci., 24 (1984) 70.

42. Chuan Qin, Jinghua Yin and Baotong Huang, Polymer, 31 (1990) 663.

43. T.K. Kwei, H.L. Frisch, W. Radigan and S. Vogel, Macromolecules, 10 (1977) 157.

44. V.S. Shah, J.D. Keitz, D.R. Paul and J.W. Barlow, J. Appl. Polym. Sci., 32 (1986) 3863.

45. Y.Y. Wang and S.A. Chen, Polym. Eng. Sci., 21 (1981) 47.

46. C. Belaribi, G. Maren and Ph. Monge, Eur. Polym. J., 22 (1986) 487.

47. K.E. Min, J.S. Chiou, J.W. Barlow and D.R. Paul, Polymer, 28 (1987) 1721.

48. R. Fayt, R. Jerome and Ph. Teyssie, Polym. Eng. Sci., 27 (1987) 328.

49. A.Y. Coran and R. Patel, Rubber Chem. Technol., 56 (1983) 1045.

50. W.E. Baker and M. Saleem, Polym. Eng. Sci., 27 (1987) 1634.

51. W.E. Baker and M. Saleem, Polymer, 28 (1987) 2057.

52. Daniel Serrano, Jean Peyrelasse, Christian Boned, Daniel Harran and Philippe Monge, J. Appl. Polym. Sci., 39 (1990) 679.

53. S. Cimmino, L. D'Orazio, R. Greco, G. Maglio, M. Malinconico, C. Mancarella, E. Martuscelli R. Palumbo and G.Rogosta, Polym. Eng. Sci., 24(1) (1984) 48.

54. C.B. Bucknall, "Toughened Plastics", Applied Science Publishers, London, 1977.

55. S. Wu in Polymer Blends eds D.R. Paul and S. Newman, Vol. 1, Academic Press, Inc., New York, 1978, Ch. 6.

56. A. Ahagon and A.N. Gent, J. Polym. Sci., Phys. Edn., 13 (1975) 1285.

57. E.P. Plueddermann in `Interfaces in Polymer Matrix Composites' (E.P. Plueddermann, ed.), Academic Press, New York, 1974, p. 174.

58. T.J. Mao and S.L. Reegen in "Adhesion and Cohesion, P. Weiss, ed., Elsevier, Amsterdam, 1962, p. 209.

59. W.H. Samaroot and S. Bonotto, Polym. Eng. Sci., 8 (1968) 41.

60. W.J. Macknight, F.E. Karasz and J.R. Fried, "Polymer Blends", Ed., D.R. Paul and S. Newman, Academic Press, New York, Ch. 5, p. 186.

61. S. Krause, J. Macromol. Sci. Rev. Macromol Chem., 7(2) (1972) 251.

62. B.D. Gesner, Encycl. Polym. Sci. Technol., 10 (1969) 694.

63. T.G. Fox, Bull. Amer. Phys. Soc., 2 (1956) 123.

64. M. Gordon and J.S. Taylor, J. Appl. Chem., 2 (1952) 493.

65. G.A. Zakrzewski, Polymer, 14 (1973) 347.

66. J.J. Hickman and R.M. Ikeda, J. Polym. Sci., Polym. Phys. Edn., 11 (1973) 1713.

67. A.R. Schultz and B.M. Beach, Macromolecules, 7 (1974) 902.

68. L.M. Robeson and A.B. Fartek, J. Appl. Polym. Sci., 23 (1979) 645.

69. J. Koleske and R. Lundberg, J. Polym. Sci., A-2, 7 (1969) 795.

70. F.N. Kelley and F. Bueche, J. Polym. Sci., 50 (1961) 549.

71. W.M. Prest and R.S. Porter, J. Polym. Sci., Polym. Phys. Edn., 10 (1972) 1639.

72. D.R. Paul and J.W. Barlow, J. Macromol. Sci. Rev., Macromol. Chem., C18 (1980) 109.

73. E. Nolley, D.R. Paul and J.W. Barlow, J. Appl. Polym. Sci., 23 (1979) 623.

74. E.W. Fischer, J.H. Wendorff, M. Dettenmaier, G. Lieser and I. Voigt-Martin, J. Macromol. Sci., Phys., 12 (1976) 12.

75. G.D. Patterson, J. Macromol. Sci. Phys., 12 (1976) 61.

76. Y.J. Shur and B. Ranby, J. Appl. Polym. Sci., 20 (1976) 3105.

77. Y.J. Shur and B. Ranby, J. Appl. Polym. Sci., 19 (1975) 1337.

78. J.J. Hickman and R.M. Ikeda, J. Polym. Sci., Polym. Phys. Ed., 11 (1973) 1713.

79. B.G. Ranby, J. Polym. Sci., Polym. Symp., 51 (1975) 89.

80. F.B. Khambatta, F. Warner, T. Rusell and R.S. Stein, J. Polym. Sci., Polym. Phys. Edn., 14 (1976) 1391.

81. U. Wenig, F.E. Karasz and W.J. Macknight, J. Appl. Phys., 46 (1975) 4194.

82. T. Nishi and T.T. Wang, Macromolecules, 3 (1975) 909.

83. T.K. Kwei, G.D. Patterson and T. Wang, Macromolecules, 9 (1976) 780.

84. J.D. Hoffman and J.J. Weeks, Res. Natt. Bur. Stand. (A), 66 (1962) 13.

85. J.B. Nagode and C.M. Roland, Polymer, 32 (3) (1991) 505.

86. D.R. Paul, J.W. Barlow, R.E. Bernstein and O.C. Wahrmund, Polym. Eng. Sci., 18 (1978) 1225.

87. P.B. Rim and J.P. Runt, Macromolecules., 17 (1984) 1520.

88. R.M. Briber and F. Khoury, Polymer, 28 (1987) 38.

89. H. Zhang and R.E. Prud'homme, J. Polym. Sci., Polym. Phys. Edn., 24 (1987) 723.

90. S. Hobbs, J. Macromol. Sci., Rev. Macromol. Chem., 19 (1980) 221.

91. R.W. Smith and J.C. Andries, Rubber Chem. Technol., 47 (1974) 64.

92. M. Matsuo, C. Nozaki and Y. Jyo, Polym. Eng. Sci., 9 (1969) 197.

93. L.P. McMaster, Adv. Chem. Ser., 142 (1975) 43.

94. W.H. Walters and D.N. Keyte, Rubber Chem. Technol., 38 (1965) 62.

95. G. Demma, E. Martuscelli, A. Zanetti and M. Zorzetto, J. Mater. Sci., 18 (1983) 89.

96. A.K. Bhowmick, Rubber Chem. Technol., 55 (1982) 1055.

97. S. Thomas, Wear, 116 (1987) 201.

98. M.M. Mathew and S.K. De, J. Mat. Sci., 18 (1983) 515.

99. A.N. Gent and C.T. Pulford, in "Development in Polymer Fracture -1", ed. E.H. Andrew, Applied Science, London, 1979, p. 155.

100. C.B. Bucknell, in "Toughened Plastics", Applied Science Publishers, London, 1977.

101. F.J. McGarry, Proc. R. Soc. London, A319 (1970) 59.

102. R.A. Pearson and A.F. Yee, J. Mater. Sci., 21 (1986) 2475.

103. E. Butta, G. Levita, A. Marchetti and A. Lazzer, Polym. Eng. Sci., 26 (1986) 63.

104. P.J. Flory, J. Am. Chem. Soc., 87 (1965) 1833.

105. L.W. Kleiner, F.E. Karasz and W.J. Macknight, Polym. Eng. Sci., 19 (1979) 519.

106. C.M. Roland, Rubber Chem. Technol., 62 (1989) 4567.

107. C.S. Hu, D.J. Ihm and S.C. Kim, J. Appl. Polym. Sci., 32 (1986) 6281.

108. B. Kuriakose, S.K. Chakraborty and S.K. De, Material Chem. Phys., 12 (1985) 157.

109. S. Akhtar, P.P. De and S.K. De, Material Chem. Phys., 12 (1985) 235.

110. S. Thomas, B. Kuriakose, B.R. Gupta and S.K. De, Plast. Rubb. Process. Appl., 6 (1986) 101.

111. P.J. Flory and J. Rehner, Jr., J.Chem. Phys., 11 (1943) 512.

112. P.J. Flory, J. Chem. Phys., 18 (1950) 108.

113. G. Kraus, J. Appl. Polym. Sci., 7 (1963) 861.

114. P.B. Stickney and W.J. Muller, ACS Meeting, Rubber Divn., Cleveland, Ohio, 1968.

115. C.J. Sheehan, Rubber Chem. Technol., 39 (1966) 149.

116. G. Butenuth, Rubber Age, February (1964) 737.

117. G. Kraus, Rubber World, 135 (1956) 67, 254.

118. O. Lorentz and C.R. Parks, J. Polym. Sci., 50 (1961) 299.

119. A.K. Bhowmick and S.K. De, Rubber Chem. Technol., 53 (1980) 960.

120. S.K. Chakraborty and S.K. De, J. Appl. Polym. Sci., 27 (1982) 4561.

121. S.K. Chakraborty and S.K. De, Polymer, 24 (1983) 1055.

122. S.C. Einhorn and S.B. Turetzky, J. Appl. Polym. Sci., 8 (1964) 1257.

123. A.S. Hill and B. Maxwell, Polym. Eng. Sci., 10 (1970) 289.

124. R.F. Heitmiller, R.Z. Naar and H.H. Zabusky, J. Appl. Polym. Sci., 8 (1964) 873.

125. H. Natov, L. Peera and E. Djagenora, J. Polym. Sci., C-16 (1986) 4497.

126. C.L. Sieglass, Polym. Eng. Sci., 9 (1969) 91.

127. A. Plochoki, in "Polymer Blends", Eds. D.R. Paul and S. Newman, Vol. 2, Academic Press, New York, 1978, p. 319.

128. A. Plochoki, J. Appl. Polym. Sci., 16 (1972) 987.

129. Baby Kuriakose and S.K. De, Polym. Eng. Sci., 25 (1985) 630.

130. Sania Akhtar, Baby Kuriakose, Prajna P. De and Sadhan K. De, Plastics. Rubb. Process. Appl., 7 (1987) 11.

131. K.T. Varughese, P.P. De, G.B. Nando and S.K. De, J. Vinyl Technology, 10(4) (1988) 166.

132. T.K. Bhaumik, B.R. Gupta and A.K. Bhowmick, Plast. Rubber Process. Appl., 10 (1988) 105.

133. D.M. Turner and A.C. Bickley, Plast. Rubber Process. Appl., 1 (1981) 357.

134. G. Angerer and D. Wolff, Rheol. Acta., 15 (1976) 57.

135. E.L. Ong and R. Subramaniam, Proc. Int. Rubber Conf., Kuala Lumpur, 39 (1975) 1.

136. B.L. Lee and J.L.White, Trans. Soc. Rheology, 19 (1975) 481.

137. L. Nielsen, "Polymer Rheology", Marcel Dekker, Newyork, 1977.

138. E. Boudreaux, Jr. and J.A. Cuculo, J. Appl. Polym. Sci., 27 (1982) 189.

139. S. Uemura and M. Takayanagi, J. Appl. Polym. Sci., 10 (1966) 113.

140. J.W. Teh, Plastics Rubb. Process. Appl., 4 (1984) 157.

141. J.A. Brydson, "Flow Properties of Polymer Melts", Second Ed., Pub. George Godwin Ltd., Print. Butler and Tanner Ltd., U.K., Chap. 8., p. 202 (1981).

142. Stanley Middleman, "Fundamentals of Polymer Processing", Eds. NB.J. Clark and Douglas J. Marshell, McGraw-Hill Inc., USA, Chap. 3, p. 43 (1977).

143. J.E. Callan, W.M. Hess and C.E. Scott, Rubber Chem. Technol., 44 (1971) 814.

144. P.J. Corish and D.W. Powell, Rubber Chem. Technol., 47 (1974) 481.

145. G. Avgeropoulos, F.C. Weissert, P.H. Biddison and C.G.A. Bohm, Rubber Chem. Technol., 49 (1976) 93.

146. C.J. Nelson, G.N. Avgeropoulos, F.C. Weissert and C.G.A. Bohm, Angew. Makromol. Chem., 60/61 (1977) 49.

147. N. Tokita, Rubber Chem. Technol., 50 (1977) 292.

148. T. Inoue, Nippon Gomu Kyokaishi, 1 (1981) 20.

149. W.P. Gergen, R.P. Lutz and S. Davison, Rubber Chem. Technol., 58 (1985) 857.

150. I.S. Miles and A. Zurek, Polym. Eng. Sci., 28 (1988) 796.

151. J.E. Callen, W.M. Hess and C.E. Scott, Rubber Chem. Technol., 44 (1971) 814.

152. P.J. Corish, Science and Technology of Rubber, F.R. Eirich, Ed., Academic Press, New York, 1978, Chap. 12.

153. W.M. Hess, C.E. Scott and J.E. Callen, Rubber Chem. Technol., 40 (1967) 371.

154. J.B. Gardiner, Rubber Chem. Technol., 41 (1968) 1312.

155. J.B. Gardiner, Rubber Chem. Technol., 42 (1969) 1058.

156. J.L. Leblanc, Plast. Rubber Process. Appl., 2 (1982) 361.

157. A.K. Bhowmick and S.K. De, Rubber Chem. Technol., 53 (1980) 960.

158. R.P. Mastromatteo, J.M. Mitchell and T.J. Brett, Jr., Rubber Chem. Technol., 44 (1971) 1065.

159. Technical note on USRNE Japan Synthetic Rubber Company Ltd., 1980.

160. R.W. Amidon and R.A. Gencarelli, US 3,674,824 (1972).

161. Sumitomo Chemical Company, British 1,325,064, Aug. 1 (1973).

162. K.C. Baranwal and P.N. Son, Rubber Chem. Technol., 47 (1974) 88.

163. K. Hashimoto, M. Miura, S. Takagi and Okamoto, Int. Polym. Sci., Technol., 3 (1976) 84.

164. A.Y. Coran, Rubber Chem. Technol., 55 (1982) 575.

165. W.H. Whittington, J. Int. Rubber Ind., 9 (1975) 151.

166. M.E. Wood and J.A. Davidson, Rubber Chem. Technol., 49 (1976) 1065.

167. Hashimoto, Miura and Okamoto, Nippon Gomu Kyokaishi, 49 (1976) 246.

168. Hashimoto, Miura, Sumiyoshi and Nakajima, Nippon Gomu Kyokaishi, 49 (1976) 241.

169. N. Yoshimura and K. Fujimoto, Rubber Chem. Technol., 42 (1969) 1009.

170. P.J. Corish, Rubber Chem. Technol., 40 (1967) 324.

171. K. Hashimoto, T. Harada, I. Ando and N. Okubo, J. Soc. Rubber Ind. Jpn., 43 (1970) 659.

172. R.L. Zapp, Rubber Chem. Technol., 46 (1973) 251.

173. M.E. Woods and T.R. Mass, Adv. Chem. Ser. n., 142 (1975) 386.

174. E. Hefland and Y. Tagami, J. Chem. Phys., 56 (1972) 3592.

175. I.R. Gelling, Rubber Chem. Technol. 58 (1985) 86.

176. D.R. Burfield, K.L. Lim and K.S. Law, J. Appl. Polym. Sci., 29 (1984) 1661.

177. S.C. Ng and L.H. Gan, Eur. Polym. J., 17(10) (1981) 1073.

178. C.S.L. Baker, I.R. Gelling and R. Newell, Rubber Chem. Technol., 58 (1985) 67.

179. T. Colclough, Inst. Rubb. Ind. Trans., 38 (1962) 11.

180. C.T. Loo, Proc. Int. Rubb. Conf. Rubber Research Institute of Malaysia, Kaula Lumpur, 1985, Vol. 11, p. 368.

181. C.S.L. Baker, I.R. Gelling and S. Azemi, J. Nat. Rubb. Res., 1(2) (1986) 135.

182. G. Kojima, H. Kojima and M. Morozumi, Rubber Chem. Technol., 54 (1981) 779.

183. H.P. Brown, Rubber Chem. Technol., 36 (1963) 931.

184. S.K. Chakraborty and S.K. De, J. Appl. Polym. Sci., 27 (1982) 4561.

185. E. Giannetli, R. Mozzocchi, L. Fiore and E. Crespi, Rubber Chem. Technol., 56 (1983) 21.

186. N.D. Zakharov and G.A. Maiorov, Sov. Rubber Technol., 22 (1963) 11.

CHAPTER 2

EXPERIMENTAL

This chapter deals with materials used and the experimental techniques adopted in the present investigation.

2.1 MATERIALS USED

2.1.A Rubbers

Epoxidised Natural Rubber (ENR) Epoxidised natural rubber with 50 mol % epoxidation was obtained from MRPRA, UK. Its characteristics were Mooney viscosity ML(1+4) 120°C 47, specific gravity 1.03.

Carboxylated Nitrile Rubber (XNBR) : Krynac 221 was obtained from Polysar Ltd., Canada with medium high acrylonitrile and carboxylated monomer 7 mol percent.Its characteristics were Mooney viscosity ML(1+4)120°C 26, specific gravity 0.97.

Polychloroprene : Neoprene AD was obtained from DuPont Ltd., UK.Its characteristics were Mooney viscosity ML(1+4)120°C 160, specific gravity 1.26.

2.1.B Fillers

Carbon Black

I.S.A.F. : Intermediate super abrasion furnace black (N220) was obtained from Philips Carbon Black Ltd., Durgapur.

S.R.F. : Semi reinforcing furnace black (N756) was obtained from Philips Carbon Black Ltd., Durgapur.

Silica : Vulkasils (precipitated silica) was supplied by Bayer (India) Ltd., Bombay.

2.1.C Accelerators

MBS : N - oxydiethylene benzothiazole 2- sulphenamide was supplied by IEL Ltd., Rishra,Hooghly,India

TMT : Tetramethyl thiuram disulphide was supplied by IEL Ltd., Rishra, Hooghly, India.

2.1.D Other Chemicals

ZnO : Zinc oxide was of chemically pure grade and had specific gravity of 5.4. It was obtained from S.D.Fine Chemicals Ltd., Bombay.

Stearic Acid : Stearic acid was of chemically pure grade and had a specific gravity of 0.82. It was obtained from IEL Ltd., Rishra, Hooghly.India.

Sulphur : Sulphur was of chemically pure grade and had a specific gravity of 1.9. It was obtained from S.D.Fine Chemicals Ltd., Bombay.

Solvents : Chloroform was of analytical grade and obtained from S.D. Fine Chemicals Ltd., Bombay.

Dioctyl Phthalate : It was of commercial rubber grade and was obtained from S.D. Fine Chemicals Ltd., Bombay.

ASTM Fuel C : ASTM fuel C confirming to ASTM D 471-79, isooctane, 50 volume %, toluene 50 volume %. was obtained from S.D Fine Chemicals Ltd.;Bombay.

2.2 PROCESSING OF RUBBER

2.2.A Compounding

Mixes were prepared on a laboratory size two-roll mixing mill (325 mm x 150 mm) at a friction ratio of 1:1.5 according to ASTM D 3182-74 by careful control of temperature, nip gap, time of mixing and by uniform cutting operation. The details of the two-roll mill are given in Table 2.1.

The compounding ingredients were added in the following order : filler, plasticiser and curatives. For compounding of carboxylated nitrile rubber, sulfur was added first followed by other ingredients.

In the preparation of binary blend of ENR and XNBR, both the elastomers were masticated separately and then mixed further. The total mixing time was about 8 min. The binary blend of ENR and polychloroprene was also prepared in a similar way.

Ternary blend was prepared by adding ENR to the polychloroprene-XNBR blend. Both polychloroprene and XNBR were separately masticated and mixed for about 6 minutes. ENR was added to this and mixing continued for a further period of about 4 minutes. The fillers were added after blending the rubbers. The rolls were kept cool by the circulation of cold water. The rise in temeprature during mixing of gum rubbers was 2°C. The rise in temperature after addition of filler was 7°C.

2.2.B Determination of Cure Characteristics

The curing characteristics of the experimental compounds were determined with the help of Mooney viscometer, (Negretti Mark III) and Monsanto Rheometer (R-100).

2.2.B.1 Mooney Scorch Time

Mooney viscometer (Negretti Mark III) was used to find out the Mooney viscosity and scorch time according to ASTM designation D 927-52T. The experiment was carried out at 100°C and 120°C.

Mooney scorch time is defined as the time taken in minutes to raise the viscosity by five units above the minimum viscosity. The Mooney viscosity is expressed as $ML_{(1+4)}$ at 100°C (or at 120°C), where M stands for Mooney viscosity, L stands for large rotor, 1 indicates the pre-heating time in min and 4 minutes is the time after starting the rotor at which the reading is taken.

2.2.B.2 Optimum Cure Time

Optimum cure time at different temperatures 150°C, 160°C, 170°C, 180°C was determined using a Monsanto Rheometer (R-100). The optimum cure time corresponds to the time to achieve 90 percent (t_{90}) of the cure calculated from the following equation :

$$\text{Optimum cure time} = [0.9\ (L_F - L_i) + L_i] \qquad \ldots.(2.1)$$

where L_F and L_i are the maximum and minimum rheometeric torques. In the case of blends the torque registered a progressive rise and the rise in torque was less than or equal to one unit after an hour. So for these mixes optimum cure times were taken as 60 minutes.

For comparison of technical properties, the control mixes of ENR, XNBR and CR were cured to a time corresponding to the same rheometric torque rise as that of the corresponding blend mixes. For example, the torque rise of gum ENR-XNBR binary blend was 30 units. The gum ENR and gum XNBR were also cured to the required time in order to get a rise in rheometric torque of 30 units.

2.2.C Cure Rate

Cure rate was determined from the rheographs according to following equation

$$\text{Cure rate} = \frac{100}{t_{90} - t_2} \qquad \text{....(2.2)}$$

where t_{90} and t_2 are the times corresponding to the optimum cure and two units above the minimum value respectively.

2.3 VULCANISATION

Vulcanisation was carried out in a David Bridge single daylight electrically heated press having 300 mm x 300 mm platens at 150°C or 180°C at a pressure of 4.5 MPa on the mould for the required cure time. Mouldings were cooled

immediately in water at the end of the curing cycle. For thicker samples having thickness more than 6.25 mm (like heat build-up, compression set etc.,) additional times based on sample thickness were used to obtain satisfactory mouldings.

2.4 PHYSICAL TEST METHODS

2.4.A Measurement of Technical Properties : Modulus, Tensile Strength and Elongation at Break

These properties of the vulcanisates were determined according to the ASTM D 412-80 test method using dumbbell shaped test pieces. Samples were punched out from vulcanised sheets parallel to the grain direction using a dumbbell die (C type). The thickness of the sample was measured by bench thickness gauge. Testings were done in and Instron Universal Testing Machine, model 1195. Extensometer was clamped to the specimen to get the elongation at break. The load and elongation at break were recorded on a strip chart recorder. From the recorded load the stress was calculated based on the original cross-sectional area of the specimen. The modulus and tensile strength are reported in MPa and the elongation at break in percentage of the original length.

For measurement of failure envelope the samples were tested at strain rates from 0.04 s^{-1} to 0.20 s^{-1} and at temperature from 25°C to 150°C using Zwick Universal Testing Machine, model 1445. High temperature testings were carried out in a special oven attached with the Zwick machine. Temperature was controlled within a range of ± 1°C during the

experiment.

2.4.B Tear Resistance

The tear resistance of the sample was determined as per ASTM designation D 624-81 test method, using 90° angle test specimen which were punched out from the moulded sheets along the mill grain direction. These tests were also carried out in Instron UTM model 1445 and expressed in kN/m.

2.4.C Hardness

The hardness of the sample was determined as per ASTM designation D 1415-81 test method, using Wallace IRHD test equipment. The readings were taken after 30 seconds of firm contact.

2.4.D Abrasion Resistance

The abrasion resistance of the samples were tested using a DuPont abrader. The test was carried out according to ASTM designation D 394, method A against a silicon carbide abrasive paper P180. The samples were conditioned (surface smoothening) by five minutes of abrasion. The samples were abraded for 10 mins. The abrasion loss of the sample was calculated as volume loss in cc/hr for one test specimen.

2.4.E Rebound Resilience

Dunlop tripsometer was used to measure the rebound resilience according to the ASTM designation D 1054-79. The sample was held in position by suction. It was conditioned

by striking six times with the indenting hammer. The sample was kept at a constant temperature of 40°C. Rebound resilience was calculated according to the following formula,

$$\text{Rebound Resilience} = \frac{1 - \cos\theta_2}{1 - \cos\theta_1} \cdot 100 \qquad \ldots.(2.4)$$

where θ_1 and θ_2 are the initial and rebound angles respectively. θ_1 was taken 45° in all cases.

2.4.F Heat Build-up

The Goodrich flexometer was used to measure the property according to the ASTM designation D 623-67, method A. The test was carried out with cylinderical sample of 25 mm height and 20 mm diameter. The oven temperature was kept constant at 50°C. The stroke was adjusted to 4.45 mm and the load was 10.9 kgF. The frequency of the stroke was 30/sec. The initial height of the sample was measured and the sample was preconditioned to the oven temperature for 25 minutes. The test was continued for 25 minutes. The heat generated at the base of the sample was relayed to the microvoltmeter. The temperature rise (ΔT) at the end of 20 minutes stroke was taken as the heat build-up.

Next, the sample was taken out and the thickness was measured after half an hour of relaxation. The permanent set was calculated from the residual height of the sample and expressed as

$$\text{Dynamic set, } \% = \frac{t_1 - t_2}{t_1} \cdot 100 \qquad \ldots.(2.5)$$

where t_1 and t_2 are the initial and final heights of the test specimens respectively.

2.4.G Compression Set at Constant Strain

The compression set at constant strain was carried out according to the ASTM designation D 575-81, method A. The sample 12 mm thick and 20 mm in diameter was compressed to constant deformation (25%) and kept for 22 h in an air oven at 70°C. After 22 h the samples were taken out cooled to room temperature for half an hour and the thickness was measured. The compression set was measured as follows

$$\text{Compression set, } (\%) = \frac{(t_o - t_1)}{(t_o - t_s)} \cdot 100 \qquad \ldots.(2.6)$$

where t_o and t_1 are the initial and final thicknesses of the specimen and t_s is the thickness of the spacer bar used.

2.4.H Stress Relaxation

Stress relaxation is the stress decay with time under constant strain. It was measured by a Zwick Universal Testing Machine, model 1194. Dumbbell specimens were used. The samples were pulled to the desired elongation at a strain rate of 0.03 s^{-1}. The decay of the stresses as a function of time was recorded. The slope and intercept of the stress relaxation plots (obtained from plots of (σ/σ_o) vs. log(time)

where σ_0 is the initial stress and σ is the stress at time t,) were obtained by the method reported by Scanlan and MacKenzie.[1]

2.4.I Rupture Energy

Rupture energy was evaluated by measuring the area under the stress-strain curve of the vulcanisates, obtained from the Instron UTM.

2.5 DYNAMIC MECHANICAL ANALYSIS

For dynamic mechanical testing a sinusoidal force is applied to the sample. In the case of viscoelastic material, stress and strain both will change sinusoidally under steady state condition but the strain lags behind the stress by an angle which is called phase angle (Fig. 2.1). This behaviour is represented in terms of real and imaginary components of the complex modulus as $E^* = E' + iE''$, where E' is the elastic or storage modulus, the energy which is recoverable when a cycle deformation comes to zero position and E" is the viscous or loss modulus, the energy associated with this is converted to frictional heat and it is unrecoverable. This is shown in Fig. 2.2. The ratio E"/E' is known as $\tan\delta$.

All the dynamic mechanical measurements were done on a dynamic mechanical analyser (Rheovibron, DDV-III-EP) comprised of a temperature programmer and controller. A schematic diagram of the instrument is given in Fig. 2.3. The storage modulus, loss modulus (E' and E") and $\tan\delta$ were

recorded under oscillatory load in tension mode as a function of temperature.

The measurement of dynamic mechanical analysis was carried out on vulcanised samples. The dimension of the sample was 0.50 cm x 0.30 cm and length about 6 cm. The experiment was conducted in tension mode over a temperature range of -100°C to +50°C with a programmed heating rate of 2°C/min. The frequency was 3.5 Hz and dynamic strain was 0.0025 cm. Mechanical loss factor ($\tan\delta$) and dynamic modulus (E', E"), were calculated by the microcomputer.

Method of Calculation

Outputs of the stress and strain transducer s are converted to provide direct $\tan\delta$ readings. The absolute value of complex tensile modulus E^* ($E^* = E' + iE''$) is given by

$$E^* = Fl / \Delta L A \qquad \text{....(2.7)}$$

where F = tensil: force, A = cross-sectional area, l = length of specimen, ΔL = amplitude of elongation, E' = storage modulus and E" = loss modulus.

The storage modulus, the real part or the in-phase portion of complex modulus, is an indicator of the elastic nature of the material, while the loss modulus the imaginary part or the out-of-phase portion of complex modulus, is an indicator of the viscous nature of the material.

$$E' = |E^*| \cos\delta \quad ...(2.8)$$

$$E'' = |E^*| \sin\delta \quad ...(2.9)$$

the $\tan\delta$ or the damping factor is given by the relation

$$\tan\delta = E'' / E' \quad ...(2.10)$$

2.6 DIFFERENTIAL SCANNING CALORIMETRY

The enthalpy changes associated with the transactions in rubbers were measured by differential scanning calorimeter (DuPont 910). The thermogravimetric analysis was done by a DuPont thermal analyser, model 951. The thermogravimetric analysis was done at a heating rate of 10°C/min. For DSC studies the sample was cooled to -170°C with liquid nitrogen and then heated at a rate of 20°C/min to about 100°C in nitrogen atmosphere. Thermograms were recorded between -100°C to +100°C. The glass transition temperature (Tg) is indicated as an endothermic shift. From the shift, Tg was calculated by taking mid-point of the step in the scan.

2.7 RHEOLOGICAL MEASUREMENTS

2.7.A Equipment Details

The rheological measurements were carried out using a capillary rheometer MCR 3210 attached to an Instron UTM, model 1195. The extrusion assembly consisted of a barrel, made of hardened steel, mounted on a special support underneath the moving crosshead of the Instron UTM. A hardened plunger, which was accurately ground to fit inside the barrel, was driven by the moving crosshead of the

machine. The plunger was held to the load cell extension with the help of a latch assembly. The barrel was mounted on a ball and socket system on the support, so that the system would be self-aligning. The capillary was inserted through the bottom of the barrel and was locked using a clamping device. The capillary was made of tungsten carbide material. A teflon O-ring and a split ring around the capillary prevented the leakage of the material through the gap between the barrel and the capillary. An O-ring and a split ring were also used on the plunger so that the combination acted as a piston seal. The barrel was heated electrically using a three zone temperature control system. The differences between the successive temperature zone in the barrel was 5°C, and the temperature of the lower zone, where the capillary was located, was taken as the test temperature. Typical capillary details are shown in Fig 2.4.

The moving crosshead of the Instron UTM runs the plunger at a constant speed irrespective of the load in the melt, maintaining a constant volumetric flow-rate through the capillary. The crosshead speeds varied from 0.5 mm/min to 500 mm/min. The forces corresponding to the specific plunger speeds were recorded on the strip chart recorder. This was then converted to shear stress.

2.7.1 Test Procedure

About 3 g of the test samples (cut into small [illegible]) were placed inside the barrel of the extrusion

assembly, and forced down to the capillary with the plunger attached to the moving crosshead. The melt was extruded through the capillary at pre-selected speeds of the crosshead which varied from 0.5 to 200 mm/min. With the use of area compensator the shear stress was recorded directly, using a strip chart recorder assembly. The force and crosshead speed were converted into shear stress and apprarent shear rate $\dot{\gamma}_{wa}$ using the following equations involving the geometry of the capillary and the plunger.

$$\tau_w = \frac{\Delta P \times r_c}{2\ lc} = \frac{F}{4A_p} \cdot \frac{dc}{lc} \qquad \text{....(2.11)}$$

where ΔP is the pressure drop in N/mm^2

r_c is the radius of the capillary in mm

lc is the length of the capillary in mm

F is the applied force at a particular shear rate in Newton

A_p is the cross-sectional area of the plunger in mm^2

dc is the diameter of the capillary in mm

$$\dot{\gamma}_{wa} = \frac{2}{15} \times Vxh \times \frac{d_p^3}{d_c^3} \qquad \text{....(2.12)}$$

where Vxh is the velocity of crosshead in mm/min and

d_p is the diameter of the plunger in mm

Since the flow is not assumed to be parabolic Rabinowitsch correction[2] is given so that the corrected wall shear rate $\dot{\gamma}_w$ is

$$\dot{\gamma}_w = \frac{3n' + 1}{4n'} \cdot \frac{8v}{d_c} \qquad \ldots(2.13)$$

where V is the volumetric flow rate in mm s^{-1} and n' is the flow behaviour index[2] defined by d log τ_w)/d log $\dot{\gamma}_{wa}$.

Flow activation energy was calculated from the viscosity temperature dependence using an Arrhenius type equation.

Extrudates emerging from the capillary were collected for die swell measurement avoiding any further deformations. The diameter of the extrudate at several points were measured using a travelling microscope. The die-swell ratio is measured at room temperature as De/Dc, where De = extrudate diameter; Dc = capillary diameter.

The principal normal stress difference ($\tau_{11} - \tau_{22}$) was calculated from die swell values and shear stress according to Tanner's equation[3].

$$\tau_{11} - \tau_{22} = 2\tau_w [2(De/Dc)^6 - 2]^{1/2} \qquad \ldots.(2.14)$$

Recoverable shear strain S_R and the elastic shear modulus G were calculated from the equation[4].

$$S_R = \tau_{11} - \tau_{22} / 2\tau_w \qquad \ldots.(2.15)$$

$$G = \tau_w / S_R \qquad \ldots.(2.16)$$

where τ_w is the wall shear stress.

2.8 INFRARED SPECTROSCOPY

2.8.A Dispersion of the Sample in Low Density Polyethylene (LDPE) matrix

The sample was dispersed in the LDPE matrix[5] by a melt blending technique in a Brabender Plasticorder (PLE-330). LDPE was first melted in the Brabender chamber at 120°C with a rotor speed of 60 cycles/s and a fill factor of 100%. The elastomer sample was introduced to the molten LDPE and mixed for 4 min. at the same speed. The whole mix was then dumped and passed (single pass) through a two-roll mill and sheeted out (approximately 2 mm thickness). The sheet was cut into small pieces and remixed in the Brabender for another 2 min. Then again it was sheeted in the same way on a two-roll mill having 4 mm thickness. In all cases a blend ratio of 5.5:1 was maintained for LDPE:polymer.

2.8.B Preparation of Thin Film Samples

About 0.75 g of the blended material was weighed out and kept between two aluminium foils of the size 8 x 5 cm and subjected to a temperature of 120°C at a pressure of 0.25 ton for 2 min in a laboratory automatic hydraulic press (Labo Press, Model No.T10). Then the temperature was brought down to room temperature using circulating water. Since the temperature, pressure, size of aluminium foils and weight of samples were kept fixed the average film thickness was almost constant. These films were totally free of shrinkage. The

binary blend mix ENR/XNBR and the ternary blend mix ENR/XNBR/CR, were vulcanised for 60 min. at 150°C. The binary blend ENR/CR was vulcanised for 60 min at 180°C.

2.9 SCANNING ELECTRON MICROSCOPY STUDIES

2.9.A Principles of Scanning Electron Microscope (SEM)

The working principle of SEM[6] is shown in Fig. 2.5. Electrons ejected from a filament or other emission source were subjected to an accelerated potential between 1 to 30 kV and were allowed to pass through the centre of an electron optical column consisting of two or three magnetic lenses. These lenses caused a fine electron beam to be focused onto the specimen surface. Scanning coils placed just before the final lens caused the electron spot to be scanned across the specimen surface in the form of a square raster similar to that of a television screen. Current passing through the scanning deflection coil of a cathode ray tube produced a similar but magnified raster on the viewing screen in a synchronous manner.

The emitted secondary electrons from the sample stroke the collector and the resulting current was amplified and used to modulate the brightness of the cathode ray tube. The time for the emission and collection of the secondary electrons is negligibly small compared to the time for scanning of the incident electron beams across the specimen surface. Hence, there is a one to one correspondance between the number of secondary electrons collected from any particular point of

the specimen surface and the brightness of the analogous point on the screen and thus an image of the surface was progressively built upon the screen.

In SEM, the image magnification was determined by the ratio of the size of the rasters on the screen and on the specimen surface. In order to increase the magnification, it was only necessary to reduce the current in the SEM scanning coils. As a consequence of this, it was easy to obtain high magnification in SEM, for every low magnification of 10X, it would be necessary to scan the specimen approximately 10 mm across.

2.9.B Scanning Electron Microscopy of Fractured Surfaces

The SEM observations reported in the present study were made using a cam scan series 2 Scanning Electron Microscope (Table 2.2). Abraded surfaces were carefully cut from the failed surfaces (Fig. 2.6) after abrasion for 10 min. The surfaces were then sputter coated with gold within 24 hours of testing. The tilt was adjusted according to convenience. The gold coated samples were kept in desiccators before the SEM observations were made.

2.10 CHEMICAL TEST METHODS

2.10.A Determination of Volume Fraction of Rubber

Samples of approximately 1 cm diameter, 0.25 cm thickness and 0.30 gm in weight were punched out from the central portion of the vulcanisate and allowed to swell in

chloroform at 30°C in a thermostatically controlled water bath. Swollen samples, taken out after 1, 4, 9, 16, 25, 36 and 49 hours intervals were blotted with filter paper and weighed quickly in stoppered weighing bottles. 49 hours were found to be sufficient for obtaining equilibrium swelling. Samples were then dried in an oven for 24 hours at 70°C, then in vacuum and finally weighed after allowing them to cool in a desicator. The volume fraction of rubber V_r was calculated by the method reported by Ellis and Welding[7].

$$V_r = \frac{(D - FT) / \rho_r}{(D-FT)/ \rho_r + A_o / \rho_s} \qquad \text{....(2.17)}$$

where D is the deswollen weight of the specimen, F the weight fraction of insoluble components, A_o is the weight of absorbed solvent corrected for swelling and ρ_r and ρ_s are the densities of rubber and solvent respectively.

2.10.3 Ageing Studies

Ageing studies were carried out using dumbbell shaped tensile test specimens. The test specimens were subjected to ageing and the change in tensile properties after ageing were measured in Zwick UTM (1194). The samples were subjected to the following four conditions of ageing.

(1) Air ageing at 70°C for 7 days, in an air oven,
(2) Aqueous acid ageing, 25% HCl, at 70°C for 7 days,
(3) Aqueous alkali ageing, 25% NaOH, at 70°C for 7 days,
(4) Fuel ageing (ASTM fuel C) at 30°C for 7 days.

3.10.C Solubility Parameter

A list of solvents of gradually increasing solubility parameter was arranged such that the rubbers (ENR, XNBR and CR) were soluble in all the solvents grouped within a certain range. Raw rubber sample of known weight was put in the solvent. The solubility parameter (δ) of the rubber corresponded to the solubility parameter of the particular solvent which showed maximum solubility.

Table 2.1 Details of the Two-roll open mill

1. Manufacturer	SCHWABENTHAN, BERLIN
2. Type	Industrial Drive
3. Dimension of the roll	7.52 cm x 3.43 cm
4. Cooling system	Peripheral drilled holes
5. Ampere rating	78
6. Motor drive power kw	4.8 each

Table 2.2 Operating conditions of SEM

Specimen position tilt, degree	Adjustable (10-45°)
Maximum resolution, A	40
Emission current, amp	2.5
Aperture, microns	300
E.T., kv	20

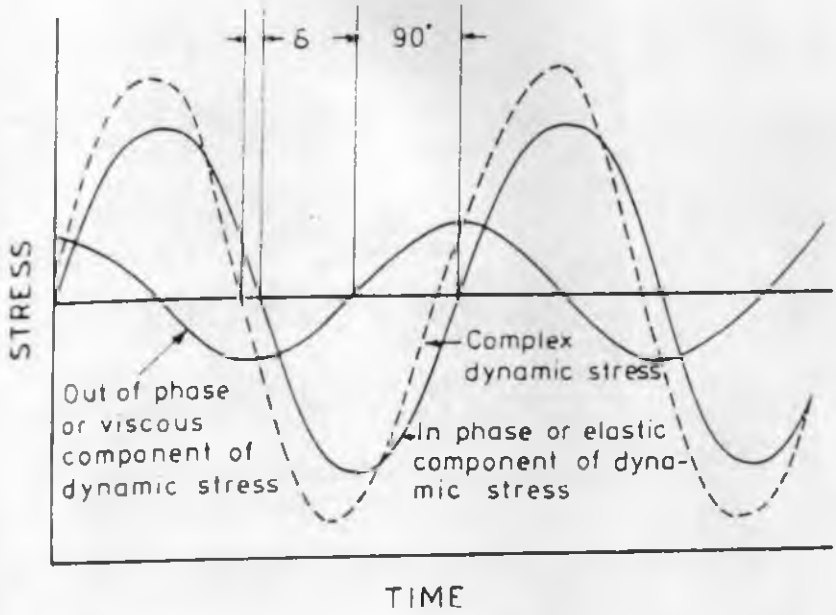

Fig.-2.1 STRESS DUE TO SINUSOIDAL DEFORMATION OF A SAMPLE SHOWING IN PHASE OR OUT-OF PHASE COMPONENTS OF DYNAMIC TENSILE STRESS.

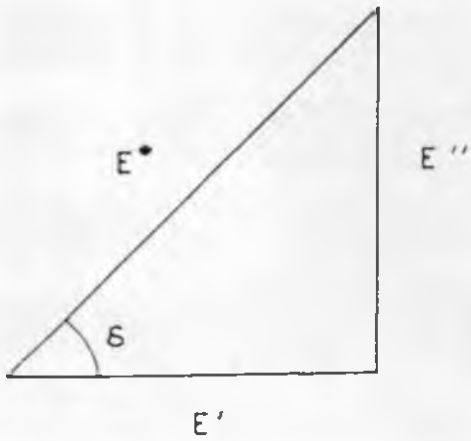

Fig.-2.2 VECTORIAL RESOLUTION OF MODULUS COMPONENTS IN SINUSOIDAL DEFORMATION.

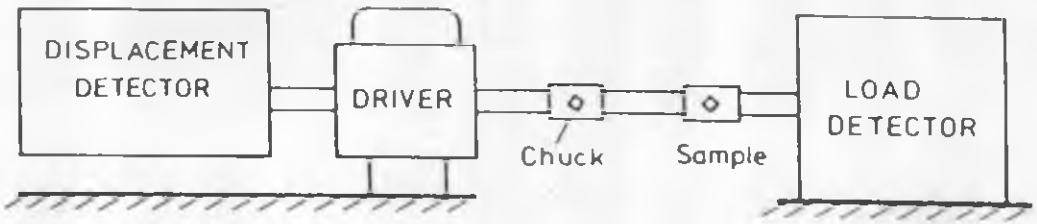

Fig-2.3 SCHEMATIC DIAGRAM OF RHEOVIBRON DDV III EP.

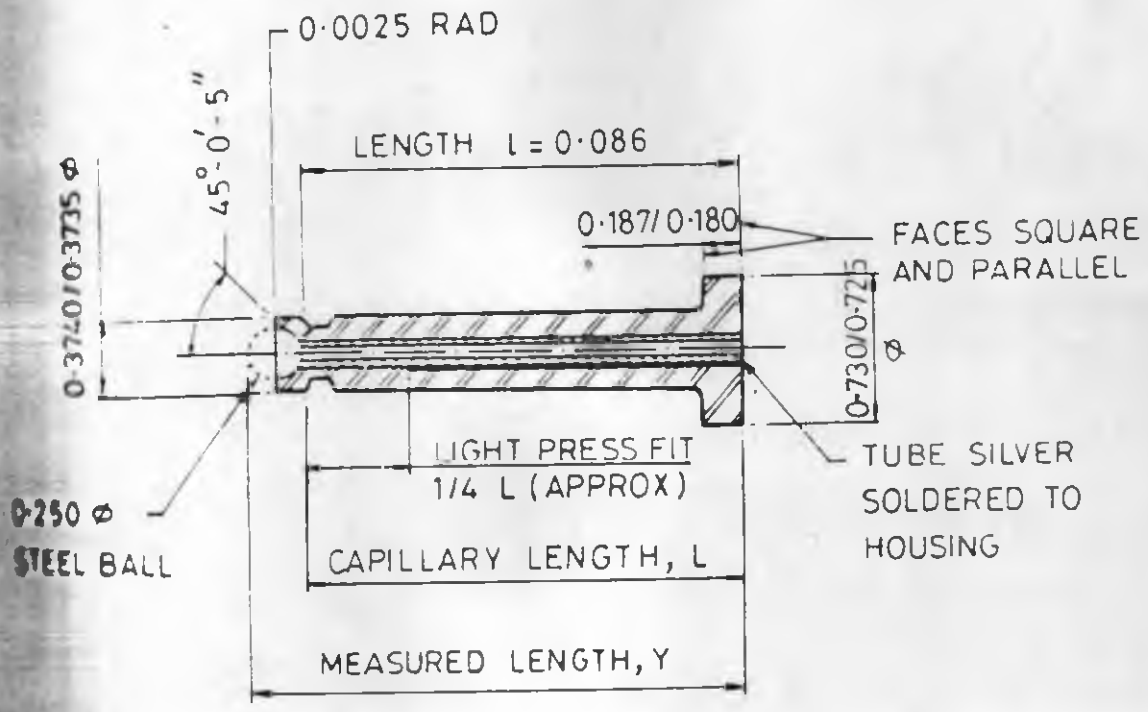

L = 2·0066 ± 0·0001 INCH
CAPILLARY DIA = 0·0495 ± 0·005 INCH

Fig. 2·4 Typical capillary details.

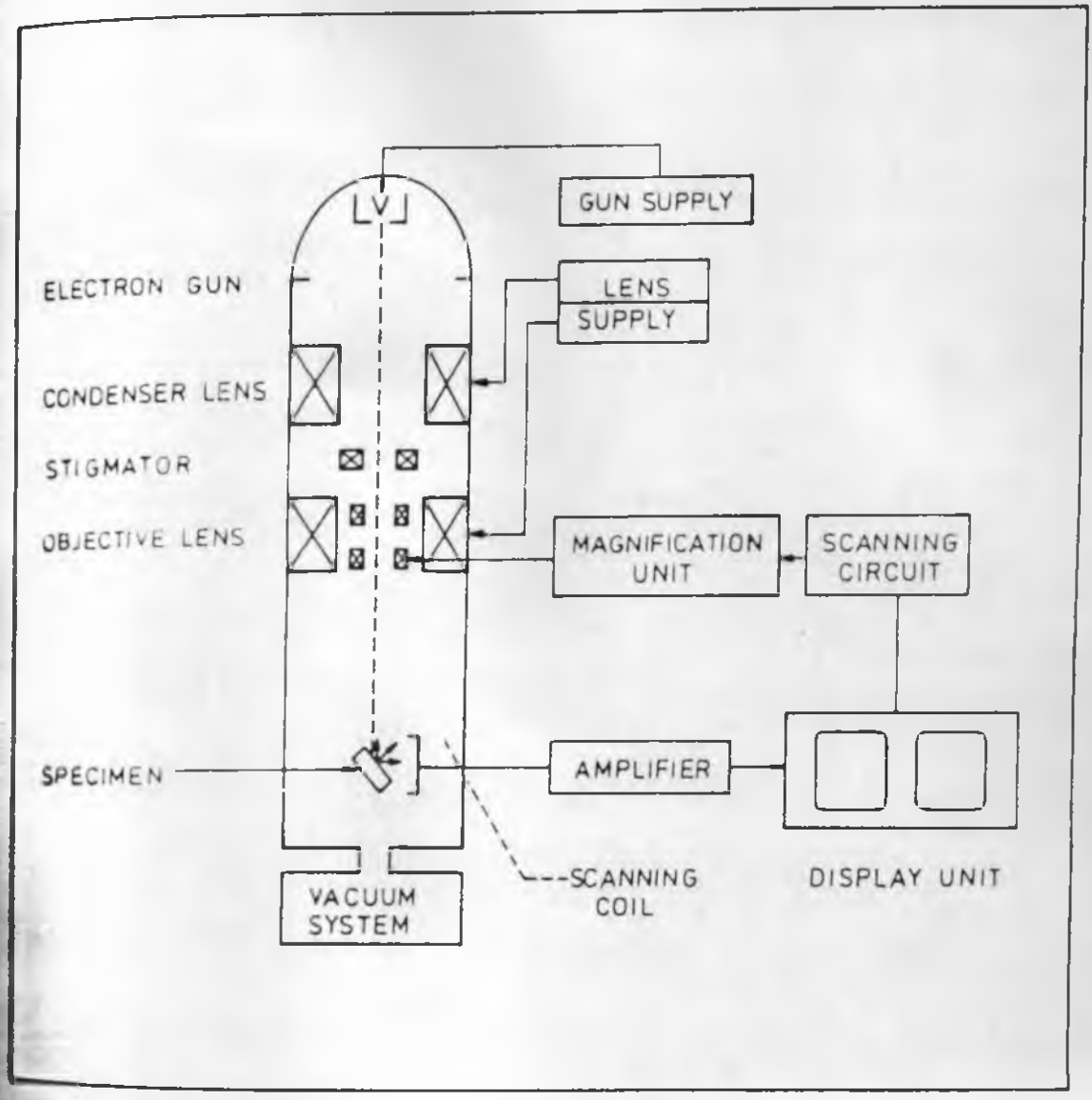

Fig.-2.5 SIMPLIFIED BLOCK DIAGRAM OF SEM.

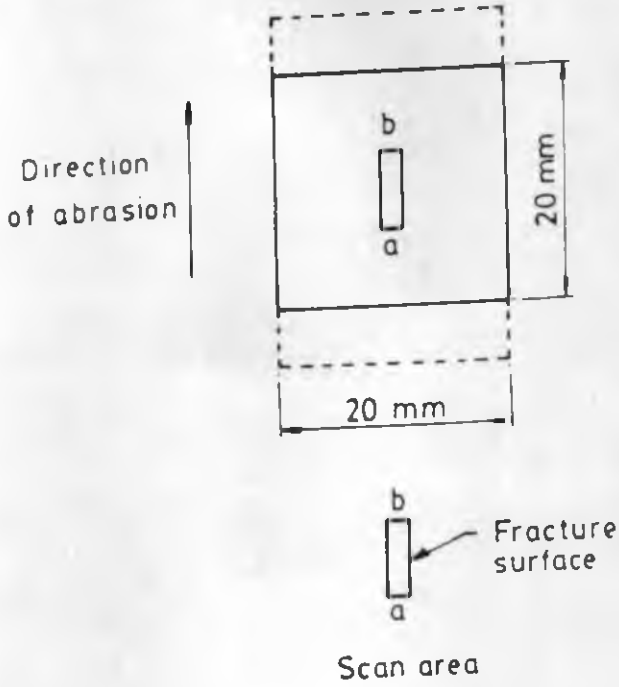

Fig 2.6 Abrasion sample showing direction of abrasion and scan area.

REFERENCES

1. C.I. MacKenzie and J. Scanlan, Polymer, 25 (1984) 559.
2. J.A. Brydson, "Flow properties of Polymer Melts", Second ed. Pub. George Godwin Ltd.; U.K. 1981, Chap.2.
3. R.I. Tanner, A theory of die swell, J. Polym. Sci., 14 A 2.8 (1970) 2067.
4. C.D. Han, Rheology in Polymer Processing, Academic Press, New York, 1976, p. 115.
5. S. Roy and P.P. De, Polymer Testing (in press).
6. J.T. Black, in "Principles and Techniques of Scanning Electron Microscopy",Ed.; M.A. Hayat, Van Nostrand Reinhold Company, New York, 1974, Vol. 1, Chap. 1.
7. B. Ellis and G.N. Welding, Rubber Chem. Technol., 37 (1964) 571.
8. Harry Burrell, `Solubility Parameters for film formers' presented to the American Chemical Society meeting in Cincinnati, Ohio, April, 1955; Official Digest, October, 1955.

CHAPTER 3

SELF-VULCANISABLE RUBBER BLENDS BASED ON EPOXIDISED NATURAL RUBBER (ENR) AND CARBOXYLATED NITRILE RUBBER (XNBR)

CHAPTER 3 - PART I

CHARACTERISATION

• This part of the work has been published in Kautschuk Gummi Kunststoffe 43 (11) (1991) 1002

Epoxidised natural rubber (ENR) prepared by the partial epoxidation of natural rubber latex[1] is gaining wide commercialisation due to the versatality of properties like oil resistance, low gas permeability and high tensile strength. ENR is generally vulcanised by conventional sulfur-accelerator systems[2]. The possibility of vulcanising ENR by other materials like dicarboxylic acids has been reported[3]. Since epoxy groups are highly reactive, crosslinking can be achieved through epoxy groups of ENR. Thus functionally active rubbers which can interact with epoxy groups can be vulcanised with ENR without the use of vulcanising agents. Carboxylated nitrile rubber (XNBR) is a modified form of nitrile rubber where carboxyl groups are introduced into the polymer by addition of unsaturated acids to acrylonitrile and butadiene during polymerisation[4]. XNBR is generally vulcanised by sulphur and metal oxides but can also be vulcanised by epoxy resins[5]. Since chemical interaction can take place between epoxy groups and carboxyl groups, it is possible that ENR and XNBR vulcanise without the aid of other curing agents. Such rubber blends, which are crosslinked by chemical reaction of the reactive groups of the individual rubbers in the absence of external vulcanising agents, are designated as self-vulcanisable rubber blends. Recently development of such self-vulcanisation has been reported from this laboratory and the examples include ENR-chlorosulphonated polyethylene (hypalon)[6], hypalon-XNBR[7] and polychloroprene-XNBR[8] blends.

This chapter deals with the studies on the self-vulcanisable rubber blends based on epoxidised natural rubber and carboxylated nitrile rubber. The first section gives the characterisation of self-vulcanisable blends by Monsanto rheometry, differential scanning calorimetry, thermogravimetry, infrared spectroscopy and swelling.

The formulations of the blends are shown in Table 3.1.1.The cure characteristics of the blends are shown in Table 3.1.2. In all the three blends of ENR and XNBR, increase in XNBR content in the blend increased the minimum Mooney viscosity and decreased the scorch time. Since oxirane rings are opened readily in presence of acids[9,10] the reactions involving carboxyl groups are likely to start earlier and accordingly such mixes become very scorchy[11]. Due to the early onset of reaction, with increase in XNBR content in the blends, the scorch times decreased.

3.1 Characteriaation of the Blend

3.1.A Monsanto Rheometry

The Monsanto rheographs of the blend are shown in Fig. 3.1.1. The blends showed marching increase in rheometric torque both at 150°C and 180°C. Blend Exa (ENR/XNBR in the ratio 75/25) showed comparatively low crosslinking at both temperatures. As the XNBR content in the blend increased (as in Exb), crosslinking was greatly decreased,and with further increase in XNBR (as in Exc) there was no more increase in crosslinking and at 180°C the

This chapter deals with the studies on the self-vulcanisable rubber blends based on epoxidised natural rubber and carboxylated nitrile rubber. The first section gives the characterisation of self-vulcanisable blends by Monsanto rheometry, differential scanning calorimetry, thermogravimetry, infrared spectroscopy and swelling.

The formulations of the blends are shown in Table 3.1.1.The cure characteristics of the blends are shown in Table 3.1.2. In all the three blends of ENR and XNBR, increase in XNBR content in the blend increased the minimum Mooney viscosity and decreased the scorch time. Since oxirane rings are opened readily in presence of acids[9,10] the reactions involving carboxyl groups are likely to start earlier and accordingly such mixes become very scorchy[11]. Due to the early onset of reaction, with increase in XNBR content in the blends, the scorch times decreased.

3.1 Characterisation of the Blend

3.1.A Monsanto Rheometry

The Monsanto rheographs of the blend are shown in Fig. 3.1.1. The blends showed marching increase in rheometric torque both at 150°C and 180°C. Blend Exa (ENR/XNBR in the ratio 75/25) showed comparatively low crosslinking at both temperatures. As the XNBR content in the blend increased (as in Exb), crosslinking was greatly increased,and with further increase in XNBR (as in Exc) there was no more increase in crosslinking and at 180°C the

rheometric torque for Exc was less than that for Exb.

In Exa, the concentration of carboxyl groups might not be sufficient to cause enough crosslinking and as XNBR content increased the availability of carboxyl groups increased resulting in higher extent of crosslinking as in Exb. In Exc, however, the concentration of epoxide groups available for crosslinking was less. Epoxidation is a random process[1,12] and Davey et al.[9] have shown that when a reaction between an acid and epoxy group is initiated at one epoxide group of a block, the remaining epoxide groups undergo furanisation and are destroyed before other reactions can occur. In Exc, even though there may be sufficient epoxide groups, the number of epoxide groups available for reaction was likely to be less due to furanisation or follow-up reactions. Due to the nonavailability of epoxide groups, crosslinking in Exc reached a state of completion.

3.1.B Differential Scanning Calorimetry (DSC)

Figure 3.1.2 illustrates the DSC profiles for cure of blends of ENR and XNBR and also control ENR and XNBR. It was evident that there was no change in enthalpy in the temperature range from 170°C to 300°C for the two neat polymers, while the blends registered an exothermic enthalpy[13] due to self-vulcanisation. TGA plots (Figure 3.1.3) indicated that the thermal degradation of neat polymers and the blend occurred at sufficiently high temperatures, above 300°C, resulting in main chain scission

and loss of volatile fragments.

In Exa, where the state of cure was low, cure initiation started at a higher temperature. As the XNBR content in the blend increased the cure initiation started at lower temperatures(Table 3.1.3). This was in agreement with Mooney scorch times of the blend. The plot of Mooney scorch times versus cure initiation temperature obtained from DSC studies as shown in Fig. 3.1.4 revealed that as the ENR content in the blend increased both cure initiation temperature and scorch time increased. The vulcanisation reaction as observed from the exotherms, showed completion only when XNBR content in ENR/XNBR blend was high as in Exc. At a lower XNBR content, as in Exa and Exb, the crosslinking proceeded till degradation and crosslinking reaction was overlapped by degradation reaction. At sufficiently high temperature above 300°C thermal degradation occurred for all the polymers resulting in main chain scission and loss of volatile fragments as determined by thermogravimetric analysis and shown in Fig. 3.1.3.

3.1.C Infrared Spectrophotometry (IR)

The IR spectra of XNBR and ENR are shown in Fig. 3.1.5 and their characteristic absorption peaks are shown in Table 3.1.4. Pure XNBR showed absorption at 1734 cm^{-1} and 1700 cm^{-1} due to free and hydrogen bonded acid groups, respectively. Pure ENR showed absorption at 870 cm^{-1} and 1245 cm^{-1} due to epoxy group and at 885 cm^{-1} for cis double bond. ENR also

showed carboxyl absorption due to traces of acids. In addition there was absorption at 1114 cm^{-1} due to aliphatic ethers and at 1065 cm^{-1} due to tetrahydrofuran. It is known that epoxidation reaction is very difficult to be controlled and that epoxide rings open up in the presence of acids and undergo furanisation[14,15]. Other cyclic ethers and ether linkages between two adjacent molecules may also form. The difference spectrum (ENR/XNBR blend minus ENR minus XNBR) is shown in Fig. 3.1.5 and the characteristic absorption peaks are summarised in Table 3.1.4. Esters showed absorption in the range of 1725 cm^{-1} to 1750 cm^{-1} due to C=O stretching of the ester groups. In the case of intramolecularly hydrogen bonded esters, it has been observed that[16] the absorption is lowered by about 40 cm^{-1}. In the case of unsaturated esters the absorption is around 1660 cm^{-1}. The absorption at 1698 cm^{-1} in difference spectrum could be due to H-bonded ester formed during vulcanisation and absorption at 1660 cm^{-1} could be due to intramolecularly hydrogen bonded unsaturated esters. Absence of absorption at 870 cm^{-1} in the blend showed that after reaction no epoxide groups remained. The absorption at 1134 cm^{-1} could be due to formation of ether linkages. Hence during curing at 150°C, the binary blend of ENR and XNBR formed ester crosslinks along with ether crosslinks. The crosslinking reaction between ENR and XNBR is shown in Fig. 3.1.6.

3.1.D Solvent Swelling

Both ENR and XNBR were found to be soluble in chloroform while the moulded blends were insoluble in the same solvent , showing that during moulding ENR and XNBR get crosslinked. The volume fraction of rubber in the swollen vulcanisate calculated from equilibrium swelling data (Table 3.1.5) revealed that in Exa degree of crosslinking was less than that in Exb and Exc.

3.1.E Physical Properties

The physical properties of blends ENR and XNBR are summarised in Table 3.1.5. As the XNBR content increased, tensile strength, modulus, tear strength and abrasion resistance increased whereas elongation at break decreased. This is also evident from the stress-strain plots (Fig.3.1.7). The properties of ENR-XNBR blend are comparable to rubber crosslinked by conventional vulcanisation systems.

Table 3.1.1 Formulation of the mixes[a]

	Exa	Exb	Exc
NBR	75	50	25
XNBR (Krynac 221)[b]	25	50	75

[a] figures are in parts by weight

[b] carboxylated monomer level, 7 mole %.

Table 3.1.2 Cure characteristics of the blends obtained from Mooney viscometer and Monsanto rheometer studies.

	Exa	Exb	Exc
Mooney viscometry			
Minimum Mooney viscosity at 120°C	23	35	45
Mooney scorch time at 120°C, min.	14.5	7.0	5.7
Monsanto rheometry			
Minimum torque at 150°C, dN.m	5	6	8
Maximum torque at 150°C, dN.m (in 60 min.)	13	36	36
Minimum torque at 180°C dN.m	4	5	6
Maximum torque at 180°C, dN.m (in 60 min.)	25	61	46

Table 3.1.3 Cure characteristics of the blends obtained from thermal analysis

Sample	Cure initiation temperature, °C	Cure termination temperature, °C	Degradation temperature, °C[a]
[illegible]	213	b	300
[illegible]	186	b	300
[illegible]	171	300	300

a obtained from thermogravimetric analysis
b cure termination overlapped by degradation of polymer.

Table 3.1.4 : IR Peak Assignments

Wave No. cm^{-1}	Functional group	Assignment of bond	ENR	XNBR	Difference Spectrum (Blend-ENR-XNBR)	Reference
1760	Carboxyl	C=O str. (monomer)	-	1760	-	16
1740	Ester (acetate)	C=O str.	-	-	1736	16,17
1710-1730	Carboxyl	C=O str.	1728	1700	-	16
1690-1725	Ester Intra-molecularly (H-bonded)	C=O str.	-	-	1699	16
1245	Epoxy group	C-O str.	1245	-	-	16
Around 1660	unsaturated esters	C=O str.	-	-	1660	16
Around 1114 (1060-1150)	aliphatic ether	assym. C-O str.	1114	-	1134	16
1065-1070	Tetrahydro-furan	ring str.	1065	-	-	18
885	cis double bond	C=C str.	885	-	885	16
785-875	cis epoxides	ring vibrn.	873	-	-	16

Table 3.1.5 Physical properties of blends, moulded for 60 min at 150°C

	Exa	Exb	Exc
Modulus 300%, MPa	1.9	3.2	-
Tensile strength, MPa	2.2	3.2	3.6
Elongation at break,%	380	300	220
Tear strength, kN/m	11.0	12.6	16.8
Hardness, shore A	30	47	50
Resilience at 40°C,%	55	69	58
Compression set for 22h. at 70°C, %	27	12	12
Abrasion loss, cc/hr	a	4.5	1.8
Heat build-up by Goodrich flexometer with a load of 24lb and stroke of 4.5 mm T, °C	b	17	30[c]
$\tan\delta$	0.07	0.12	0.12

a sample could not be abraded
b sample blown out before 20 min.
c value after 20 min.

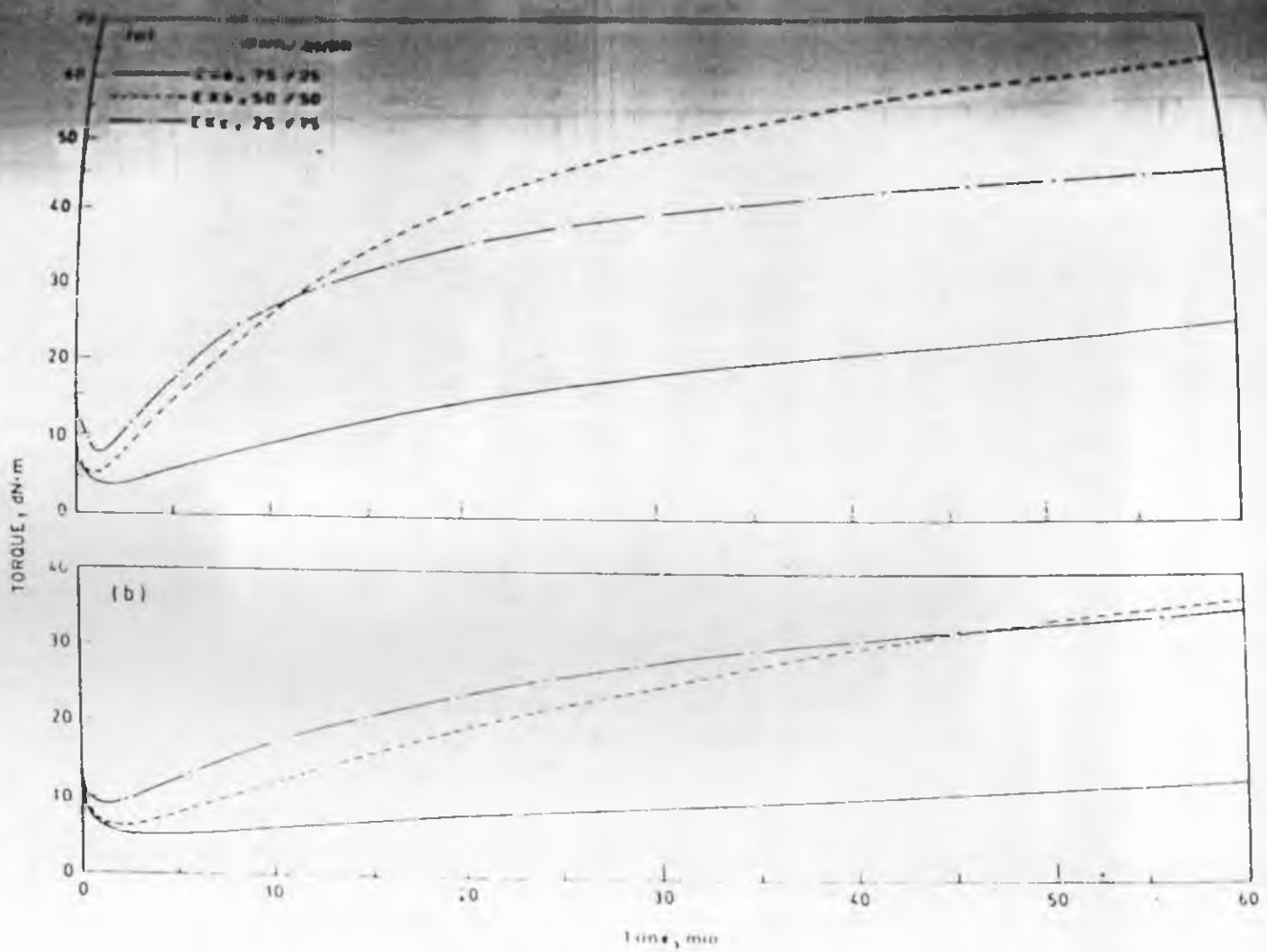

Figure 3.1.1: Rheographs of blends of ENR and XNBR
(a) 180°C (b) 150°C.

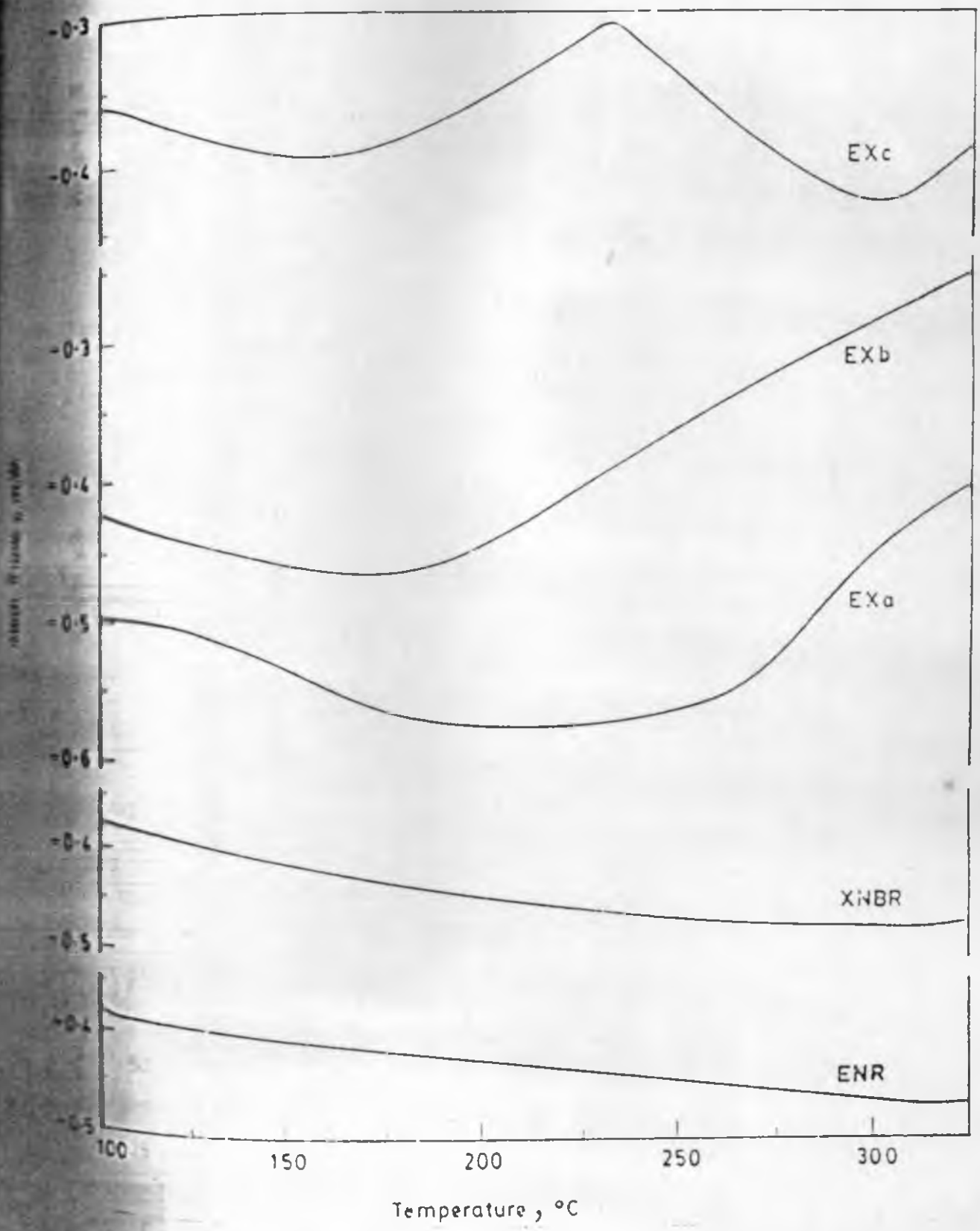

Fig. 3.1.2 : DSC scan for blends of ENR and XNBR and of neat ENR and XNBR.

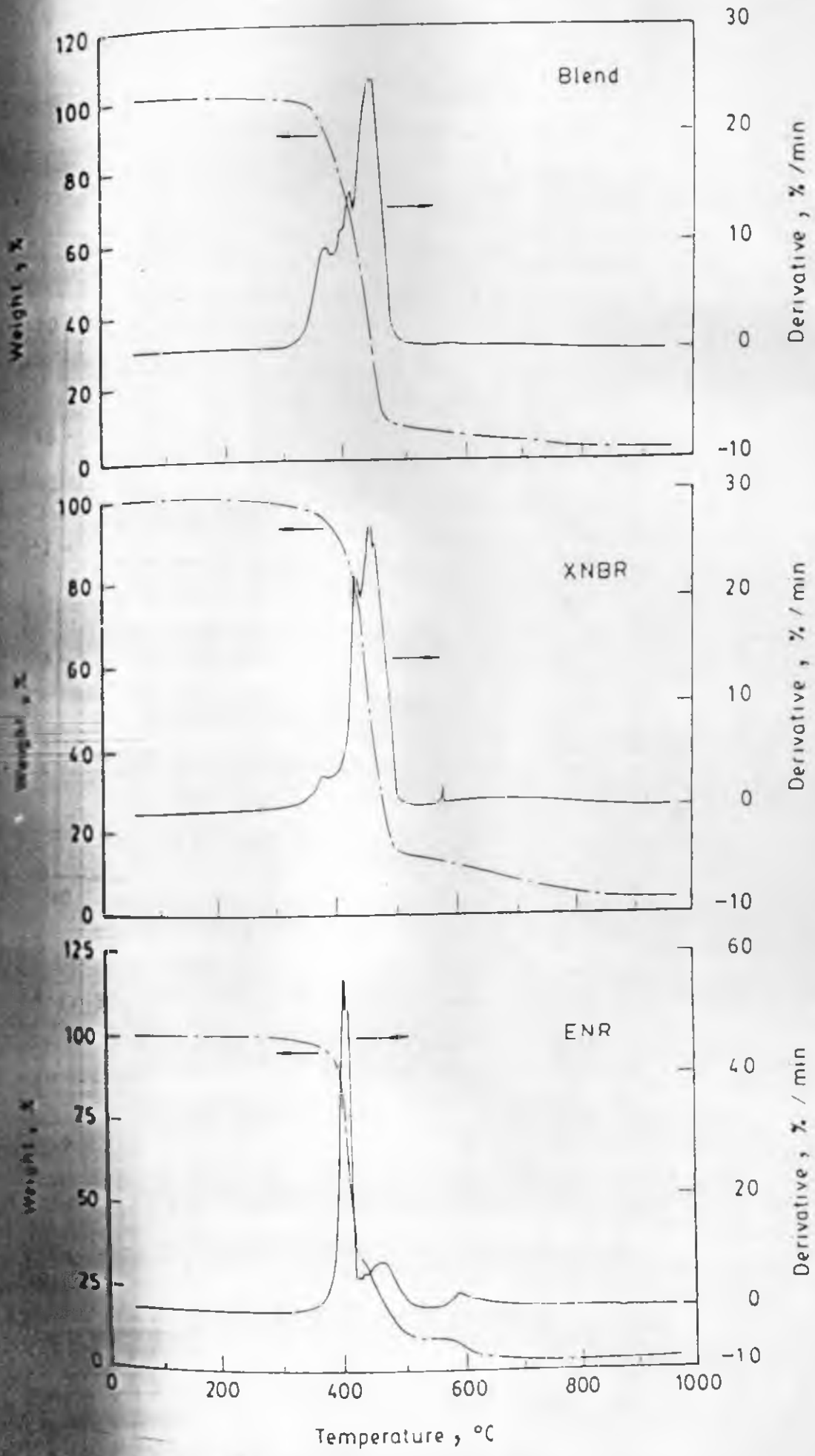

Fig. 3.1.3 : TGA curves of neat ENR, XNBR and 1:1 ENR-XNBR blend.

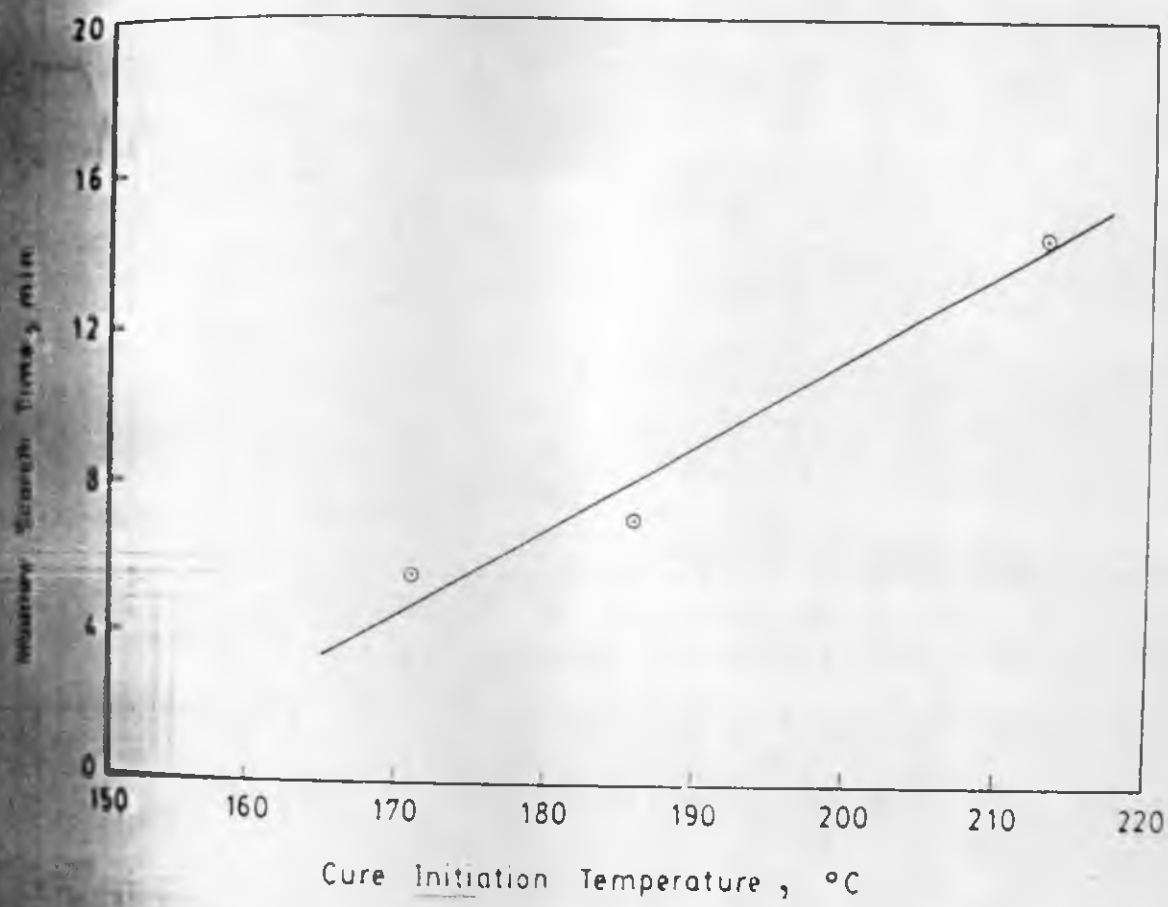

Fig. 3.1.4 : Plot of Mooney scorch time versus cure initiation tempeature (DSC thermogram).

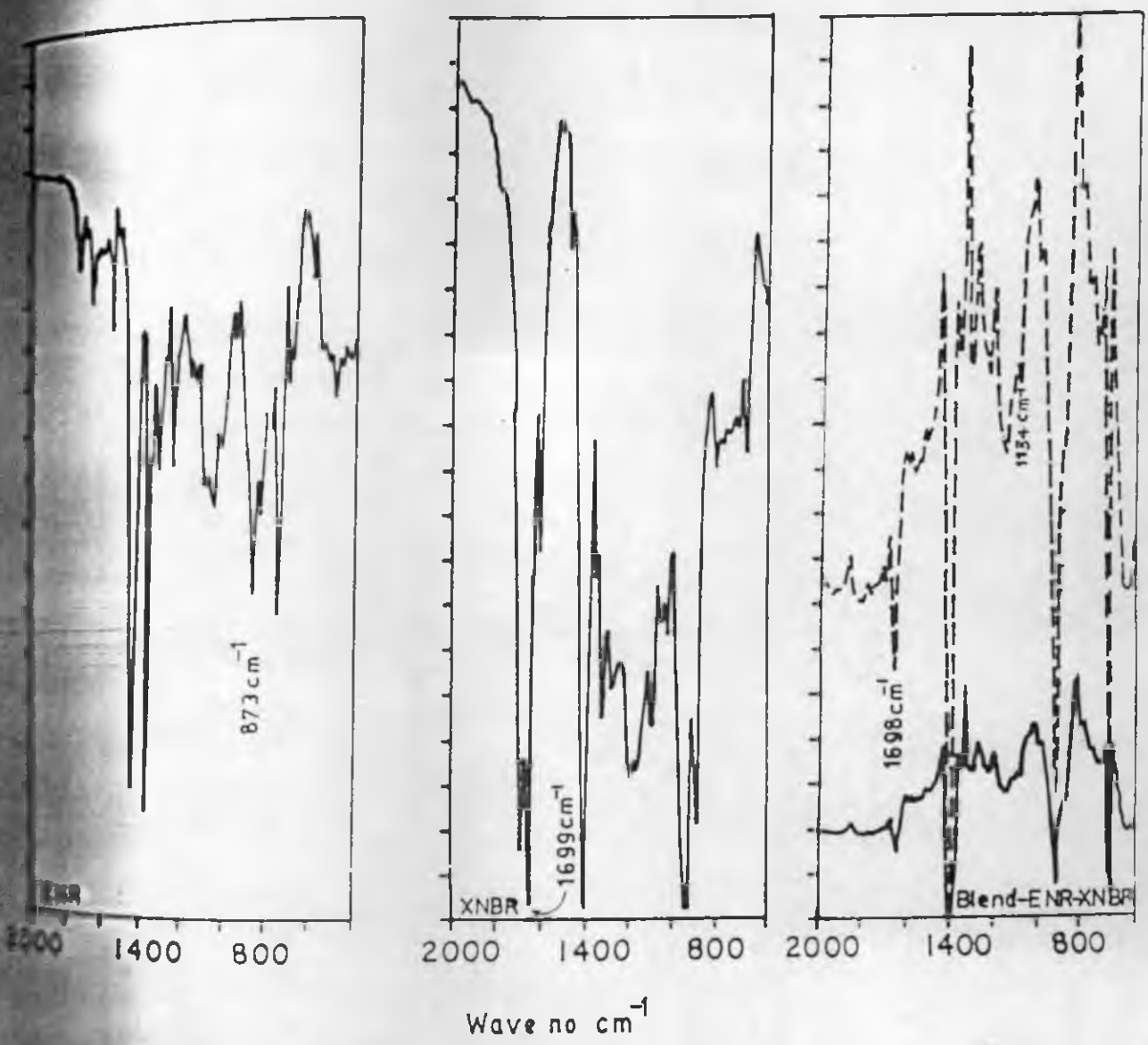

Fig. 3.1.5: IR spectra of their films of ENR, XNBR and the difference spectrum, blend-ENR-XNBR.

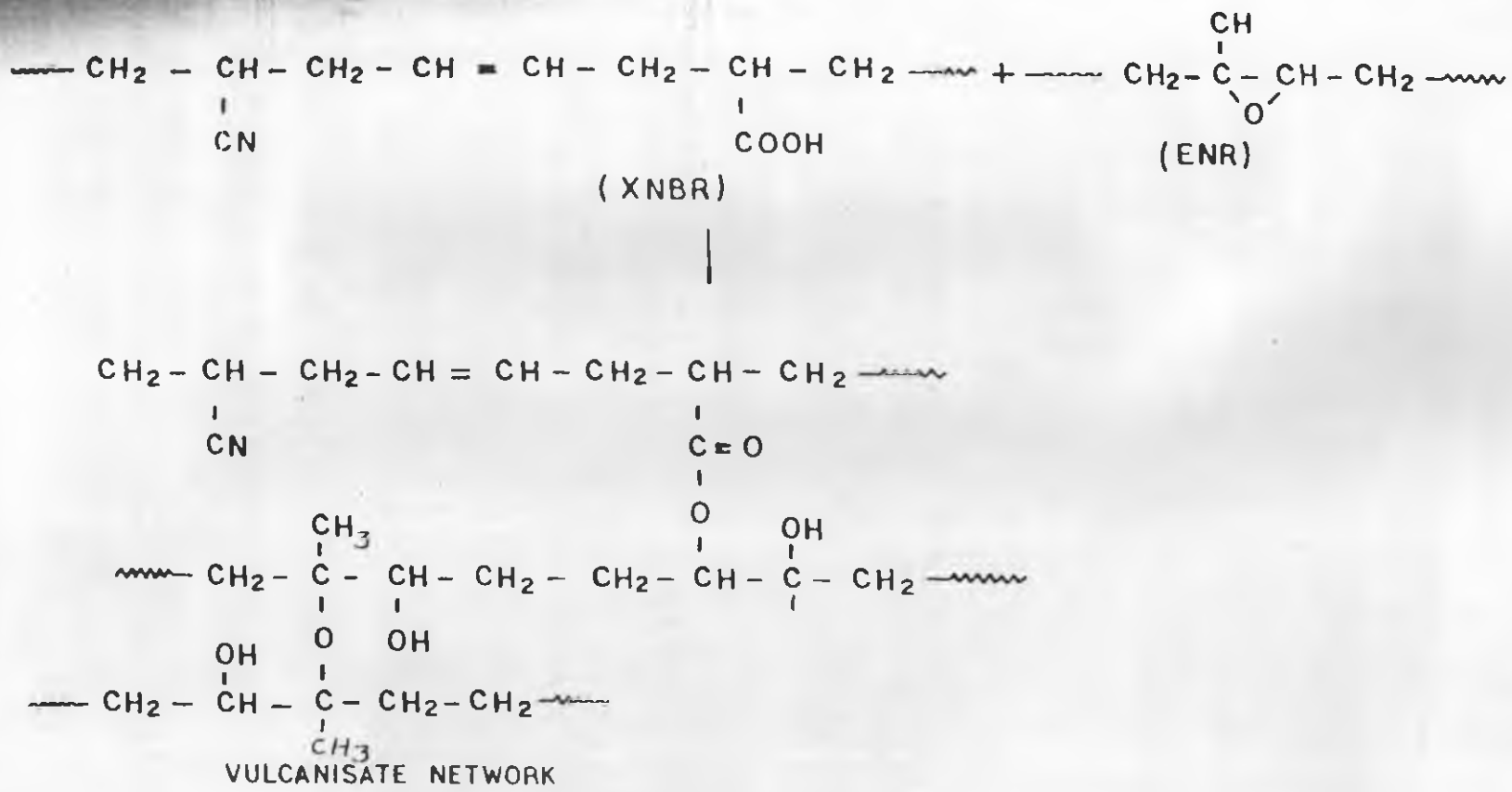

Fig. 3.1.6: The possible mechanism of crosslinking between ENR and XNBR.

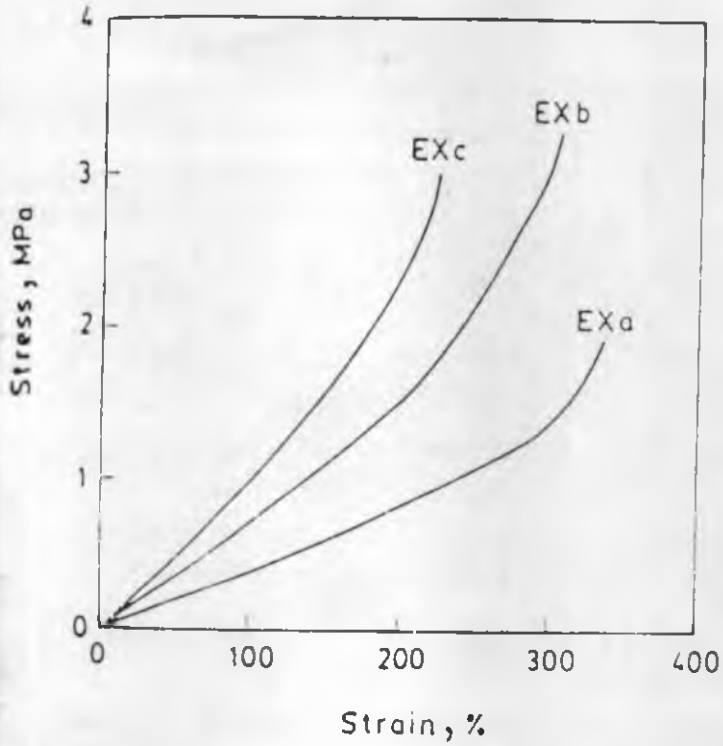

Fig. 3.1.7 : Tensile stress strain curves of blends of ENR and XNBR, moulded for 60 min. at 150°C.

CHAPTER 3 - PART II

PROCESSING CHARACTERISTICS

& PHYSICAL PROPERTIES

• This part of the work has been published in Plast. Rubb. Proc. Appl. 14 (4) (1990) 223

The properties of rubber vulcanisates are known to depend on the crosslink density and the type and amount of fillers used. Crosslink density can be controlled by varying the temperature and time of moulding.

This section reports the results of studies on the moulding conditions, and incorporation of three different kinds of fillers (ISAF black, SRF black and silica filler) on the cure characteristics and technical properties of the self-vulcanisable ENR-XNBR blend, the failure envelope studies and stress relaxation behaviour.

3.2 Processing Characteristics

3.2.A Cure Characteristics

Mix formulations are given in Tables 3.2.1(a), 3.2.1(b) and 3.2.2. Minimum Mooney viscosities and Mooney scorch times of the gum and filled blends are given in Tables 3.2.3(a) and 3.2.3(b). It is evident that an increase of filler loading increased the minimum viscosity and decreased the scorch time. Also, the increase in Mooney viscosity and decrease in scorch time were most prominent in the case of silica filled mixes and least prominent in the case of SRF black-filled mixes, while the ISAF black-filled mixes occupied an intermediate position. For example, at 40 phr loading, Mooney viscosity at 120°C increased from 35 for the unfilled blend to 49 for SRF black, to 63 for ISAF black and to 100 for silica-filled blend. The higher Mooney viscosity

of silica-filled mix was probably due to strong interaction of silica with rubber during mixing. It is well known that ISAF black is more reinforcing than SRF black and hence the higher viscosity is found in the case of ISAF black-filled mix[19]. Samples of neat ENR and neat XNBR were masticated for 8 min., which was also the blending time for the two rubbers, and the Mooney viscosity values, ML (1+4) at 120°C were determined. The values were as follows : ENR 10, XNBR 30 and blend 35. It was evident that reaction between ENR and XNBR took place to limited extent even at 120°C, during Mooney viscosity determination. The minimum Mooney viscosity and scorch time for the control mixes of ENR and XNBR are shown in Table 3.2.4. The mixes of XNBR were very scorchy compared to ENR mixes. It has been reported earlier that mixes of NBR containing ZnO have low scorch time and high Mooney viscosity, where metal carboxylate crosslinks are formed[11]. In such mixes the low scorch time was due to the early onset of reaction of carboxyl group with metal oxide. The epoxy group of ENR permitted effective crosslinking with chemicals like dibasic acids and polyamines[20,21]. Hence the low scorch time of the blend of ENR and XNBR was due to the early onset of reaction of carboxyl group of XNBR with the epoxy group of ENR.

Rheographs of the gum blend (formulation Exb) at different temperatures 150°, 160°, 170° and 180°C are shown in Fig. 3.2.1. For comparison rheographs of one control XNBR mix and one control ENR mix were chosen (Table 3.2.2). It

was evident that rheometric torque of the blend progressively increased with moulding time and with moulding temperature. This showed that in the blend both XNBR and ENR crosslinked each other during moulding and that both prolonged time and enhanced temperature caused progressive increase in crosslinking. At 150°C the self-vulcanisable blend registered marching rheometic torque like control XNBR compounds, while the ENR compounds showed reversion. However, crosslinking of ENR with dibasic acids have been reported to show marching increase in modulus with cure time . The XNBR system at 150°C showed much higher rheometric torque than that of the blend. Fig. 3.2.2 shows the rheographs of the filled systems at 150°C. It was evident that addition of filler increased the rheometric torque as in the case of conventional rubber systems. The nature of the rheographs with repect to moulding time and temperature was similar to that of gum blend. Increase of filler loading increased the rheometric torque.

In blend the chemistry of vulcanisation and nature of crosslinks was different from conventionally cured ENR or XNBR. In conventionally cured ENR, crosslinking was by sulphur linkages[2], and in XNBR crosslinking was by sulphur linkages and metal carboxyl linkages[11]. In blends of ENR and XNBR the crosslinking reaction occurred between epoxy and carboxyl groups to form ester linkages. Due to this difference in the mechanism of vulcanisation in blends, the rheographs of blends showed absence of cure reversion, and thermal stability of the crosslinked structure.

Fig. 3.2.3 showed the effect of ISAF black loading at 150°C. The cure characteristics of these mixes at temperatures 150°C and 180°C are shown in Table 3.2.3(b). Enhancement of torque followed the order, silica $\geq$ ISAF > SRF. As we shall see later, polymer-filler interaction also followed the same order.

Kinetics of cross linking reaction could be followed from the changes in rheometric maximum torque with time. For the first order reaction[22,23].

$$\ln (M_\alpha - M) = - kt + \ln (M_\alpha - M_o).$$

where, M is the torque at time t, Mo is the torque at zero time and M_α is the maximum torque. For marching modulus cure curves, M_α was taken as the torque when rise in torque was less than one unit in five minutes; at this stage it was assumed that the reaction had almost come to an end. From the linear plot of ln $(M_\alpha - M)$ versus time the rate constant of the first order crosslinking reaction could be determined. The activation energy for the initial vulcanisation reaction was calculated by using an Arrhenius equation. Figures 3.2.4 and 3.2.5 showed typical plots for calculation of rate constants and activation energies. Table 3.2.5 summarises the rate constants of blend and control mixes at two temperatures and Table 3.2.6 gives the values of the activation energy for vulcanisation. The activation energy for self-vulcanisation of NR-XNBR system was found to lie between 65-70 kJ/mole. This was of the same order of magnitude as reported by other

workers for conventional rubbers[24].

3.3.3 Physical Properties

Tensile stress-strain behaviour of the gum blend moulded under different conditions is shown in Figure 3.2.6. Similar plots for ISAF black and silica filled compositions are shown in Figures 3.2.7 and 3.2.8. It was evident that both moulding time and temperature altered the stress-strain behaviour and the effect was prominent in filled systems. The effect of filler loading on stress strain behaviour is shown in Figures 3.2.9 - 3.2.11. Energy at rupture increased with increase in filler loading and the trend continued up to the highest filler loading studied. The variation of rupture energy with the filler loading is given in Figure 3.2.12.

Table 3.2.7 summarises the results of the effect of moulding time at 150°C on some physical properties like modulus, tensile strength, elongation at break and tear resistance. It is evident that increase in moulding time at a constant temperature caused lowering of both tensile strength and tear resistance. However, modulus increased and elongation at break decreased. Table 3.2.8 showed the results of variation of moulding temperature at a constant moulding time on physical properties . It was observed that increase of moulding temperature from 150°C to 180°C caused increase in hardness and resilience and decrease in abrasion loss, compression set, heat build-up and dynamic set. From the evidence of Vr values (Table 3.2.8) these changes were

ascribed to the formation of additional crosslinks at elevated temperatures.

Effects of filler loading on the physical properties are summarised in Tables 3.2.9 - 3.2.11. Expectedly, the following properties showed gradual increase with increase in filler loading : modulus, tensile strength, tear strength, abrasion resistance, hardness, heat build-up and dynamic set. Resilience decreased gradually and compression set increased with filler loading.

In order to understand abrasion mechanism we had analysed SEM photographs of the abraded surfaces. In abrasion, mechanical, chemical and thermal processes are involved[25]. Reznikoiskii and Brodskii have described different types of wear in elastomers[26]. High abrasion resistance was observed in vulcanisates with high hardness, modulus, tensile strength, tear strength, resistance to thermo-oxidative degradation and crack growth resistance under dynamic conditions[27]. Such elastomeric vulcanisates showed ridge formation during abrasion[28,29]. Figure 3.2.13 and 3.2.14 show the failure surfaces of E and EIS 20 (formulation in Table 3.2.2). In ENR the abrasion resistance was very poor and the material seemed to be chipped by the abrasive. This was due to low matrix strength as seen from tensile properties and hardness. The cut growth resistance was also poor as rubber was removed in lumps by the abrasive. When filler was added the abrasion resistance was improved

due to high matrix strength. There was ridge formation in XNBR vulcanisates and blends as seen from figures (3.2.15 - 3.2.19). Gum XNBR and ISAF black-filled XNBR showed high abrasion resistance and followed frictional type wear (Fig. 3.2.15 and Fig. 3.2.16).

The gum blend showed abrasive type of wear (Fig. 3.2.17). Here the abrasion resistance was better than pure XNBR due to higher matrix strength. At low loading of ISAF black (20 phr) also, the blend showed the abrasive type of wear, and at higher loading of ISAF black (40 phr) the mechanism of wear changed from abrasive to frictional type (Figure 3.2.18 and Figure 3.2.19). In EXbIS 40 (Fig. 3.2.19) the ridge height was considerably reduced and the spacing between the ridges became less. It is known that reduction of ridge height and closer spacing of ridges are manifestations of high abrasion resistance[30].

It is noted from the above discussion that the self-vulcanised rubber blend system is similar to conventional rubber vulcanisates as regards the influence of filler. However, silica reinforcement in such blend occurred even in absence of coupling agent and the extent of silica reinforcement was similar to the reinforcement by ISAF black. The degree of reinforcement followed the order, SRF < ISAF = silica. Reinforcement could be related with the polymer-filler interaction. An indication of the polymer-filler interaction could be obtained from the Kraus plot[31]. It has been shown elsewhere that both ENR and XNBR vulcanisates are

reinforced by silica in the absence of coupling agent[32,33].

The plot of Vro/Vrf against Ø / (1-Ø) is shown in Figure 3.2.20. The slope of the plot was maximum in silica-filled blend and minimum in SRF black-filled blend. The slope of the ISAF black-filled blend was close to the silica-filled blend. Accordingly, we observed that polymer-filler interaction increased in the order SRF < ISAF ≤ silica. It had been noted earlier in this section that reinforcement in physical properties also followed the same order. The plot of relative modulus versus volume fraction of filler is shown in Fig. 3.2.21. The increase in relative modulus with filler loading also followed the same trend. Accordingly, it was concluded that filler reinforcement of the self vulcanised rubber-rubber blend system was similiar to the filler reinforcement of conventional rubber vulcanisates.

For comparison, studies of two control systems based on XNBR alone and ENR alone are included here. These mixes were cured in such a way as to have similar crosslink density as the corresponding blend mixes.

Table 3.2.12 shows properties of XNBR-ENR blend and the control vulcanisates, for both gum and filled systems. The blend showed higher resilience and lower compression set than the corresponding control ENR and XNBR vulcansates. Since the crosslink density of the blend was similar to the corresponding control rubbers, the difference in the properties could be ascribed to the type of vulcanisate

network structure.

Plot of tensile strength values obtained at different temperatures and rates against elongation at break on a logarithmic scale generates a mastercurve. Smith[34,35] termed this mastercurve as failure envelope. Failure envelopes generated by tear and tensile rupture measurements were done by Greensmith[36]. The failure envelopes of SBR rubber was analysed by Landel and Fedors[37]. Bhowmick et al. analysed the failure of carbon black filled NR and SBR vulcanisates[38,39]. This section deals with the failure envelope generated by the self-vulcanised ENR-XNBR blend.

3.1.C Failure Envelope

The tensile strength data of the 1:1 ENR-XNBR blend obtained at different temperatures and rates were modified by a reduction factor, 298/(298+T), where T was the working temperature in Kelvin. The plots of breaking stress against breaking elongation for the blend is given in Fig. 3.2.22. It was observed that the self-vulcanised blend yielded a failure envelope when tensile strength obtained at different temperatures and rates were plotted against elongation at break on a logarithmic scale.

The failure envelope generated by the blend was similar to that of conventional rubber vulcanisates[38,39]. At [illegible] temperatures and high shear rates, there was an [illegible] in strength with a reduction of elongation at break.

at higher temperatures the tensile strength decreased considerably. The co-efficient of friction of molecules was high at low temperature. Hence, greater energy was required at low temperature and higher shear rates to break the chains. At lower temperature the energy dissipation in the vulcanisates is higher and the tensile strength of elastomers is governed by the extent to which they dissipate the energy of deformation[40,41]. So at lower temperature the tensile strength was high, but at higher temperature both tensile strength and elongation at break was low.

Under constant strain stress of a rubber vulcanisate decreases with time. This is called stress relaxation. Stress relaxation in rubber vulcanisates has been widely studied[42-47]. It was shown by Gent[42] that both gum and carbon black filled natural rubber vulcanisates showed linear plots of stress against log(time).

In this section the result of stress relaxation studies on self-vulcanised ENR-XNBR blend is reported. For comparison, stress relaxation data of single ENR and XNBR vulcanisates are included as control.

3.2.A Stress Relaxation

Formulation of the mixes are shown in Tables 3.2.1(a), 3.2.1(b) and 3.2.2. Plots of (σ/σ_o) (σ_o is obtained from the maximum stress at t = 0, when the desired strain is reached, σ is the stress at subsequent times) versus log(t) are shown in Figs. 3.2.23 and 3.2.24. The stress relaxation

parameters[48] obtained are shown in Table 3.2.13.

The stress relaxation behaviour of all gum vulcanisates could be fitted in two straight lines as observed earlier for unfilled rubber vulcanisates[49-52]. The slope of the second line was less than the slope of the first line. This showed that there were two different relaxation mechanisms, operating, in the time range studied. The first relaxation could be due to small segments or domains of molecular chains[48] and the second due to rearrangement of molecular chains or aggregates[42]. It was observed that the time after which the slope changes was high for ENR and low for XNBR, while the blend had a value which was inbetween the two single rubbers. The slope (of the first process), which gives an idea of the rate of relaxation, was high for XNBR and low for ENR while the blend showed an intermediate behaviour. The comparatively high stress relaxation of XNBR could be due to the high hysteresis caused by ionic crosslinks in XNBR[4,11].

The slopes of all mixes increased with addition of filler showing that filler increased the stress relaxation behaviour. The intercept on time axis (Table 3.2.13) shifted to a higher time showing that the greater polymer-filler interaction affected the stress relaxation of molecular chains.

The stress relaxation behaviour of these vulcanisates showed that the self-vulcanised ENR-XNBR blend behaved like conventional rubber vulcanisates.

Table 3.2.1(a) : Formulation of XNBR-ENR Blend Mixes[a]

Mix No	EXb	Exb Si10	Exb Si20	Exb Si30	Exb Si40
XNBR-50	50	50	50	50	50
ENR (Krynac 221)	50	50	50	50	50
Silica[b]	-	10	20	30	40

[a] Formulation is in parts by weight

[b] Vulkasil S (precipitated silica), obtained from Bayer (India) Ltd.

[illegible] : Formulation of XNBR-ENR Blend Mixes[a]

[illegible]	Exb IS5	Exb IS10	Exb IS15	Exb IS20	Exb IS30	Exb IS40	Exb SR5	Exb SR10	Exb SR15	Exb SR20	Exb SR30	Exb SR40
[illegible]	50	50	50	50	50	50	50	50	50	50	50	50
[illegible] (221)	50	50	50	50	50	50	50	50	50	50	50	50
[illegible]	5	10	15	20	30	40	-	-	-	-	-	-
[illegible]	-	-	-	-	-	-	5	10	15	20	30	40

[a] Formulation is in parts by weight

Table 3.2.2 : Formulation of Control Mixes[a]

[illegible]	E	Ec	Es	X	Xc	Xs
[illegible] (krynac 221)	-	-	-	100	100	100
[illegible] - 50	100	100	100	-	-	-
[illegible] CO_3	0.25	0.25	0.25	-	-	-
[illegible]	5	5	5	5	5	5
[illegible]ric Acid	2	2	2	2	2	2
[illegible] black	-	20	-	-	20	-
[illegible]	-	-	20	-	-	20
[illegible]tic oil	-	2	2	-	-	-
[illegible]yl phthalate	-	-	-	-	2	2
[illegible][b]	1.6	-	-	-	-	-
[illegible][c]	2.4	1	1	1	1	1
[illegible]	0.3	2.8	2.8	2.4	2.4	2.4

a. Formulation is in parts by weight
b. Tetramethylthiuram disulphide
c. N-oxydiethylenebenzothiazole - 2 - sulphenamide

Table 3.2.3(a) : Cure Characteristics of Different Blends

[illegible]	EXb	Exb Si10	Exb Si20	Exb Si30	Exb Si40
[illegible] Mooney viscosity at 120°C	35	43	59	66	100
[illegible] scorch time at [illegible]°C,min.	7.0	6.1	5.0	4.3	3.0
[illegible] Rheometry					
[illegible] torque at [illegible]°C,dN.m	6	9	10	17	25
[illegible] torque at [illegible]°C(in 60 min.) dN.m	37	53	58	76	96
[illegible] torque at [illegible]°C,dN.m	6	8	9	12	20
[illegible] torque at [illegible]°C(in 60 min.)dN.m	62	74	91	100	118

[illegible] Cure Characteristics of Different Blends

[illegible]	Exb IS5	Exb IS10	Exb IS15	Exb IS20	Exb IS30	Exb IS40	Exb SR5	Exb SR10	Exb SR15	Exb SR20	Exb SR30	Exb SR40
[illegible] at [illegible]°C	35	39	43	43	58	63	36	39	39	39	41	49
[illegible] Time at [illegible]	6.8	6.7	6.0	5.0	4.8	4.5	6.7	5.8	5.7	5.3	5.2	5.1
[illegible] Rheometry												
[illegible] at [illegible]	8	8	9	10	13	13	9	9	10	10	10	11
[illegible] at [illegible]	44	48	54	62	76	86	48	50	52	57	60	69
[illegible] at [illegible]	8	8	8	8	10	10	7	7	8	8	8	8
[illegible] at [illegible]	75	87	92	92	113	130	69	75	84	88	106	109

Table 3.1.8 : Cure Characteristics of Control Mixes.

	E	Ec[a]	Es[b]	X	Xc[a]	Xs[b]
Mooney viscosity at 120°C	5	9	6	40	50	53
Mooney scorch time at 120°C, min	10.0	6.5	20.0	3.8	2.0	2.5
Monsanto rheometry						
Minimum torque at 160°C, dN.m	2	3	2	11	12	12
Maximum torque at 160°C, dN.m	33.0	80.0	63.0	87.0	115.0	118.0

a 40 phr ISAF black-filled

b 40 phr Silica-filled

Table 3.2.5 : Rate constant (k) of vulcanisation of the blend and control mizes at 150°C and 180°C.

	Rate constant, k, min^{-1} $x10^2$					
	E		X		Blend	
	150°C	180°C	150°C	180°C	150°C	180°C
Gum[a]	12.3	72.3	7.0	23.5	3.3	3.8
Carbon black-filled[a]	21.0	194.6	7.0	26.2	3.2	4.6
Silica-Filled[a]	-	-	-	-	3.7	5.9

[a] Mix No. Exb, ExbIS 20 and ExbSi 20 (Table 1)

Table 3.2.6 : Activation Energy for vulcanisation.

	Activation energy , E, kJ /mole.		
	E	X	Blend
Gum[a]	77	34	65
Carbon black-filled[a]	86	43	65
Silica-filled[a]	-	-	70

[a] Mix No. Exb, ExbIS 20 and ExbSi 20 (Table 1)

Table 3.2.7 : Effect of Moulding Time at 150°C on Physical Properties of 1:1XNBR-ENR blend.

	Gum			ISAF black[a]			Silica[a]		
Time of Moulding, min	30	45	60	30	45	60	30	45	60
Modulus 100% , MPa	0.5	0.8	0.8	0.6	0.7	1.1	1.3	1.4	1.5
Modulus 200% , MPa	1.0	1.5	1.5	2.9	3.3	4.3	2.7	3.6	4.2
Modulus 300% , MPa	2.0	2.8	3.2	6.2	7.0	8.9	5.3	7.1	9.2
Tensile strength, MPa	3.0	3.1	3.2	17.0	16.0	13.5	12.0	12.0	13.0
Elongation at break, %	340	310	300	500	470	410	400	370	370
Tear strength, kN/m	17.0	16.0	12.6	53.0	47.0	38.0	33.0	29.0	29.0

[a] at 30 phr loading

Table 3.2.8 : Effect of Moulding temperature at Constant Moulding Time of 60 minutes on Physical Properties of 1:1 XNBR-ENR Blend.

	Gum		ISAF black[a]		Silica[a]	
	150°C	180°C	150°C	180°C	150°C	180°C
Modulus 300%, MPa	3.2	-	8.9	-	9.2	-
Tensile strength, MPa	3.2	3.2	13.5	10.0	13.0	8.0
Elongation at break, %	300	200	410	200	370	200
Tear strength, kN/m	12.6	11.8	38.0	27.0	29.0	23.0
Hardness, Shore A	47	50	58	60	57	74
Resilience at 40°C, %	69	74	61	67	64	70
Abrasion loss, cc/hr	4.5	3.7	1.6	1.1	1.4	0.9
Compression set at 70°C 22 hr., %	12	4	14	6	12	7
Heat build-up by Goodrich flexometer with a load of 1 kg and stroke of 4.5 mm.						
ΔT^{b}, °C	17	11	26	21	22	18
Permanent set, %	0.6	0.5	1.3	0.5	1.0	0.5
	0.12	0.18	0.17	0.24	0.15	0.19

a at 20 phr loading

b Ambient temperature, 50°C.

Table 3.2.9 : Physical Properties of ISAF Black Filler 1:1 XNBR-ENR Blend Moulded at 150°C for 60 Minutes.

	Filler loading (parts per 100 of rubber)						
	0	5	10	15	20	30	40
[illegible] 300%, MPa	3.2	3.3	4.0	6.4	8.9	11.6	15.9
[illegible] strength, MPa	3.2	5.2	8.6	10.7	13.5	15.0	17.8
[illegible]ation at break, %	300	395	460	410	410	350	340
[illegible] strength, kN/m	12.6	25.8	28.4	29.0	38.0	46.7	55.0
[illegible]ness, Shore A	47	49	53	55	58	67	76
[illegible]lience at 40°C, %	69	65	63	62	61	52	48
[illegible]ion loss, cc/hr	4.5	3.6	1.8	1.7	1.6	1.1	0.7
[illegible]sion set at 70°C [illegible], %	12	13	14	14	14	15	17
[illegible] build-up by Goodrich [illegible]ter with a load of [illegible] stroke of 4.5 mm.							
[illegible] °C	17	19	21	25	26	30	33
[illegible]ic set, %	0.6	1.1	1.2	1.3	1.3	1.6	1.6
	0.12	0.13	0.14	0.15	0.17	0.19	0.20

[illegible] Ambient temperature 50°C.

Table 3.2.10 : Physical Properties of SRF Black Filled 1:1 XNBR-ENR Blend Moulded at 150°C for 60 Minutes.

	Filler loading (parts per 100 of rubber)						
	0	5	10	15	20	30	40
Modulus 300%, MPa	3.2	3.7	4.9	6.3	7.3	7.6	9.8
Tensile strength, MPa	3.2	5.2	7.6	9.2	10.5	11.5	14.5
Elongation at break, %	300	310	385	390	390	440	460
Tear strength, kN/m	12.6	26.0	28.0	29.5	30.9	36.0	47.0
Hardness, Shore A	47	48	49	51	55	60	65
Resilience at 40°C, %	69	69	68	68	66	59	57
Abrasion loss, cc/hr	4.5	2.7	2.1	1.8	1.6	1.5	1.0
Compression set at 70°C for 24h., %	12	13	14	15	16	16	16
Heat build-up by Goodrich flexometer with a load of 10 kg and stroke of 4.5 mm.							
ΔT^{a}, °C	17	18	19	20	21	23	30
Dynamic set, %	0.6	0.6	0.6	0.7	0.7	0.7	1.0
T_g	0.12	0.13	0.13	0.14	0.15	0.16	0.18

a Ambient temperature 50°c

Table 3.2.11 : Physical Properties of Silica Filled 1:1 XNBR-ENR Blend Moulded at 150°C for 60 Minutes.

	Filler loading (parts per 100 of rubbe)				
	0	10	20	30	40
[illegible] 300%, MPa	3.2	5.0	9.2	13.4	16.0
[illegible] strength, MPa	3.2	8.0	13.0	15.3	18.0
[illegible]ation at break, %	300	400	370	330	330
[illegible] strength, kN/m	12.6	26.0	29.0	40.0	49.7
[illegible], Shore A	47	51	57	67	76
[illegible]lience at 40°C, %	69	64	64	60	55
[illegible] loss, cc/hr	4.5	1.9	1.4	1.1	0.76
[illegible]ression set at 70°C [illegible], %	12	12	12	15	16
[illegible] build-up by Goodrich [illegible]ler with a load of [illegible] stroke of 4.5 mm.					
[illegible] 43°C	17	19	22	24	30
[illegible]mic set, %	0.6	1.0	1.0	1.1	1.4
[illegible]	0.12	0.13	0.15	0.19	0.20

[illegible] Ambient temperature, 50°C

Table 3.2.12 : Physical Properties of XNBR-ENR Blend with Control XNBR and ENR Systems.

	E	X	Exb	Ec	Xc	EXb IS20	Es	Xs	EXb Si20
Modulus 300%, MPa	1.2	3.9	3.2	9.0	15.5	8.9	6.9	13.0	9.2
Tensile strength, MPa	4.2	18.7	3.2	23.0	24.0	13.5	18.0	25.1	13.0
Elongation at break, %	650	470	300	595	380	410	500	400	370
Tear strength, kN/m	18.4	34.2	12.6	49.0	69.7	38.0	39.0	60.7	29.0
Hardness, Shore A	30	69	47	61	83	58	53	81	57
Resilience at 40°C, %	56	62	69	49	54	61	49	52	64
Abrasion loss, cc/hr	19.0	0.05	4.5	1.0	0.1	1.6	4.6	0.1	1.4
Compression set at 70°C for 22h., %	16	70	12	35	53	14	23	45	12
Heat build-up by Goodrich flexometer with a load of 24 lb and stroke of 4.5 mm.									
Δ T°C	20	-	17	16	58	26	18	41	22
Dynamic set, %	1.6	-	0.6	7.3	4.2	1.3	8.0	13.0	1.0
	0.09	0.05	0.12	0.12	0.10	0.17	0.12	0.16	0.15

Ambient temperature 50°C.

Table 3.2.13 : Results of stress relaxation measurements for the gum and filled vulcanisates

Sample[a]	Slope		Intercept point on time axis (sec)
	Early	Later	
[illegible]	.03	.02	600
[illegible]	.09	.06	400
Blend (Exb)	.05	.02	450
[illegible]	.04	.02	2500
[illegible]	.09	.08	80
Blend(ExbIS20)	.05	.03	1000

[a] Refernce : Table Nos. 3.2.1(a), 3.2.1(b), 3.2.2

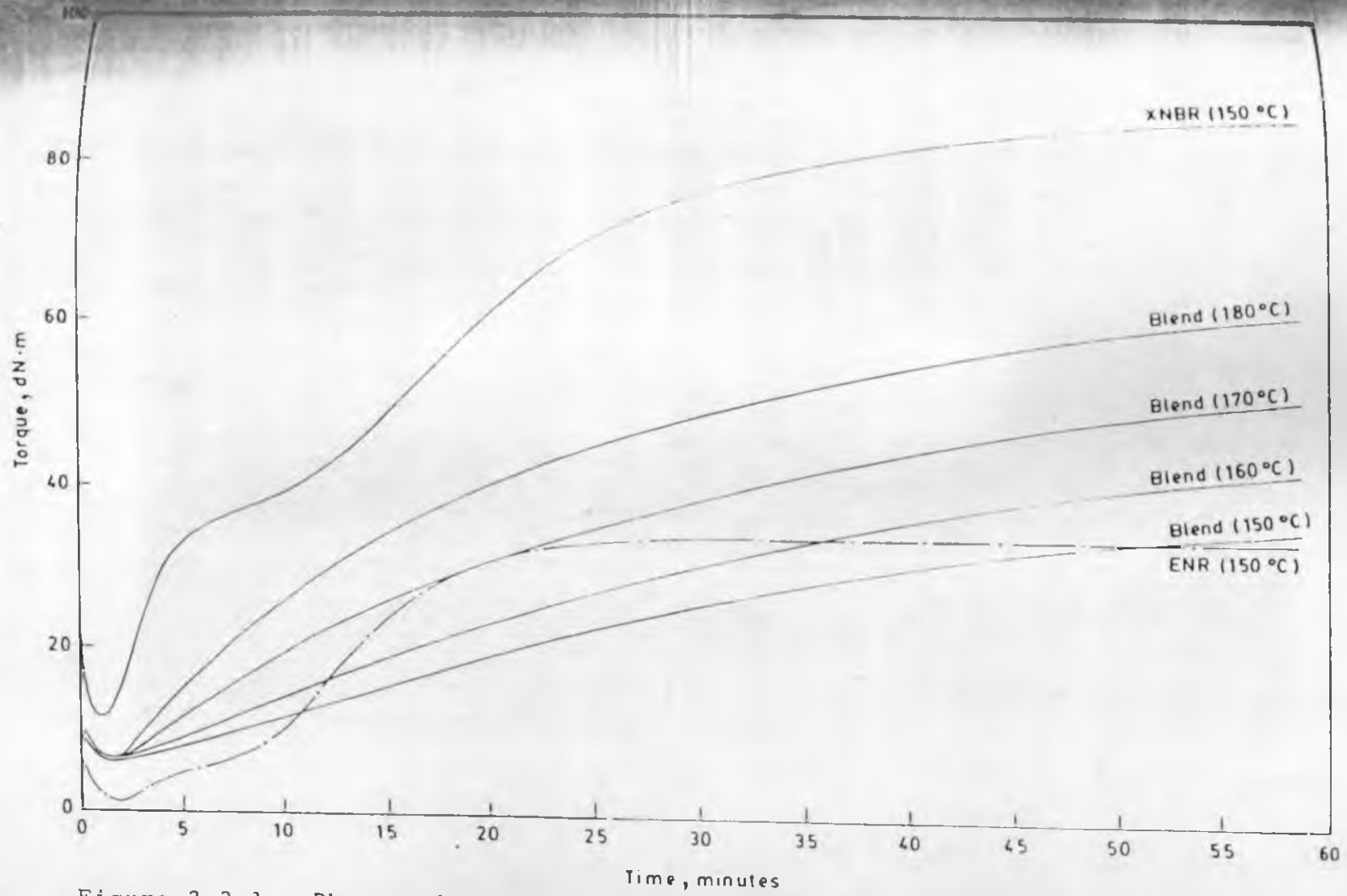

Figure 3.2.1 : Rheographs of gum 1:1 ENR-XNBR blend at different temperatures and of control gum XNBR and ENR mixes at 150°C.

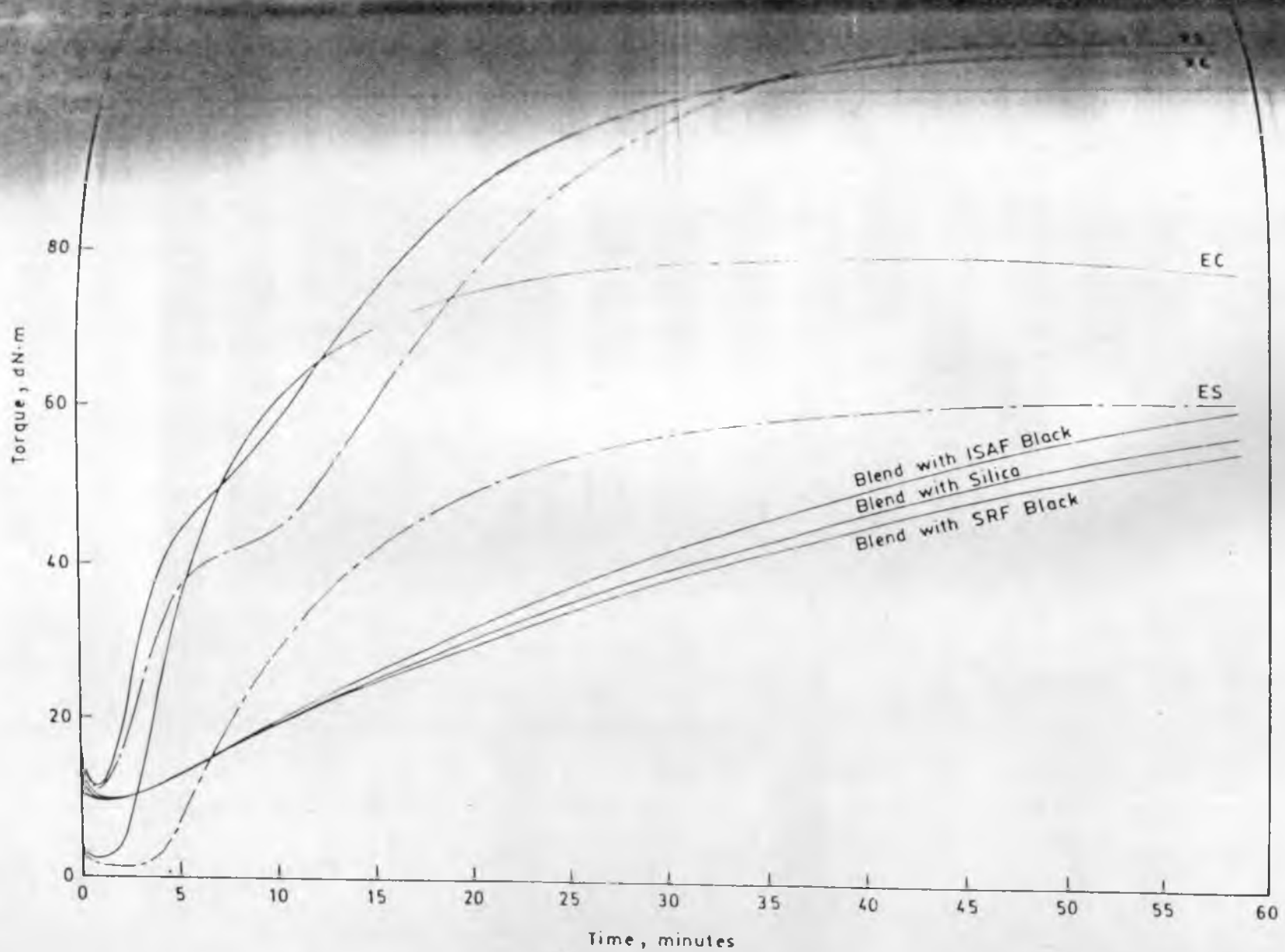

Figure 3.2.2 : Rheographs at 150^{0}C. of ENR, XNBR and 1:1 ENR-XNBR blend filled with 20phr loading of ISAF black, SRF black and silica filler.

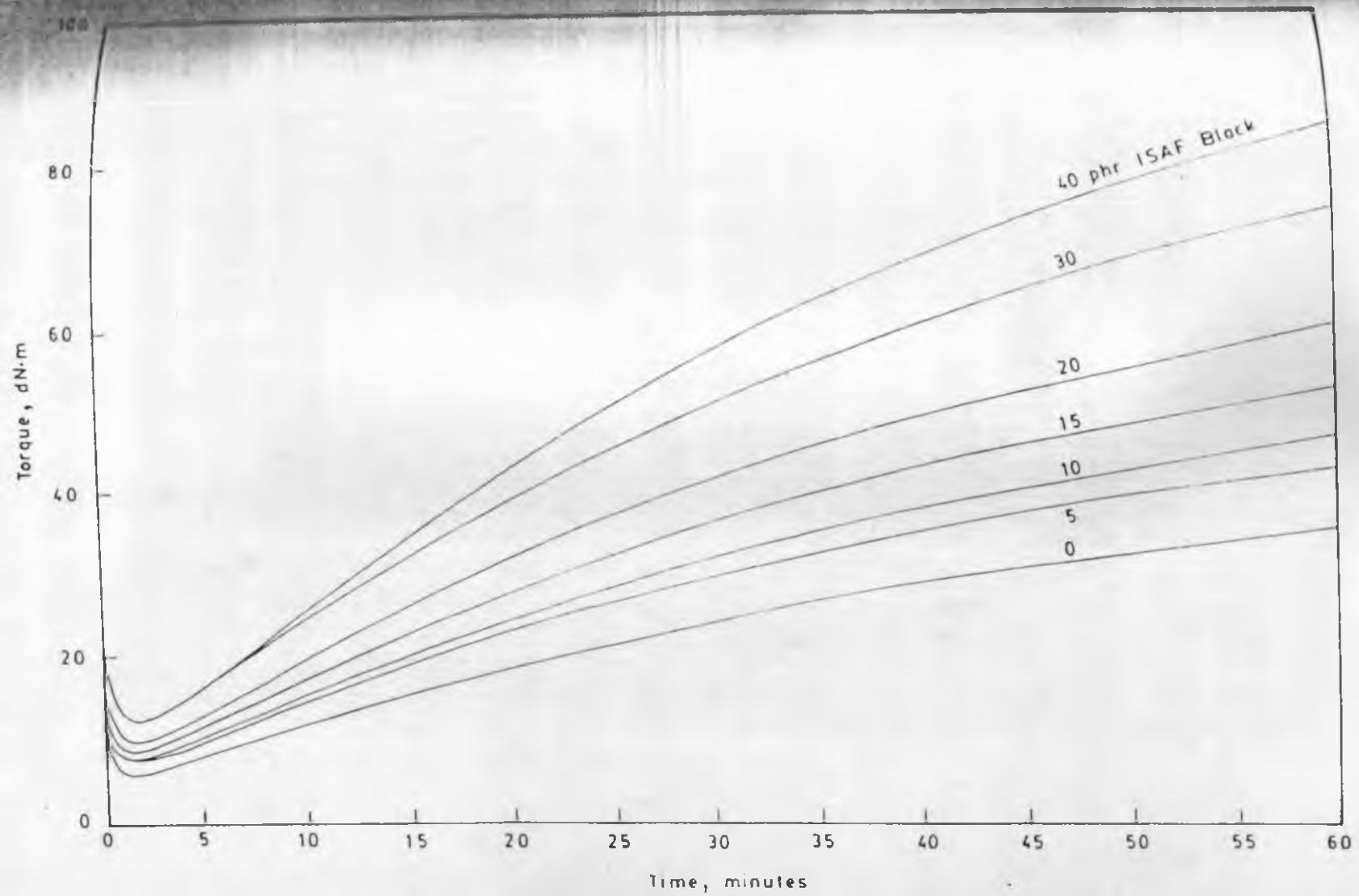

Figure 3.2.3 : Rheographs at 150°C of the 1:1 ENR-XNBR blend filled with different loadings of ISAF black filler.

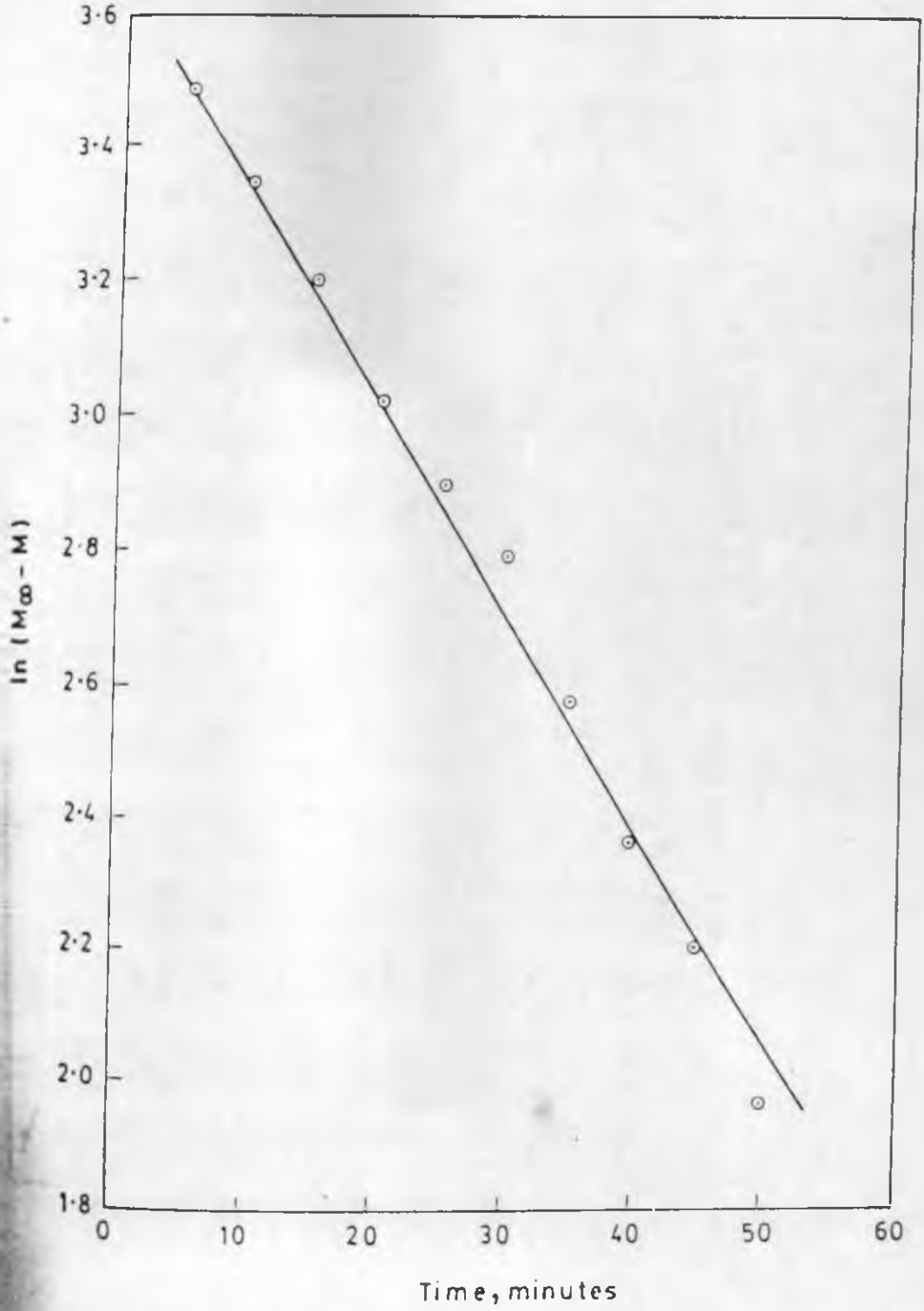

Figure 3.2.4 : Plot of ln (M_∞- M) versus time for the gum 1:1 ENR-XNBR blend at 150°C.

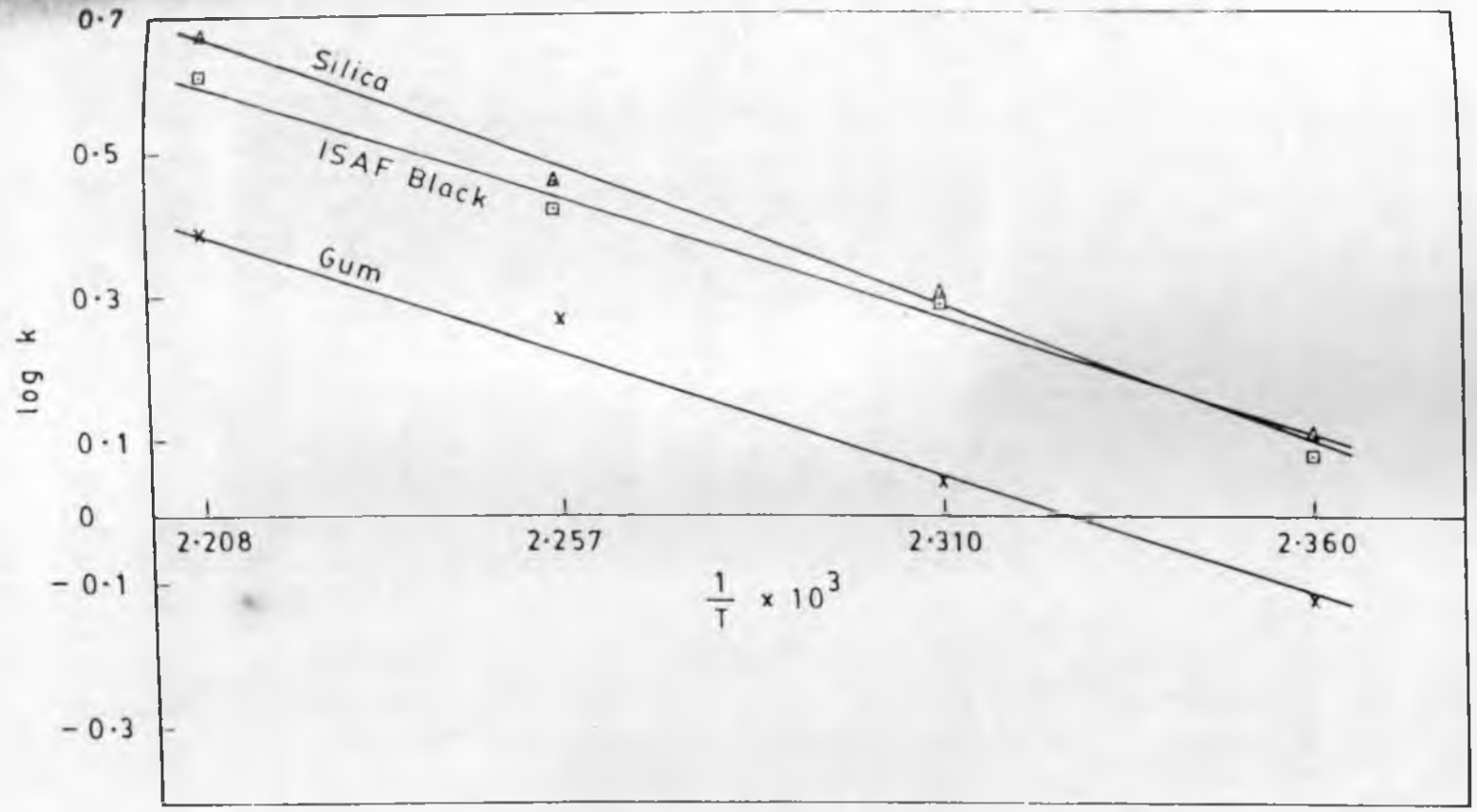

Figure 3.2.5 : Plot of log cure rate (10g k) versus reciprocal of absolute temperature for 1:1 ENR-XNBR blend and for the blend filled with 20 phr ISAF black and silica filler.

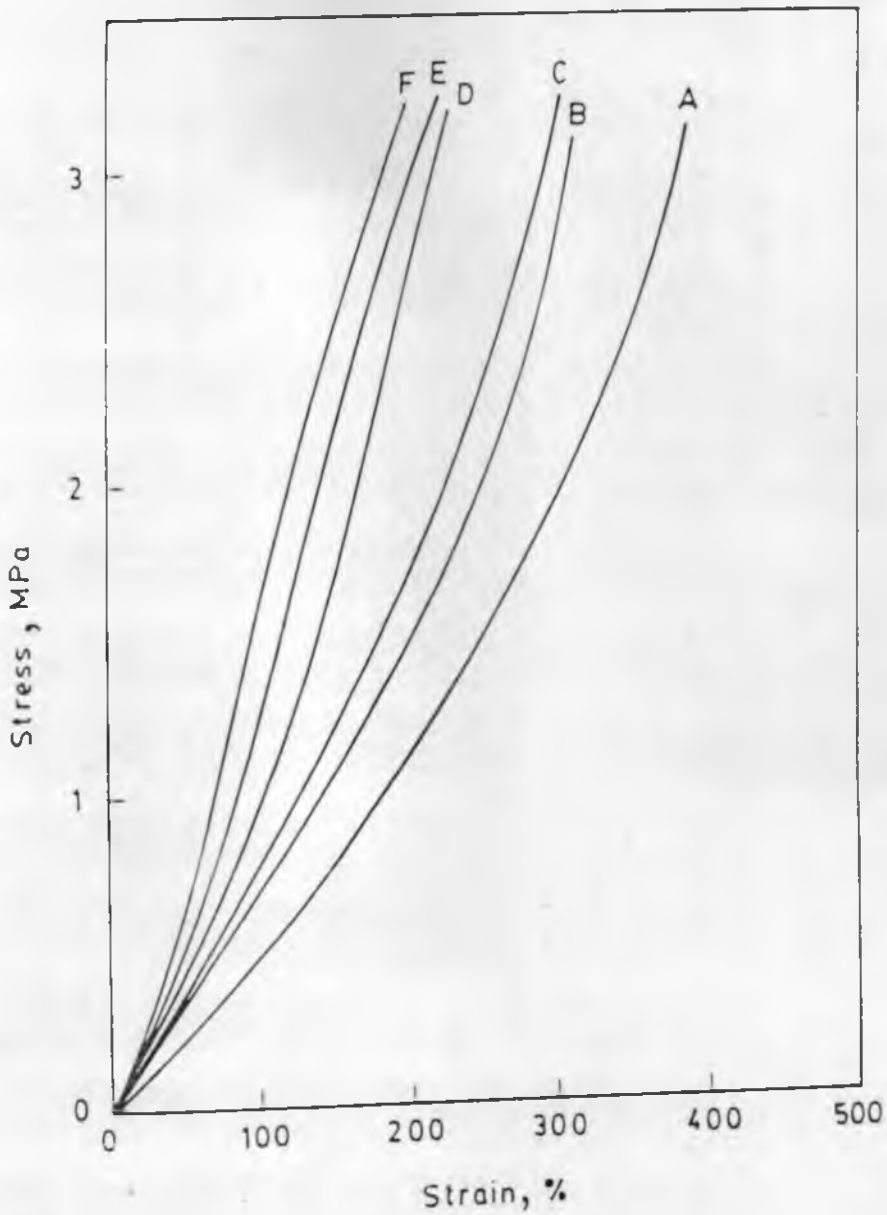

Figure 3.2.6 : Tensile stress-strain behaviour of gum 1:1 ENR-XNBR blend moulded under different conditions of moulding time and temperature
A) 150°C / 30min; B) 150°C/45min;
C) 150°C/60 min; D) 160°C/60min;
E) 170°C/60 min; F)180°C/60min.

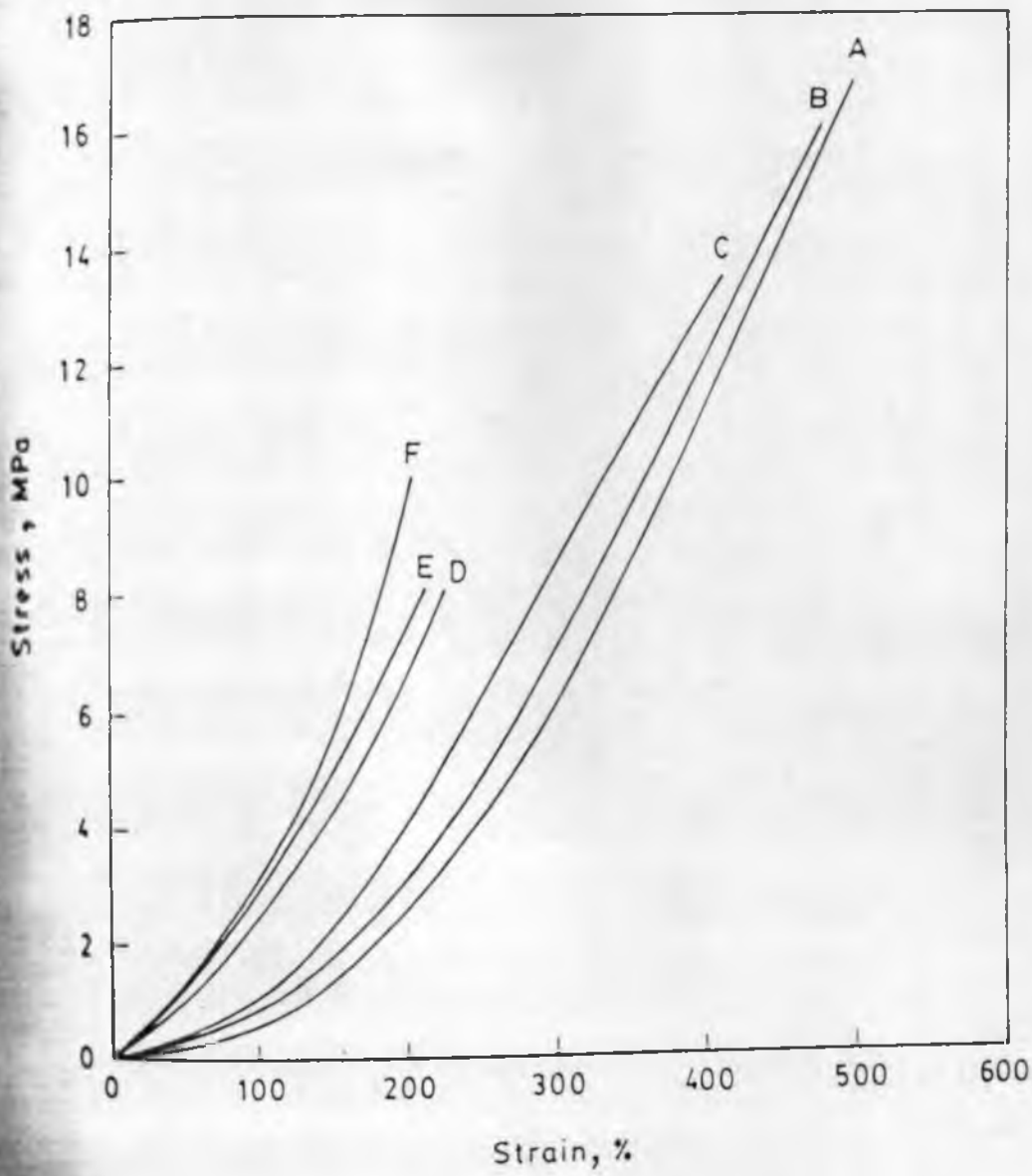

Figure 3.2.7 : Tensile strees-strain behaviour of 1:1 ENR-XNBR blend filled with 20 phr ISAF black and moulded under different conditions of time and temperature.

A) 150°C/30 min; B) 150°C / 45 min;

C) 150°C / 60 min ; D) 160°C / 60 min;

E) 170°C/60 min; F) 180°C/60 min.

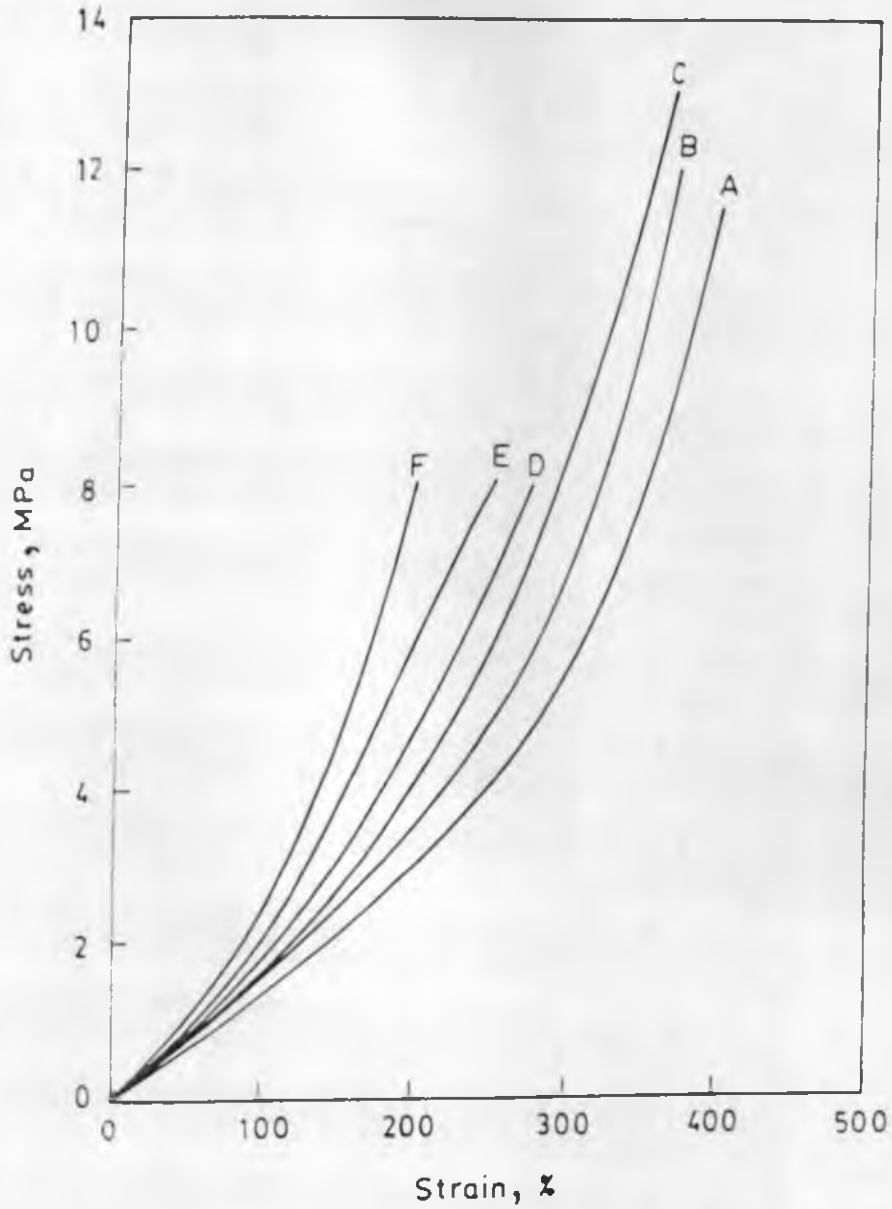

Figure 3.2.8 : Tensile stress-strain behaviour of 1:1 ENR-XNBR blend filled with 20 phr silica and moulded under different conditions of time and temperature

A) 150°C/30min; B) 150°C/ 45min;

C) 150°C / 60 min; D) 160°C / 60 min; E)170°C/60min;

F) 180°C / 60 min.

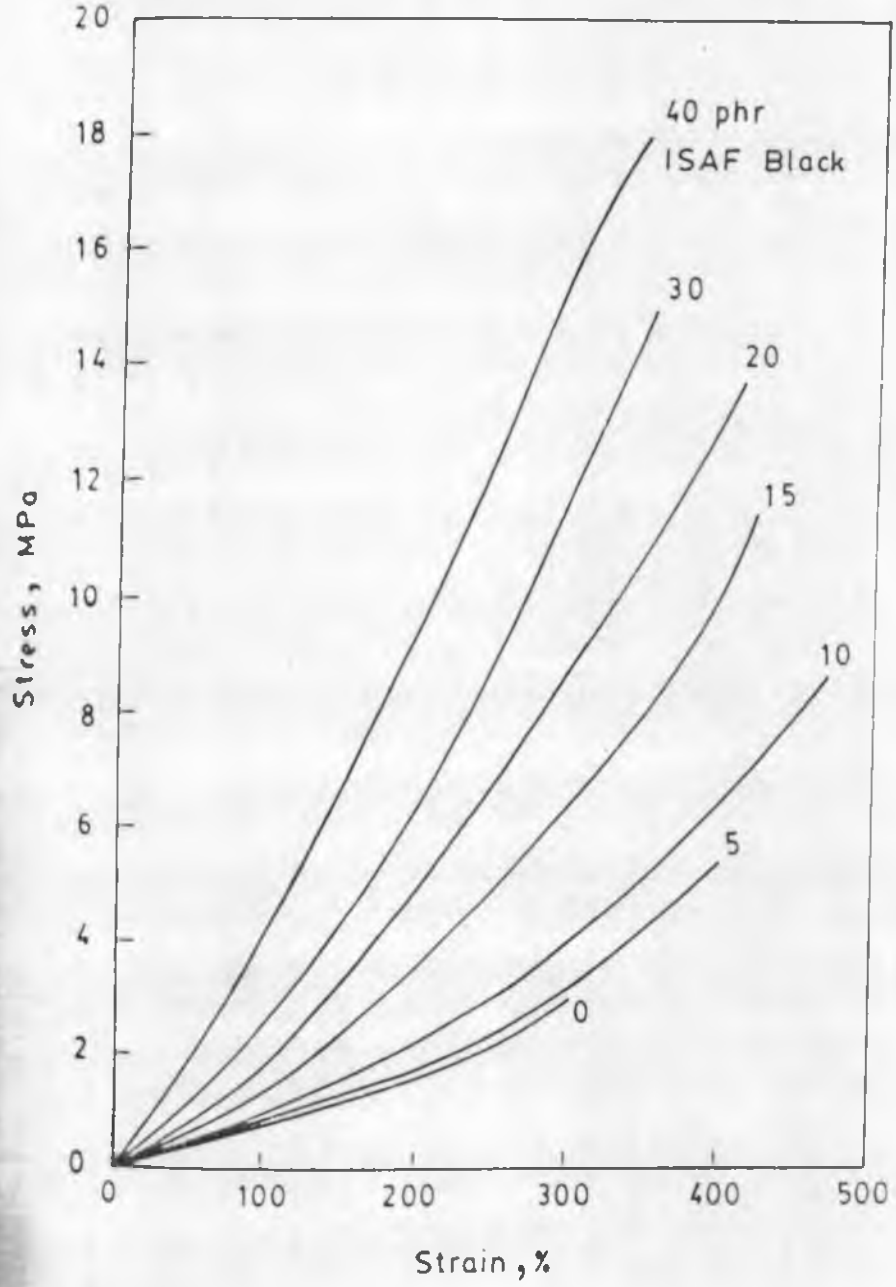

Figure 3.2. 9 : Tensile stress-stain plots of 1:1 ENR-XNBR blend filled with different loadings of ISAF black, moulded at 150°C for 60 min.

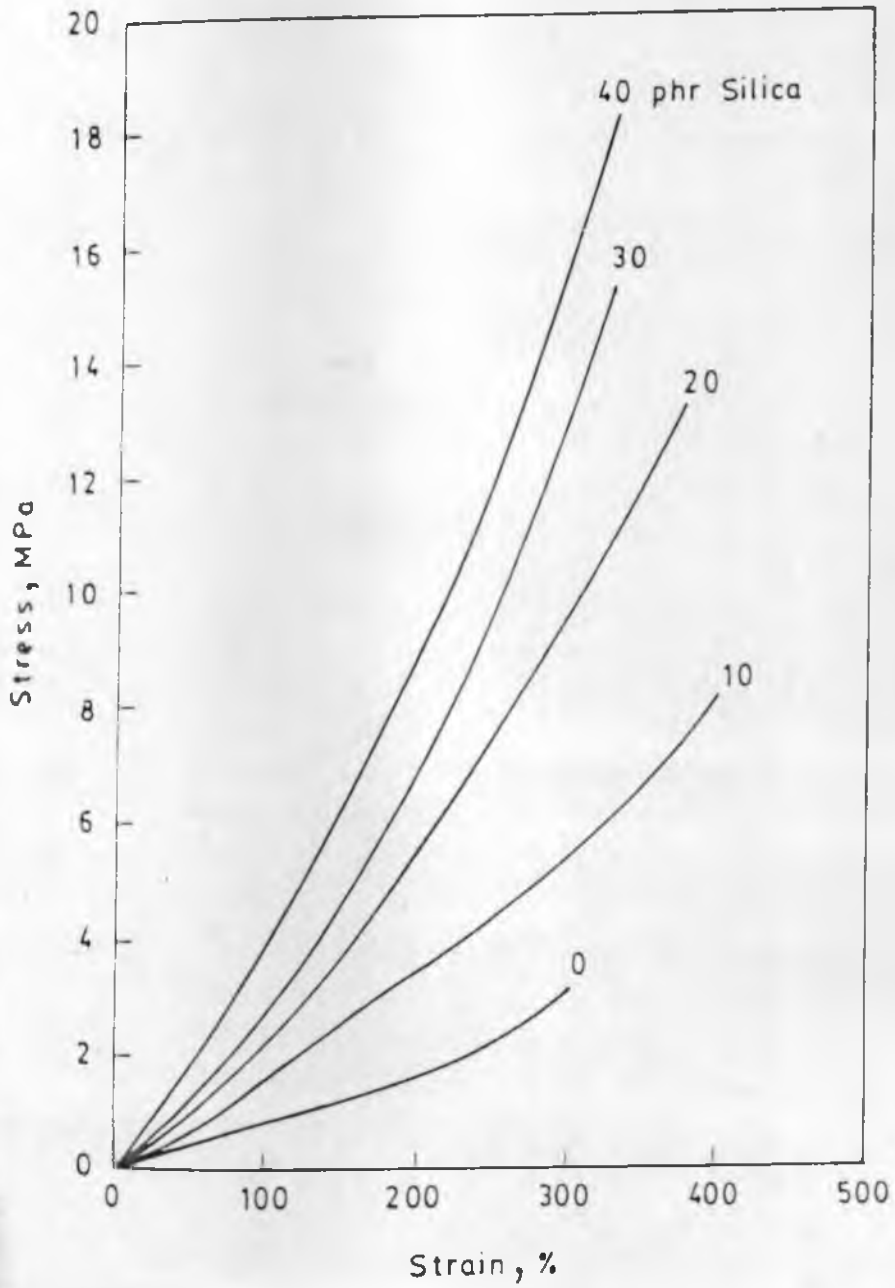

Figure 3.2.10 : Tensile stress-strain plots of 1:1 ENR-XNBR blend filled with different loadings of silica moulded at 150°C for 60 min.

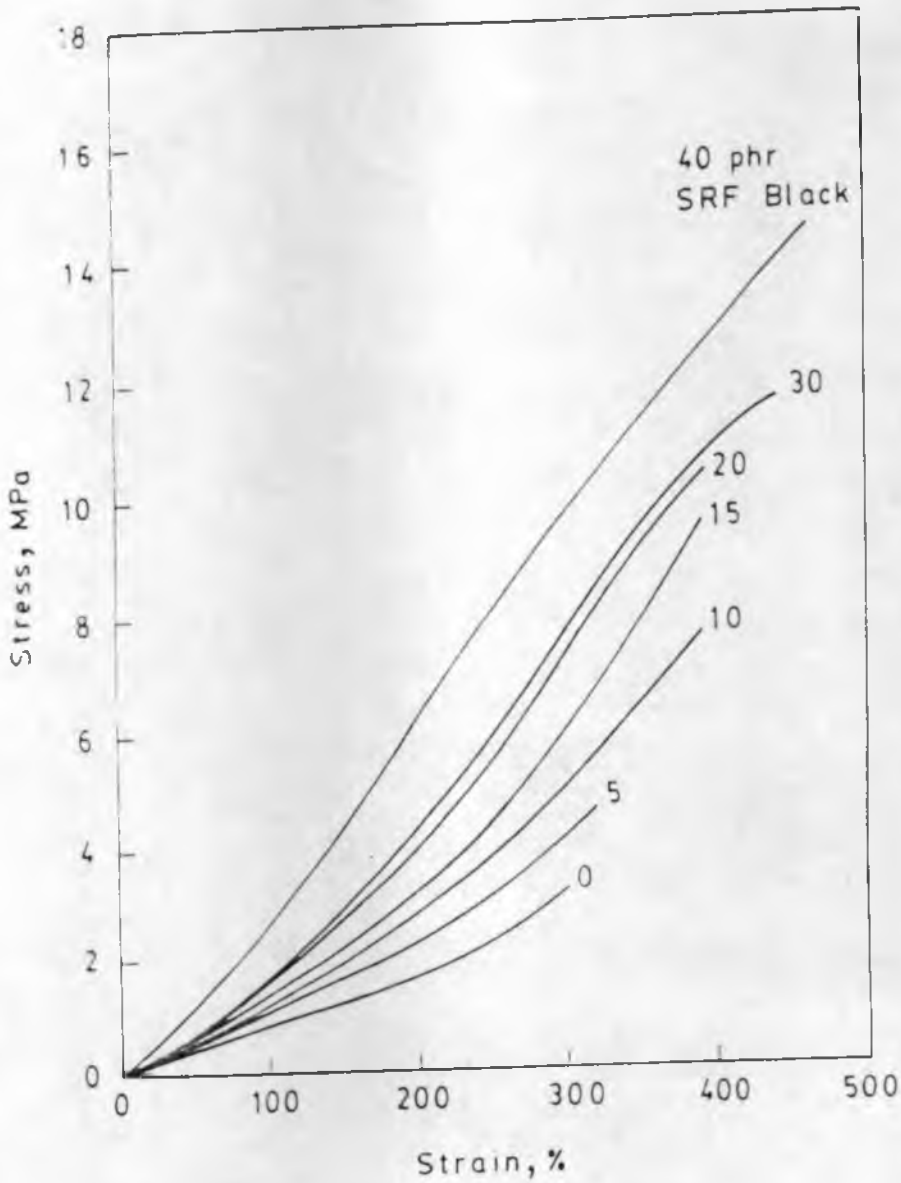

Figure : 3.2.11 : Tensile stress-strain plots of 1:1 ENR-XNBR blend filled with different loadings of SRF black, moulded at 150°C for 60 min.

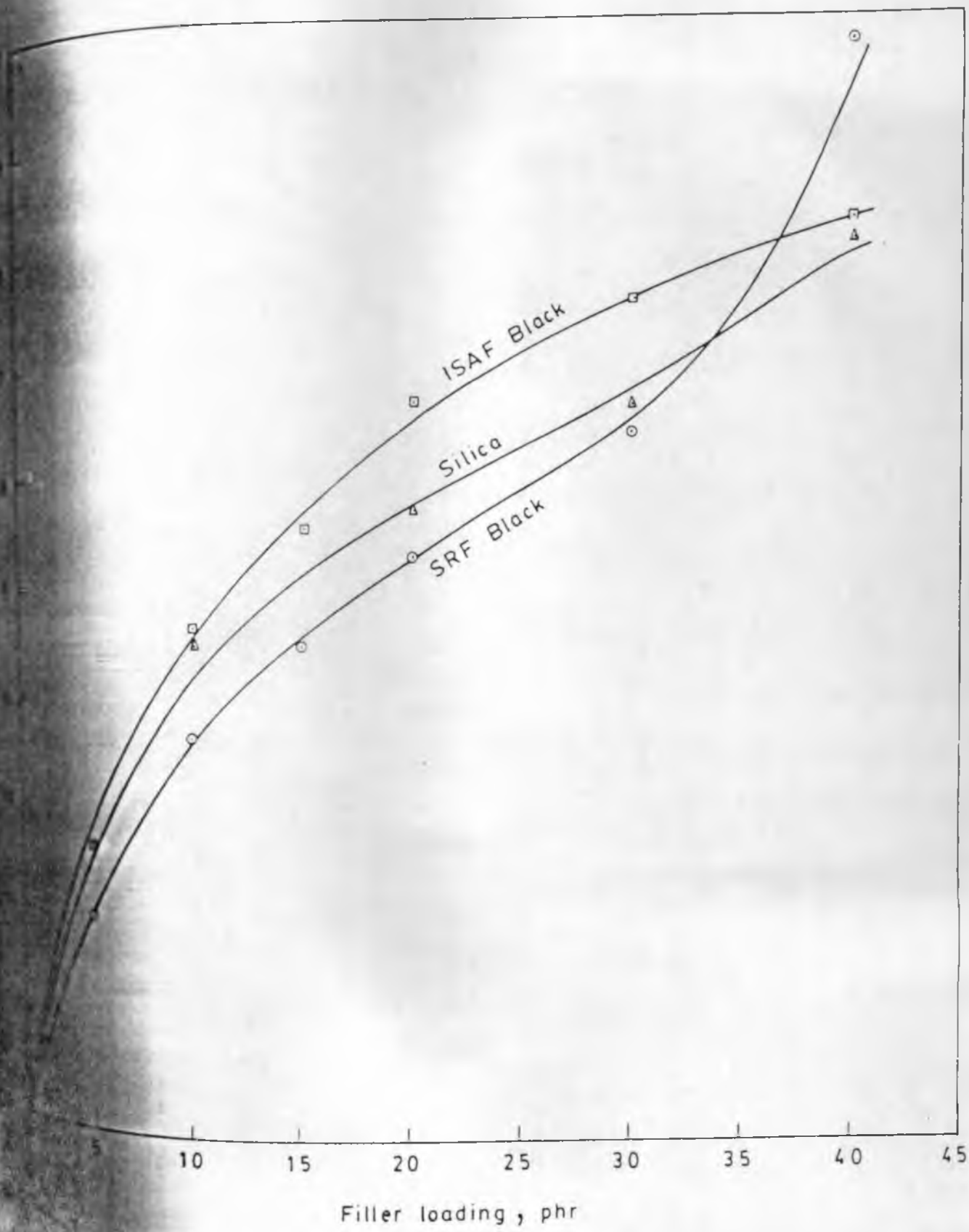

2.12 : Plots of relative rupture energy versus filler loading for ISAF black, SRF black and silica filled 1:1 ENR-XNBR blend.

Fig. 3.2.13 : Scanning electron micrographs of gum ENR vulcanizate showing coarse abrasion pattern.

Fig. 3.2.15: Abraded surface of gum XNBR vulcanizate showing clear surface.

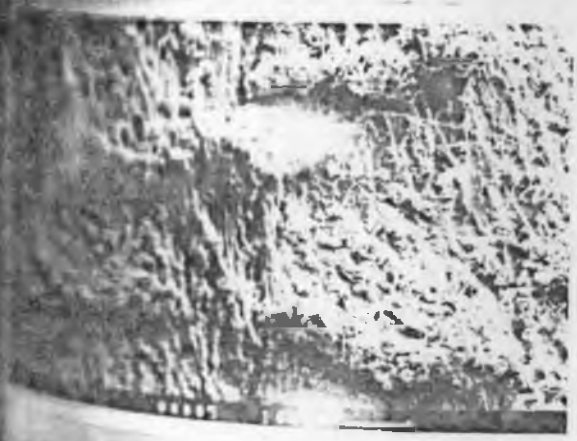

Fig. 3.2.14: Scanning electron micrograph of filled (20 phr ISAF black) ENR vulcanizate showing material removal.

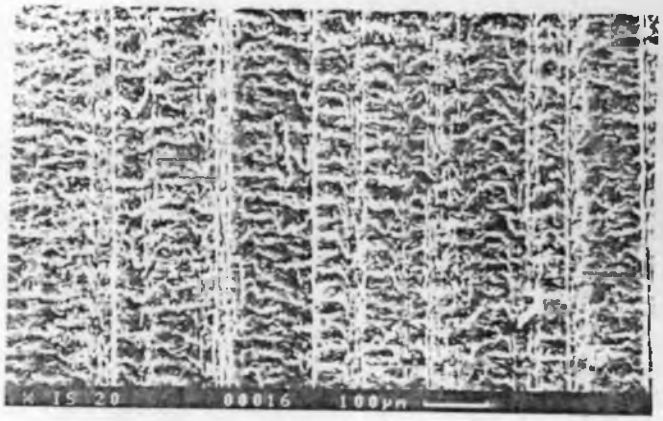

Fig.3.2.16: Abraded surface of 20 phr ISAF black-filled XNBR vulcanizate showing fine and closely spaced ridges.

Fig.3.2.17 : Abraded surface of 1:1 ENR-XNBR blend showing abrasive type of wear.

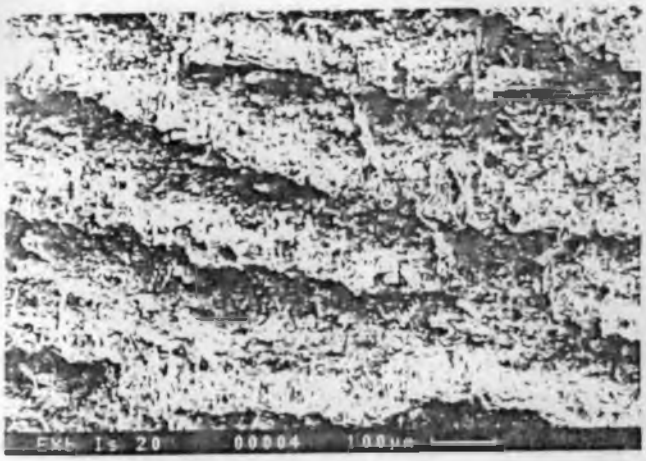

Fig.3.2.18 : Abraded surface of 1:1 ENR-XNBR blend filled with 20 phr ISAF black showing ridges which are not closely spaced.

Fig.3.2.19 : Abraded surface of 1:1 ENR-XNBR blend filled with 40 phr ISAF black showing closely packed fine ridges.

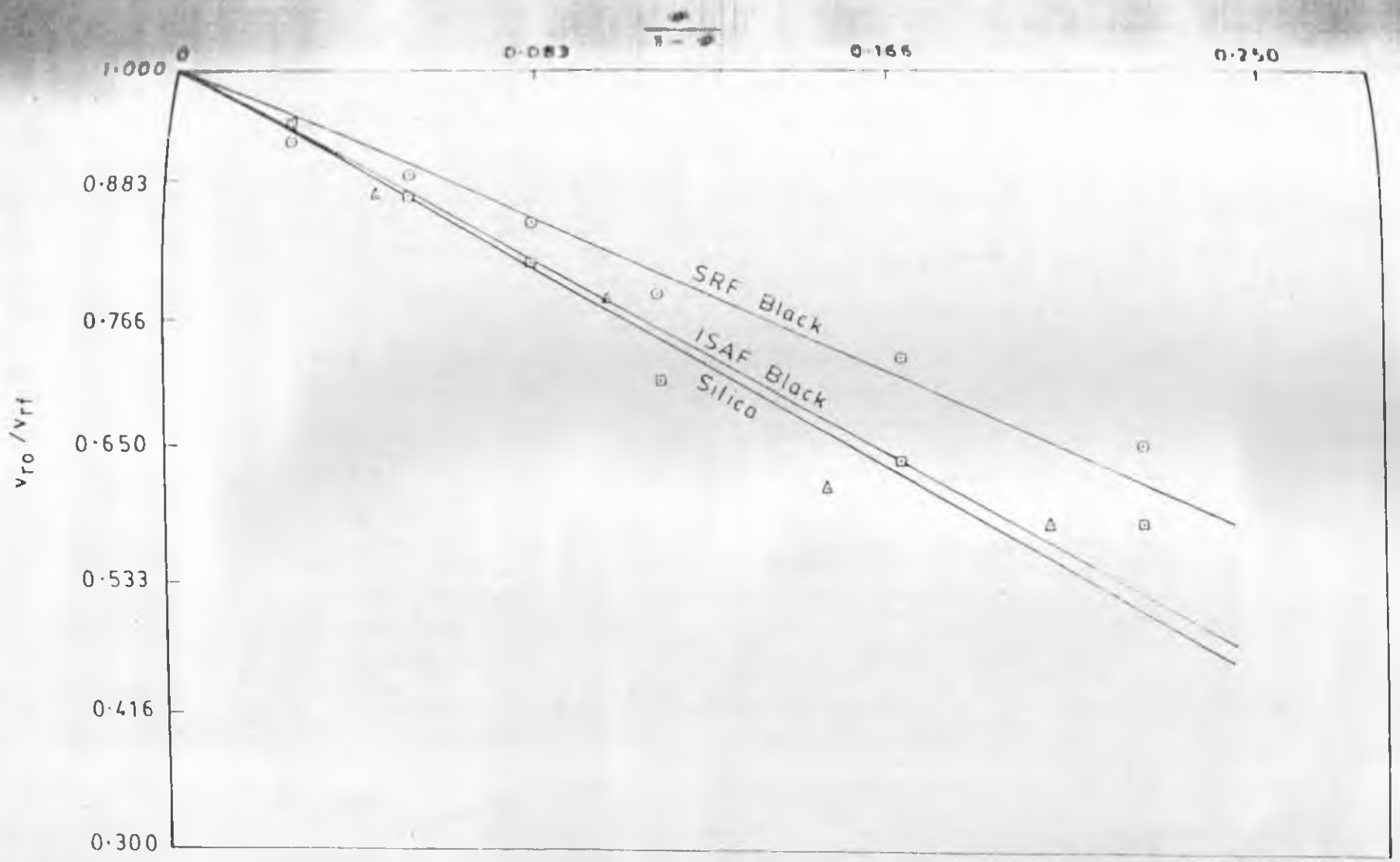

Figure : 3.2.20 : Kraus plots for ISAF black, SRF black and silica-filled 1:1 ENR-XNBR blend.

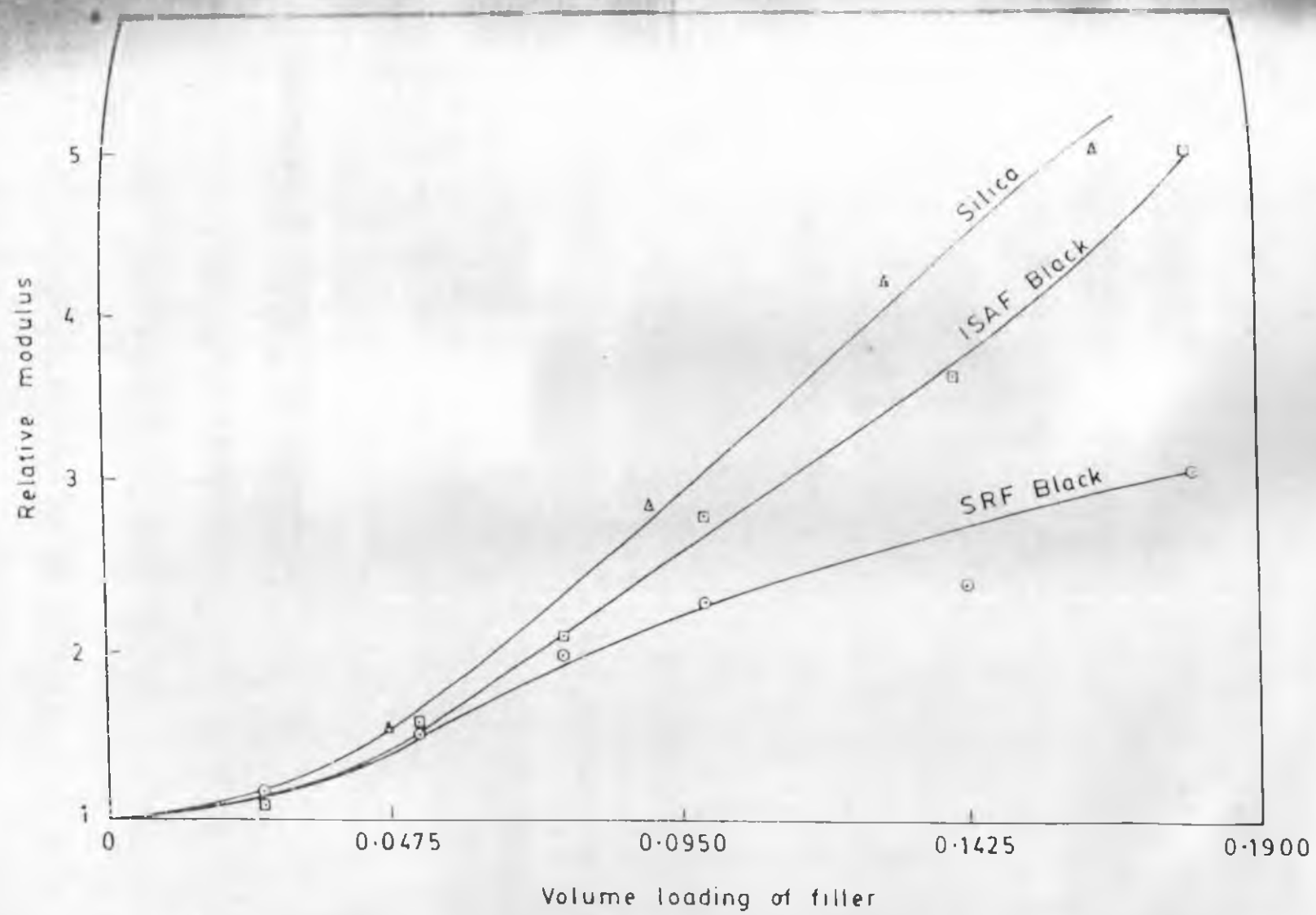

Figure 3.2.21 : Variation of relative modulus with volume fraction of filler for 1:1 ENR-XNBR blend filled with silica, ISAF black and SRF black and moulded at 150°C for 60 min.

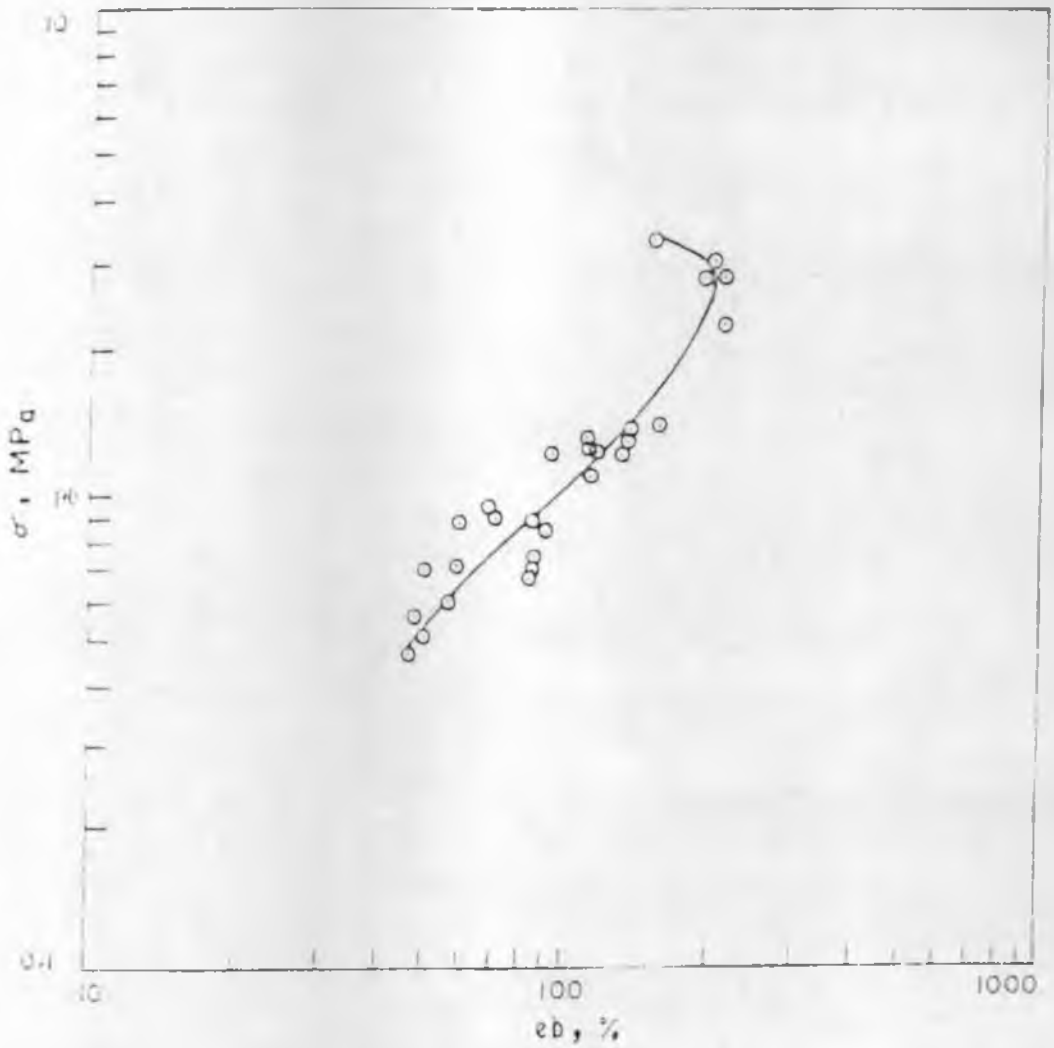

Fig. 3.2.22: Plots of breaking stress versus breaking elongation for the 1:1 ENR-XNBR blend vulcanisate.

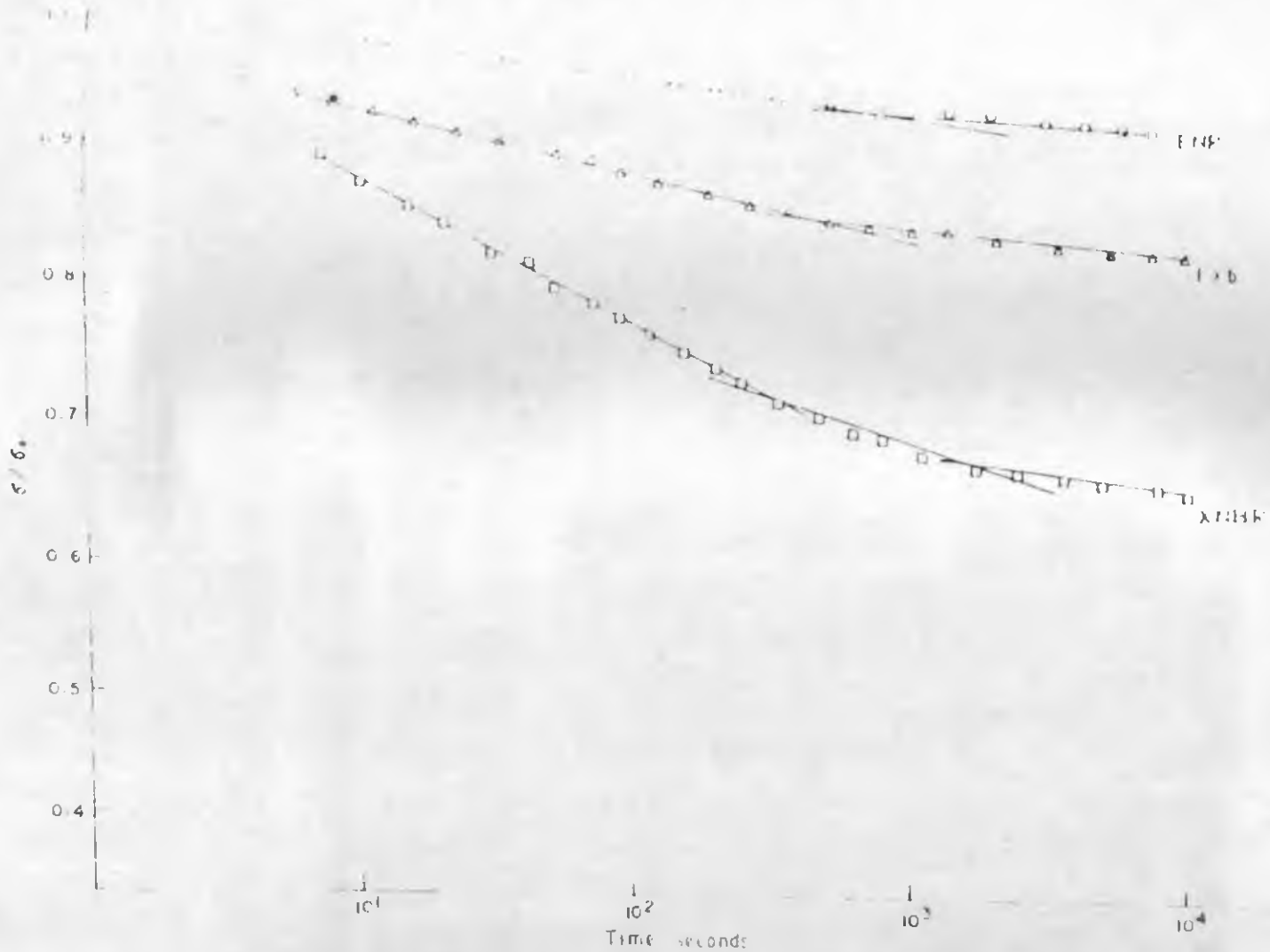

Fig.3.2.23 : Semilogarithmic plots of stress decay as a function of time, for the gum IKR, XNBR and 1:1 blend.

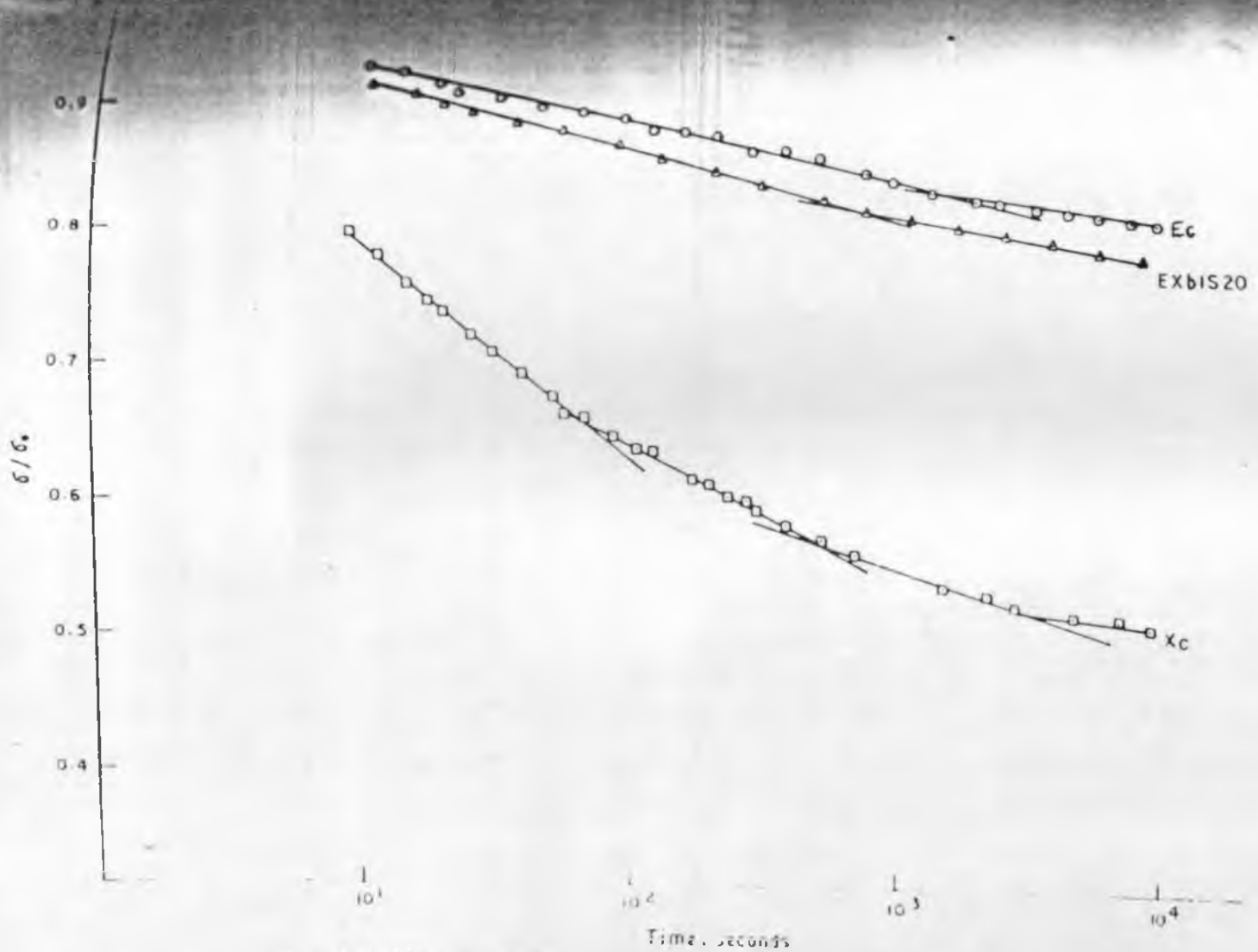

Fig. 3.2.24: Semilogarithmic plots of stress decay as a function of time for the 20 phr ISAF black filled ENR, XNBR and 1:1 blend.

CHAPTER 3 - PART III

DYNAMIC MECHANICAL PROPERTIES

* This part of the work has been Communicated to Indian Journal of Natural Rubber Research

Dynamic mechanical properties give ideas about the kinds of molecular motion, structural heterogeneities, morphology of multiphase systems, and polymer-filler interaction in rubber vulcanisates. Glass transition temperature or Tg values depend on flexibility of the molecular chains[53,54]. The dynamic mechanical characteristics of gum and filled rubbers have been investigated and it has been shown that addition of filler usually does not change the Tg[55]. However, highly reinforcing fillers are known to increase the damping peak height and increase the width of damping peak[55,56].

This section reports the results of studies on the dynamic mechanical behaviour of binary blends of ENR and XNBR with special reference to the effect of fillers, ISAF black, HAF black and silica.

3.3.1. Dynamic Mechanical Properties

3.3.1 Effect of Blending

Formulations of the mixes are shown in Tables 3.1.1, 3.1.1(a) and 3.2.1(b).

The damping plots of conventionally vulcanised ENR and and self-vulcanised binary blend of ENR and XNBR are shown in Fig. 3.3.1. The conventionally vulcanised ENR and were cured to a time corresponding to the same torque rise as that of the binary blend. ENR has Tg at -3°C along with tan δ peak value of 1.90,

while XNBR showed Tg at -8°C and tan δ peak value of 0.90. The binary blend showed Tg at -10°C and tan δ peak value of 1.65. The damping behaviour is related to chain flexibility and free volume of the polymer[54,57]. The higher chain flexibility and lower Tg of the self-vulcanised ENR-XNBR blend were likely to be due to the flexible ester crosslinks[53]. It was interesting to note that the tan δ peak height of the blend occupied a position which was inbetween the two single rubbers.

Plots of viscous modulus versus temperature and elastic modulus versus temperature are shown in Figures 3.3.2 and 3.3.3 respectively. As in the case of damping plots the value of viscous modulus and elastic modulus occupies a position which was inbetween the control rubbers but the transition from glassy to rubbery region started at an earlier temperature than the control mixes. As stated earlier, this could be ascribed to the increased chain flexibility of the self-vulcanised blends than the conventionally vulcanised single rubbers.

Figure 3.3.4 shows the damping plots of the binary blend vulcanised at two different temperatures, 180°C and [illegible]°C. When moulding was done at high temperature, the crosslinking was more (Table 3.2.8) and hence, free ends were reduced[62]. As a consequence of this, Tg was shifted to higher temperature and the height of damping peak reduced.

3.3.B Effect of Blend Ratio Variation

The effect of blend composition on the damping behaviour is shown in Fig. 3.3.5. Exc contained a higher proportion of XNBR and as discussed earlier the extent of crosslinking was more in this case and hence, Tg was shifted to a slightly higher temperature and there was reduction in damping height, as compared to other blend ratios (Exa and Exb). Results of the dynamic mechanical studies are summarised in Table 3.3.1.

3.3.C Effect of Addition of Fillers

The effect of addition of 40 phr loading of three fillers, ISAF black, SRF black and silica on the damping as a function of temperature is illustrated in Fig. 3.3.6 and Table 3.3.1.

It was seen that the reduction in tan δ peak height and spread of the peak, for the three fillers were of the order ISAF>silica>SRF black. As discussed earlier, this is also the trend of reinforcing ability of the fillers as determined by physical properties and swelling studies. The glass transition temperatures remained the same. The glass transition in rubber is generally considered to be largely unaffected by the incorporation of reinforcing fillers, such as carbon black[56].

It is well known that carbon black filler has high reinforcing action in rubbers and silica filler has high

reinforcing action without addition of any coupling agent in rubbers like ENR[33] and XNBR[32] due to the specific interaction of silica with these rubbers. In carbon black filled vulcanisates a portion of rubber gets adsorbed on the filler surface[58] and this adsorbed rubber behaves in a manner different from bulk rubber. So interacting fillers have a complex nature in the rubber matrix[59]. It has been shown that incorporation of filler which has interaction with rubber matrix, showed reduced tan δ value more spread of the tan δ peak and higher damping in the rubbery region[55,56]. The present results are in conformity with these observations.

3.3.D Miscibility of the System

Thermodynamic concept of miscibility is given by

$$\Delta G_{mix} < \Delta H_{mix} - T \Delta S_{mix} \qquad ...(2)$$

where ΔG is the free energy change, ΔH is the enthalpy change, ΔS is the entropy change and T is the absolute temperature.

Miscibility of nonpolar polymers of high molecular weights occurs only when the solubility parameters are precisely matched. The interaction parameter χ_{AB} is given by[61].

$$\chi_{AB} = (V_r/RT)(\delta_A - \delta_B)^2 \qquad ...(2)$$

The enthalpy term[61,62] for non-polar polymers can be related to solubility parameters,

$$\Delta H_m = RTV/V_r\ (\chi_{AB}\ \phi_A\ \phi_B) = V\ \phi_A\ \phi_B\ (\delta_A-\delta_B)^2$$

where V_r is the volume occupied by the smallest possible repeat unit, R is the universal gas constant and T is the temperature, δ_A and δ_B are the solubility parameters of the two polymers, ϕ_A and ϕ_B are the volume fractions of the two polymers and V is the total volume of the mixture. The situation is different in polar polymers, where there is specific interaction between the two polymers. In such cases due to specific interaction there is exothermic enthalpy and as a result ΔG_m becomes negative and the system becomes miscible. Strong chemical interactions which leads to attachment of the polymers to each other via block and graft copolymers or formation of covalent bonding between the polymers through crosslinking is reported to enhance the degree of miscibility[63]. It has been shown that in blends of SBR-BR[64] (styrene butadiene rubber and polybutadiene rubber) and NR-BR[65] (natural rubber-polybutadiene rubber), miscibility was enhanced by vulcanisation.

In the present case the solubility parameters were determined by swelling of raw rubbers[66]. The following values were obtained : ENR 9.3; XNBR 9.1. The enthalpy of mixing could be negative due to specific interaction between the epoxy group and the carboxyl group. Hence the binary blends of ENR and XNBR were miscible due to specific interaction between the functional groups.

Films of miscible polymers are optically clear. A very small amount of incompatible polymer (.01 wt %) could cause opacity in film[67]. In rare cases incompatible polymers had optical clarity if their refractive indices were the same. In the present case blends of ENR and XNBR were optically clear, confirming that the vulcanisates obtained were miscible.

Table 3.3.1 : Results of D.M.A. studies

	tan $\delta_{(max)}$	Tg, ^{o}C	
		tan δ	viscous modulus
[illegible]	1.90	- 3	-14
[illegible]	0.90	- 8	-16
[illegible]	1.65	-11	-19
[illegible]	1.60	- 9	-16
[illegible]	0.71	- 8	-16
[illegible]1840	0.71	- 7	-17
[illegible]2840	1.19	- 7	-17
[illegible]3/40	0.71	- 7	-17

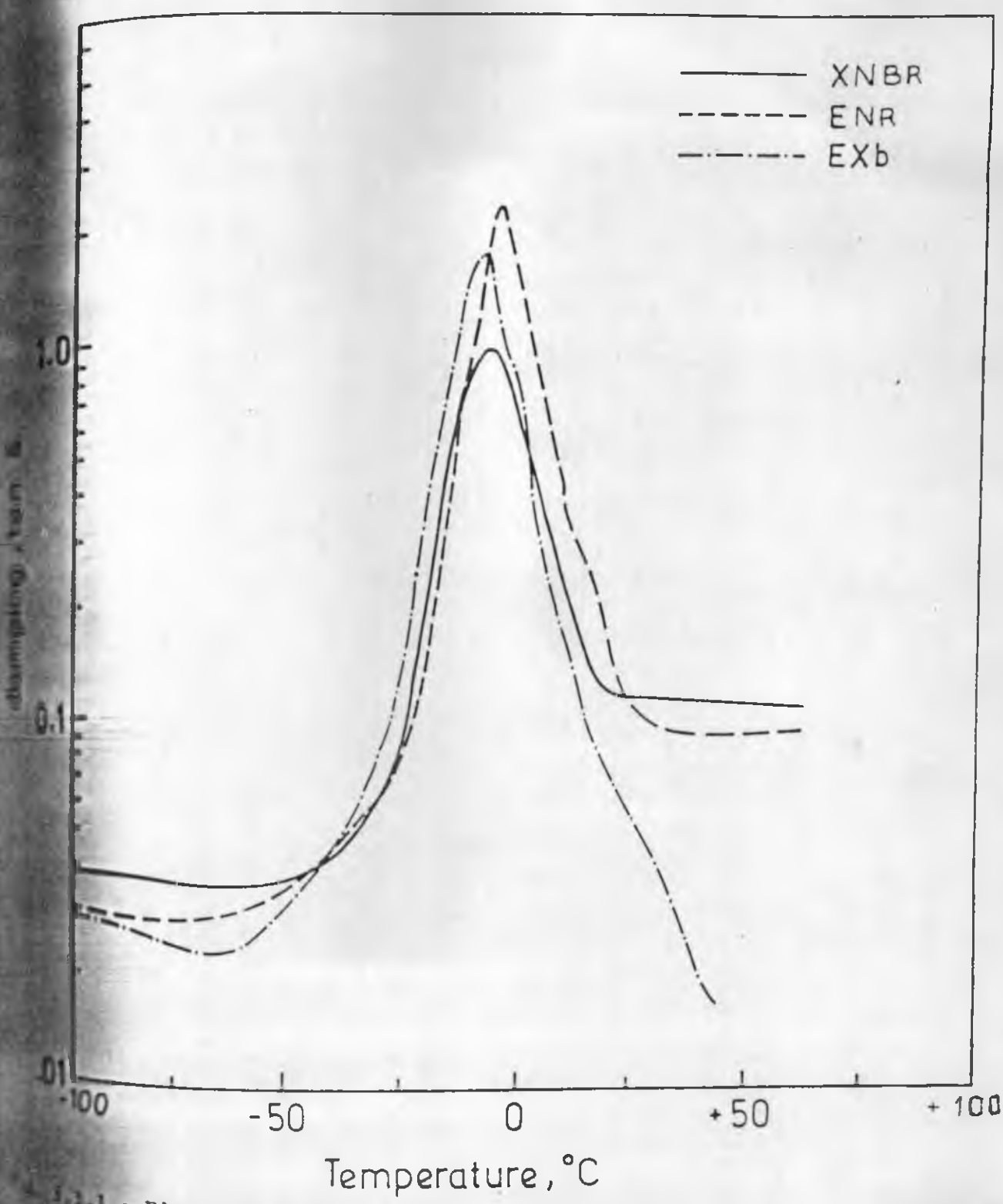

4.1.1 : Plots of damping (tan δ) versus temperature for ENR, XNBR and the 1:1 binary blend.

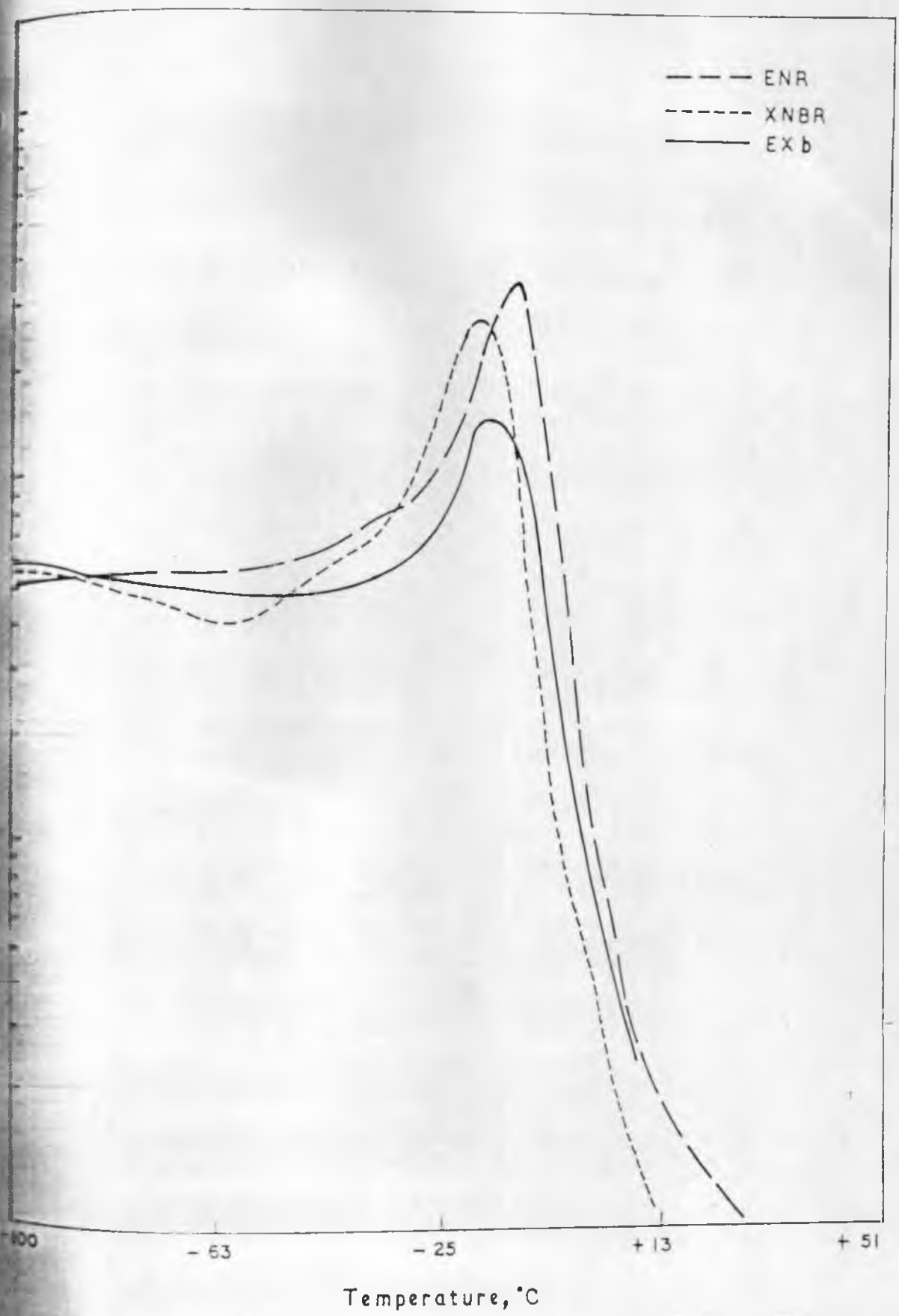

Fig. 3.3.2 : Plots of viscous modulus versus temperature for ENR, XNBR and the 1:1 ENR-XNBR blend vulcanisates.

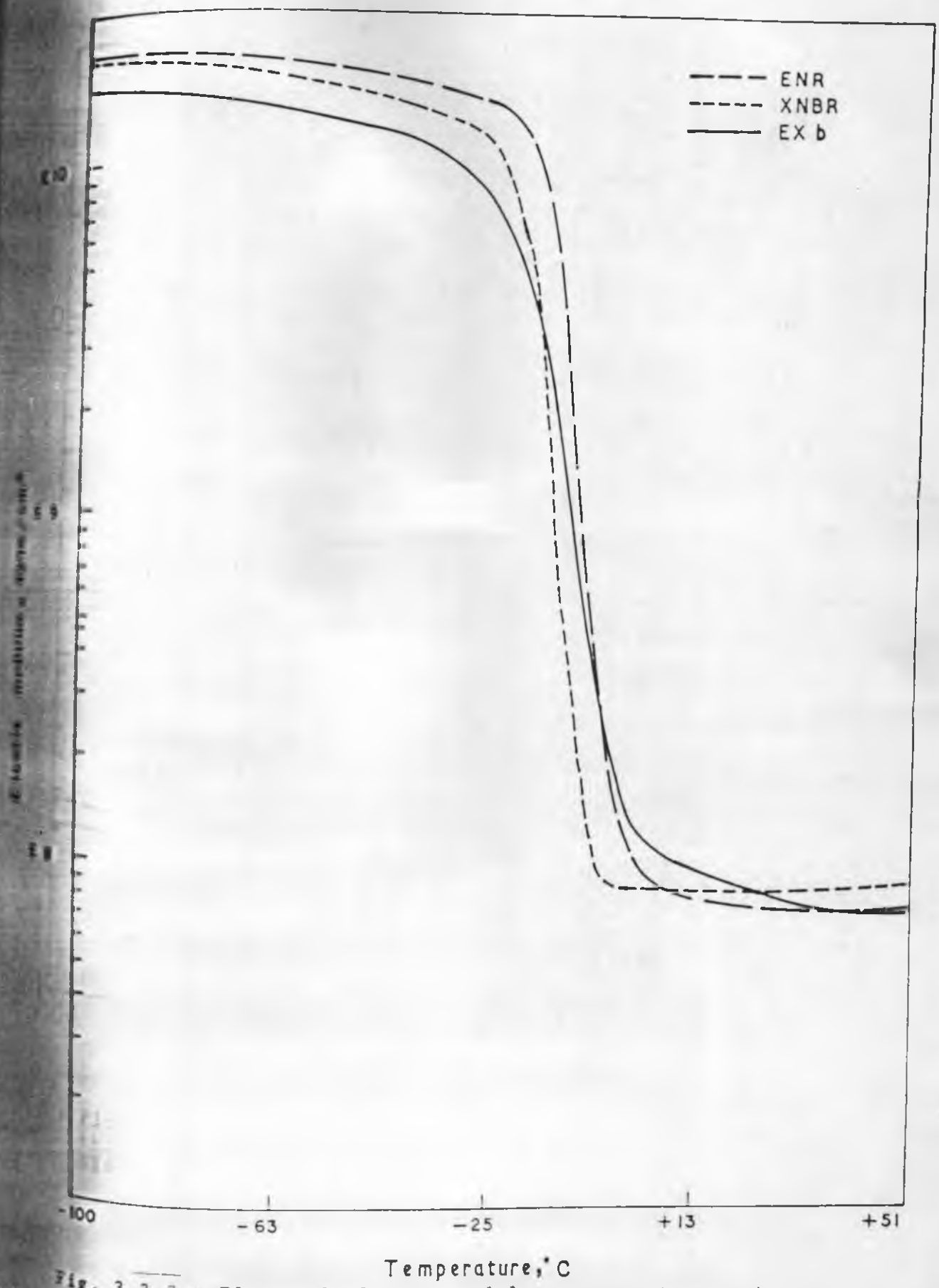

Fig. 3.3.3 : Plots of elastic modulus versus temperature for ENR, XNBR and the 1:1 ENR-XNBR blend vulcanisates.

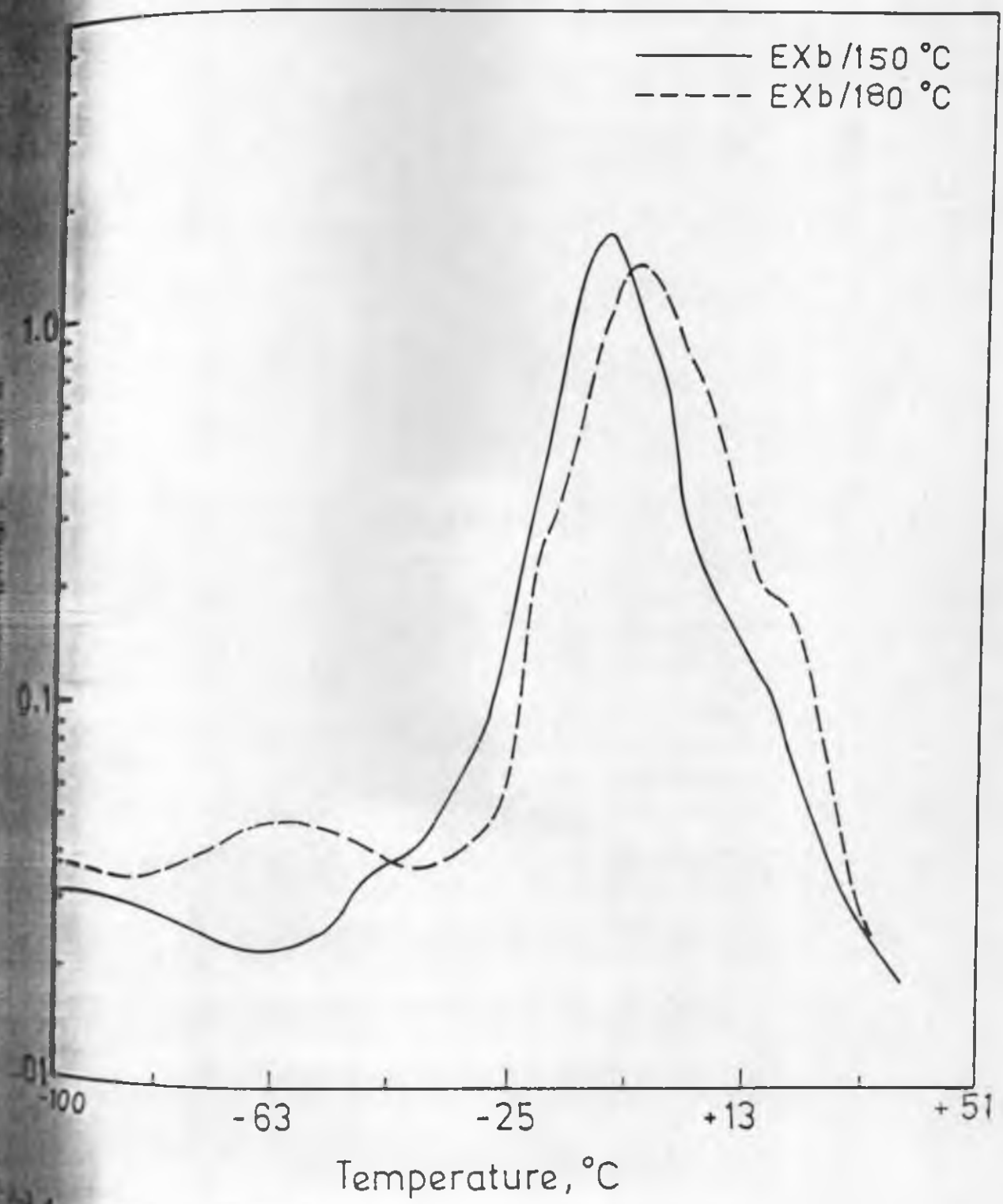

Fig.4 : Plots of damping (tan δ) versus temperature for the binary blend vulcanised at two temperatures 180°C and 150°C for 60 min.

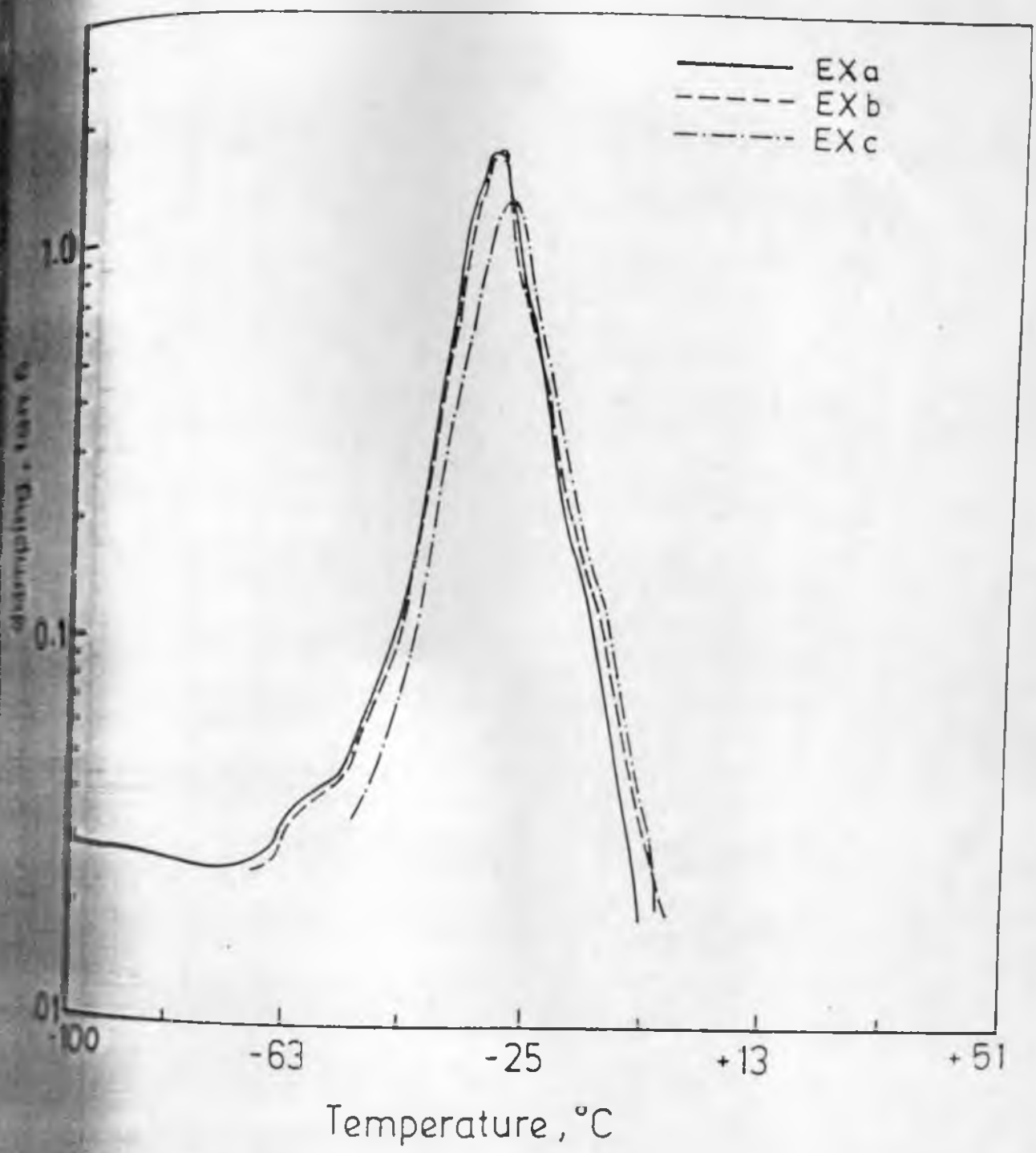

Fig. 3.3.5 : Plots of damping (tan δ) versus temperature for the binary blend showing the effect of blend ratio variation.

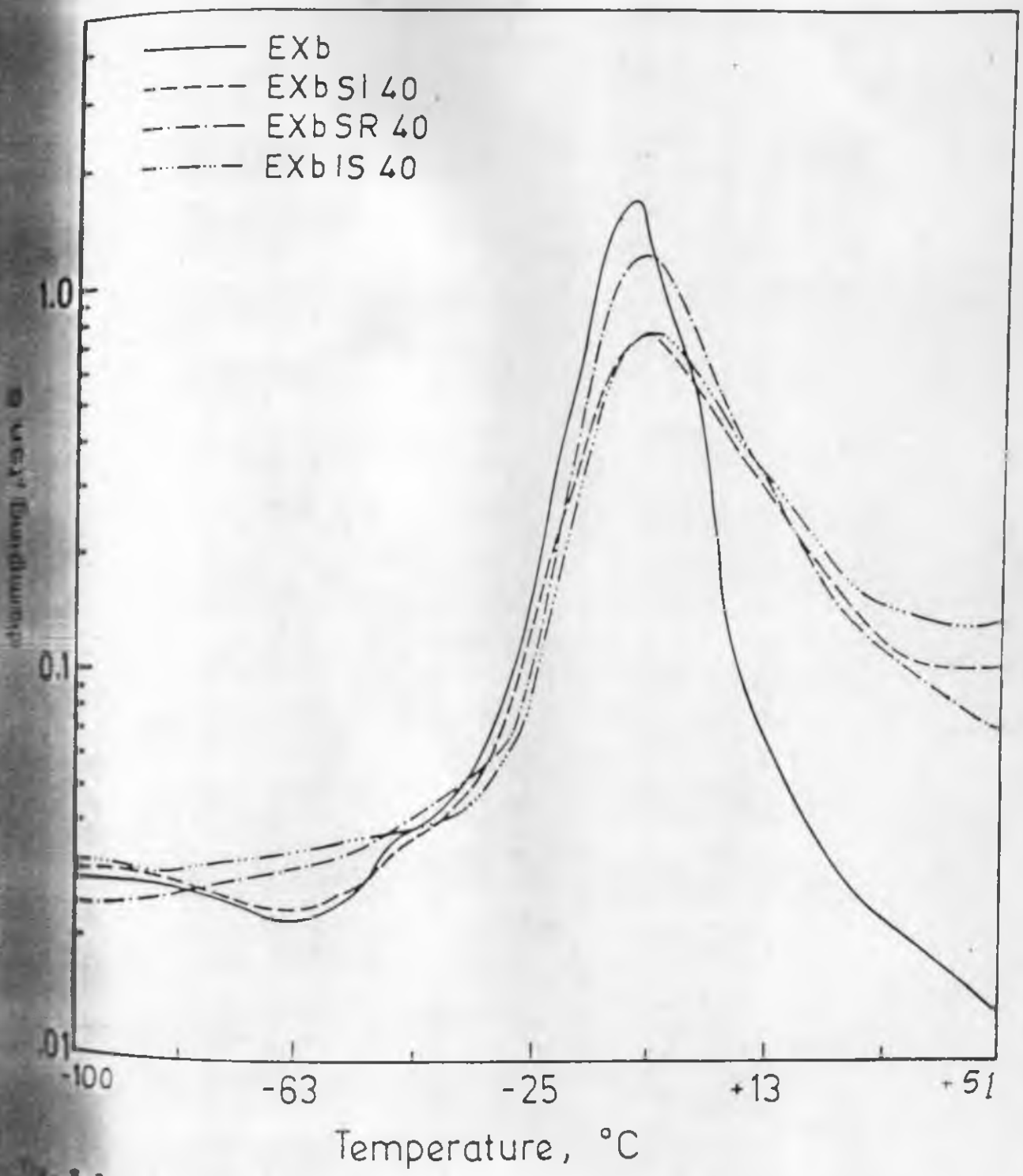

Fig. 3.3.6 : Plots of damping (tan δ) versus temperature for the binary blend showing the effect of fillers ISAF black SRF black and silica.

CHAPTER 3 - PART IV

AGEING STUDIES

Rubber products undergo ageing during application under different environments like elevated temperature, corrosion media and oil. A crosslinked elastomer which gives optimum properties under normal conditions may show poor properties under conditions like exposure to chemicals and higher temperature. Rubber vulcanisates are degraded thermally, mechanically and chemically and the extent of these reactions depends on the type and nature of crosslinks in addition to the type of polymer matrix. Ageing in unblended rubbers have been investigated extensively[68-71]. Both ENR and XNBR are known to crosslink in presence of oxygen[15,72].

This chapter reports the results of ageing studies of the blends formed by self-vulcanisation of ENR and XNBR under the following four different ageing conditions.

(1) Air at 70°C for 12 days

(2) Hydrochloric acid (aqueous 25%) at 70°C for 7 days

(3) Sodium hydroxide (aqueous 25%) at 70°C for 7 days

(4) ASTM fuel C at 30°C for 7 days.

3.4 Ageing Studies

3.4.1 Air Ageing

The formulation of the mixes are given in Table 3.2.1 and 3.2.2. Tensile properties of aged and unaged vulcanisates are given in Table 3.4.1 and that of filled vulcanisates are given in Table 3.4.2. The retention of tensile strength for the gum and filled vulcanisates

subjected to the various ageing conditions are given in Figs. 3.4.1 and 3.4.2.

Gum ENR vulcanisate after air ageing showed an increase in modulus and decrease in tensile strength and elongation at break. The filled ENR vulcanisate also showed a similar change in tensile properties but the change was more prominent. The poor ageing of ENR vulcanisates was due to the ring opening of epoxide groups forming ether linkage[15].

XNBR vulcanisates exhibited higher tensile and better ageing properties. Gum XNBR vulcanisate after air ageing showed increased modulus and elongation at break. In case of filled vulcanisate the tensile strength after ageing remained almost same. The change in tensile properties could be due to crosslinking by oxygen in presence of heat[71].

Gum binary blend vulcanisate showed increase in modulus and decrease in elongation at break after air ageing but the tensile strength remained almost same. Air ageing caused an increase in modulus and tensile strength and decrease in elongation at break for the filled blend vulcanisate. The blend showed better retention of tensile properties than the control ENR vulcanisates. In the binary blend XNBR imparted its good tensile and air ageing properties[73]. Since a considerable proportion of the epoxy groups reacted with XNBR during moulding, concentration of the epoxy groups available for undergoing structural changes

ageing became less.

4.4.B Acid Ageing

Both ENR gum and filled vulcanisates became brittle after acid ageing and showed a drastic reduction of elongation at break. This could be due to cyclisation taking place in ENR vulcanisates in presence of acids and hydrochlorination by the ionic addition of hydrogen chloride to the double bond[73].

The XNBR vulcanisates also were affected drastically by the acid and there was reduction of tensile strength and elongation at break. In acid medium there possibly was more degradation than crosslinking[4].

The gum blend vulcanisate showed an increase in modulus and decrease in elongation at break without any change in tensile strength. The filled binary blend showed an increase in modulus and decrease in both tensile strength and elongation at break. However, the retention of tensile properties for the filled blend was better than that of pure ENR and XNBR vulcanisates. In the blends the crosslinking reaction was predominant over the degradation reaction due to the contribution of ENR.

4.4.C Alkali Ageing

Gum ENR vulcanisate showed decrease in tensile properties, while the filled ENR vulcanisate showed an

increase in modulus and a decrease in tensile strength and elongation at break. Compared to acid aged ENR vulcanisates, the change in tensile properties was less. This was probably due to absence of self-crosslinking of ENR that normally occurs in presence of acids.

In gum XNBR vulcanisates the modulus increased while the tensile strength and elongation at break decreased and in filled XNBR vulcanisates there was an increase in modulus and decrease in both elongation at break and tensile strength. Here also the degradation reaction appeared prominant as compared to the crosslinking reaction[4].

The gum binary blend showed an increase in modulus and decrease in tensile strength while the filled binary blend showed tensile properties very similar to the unaged samples. Here there was no degradation probably in polymers containing ester groups crosslinked by hydrolysis[74] in presence of metal hydroxides.

5.4.3 Fuel Ageing

Gum ENR vulcanisate showed a reduction in tensile properties, while the filled ENR vulcanisate showed almost no change in modulus and decrease in both tensile strength and elongation at break. ENR vulcanisates get crosslinked during oxidation and this crosslinking reaction is catalysed by acids which are formed during oxidation of conventionally cured ENR vulcanisates.

Gum XNBR showed a decrease in tensile properties after fuel ageing. The filled XNBR vulcanisate, however, showed marginal increase in modulus and marginal decrease in both tensile strength and elongation at break. XNBR vulcanisates possess high resistance to hydrocarbons and during fuel ageing some degree of crosslinking take place by hydroperoxides formed in fuel by the dissolved oxygen[72].

The gum blend vulcanisates showed a decrease in tensile properties. However the retention in tensile properties improved in the filled blend systems. The retention of tensile strength for the gum 1:1 blend vulcanisate was superior to that of control mixes (Fig. 3.4.1). The filled blend vulcanisate showed better retention of tensile strength during air ageing, acid ageing and alkali ageing. In fuel ageing it was inferior to XNBR, but better than BNR (Fig. 3.4.2).

Table 3.4.1 : Tensile properties of agend and unaged gum vulcanisates

Sample	Conditions	Modulus, MPa 100%	200%	300%	Tensile strength, MPa	Elongation at break,%
I	Unaged	0.78	1.14	1.50	3.3	590
	Air/70°C/12d	0.81	1.22	-	1.4	250
	Acid/70°C/7d	-	-	-	6.4	15
	Alkali/70°/7d	0.77	1.10	1.40	2.1	440
	Fuel/30°C/7d	0.67	0.98	1.30	1.8	415
II	Unaged	2.17	3.63	5.5	15.1	600
	Air/70°C/12d	2.60	4.10	6.3	11.0	430
	Acid/70°C/7d	2.10	-	-	4.0	192
	Alkali/70°/7d	2.47	4.04	6.3	7.2	335
	Fuel/30°C/7d	1.92	3.00	4.6	5.7	352
III	Unaged	0.98	1.47	2.3	2.7	350
	Air/70°C/12d	1.35	-	-	2.6	190
	Acid/70°C/7d	1.90	-	-	2.98	181
	Alkali/70°/7d	1.65	-	-	2.30	155
	Fuel/30°C/7d	1.00	1.54	-	1.96	254

Table 3.4.2: Tensile properties of the aged and unaged samples (20 phr ISAF black filled mixes)

Sample	Conditions	Modulus, MPa 100%	200%	300%	Tensile strength, MPa	Elongation at break, %
	Unaged	2.10	3.86	6.2	25.5	790
	Air/70°C/12d	2.84	6.00	-	9.0	280
	Acid/70°C/7d	-	-	-	< .53	7
	Alkali/70°C/7d	2.45	4.68	7.5	17.5	580
	Fuel/30°C/7d	2.05	4.14	6.8	12.4	467
	Unaged	3.57	6.60	10.4	23.5	570
	Air/70°C/12d	4.80	10.00	16.0	23.3	405
	Acid/70°C/7d	4.34	-	-	8.0	173
	Alkali/70°/7d	4.57	9.3	-	13.4	268
	Fuel/30°C/7d	3.60	7.20	12.2	20.6	445
	Unaged	2.10	4.41	7.8	9.8	360
	Air/70°C/12d	2.84	6.80	-	11.0	280
	Acid/70°C/7d	4.60	-	-	6.6	145
	Alkali/70°/7d	2.39	5.41	9.6	9.9	307
	Fuel/30°C/7d	1.96	4.27	7.6	7.7	306

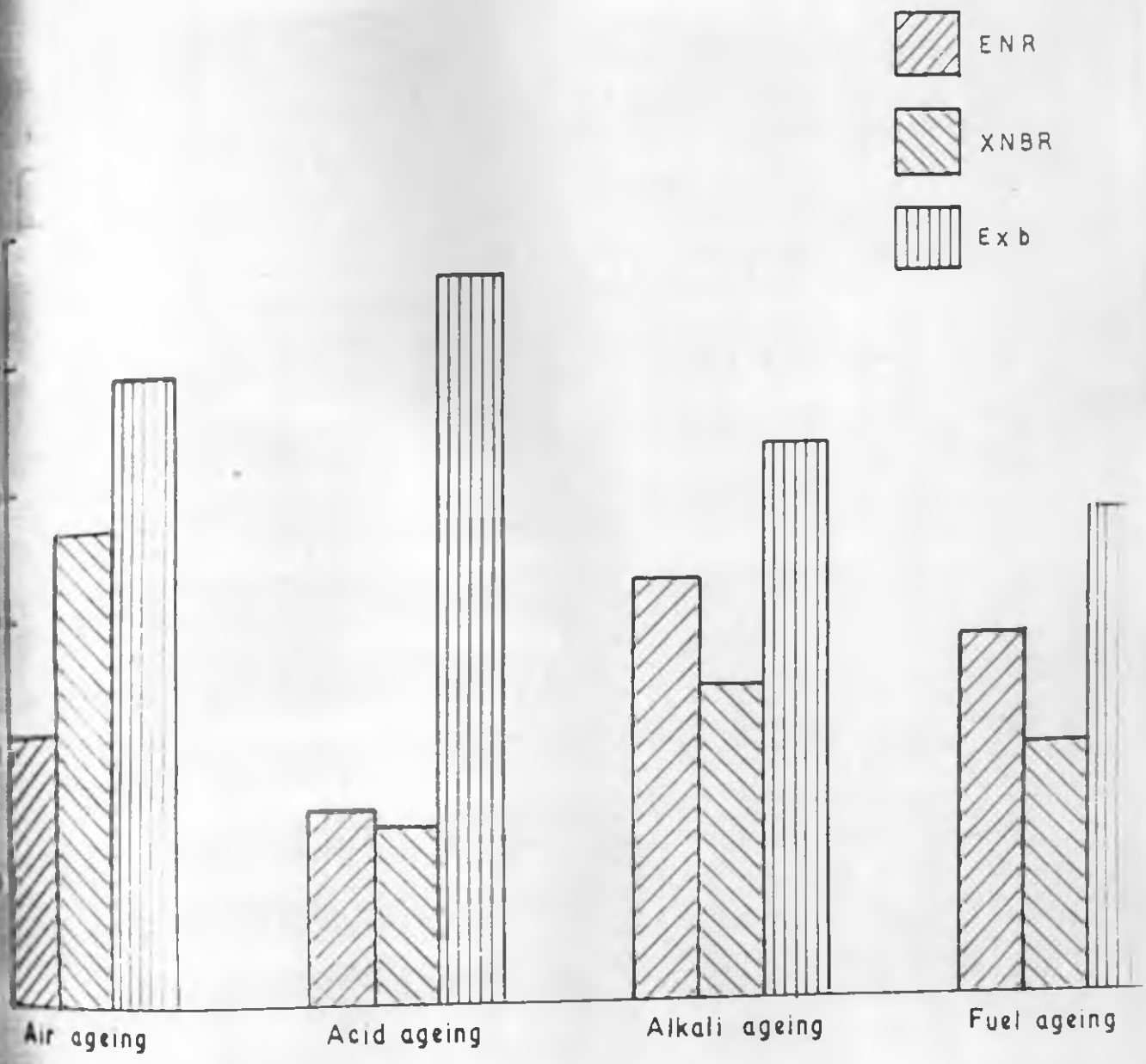

Fig. 3.4.1 : Percent retention of tensile strength for ENR, XNBR and 1:1 gum ENR-XNBR blend vulcanisates.

Fig. 3.4.2 : Percent retention of tensile strength for

REFERENCES

David R. Burfield, Kooi-Ling Lim and Kia Sang Law, J. Appl. Polym. Sci., 29 (1984) 1661.

C.S.L. Baker, I.R. Gelling and R. Newell, Rubber Chem. Technol., 58 (1985) 67.

C.T. Loo, Proc. Int. Rubb. Conf. Rubber Research Institute of Malaysia, Kuala Lumpur, 1985, 368.

H.P. Brown, Rubber Chem. Technol., 36 (1963), 931.

S.K. Chakraborty and S.K.De, J. Appl. Polym. Sci.,27 (1982) 4561.

S. Mukhopadhyay, T.K. Chaki and S.K. De, J. Polym. Sci., Polym. Lett. Ed., 28 (1990) 25.

S. Mukhopadhyay, P.P. De and S.K. De, J. Appl. Polym. Sci., 43(2) (1991) 347.

S. Mukhopadhyay and S.K. De, J. Appl. Polym. Sci., 42(10) (1991) 2773.

John E. Davey and M. John R. Loadman, Polymer,16 (1984) 134.

S. C. Ng and L. H. Gan, Eur. Polym. J. 17 (1981) 1073.

S.K. Chakraborty, A. K. Bhowmick and S.K.De, J. Appl. Polym. Sci., 26 (1981) 4011.

J. H. Bradbury and M.C.S. Perera, J. Appl. Polym. Sci., 30 (1985) 3347.

D. U. Brazier, Rubber Chem. Technol., 53 (1980) 437.

M.C.S. Perera, J.A. Elix and J.H. Bradbury, J. Polym. Sci., Part A : Polym. Chemistry, 26 (1988) 637.

I.R. Gelling and N.J. Morrison, Rubber Chem. Technol., 58 (1985) 243.

G. Socrates, in "Infrared Characteristic Group Frequencies" The Pitman Press, Bath, John Wiley and Sons Ltd., New York, Chap. 10, p. 69.

R.A. Saunder and D.C. Smith, J. Appl. Phys., 20 (1949) 953.

C. Raux, R. Pautrat, P. Cheritat, F. Ledran and J.C. Danjard, J. Polym. Sci., Part C, 16 (1969), p. 4687.

A.R.Payne, in "Reinforcement of elastomers" G. Kraus Ed., Interscience, New York, 1965, p. 92

T.Colclough, Trans. Instn. Rubb. Ind.,38 (1962) 11.

F.P. Greenspan, "Epoxidation in chemical ractions of polymers" Fetters, E. M. Ed., Interscience, New York 1964, p. 152

C.R. Cotten, Rubber Chem. Technol., 45 (1972) 129.

A.E. Juve, in " Vulcanization of Elastomers : Principles and Practice of Vulcanisation of Commercial Rubbers", G.Alliger and I.J.Sjothum, Ed., Reinhold Publishing corporation, USA 1964, p. 30

Miroslav Behal and Vratislav Duchacek, J.Appl. Polym. Sci., 35 (1983) 507.

S.U. Zhang, Rubber Chem. Technol., 57 (1984) 755.

M.M. Reznikoiskii and G.L. Brodskii in "Abrasion of Rubbers" D.I. James Ed., Maclaren,London, 1967, p.64 and p.81

A.K. Bhowmick, Rubber Chem. Technol.,55 (1982) 1055.

Sabu Thomas, Wear 116 (1987) 201.

M.M. Mathew and S.K.De, J. Mat. Sci., 18 (1983) 515.

A.N. Gent and C.T.R Pulford in "Development in polymer fracture-I", E.H. Andrew Ed., Applied science, London, 1979, p.155

G. Kraus, J. Appl. Polym. Sci., 7 (1963) 861.

S.K. Chakraborty and S.K.De, Rubber Chem. Technol., 55 (1982) 990.

C.S.L Baker, I.R. Gelling and Azemi Bin Samsuri, J.Nat. Rubb. Res.,1(1986) 135.

T.L. Smith, J. Polym. Sci., Part A1 (1963) 3597.

T.L. Smith, J. Polym. Sci., 32 (1958) 99.

W.W. Greensmith, J. Appl. Phys., 3(8) (1960) 183.

R.F. Landel and R.F. Fedors, Proc. Int. Conf. Fract. 1st, Sendai, 2 (1966) 1247.

N. Roy Choudhury and A. K. Bhowmick, J. Mater. Sci., 25 (1990) 161.

Chanchal Neogi, S.P. Basu and Anil K. Bhowmick, J. Mater. Sci., Lett., 9 (1990) 1379

A.K. Grosch, J.A.C. Harwood and A.R. Payne, Nature, 212 (1966) 497.

A.N. Gent, in "Elastomers : Criteria for Engineering Design", Eds. C. Hepburn and R.J.W. Raynolds, Applied Science Publishers Ltd., London, 1979, Chap. 5, p. 57.

A.N. Gent, Rubber Chem. Technol., 36 (1963) 397, 697.

G.R. Cotten and B.B. Boonstra, J. Appl. Polym. Sci., 9 (1965) 3395.

A. Voet, A.K. Sircar and F.R. Cook, Rubber Chem. Technol., 44 (1971) 175, 185.

G.M. Bartenev and N.M. Lyalina, Vysokomol. Soed., A-12 (1970) 368, 922.

G.M. Batenev, A.A. Valishin and I.I. Panchuk, Vysokomol Soed, A-19 (1977) 187.

G.M. Bartenev, L.A. Sheklovnikova and L.A. Akopyan, Mekhanika Polimerov, 1 (1973) 151.

C.I. Mackenzie and J. Scanlan, Polymer, 25 (1984) 559.

Per Flink and Begnt Slenberg, British Polymer Journal, 22 (1990) 193.

T. Kusano and K. Murakami, J. Polym. Sci., Polym. Chem. Ed., 10 (1972) 2823.

S.S. Bhagwan, D.K. Tripathy and S.K. De, J. Appl. Polym. Sci., 33 (1987) 1623.

A. Saha Deuri, P.P. De, A.K. Bhowmick and S.K. De, Polymer Degrn. Stability, 20 (1988) 135.

Takayaki Murayama, "Dynamic Mechanical Analysis of Polymeric Material", Elsevier Scientific Publishing Company, Amsterdam, 1978, p. 12.

L.E. Nielsen, "Mechanical Properties of Polymers and Composites", Marcel Dekker, New York, 1974.

P.P.A. Smit, Rheol. Acta., 5 (1966) 277.

F.R. Schwarzl, H.W. Bree, C.J. Nederveen, G.A. Schwippert, L.C.E. Striuk and C.W. Vander Waal, Rheol. Acta., 5 (1966) 270.

T.T. Aklonis, W.J. Macknight and M. Shen, "Introduction to Polymer Viscoelasticity", Wiley, New York, 1972.

G. Kraus, J. Polym. Sci., Polym. Phys. Edn., 8 (1970) 601.

A.I.Medalia, Rubber Chem. Technol., 47 (1974) 411.

Sonja Krause in "Polymer Blends", Vol. 1, ed. D.R.Paul and S. Newman, Academic Press, Inc., New York, 1978, Chap. 2.

J.H. Hilderbrand and R.L. Scott, "The solubility of non-electrolytes", Van Nostrand-Reinhold, Princton, New Jersey, 1950, reprinted, Dover, New York, 1964.

J.H. Hilderbrand and R.L. Scott, "Regular solutions", Prentice-Hall, Englewood, Cliffs, New Jersey, 1962.

Olagoke Olabisi, Lloyd M. Robeson and Montgomery T. Shaw, "Polymer-polymer Miscibility, Academic Press, Inc., New York, 1979, Chap. 4.

N. Yoshimura and K. Fujimoto, Rubber Chem. Technol., 42 (1969) 1009.

P.J. Corish, Rubber Chem. Technol., 40 (1967) 324.

Harry Burrell, "Solubility parameter for film formers", presented to the American Chemical Society meeting in Cincinnati-Ohio, April 1955.

K.K. Yuen and J.B. Kinsinger, Macromolecules, 1(3) (1974) 329.

G. Meinel and A. Peterlin, J. Polym. Sci., B3 (1965) 1059.

Sania Akhtar, Prajna P. De and Sadhan K. De, Materials Chemistry and Physics, 12 (1985) 235.

Sania Akhtar, Dipak K. Setua, Prajna P. De and Sadhan K. De, Polymer Degradation and Stability, 10 (1985) 299.

Hans George Elias, 'Macromolecules, synthesis and materials' Plenum Press, New York, Vol. II, p. 843.

L.I. Sergunova, A.I., Andreeva and A.A. Dontsov, Kauchuk i Rezina., 5 (1988) 18.

E., Schoenberg, H.A. Marsh, S.J. Walters and W.M. Saltman, Rubber Chem. Technol., 52(11) (1979) 577.

S.T. Semegen and J.E. Wakelin, Rubber Age, 71 (1952) 57.

CHAPTER 4

SELF-VULCANISABLE RUBBER BLENDS BASED ON EPOXIDISED NATURAL RUBBER (ENR) AND POLYCHLOROPRENE RUBBER (CR)

• This part of the work has been published in Kautschuk Gummi Kunststoffe 44 (4) (1991) 333

Epoxy resins have been reported to cure polychloroprene (CR)[1]. Hence, it was thought that epoxidised natural rubber (ENR) could be used for crosslinking polychloroprene. The present investigation has been undertaken with the following objective in mind : preparation of self-crosslinkable rubber-rubber blend of ENR and CR.

This chapter deals with the characterisation of ENR-CR blend by Monsanto rheometry, IR spectroscopy, differential scanning calorimetry, swelling studies and determination of physical properties. The chapter also reports the results of studies on the effect of moulding temperature, addition of filler on the technical properties and dynamic mechanical properties of the blend.

4.1 Monsanto Rheometry

The formulations of the mixes are shown in Table 4.1

The rheographs of the blends of polychloroprene and epoxidised natural rubber (ENR) are shown in Figure 4.1. Polychloroprene alone has been reported to undergo thermovulcanisation[2]. It is not known whether thermovulcanisation of polychloroprene will take place in the presence of functionally active rubbers like ENR. In a blend of polychloroprene and a rubber which does not contain active functional groups (for example, natural rubber), rise in isometric torque, if any, in the blend, will be due to thermovulcanisation of polychloroprene only. Accordingly, for

comparison we have taken rheographs of blends of polychloroprene and natural rubber. The blend compositions of polychloroprene-natural rubber system were chosen to be the same as the polychloroprene-ENR system. It is believed that in the same blend composition rheometric torque rise in polychloroprene-natural rubber system corresponds to thermovulcanisation alone while in the case of the polychloroprene-ENR system the torque rise corresponds to thermovulcanisation of polychloroprene as well as self-vulcanisation between polychloroprene and ENR. At a particular curing time the difference in the two torque values will correspond to the torque due to self-vulcanisation. The calculated rheographs thus obtained are shown in Fig. 4.2. The progressive rise in rheometric torque showed that crosslinking reaction occurred between blend constituents during high temperature moulding.

The very long scorch time for the CR-ENR blends showed good processing safety. The Mooney viscosity and scorch time values are shown in Table 4.1.

4.3 Physical Properties

The physical properties of the gum blends are shown in Table 4.2. Higher proportion of polychloroprene in the blend resulted in improved physical properties. The stress-strain curves are shown in Fig. 4.3. The modulus increased with increase in polychloroprene content. As the proportion of polychloroprene in the blend increased, compression set,

abrasion loss and heat build-up decreased.

4.3 Swelling

Although both ENR and polychloroprene are known to be soluble in chloroform, the moulded blend was insoluble in the same solvent showing thereby that each blend constituent got crosslinked by the other during moulding. The weight loss after 48 h. of immersion in chloroform was less than 15% for the blends showing that during vulcanisation , both ENR and polychloroprene got crosslinked to a large extent. This was also evident from V_r (volume fraction of rubber in the swollen vulcanisate), shown in Table 4.2. The crosslink density which could be regarded as proportional to V_r was high when the polychloroprene content was high.

4.4 IR Spectroscopy

The characteristic absorption peaks of ENR and polychloroprene are shown in Table 4.3 and the corresponding IR spectra is shown in Fig. 4.4. The broad peak around 860 cm^{-1} in CR is contributed by absorption due to trans 1,4 polychloroprene unit[3].

Pure ENR showed absorption at 870 cm^{-1} and 1245 cm^{-1} due to epoxy group and at 885 cm^{-1} for cis double bond. In addition there was absorption at 1114 cm^{-1} due to aliphatic C-O and at 1065 cm^{-1} due to tetrahydrofuran[5]. It is known that epoxidation reaction is very difficult to be controlled and that epoxide rings open to form furan

rings[6,7].

The difference spectrum of binary blend -ENR-CR is shown in Fig. 4.4. The difference spectrum showed absorption in the range 1030-1270 cm^{-1} due to aliphatic ethers[4]. The absorption at 1203 cm^{-1} could be due to C-O stretching of vinyl ethers and absorption at 1162 cm^{-1} could be due to cyclic ethers having more than five members. The absorption at 1140 cm^{-1} was attributed to ether formation.

It is known that in presence of acids the epoxy groups undergo cyclisation[6,7]. The thermovulcanisation of polychloroprene has been reported by Duchacek et al[2]. During crosslinking of ENR and CR, ether crosslinks are formed by reaction of epoxy and allylic chlorine along with cyclic ethers. A probable crosslinking reaction between ENR and CR is shown in Fig. 4.5.

4.5 Effect of Filler on the Technical Properties of the Blend

The rheographs of the filled blends are shown in Fig. 4.6. The physical properties of the 1;1 blend filled with 20 phr of ISAF black moulded at 180°C are shown in Table 4.2. The observed incorporation of carbon black greatly improved the properties of the gum compound. There is an increase in crosslink density due to specific interaction between rubber matrix and filler. The physical properties are governed by factors like rubber-filler interaction[8], the nature of crosslinks[9] and distribution of carbon black in the different phases. The migration of carbon black in the two phases

[illegible]ration of carbon black in the two phases depends on [illegible]tors like viscosity and unsaturation of polymers and [illegible]ller characteristics[11]. It has been reported that [illegible]steresis behaviour improves by unequal distribution of [illegible]ller[12,13] and also by an increase in crosslink density. [illegible] decrease in heat build-up observed for the filled [illegible]ary blend was due to the combined effect of these two [illegible]tors. As will be seen later, the distribution of filler [illegible] more unequal as the ratio of CR in the blend increased. [illegible]pression set, hardness and the failure properties were also [illegible]proved by the addition of filler.

[illegible] Dynamic Mechanical Properties

Dynamic storage modulus or elastic modulus (E'), [illegible]mic viscous modulus or loss modulus(E'') and mechanical [illegible]ping ($\tan \delta$) at different compositions are shown in [illegible]gures 4.7 to 4.9. The temperature corresponding to maximum [illegible]ping and maximum viscous modulus, were taken as T_g s. The [illegible] of the samples thus obtained are shown in Table 4.4. [illegible] the T_g region as a general trend loss modulus and damping [illegible]creased until they attained their maxima and then dropped [illegible] increase in temperature whereas the dynamic storage [illegible] dropped rapidly. Neat ENR showed single transition in [illegible] region. Neat CR showed two transitions in the rubbery [illegible] as reflected from plots of damping and elastic [illegible]. For CR there was a sharp transition in the elastic [illegible]ound -46°C and a slow second transition around -13 [illegible]°C. In the plots of damping versus temperature the

maximum damping occurred at -29°C.

In CR the first sharp transition observed in damping and elastic modulus could be ascribed to transition from the glassy to the rubbery state, and the second transition to the melting of the crystallites in the polymer. CR has been reported to contain about 90% trans 1,4 configuration[14]. Development of crystallinity at low temperatures for elastomers which are substantially amorphous at room temperature has been reported earlier[15].

In blends of CR and ENR, considerable broadening of the T_g zone occurred. This showed that there was microlevel inhomogeniety or partial miscibility for the blends. When the CR content was more, the transition to rubbery region started at a lower temperature. In blend NEa the damping was high in the region -27°C to +1°C. However, maximum damping was observed at -27°C. In NEb blend vulcanisate the maximum damping was observed at -15°C. The transition in elastic modulus occurred in a wider range of temperature, -43 to -6°C for NEa. This wide temperature range of transition in the Tg region was also observed in the loss modulus plots of the blends. Thus the blends showed high damping over a wide range of temperature depending on the blend ratio. The dynamic mechanical data is summarised in Table 4.4.

Fig. 4.10 shows the dynamic mechanical behaviour of thermovulcanised CR and HCl catalysed self-crosslinked ENR. Tg of crosslinked ENR was -1°C and thermovulcanised CR was

-37°C, which were close to the Tg s of the corresponding conventionally cured vulcanisates. Since the Tg's of the rubbers vulcanised by two methods did not differ appreciably, it was difficult to characterise the individual rubber phases. Accordingly, it could be proposed that the vulcanisate network structure was composed of : thermovulcanised polychloroprene, self-vulcanised ENR/CR blend, and crosslinked ENR.

Fig. 4.11 shows the effect of 20 phr loading of carbon black in the 3;1 CR -ENR blend on damping characteristics. Incorporation of 20 phr loading of carbon black caused high damping over a wider range of temperature with a maximum at -37°C, showing that filler affects miscibility of the system. Since ENR is less viscous than CR, carbon black is likely to migrate preferentially to ENR phase.

Fig. 4.12 shows the effect of addition of filler on the damping behaviour of the 1:1 blend. Here the broadening of Tg was over a lesser temperature range. Though the possible vulcanised network structure consisted of thermovulcanised polychloroprene, self-vulcanised ENR and CR and self-crosslinked ENR, there was only a single transition.

Extensive investigations of the morphology of carbon black[16-19] have shown that a persistant, irreversible primary structure originated from reticular particle aggregates, which appeared to be fused together in the formative stage of carbon black at the extremely high temperature in the

surface. Investigations by Medalia[20] and Kraus[21] have shown that polymer occluded within the internal void of the primary structure aggregate was not free to fully share the microscopic deformation of carbon black filled rubber. Some investigators[22,23] identified this immobilized rubber with 'bound rubber' measured by solvent extraction, whereas others, through microscopic study[24,25] modulus[26] and tensile measurements[27-29], indicated the existance of a shell of immobilized rubber of definite thickness around the vulcanisate. Medalia[30] suggested that the independent nature of occluded rubber, bound rubber and shell rubber might result in the overlapping of each other forming a complicated interlinked system. Thus, filled polymers constituted a system with a complex structure of two components, the absorbed hard rubber and the bulk rubber. The absorbed, hard, immobilized rubber would cause a perturbed relaxation response and the character of these layers would shift towards the glassy state. The tan δ peak could be ascribed to the glass transition relaxation of the bulk rubber and thus the tan δ peak decreased on introduction of carbon black. A shift of relaxation spectra to higher temperature with the addition of reinforcing filler has been reported by many workers[31-33]. The broad maxima could be attributed to the superposition of different relaxation processes. A similar observation of reduction of tan δ peak height and broadening of transition zone was observed in self-vulcanised blends of ENR and Hypalon[34]. The plots of loss modulus versus temperature for the filled binary blends are shown in

figures 4.13 and 4.14. It was seen that though there was single transition, the transition zone was broadened after addition of filler.

The Fig. 4.15 shows plots of elastic modulus versus temperature for the NEa system. In the glassy region modulus of CR was higher than that of ENR. The binary blend showed elastic modulus very close to that of ENR. Addition of filler increased the elastic modulus of the gum blend till room temperature, beyond which the modulus dropped. Filler in general increased the elastic modulus. The higher elastic modulus of CR vulcanisates in the rubbery region could be due to the crystallinity of the CR . Fig. 4.16 shows the plots of elastic modulus versus temperature for the filled 1:1 binary blend. Filler increased the modulus in the transition region, similar to the behaviour shown by CNEa blend.

DSC thermograms shown in Fig. 4.17 give additional support for the partial miscibility of ENR-CR blend vulcanisate. Blends exhibited a single T_g which shifted to a higher temperature as CR content increased. As observed in the case of DMA results here also, the T_g zone became broadened in the case of blends. This broadening showed partial miscibility of the components in the blend. Radivoje Vukovic et al.[35] while studying compatibility of poly(2.6 dimethyl 1,4-phenylene oxide) / poly(fluorostyrene-co-chlorostyrene) have observed that there is increase in T_g width of DSC thermograms with blend composition till there is phase separation.

Table 4.1 : Formulations[a] and Processing Characteristics

	NEa	NEb	CNEa	CNEb
Polychloroprene	75	50	75	50
NR	25	50	25	50
HAF black	-	-	20	20
Minimum Mooney viscosity at 120°C	38	31	42	36
Mooney scorch time at 120°C, min	38	132	29	72

[a] figures in parts by weight

Table 4.2 : Physical properties of the blends moulded at 180°C for 60 minutes

	Blend designation		
	NEa	NEb	CNEb
Modulus 300%, MPa	1.8	1.1	4.0
Tensile Strength, MPa	5.7	3.8	11.3
Elongation at break, %	460	570	600
Tear strength, kN/m	16.8	13.0	30.0
Hardness, shore A	41	30	50
Resilience at 40° C, %	55	55	40
Compression set, 22hrs at 70°C, %	4	11	8
Heat build-up by Goodrich flexometer			
(a) ΔT, °C.	14	a	3.6
(b) Dynamic set %.,	1	a	2.4
Abrasion loss, cc/hr	1.1	4.8	2.6
Volume fractoin, V_r	0.14	0.05	0.12

a sample blown out in the 10th minute.

Table 4.3 : IR Peak Assignments

Band No. cm^{-1}	Functional group	Assignment of band	ENR	CR	Blend-ENR-CR	Reference
1710-1730	Carboxyl	C=O str.	1728	-	-	4
1245	Epoxy	C-O str.	1245	-	-	4
Around 1114 (1040-1150)	aliphatic ether	assym. C-O str.	1114	-	1120	4
Around 1162	Cyclic ether more than 5 membered rings	assym. C-O str.	-	-	1162	4
1065-1070	Tetrahydro-	ring strt.	1065	-	-	5
865-875	cis epoxides	ring vibrn.	873	-	-	4
885	cis double bond	C=O str	885	-	885	4
Around 840	trans 1,4 polychloro-prene	C-Cl strt.	-	860	-	3

Table 4.4 : Damping and loss modulus, obtained from dynamic mechanical analysis with a frequency of 3.5 Hz.

Sample	Damping tan δ (max)	Tg, °C	
		Damping	Loss modulus
[illegible][a]	0.42	-29	-37
[illegible][b]	1.02	-29	-36
[illegible][c]	2.13	- 5	-13
[illegible][d]	1.40	-1	-12
[illegible]	0.55 to 0.33	-27 to -1	-35
[illegible]	0.62	-17	-21
[illegible]	0.40 to 0.30	-17 to +30	-22
[illegible]	0.62	-1	-21

a = Conventionally vulcanised polychloroprene (Ch.5)
b = Thermovulcanised polychloroprene
c = Conventionally vulcanised ENR (Ch.5)
d = acid catalysed self-crosslinked ENR

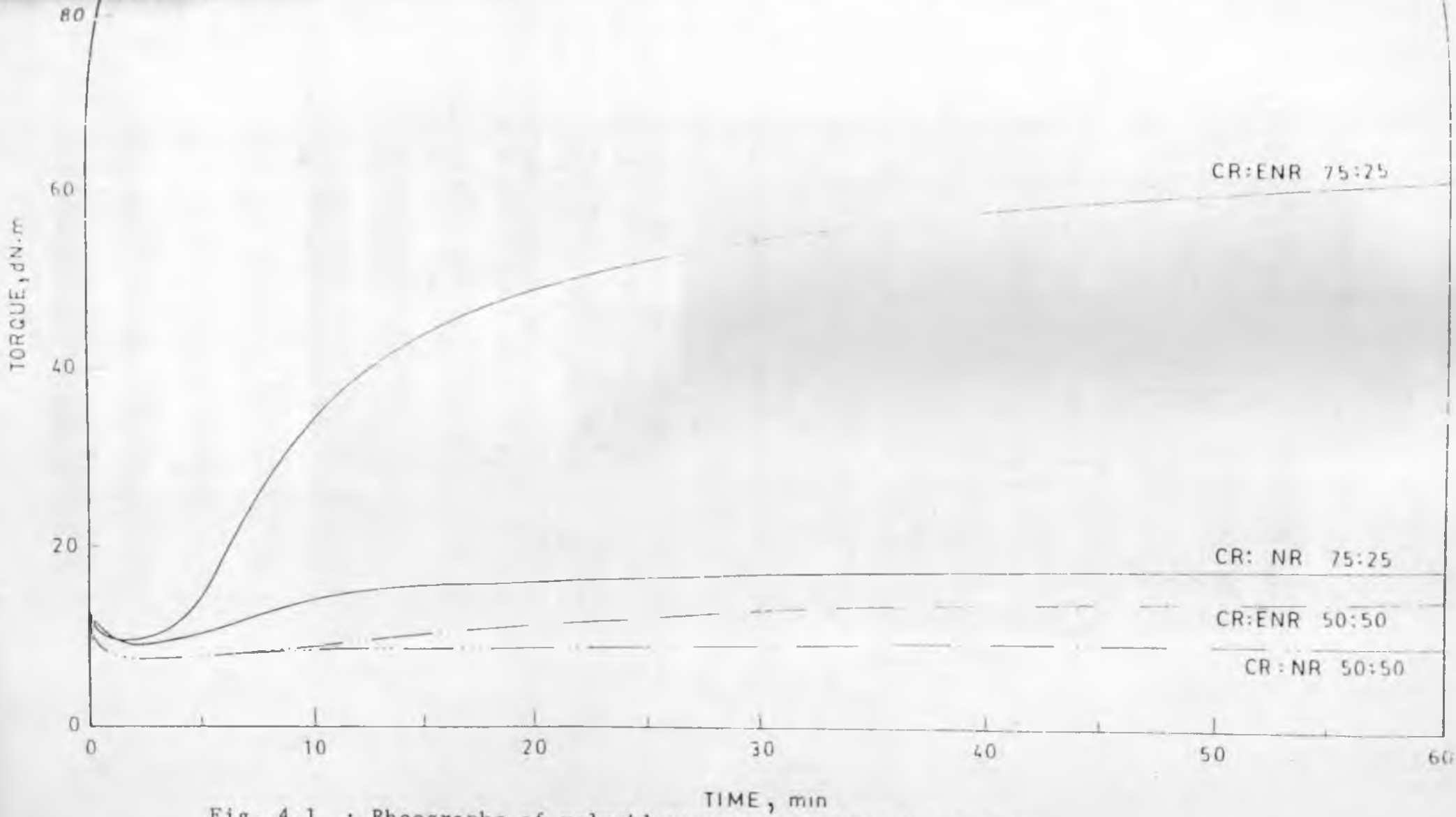

Fig. 4.1 : Rheographs of polychloroprene-epoxidised natural rubber and polychloroprene-natural rubber blends at 180°C.

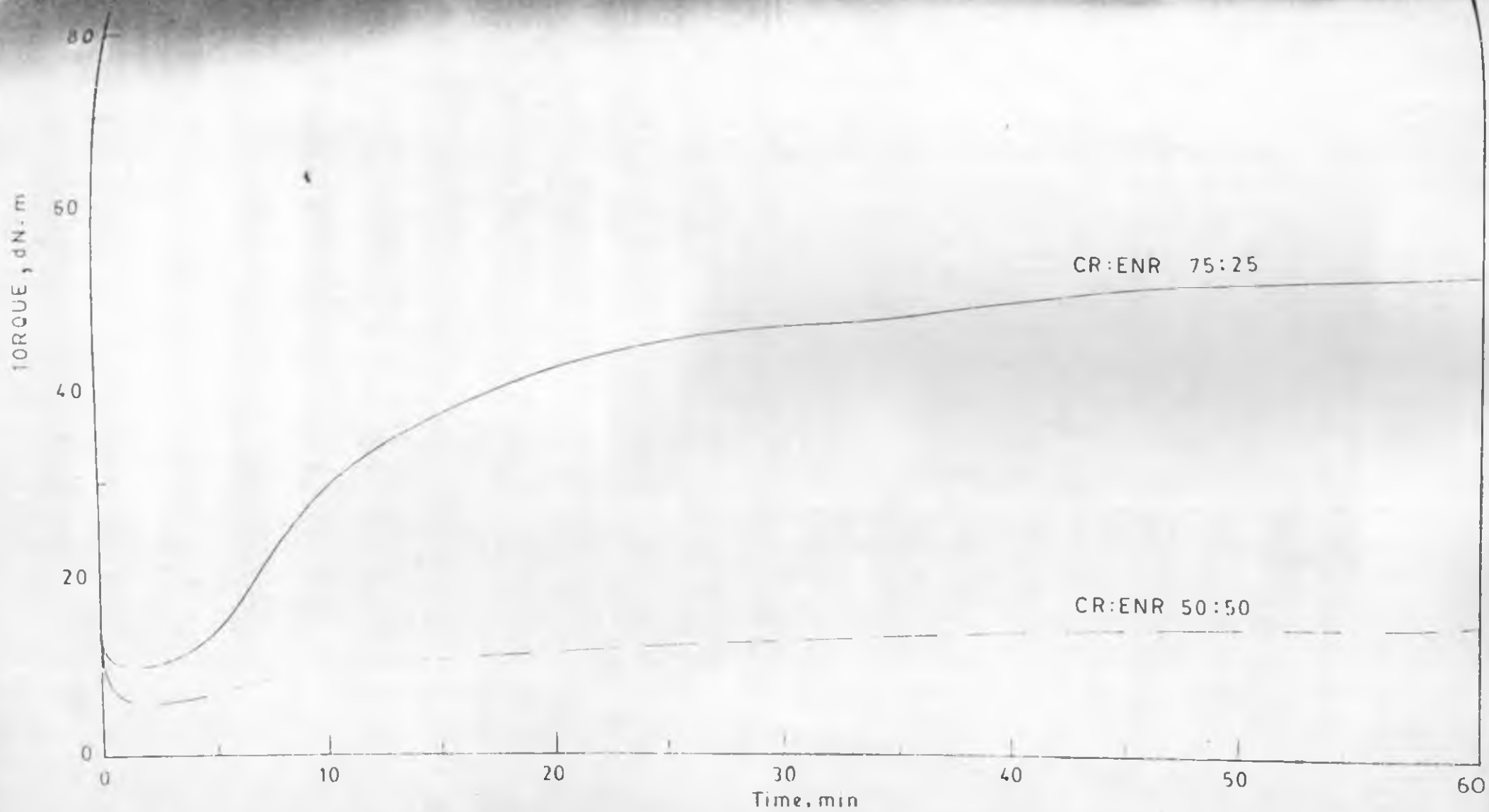

Fig. 4.2 : Calculated rheographs of the self-vulcanisable CR-ENR blend after deducting the effect due to thermovulcanisation of polychloroprene.

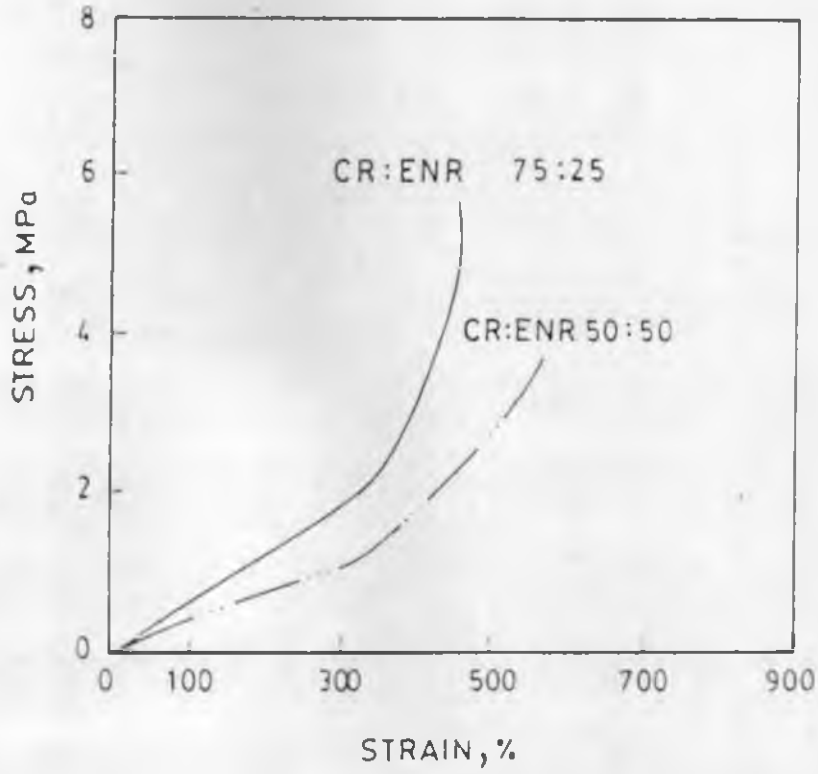

FIG.- 4.3. Stress strain curves of blends of CR and ENR.

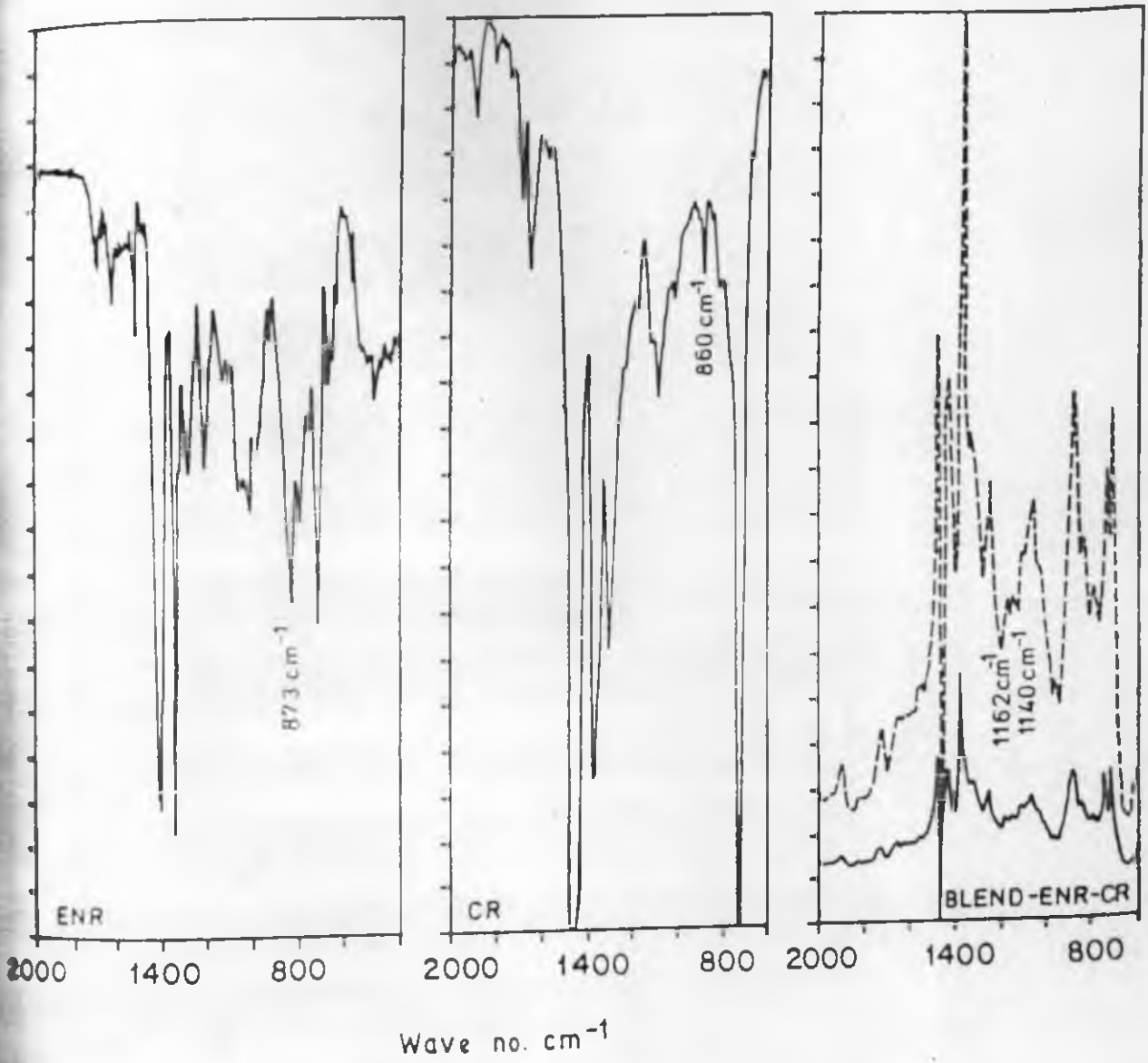

Fig.4.4. : IR spectra of thin films of ENR, XNBR and the defference spectrum(blend-ENR-CR)

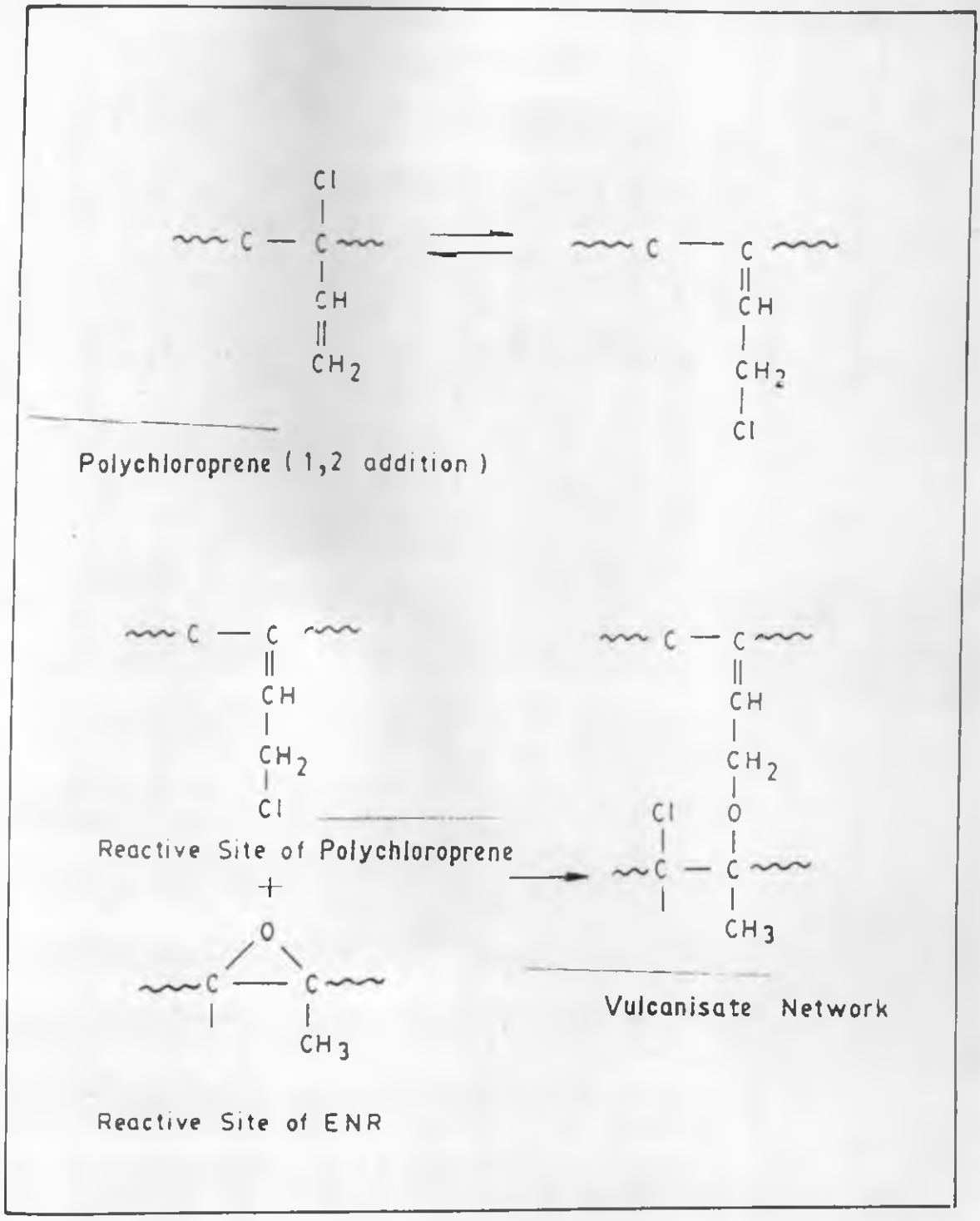

Fig. 4.5 : Possible cross linking reaction between polychloroprene and ENR.

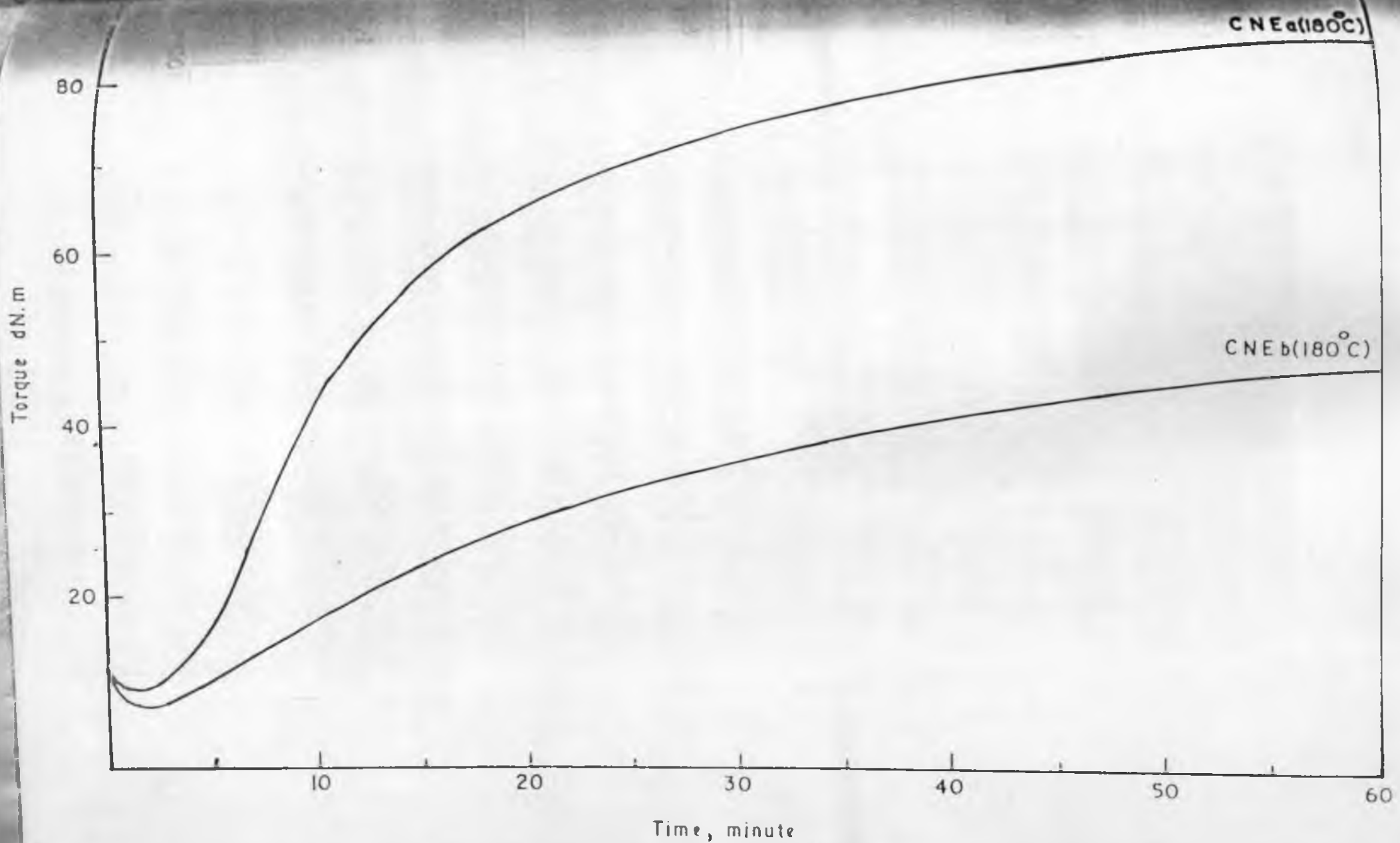

Fig. 4.6 : Rheographs of the CR-ENR blends filled with 20 phr of ISAF black.

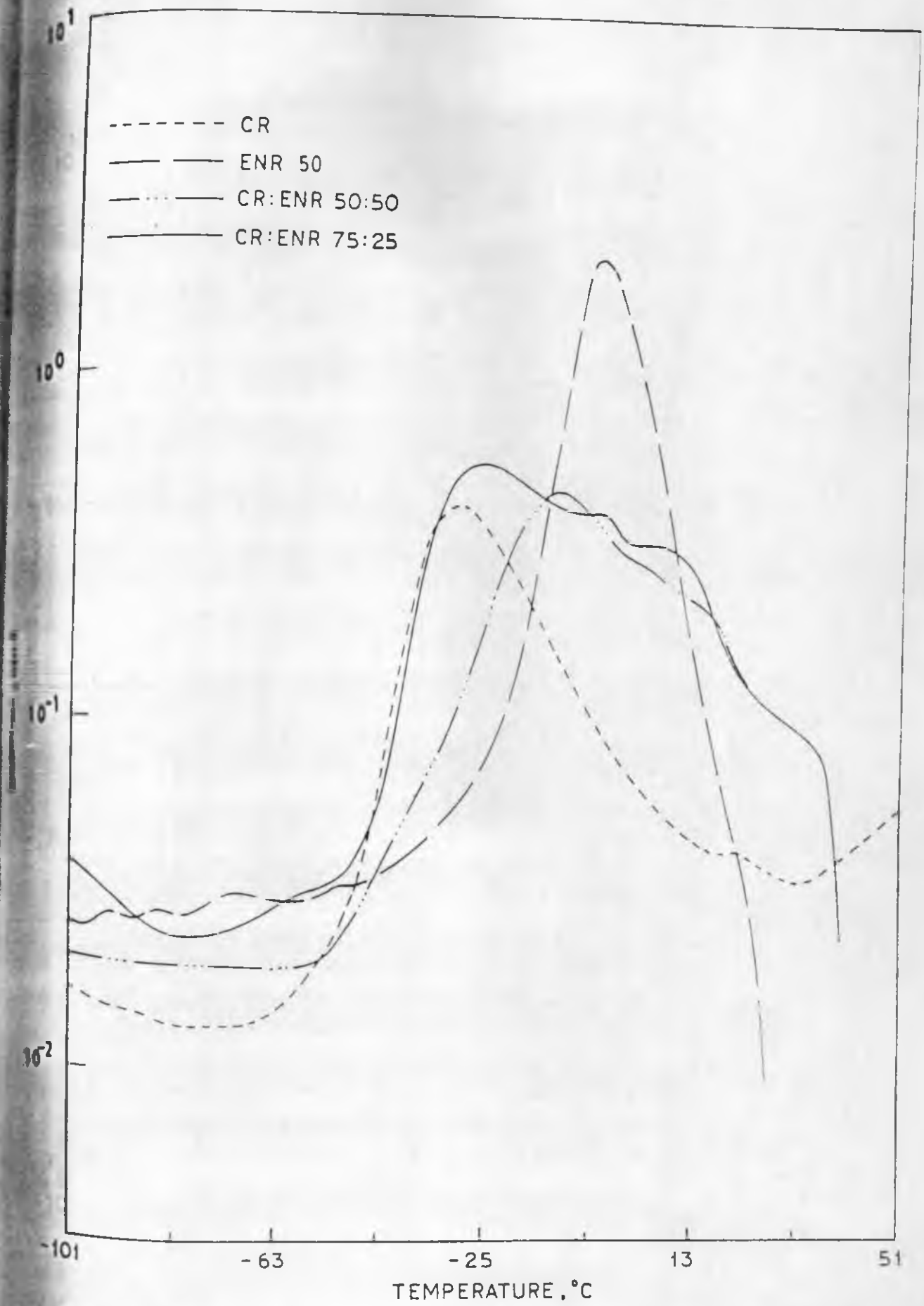

FIG.- 4.7 : Plots of damping (tan δ) versus temperature for CR, ENR and blends of CR and ENR.

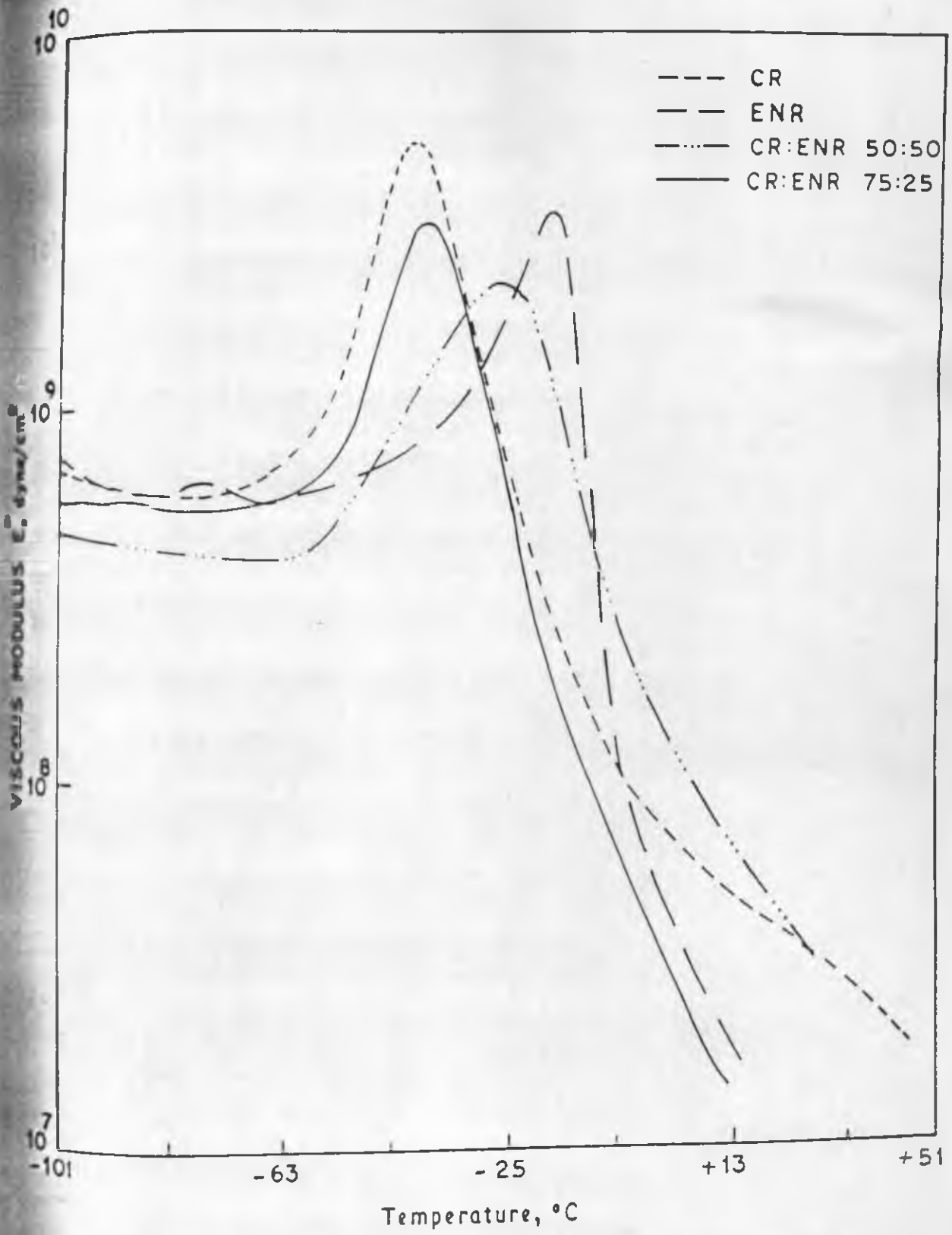

FIG.-4.8 PLOTS OF VISCOUS MODULUS VERSUS TEMPERATURE FOR CR, ENR AND BLENDS OF CR AND ENR

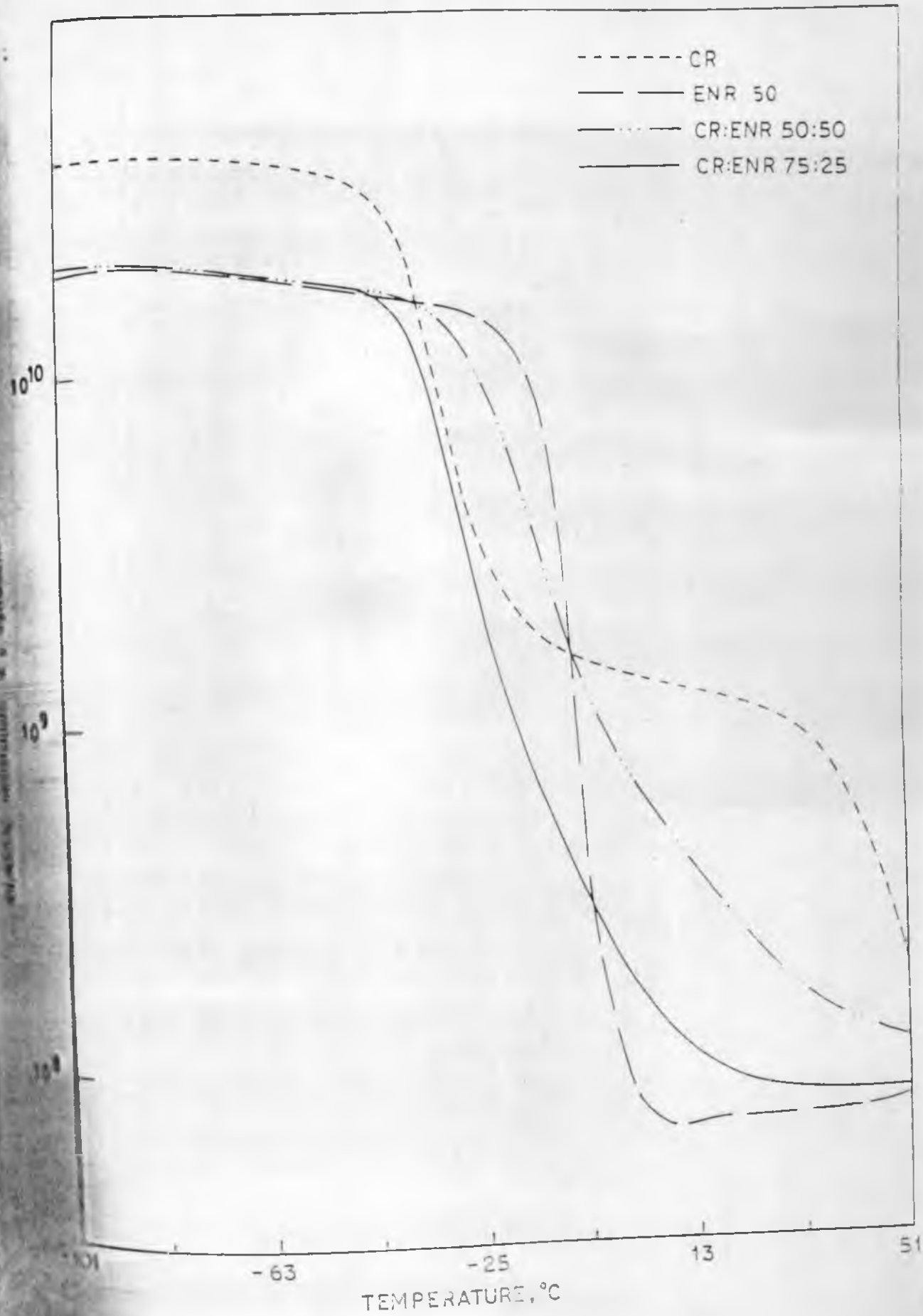

FIG.- 4.9 : Plots of elastic modulus versus temperature for CR, ENR and blends of CR and ENR.

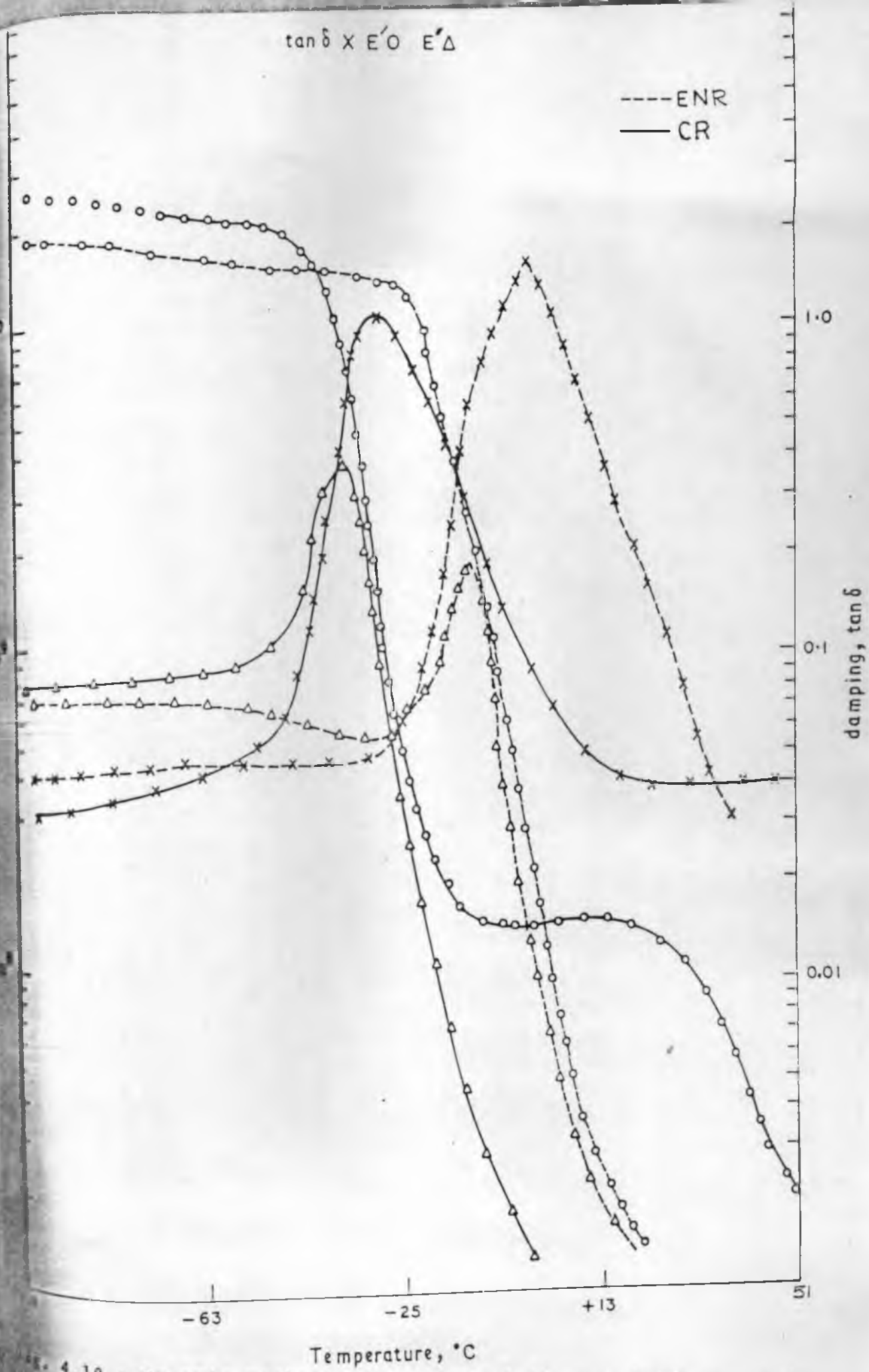

Fig. 4.10 : Dynamic mechanical spectra of thermovulcanised polychloroprene and HCl catalysed crosslinked ENR.

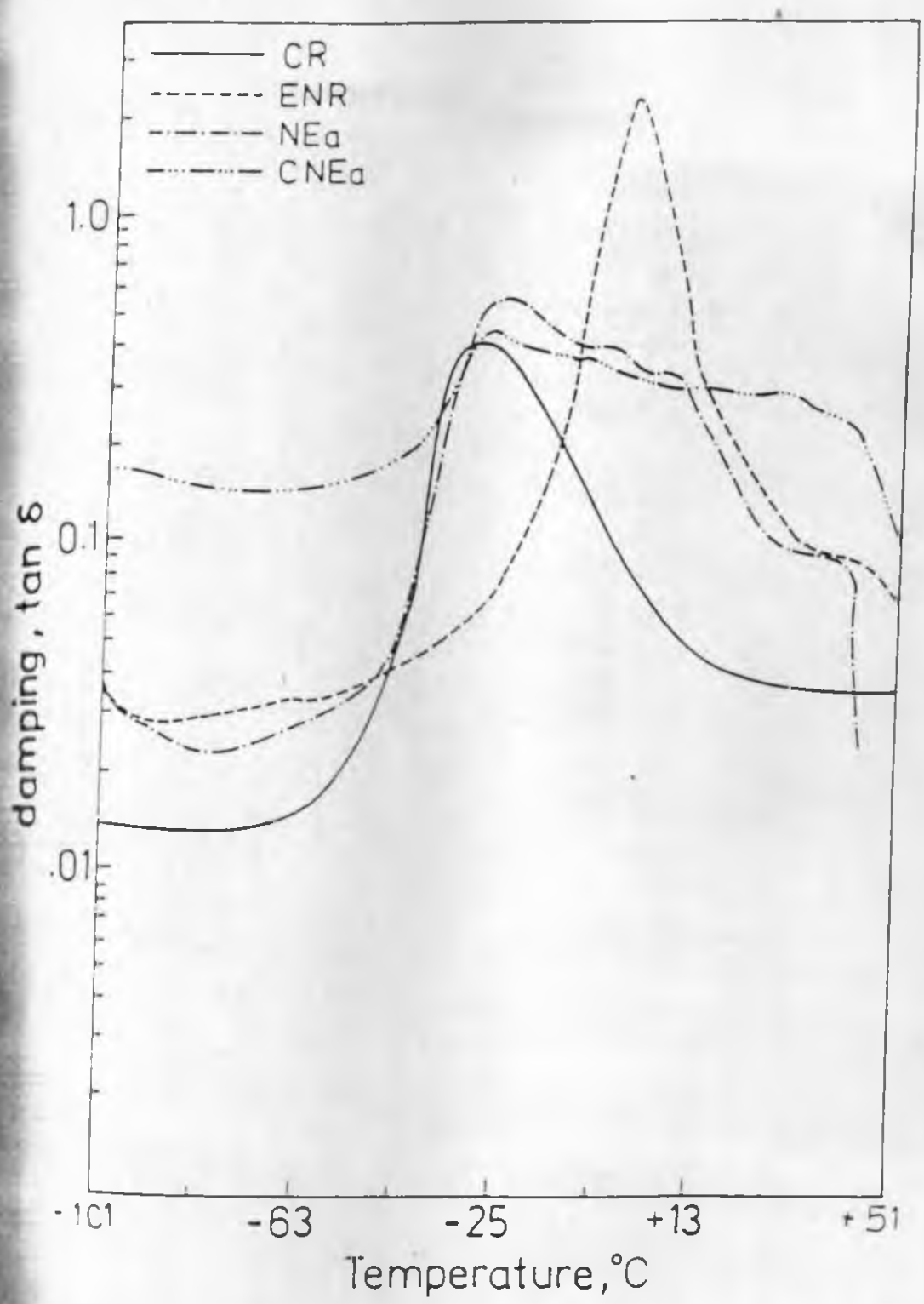

Fig. 4.11 : Plots of damping versus temperature for CR, ENR and the gum and filled 3:1 CR-ENR blend.

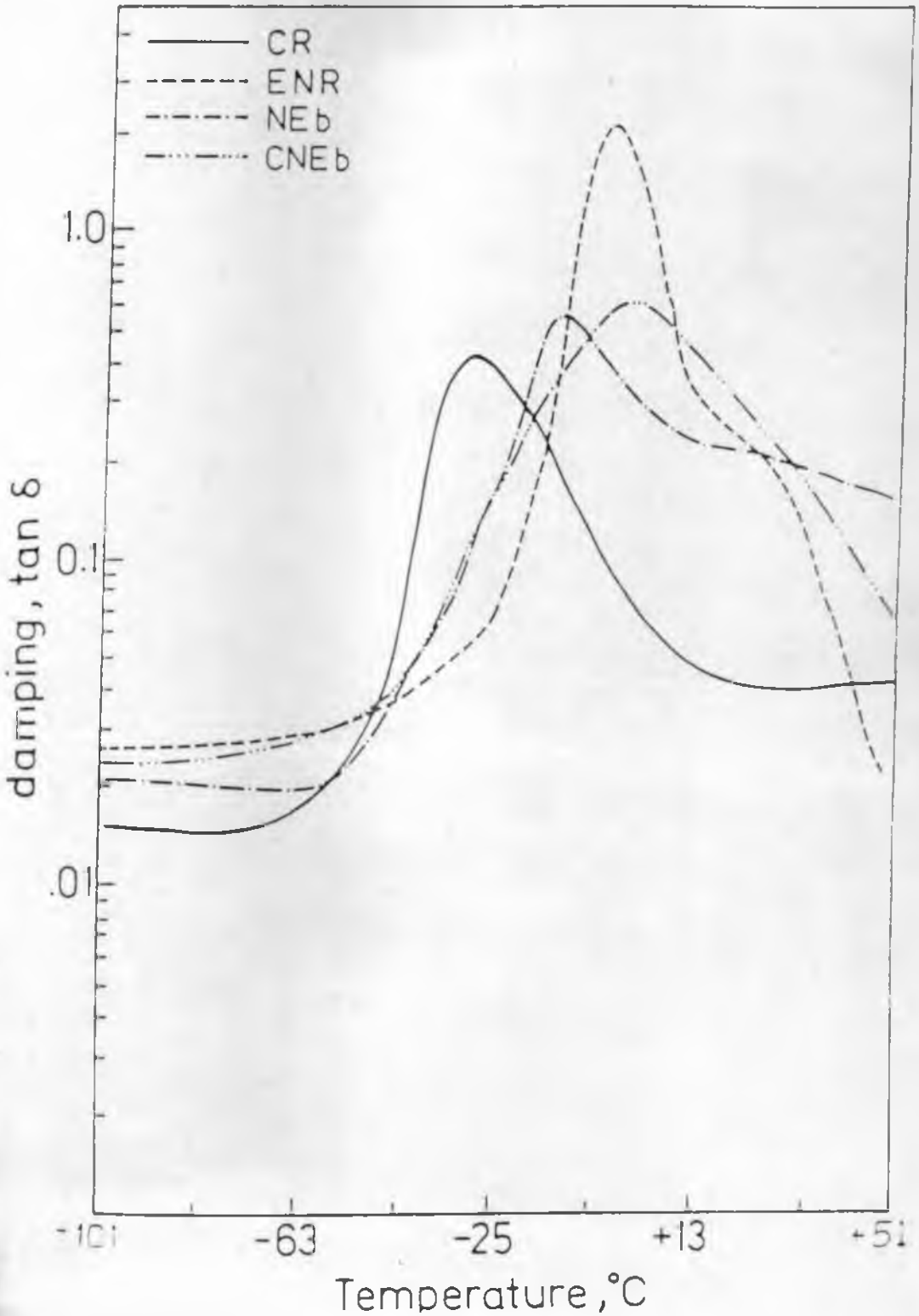

Fig. 4.12 : Plots of damping versus temperature for CR, ENR and the gum and filled 1:1 CR-ENR blend.

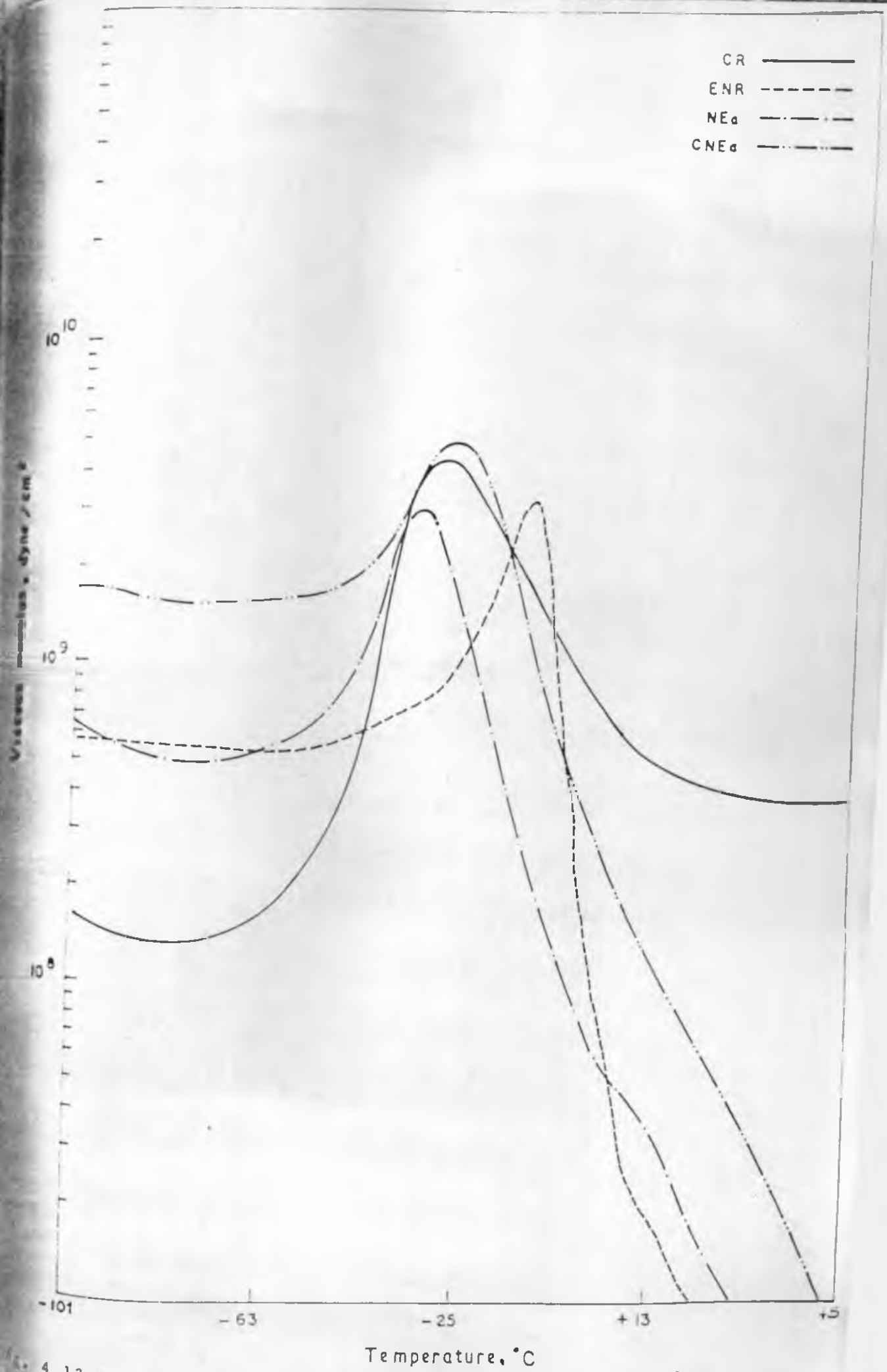

Fig. 4.13 : Plots of viscous modulus versus temperature for ENR, CR and the gum and filled 3:1 CR-ENR blend

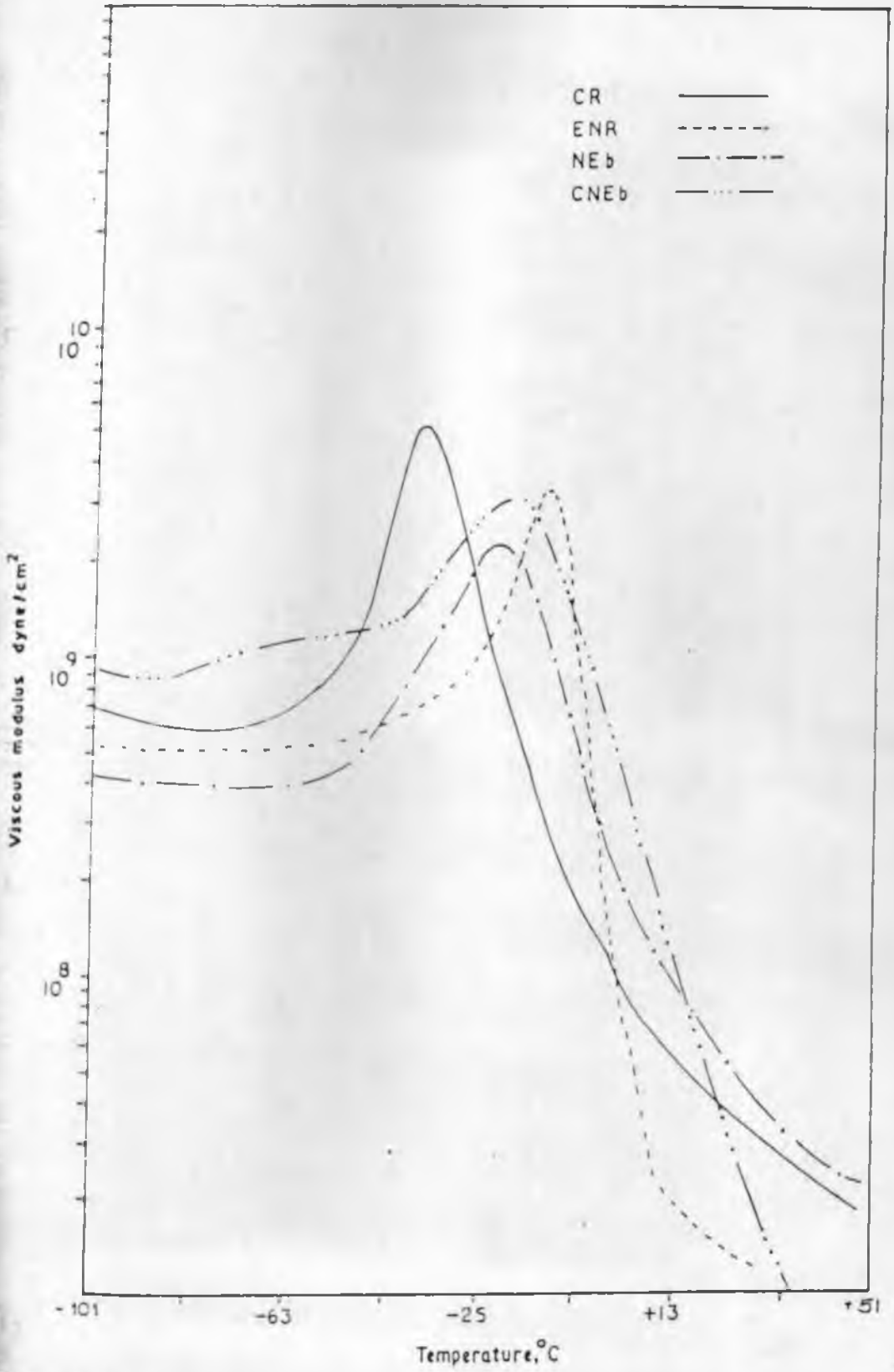

Fig. 4.14 : Plots of visscous modulus versus temperature for ENR, CR and the gum and filled 1:1 ENR-CR blend.

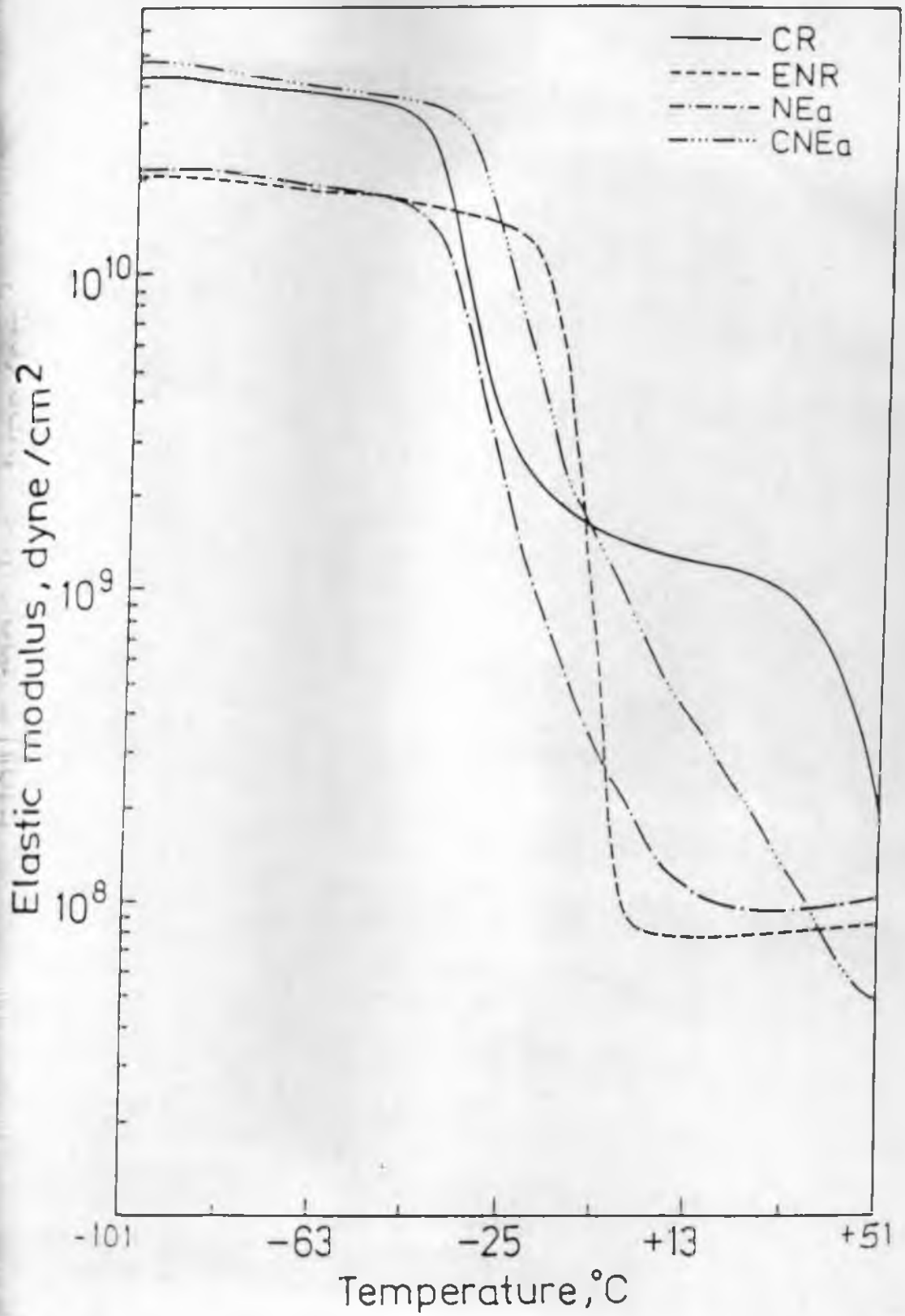

Fig. 4.15 : Plots of elastic modulus versus temperature for ENR, CR and the gum and filled 3:1 CR-ENR blend.

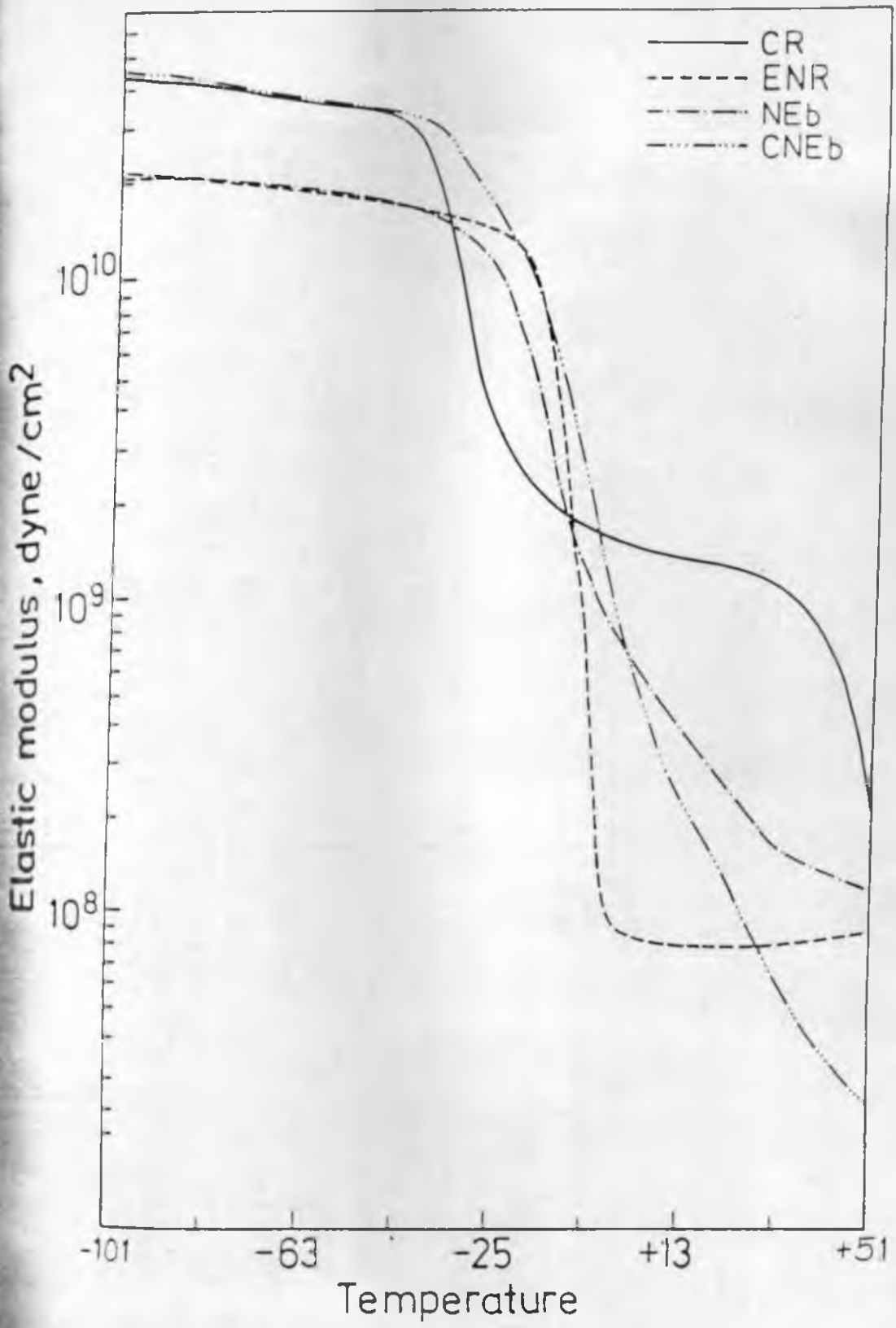

Fig. 4.16 : Plots of elastic modulus versus temperature for ENR, CR and the gum and filled 1:1 CR-ENR blend.

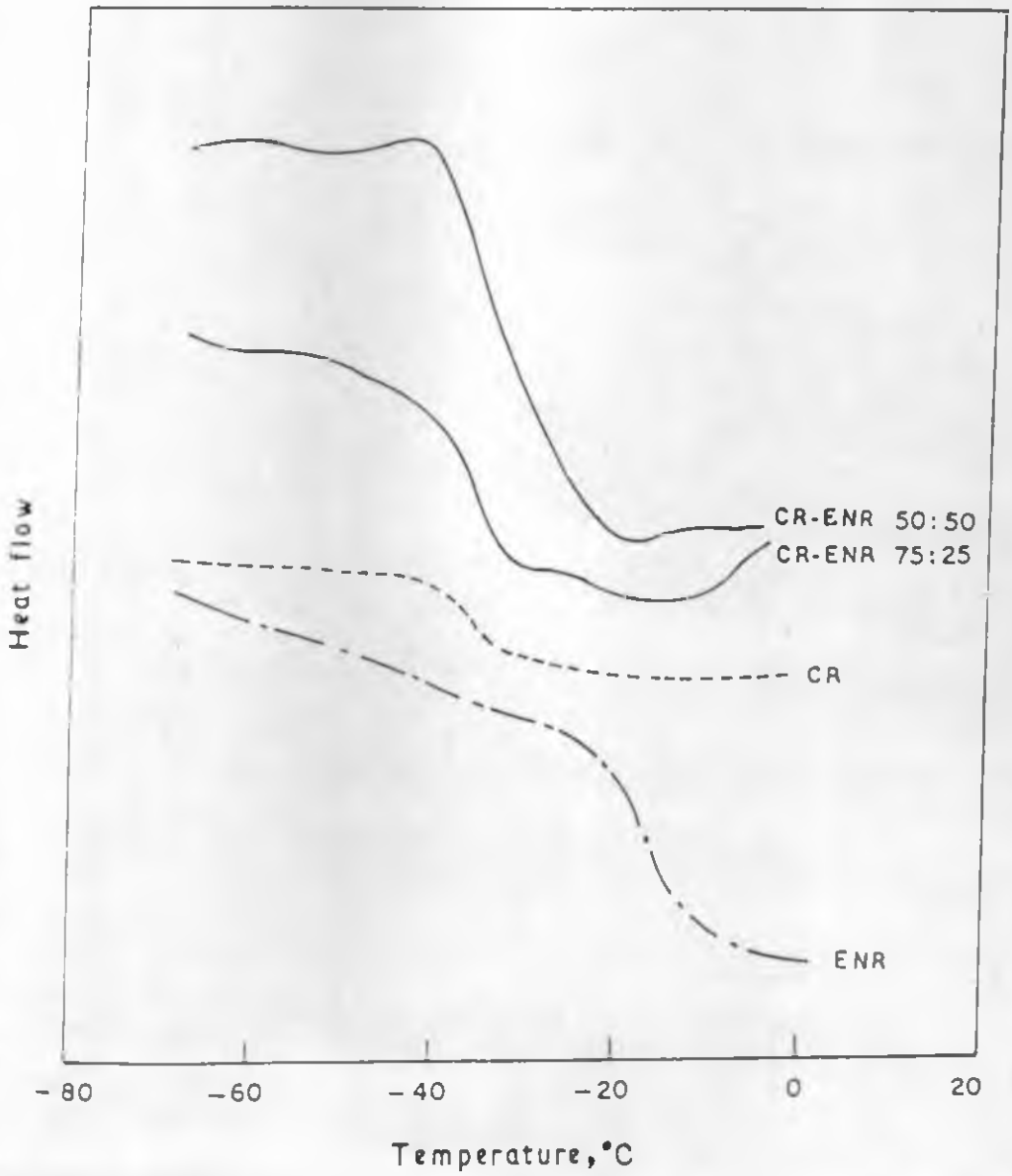

Fig. 4.17 : DSC thermograms of ENR, CR and the binary blends.

REFERENCES

1. N. D. Zakharov and G.A. Mairov, Sov. Rubber Technol. 22(1963) 11.
2. Miroslav Behal, and Vratislav Duchacek, J. Appl. Polym. Sci.,35 (1988) 507
3. Annual Book of ASTM standards,Part 37 (1981).
4. G. Socrates,`Infrared Characteristic Groups Frequencies', John Wiley & Sons Ltd., New York (1980).
5. C.Raux, R.Pautrat,R.Cheritat,F.Lederan and J.C.Danjard, J.Polym.Sci., Part C, 16 (1969) 4687.
6. I.R.Gelling and N.J.Morrison, Rubber Chem. Technol.,58 (1985) 243.
7. M.C.S. Perera, J.A. Elex and J.H. Bradbury, J. Polym. Sci., Part A : Polym. Chem., 26 (1988) 637.
8. R. Mukhopadhyay and S.K. De, Rubber Chem. Technol., 51 (1978) 704.
9. S.K. Chakraborty, A.K. Bhowmick and S.K. De, J. Macromol. Sci., Review (Chem.), 21 (1982) 313.
10. W.M. Hess, R.A. Swor and P.C. Vegvari, Kautschuk Gummi Kunststoffe, 38 (1985) 1114.
11. J.E. Callen, W.M. Hess and C.E. Scott, Rubber Chem. Technol., 44 (1971) 814.
12. C.M. Roland, Rubber Chem. Technol., 62 (1989) 456.
13. W.M. Hess and V.E. Chirico, Rubber Chem. Technol., 50 (1977) 301.

14. M. Steinfink, 'Handbook of Adhesives', Irving Skeist, Ed., 2nd Ed., Van Nostrand Reinhold Company, Inc., New York, 1977, Chap. 21, p. 346.

15. M.A. Mohsen, J.P. Berry and L.R.G. Treloar, Polymer, 26 (1985) 1463.

16. A. Voet, J. Phys. Chem., 51 (1947) 1037 and 61 (1957) 301.

17. A. Voet and W.N. Whitten, Jr., Rubber Age, 86 (1960) 811.

18. A.I. Medalia and F.A. Heckmana, Carbon, 7 (1969) 567.

19. W.M. Hess, L.L. Ban and G.C. McDonald, Rubber Chem. Technol., 42 (1969) 1209.

20. A.I. Medalia, J. Colloid Interface Sci., 32 (1970) 115.

21. G. Kraus, J. Polym. Sci., Polym. Phys. Edn., 8 (1970) 601.

22. J.J. Brennan, T.E. Jermyn and B.B. Boonstra, J. Appl. Polym. Sci., 8 (1964) 2687.

23. A.M. Gesslar, Rubber Age, 101 (1969) 54.

24. K.A. Grosch, J. Appl. Polym. Sci., 12 (1968) 915.

25. H. Westlinning, Kautschuk Gummi Kunststoffe., 15 (1962) 475.

26. P.P.A. Smit, Rheol. Acta., 5 (1966) 277.

27. A.R. Payne and R.E. Whittaker, J. Composites, 1 (1970) 203.

28. J.A.C. Harwood, A.R. Payne and J.F. Smith, Kautschuk Gummi. Kunststoffe., 22 (1969) 548.

29. T.G.F.Schoon and K.Adler, Kautschuk Gummi.Kunststoffe., 19 (1966) 414.

30. A.I. Medalia, Rubber Chem. Technol., 47 (1974) 411.

31. L.E. Nielsen, 'Mechanical Properties of Polymers and Composites', Marcel Dekker, New York, 1974, Vol. 2, Ch. 7.

32. T.B. Lewis and L.E. Nielsen, J. Appl. Polym. Sci., 14 (1970) 1449.

33. V.P. Chacko, F.E.Karasz and R.J.Farris, J. Polym. Eng. Sci., 22 (1982) 970.

34. S.Mukhopadhyay and S.K.De, Polymer, 32 (1991) 1223.

35. R. Vukovic, V. Kuresevic, N. Segudovic, F.E. Karasz and W.J. MacKnight, J. Appl. Polym. Sci., 28 (1983) 1379.

CHAPTER 5

ELF-VULCANISABLE RUBBER BLENDS BASED ON EPOXIDISED NATURAL RUBBER (ENR), ARBOXYLATED NITRILE RUBBER (XNBR) AND POLYCHLOROPRENE RUBBER (CR)

CHAPTER 5 - PART I

EFFECT OF BLEND RATIO, MOULDING TIME AND FILLERS ON MISCIBILITY

• This part of the work has been published in Polymer. 32 (1991) 2345

It has been observed that the miscibility of the self-vulcanised binary blends depend on the blend ratio, concentration, nature of reactive groups and moulding conditions[1]. Three examples are worth mentioning in this context. The binary blend vulcanisate of CR and XNBR is miscible in all proportions[2]. On the other hand ENR-CR vulcanisate is partially miscible and ENR-XNBR vulcanisate is miscible at any compositions. There are a few examples wherein two of the binary pairs (A+B and A+C) are miscible but the third binary (B+C) is not [3-5]. It is of interest to investigate how to prepare a miscible blend on addition of A to the immiscible binary (B+C) blend. In the present series of rubber-rubber blends it is of interest to learn how much of epoxidised natural rubbrer (ENR) is to be added to the binary polychloroprene (CR) and carboxylated nitrile rubber (XNBR) blend to create a self-vulcanisable miscible ternary blend vulcanisate.

There are examples of a third component in a ternary blend acting as a polymeric compatibilizer for an incompatible or immiscible binary system. Lee and Chen[6] reported that chlorinated polyethelene, with ethylene segments similar to EPDM rubber and chlorinated sequences similar to Poly(vinylchloride)(PVC), serves as a compatibilizer for the binary blend of EPDM and PVC just as the effect of chlorinated polyethylene on PVC/polyethylene blends[7,8]. Poly(capro-lactone)/poly(vinyl chloride)(PCL/PVC) blends and poly(capro-lactone)/chlorinated poly(vinyl chloride)(PCL/CPVC) blends are miscible at any composition[5].

However, PVC and CPVC are immiscible[8]. It has been shown by Jaeduri and Prudhomme[9] that the addition of PCL to a PVC/CPVC mixture allows the observation of a single glass transition temperature (Tg) at PCL contents larger than 40 % at high PVC/CPVC ratios and at PCL contents larger than about 26% at low PVC/CPVC ratio. Min et al.[10] have identified a ternary miscible system based on poly(methyl methacrylate) - poly(epichlorohydrine) - polyethylene oxide. There is no published report in literature on self vulcanisable ternary rubber blend.

This chapter deals with the effect of blend ratio, moulding time and fillers on the miscibility of the ENR-XNBR-CR ternary blend system. In this chapter the mechanism of crosslinking between the rubbers is also studied by IR spectroscopy

5.1.A Effect of blend ratio on miscibility

Formulations of the blends are shown in Table 5.1.1. Miscibility of the ternary blend based on ENR/CR/XNBR was found to depend on blend composition. At constant CR/XNBR ratio, increase in ENR concentration increased the miscibility. Figures 5.1.1 -5.1.3 show the effect of ENR content at constant CR/XNBR ratio on tan δ and viscous modulus plots of the ternary blends. At 75/25 ratio of CR/XNBR, ENR concentration upto 25 phr did not result in a miscible ternary blend. In fact two Tg's were observed corresponding to two phases like CR/ENR (Tg -27°C) and XNBR/ENR (Tg -10°C). When ENR content increased to 37.5 phr

above, the miscibility improved in the sense that instead of two peaks a single broad peak was observed. As ENR content in the blend increased from 50 phr level to 75 phr level the broadness was replaced by sharpness in the peak indicating enhanced miscibility.

Similar observations were made when CR content in the binary blend CR/XNBR decreased as in 50/50 and 25/75 blend compositions. However, when CR content decreased in the blend instead of broad peak, we observed sharp peaks indicating enhanced miscibility.

Figure 5.1.4 shows that at 75 phr level of ENR the ternary blend became a miscible system irrespective of the binary CR/XNBR composition. However, the miscibility was more when the CR content was less in the binary CR/XNBR blend as evident from the sharp tan δ peak. Results are summarised in Table 5.1.2.

Results of Differential Scanning Calorimeter (DSC) studies (Fig. 5.1.5) also provide supportive evidence for the conclusions drawn from dynamic mechanical analysis (DMA) studies. Results of DSC studies are summarised in Table 5.1.2. It was evident that miscibility in a particular blend was manifested in the occurrence of sharp transition in the Tg curve. While immiscible system provided no clear cut single transition, a miscible system provided a single transition. In the present studies, formulation G was found to be a miscible system showing a sharp Tg at -18° C. But formulation C was found to be an immiscible system showing

two Tg's at -40° C and -18° C. Blend H, however, was found to be a partially miscible system wherein the two transitions merged with each other and no clear cut transition was observed.

5.1.B IR Spectroscopic studies

The IR spectra of thin films of XNBR, ENR, CR and the difference spectrum (ternary blend-ENR-CR-XNBR) is shown in fig. 5.1.6 and their characteristic absorption peaks are shown in Table 5.1.3. Pure XNBR showed absorption at 1734 cm^{-1} and 1700 cm^{-1} due to free and hydrogen bonded acid group respectively. Pure ENR showed absorption at 870 cm^{-1} and 1245 cm^{-1} due to epoxy group and at 885 cm^{-1} for cis double bond. ENR also showed carboxyl absorption due to traces of acids. In addition there was an absorption at 1114 cm^{-1} due to aliphatic ethers and at 1065 cm^{-1} due to tetrahydrofuran. It is known that epoxidation reaction is very difficult to be controlled and that epoxide rings open up in presence of acids and undergo hydrofuranisation[15].

Pure CR showed absorption at 860 cm^{-1} due to trans 1,4 polychloroprene unit[14].

The difference spectra of ternary blend showed absorption at 1697 cm^{-1} which could be due to ester crosslinks which were intramolecularly hydrogen bonded[11]. The absorption at 1120 cm^{-1} was probably due to ethers[11]. The strong absorption at 1079 cm^{-1} could be due to cyclic ethers. The absorption around 1660 cm^{-1} showed that during crosslinking some unsaturated esters could also be formed. This showed that the ternary blend during high temperature

moulding formed ester crosslinks by reaction of ENR with XNBR and XNBR with CR and ether crosslinks by reaction of ENR with CR. Epoxy groups also underwent cyclisation to give cyclic ethers. The probable mechanism of crosslinking is given in Fig. 5.1.7.

In the ternary blend vulcanisates, the broadening of the Tg zone could be ascribed to microlevel inhomogeneity. Microheterogeneity could be attributed to formation of different phases of crosslinked CR/XNBR blend, crosslinked ENR/CR blend, crosslinked ENR/XNBR blend, crosslinked ENR/XNBR/CR blend, thermovulcanised CR and acid-catalysed self-crosslinked ENR. However, it is not possible to characterise them individually, because several pairs have close Tg-values.

Next we studied the efect of crosslink density on miscibility of such blends. In self-vulcanisable blends crosslink density could be varied by changing the moulding time (Chapter 3, Section 2). The idea was to check whether miscibility of the immiscible blend could be improved by moulding for a longer time and similarly a miscible system would be made immiscible if moulded for a shorter period.

5.1.C Effect of moulding time on miscibility

Figure 5.1.8 shows the effect of moulding time on variation of tan and viscous modulus with temperature for a miscible system (blend G) and an immiscible system (blend C). When the moulding time was reduced to 15 min. from 60 min. in the case of the miscible system miscibility was not

affected. However, the tan δ peak shifted to lower temperature due to lower crosslink density at 15 min. moulding as compared to 60 min. moulding. For the immiscible system when the moulding time was increased to 120 min. the miscibility again did not change, but the tan δ peak shifted to higher temperature due to higher crosslink density at 120 min. moulding as compared to 60 min. moulding. The lowering of damping level and broadening of the damping peak due to increase of crosslinking has been reported earlier[16].

5.1.D Effect of filler on miscibility

Figure 5.1.9 shows the dynamic mechanical spectra of the miscible ternary blend system (Blend G) filled with three fillers namely silica, ISAF black and SRF black. The miscibility of the ternary blend was altered as evident from the two peaks in both tan δ and viscous modulus plots in the case of ISAF black (at -33° C and -5° C) and silica filled (at -21° C and -7° C) blends. However, in case of SRF black filled mix we observed a single peak at -5° C and a hump at -16° C. It was evident that reinforcing filler like SRF black and silica cause phase separation in a miscible ternary blend presumably due to varying extent of affinity of the filler to different rubber blend systems. SRF black was less reinforcing and accordingly rubber-filler interaction was expected to be less and less pronounced was the effect of the filler on miscibility. It was shown by Medalia[17] and [illegible][18] that polymer occluded within the internal void of the primary structure of carbon black is not free to fully

share in the macroscopic deformation of carbon black filled rubber. Some investigators[19,20] identified this immobilised rubber with 'bound rubber' measured by solvent extraction, whereas others through microscopic study[21-22] modulus[23] and tensile measurements[24-26] indicated the existence of a shell of immobilised rubber of definite thickness around the vulcanisate. The absorbed, hard, immobilized rubber would cause a perturbed relaxation response and the relaxation character of these layers would shift towards the glassy state. Then the tan δ peak might be ascribed to the glass transition relaxation of the bulk rubber and thus the tanδ peak would decrease on introduction of carbon black.

DSC results showing effect of different fillers on 25/75/75 CR/XNBR/ENR blend are shown in Figure 5.1.10. It was evident that addition of SRF black caused broadening of the transition with no clear cut glass transition. ISAF black also broadened the transition zone. Silica filler showed two transitions at -40°C. and -22°C. It was evident that reinforcing fillers affect the miscibility of the self-vulcanised ternary blend, as evident from the dynamic mechanical analyses (DMA) and differential scanning calorimetry (DSC) studies. However, it is to be noted that transitions in DSC studies were not as conclusive as that of DMA results.

Table 5.1.1 : Formulation of blends[a]

Blend designation	A	B	K	C	J	D	E	F	M	G	L	H	I
CR	75	75	75	75	75	50	50	50	25	25	25	25	25
XNBR	25	25	25	25	25	50	50	50	75	75	75	75	75
ENR	75	50	37.5	25	12.5	75	50	25	87.5	75	62.5	50	25

[a] Figures are in parts by weight

Table [illegible] Glass transition temperatures (Tg) of various [illegible] blends as obtained from dynamic mechanical analyses(DMA) and Differential Scanning Calorimeter (DSC) studies

Blend Designation	Blend Composition (CR/XNBR/ENR)	DMA Tg, °C. tan δ	DMA Tg, °C. loss modulus	DSC Tg, °C
A	75/25/75	-11	-27	-26
B	75/25/50	-11	-27	a
K	75/25/37.5	-5	-30	-
C	75/25/25	-29, -1	-35, shoulder at -19	-40, -18
J	75/25/12.5	-33, +8	-38, shoulder at -19	-
D	50/50/75	-10	-25	-19
E	50/50/50	-10	-24	-16
F	50/50/25	-29, -5	-37, -17	a
M	25/75/87.5	-9	-19	-
G	25/75/75	-7	-19	-18
L	25/75/62.5	-9	-20	-
H	25/75/50	-7	-30, shoulder at -17	a
I	25/75/25	-37 to -29, -10	-40, -20	a

a No clear cut transition.

[illegible] cm⁻¹	Functional group	Assignment of band	ENR	XNBR	CR	NEX-E-NX	Reference
1760	Carboxyl	C=O str. (monomer)	-	1760	-	-	11,12
1740	Ester (acetate)	C=O str.	-	-	-	-	11,12
1710-1730	Carboxyl	C=O str.	1728	1700	-	-	11
1690-1725	Ester(Intra-molecularly H-bonded)	C=O str.	-	-	-	1697	11
1245	epoxy group	C-O str.	1245				
Around 1114 (1060-1150)	aliphatic ether	assym. C-O str.	1114	-	-	1120	11
Around 1162	Cyclic ether more than 5 membered rings	assym. C-O str.	-	-	-	-	11
1065-1070	Tetrahydro-furan	ring str.	1065	-	-	-	13
885	cis double bond	C=C str.	885	—	-	885	11
785-875	cis epoxides	ring vibra	8[illegible]				11
Broad peak around 860	trans 1,4 polychloro-prene	C-Cl str.	-	-	860	-	13

Table 5.1.4 : Effect of fillers on glass transition temperatures (Tg) of miscible ternary blend (G) of CR/XNBR/ENR

Blend Designation	Filler type	Tg, °C.		DSC
		tan δ	loss modulus	Tg,°C
G[a]	-	-7	-19	-18
GIS40	ISAF black	-33, -5	-33, -7	b
GSI40	Silica	-21, -7	-23, -7	-40, -22
GSR40	SRF black	-5, shoulder at -16	-13	-19

a formulation in 5.2.1

b no clear cut transition

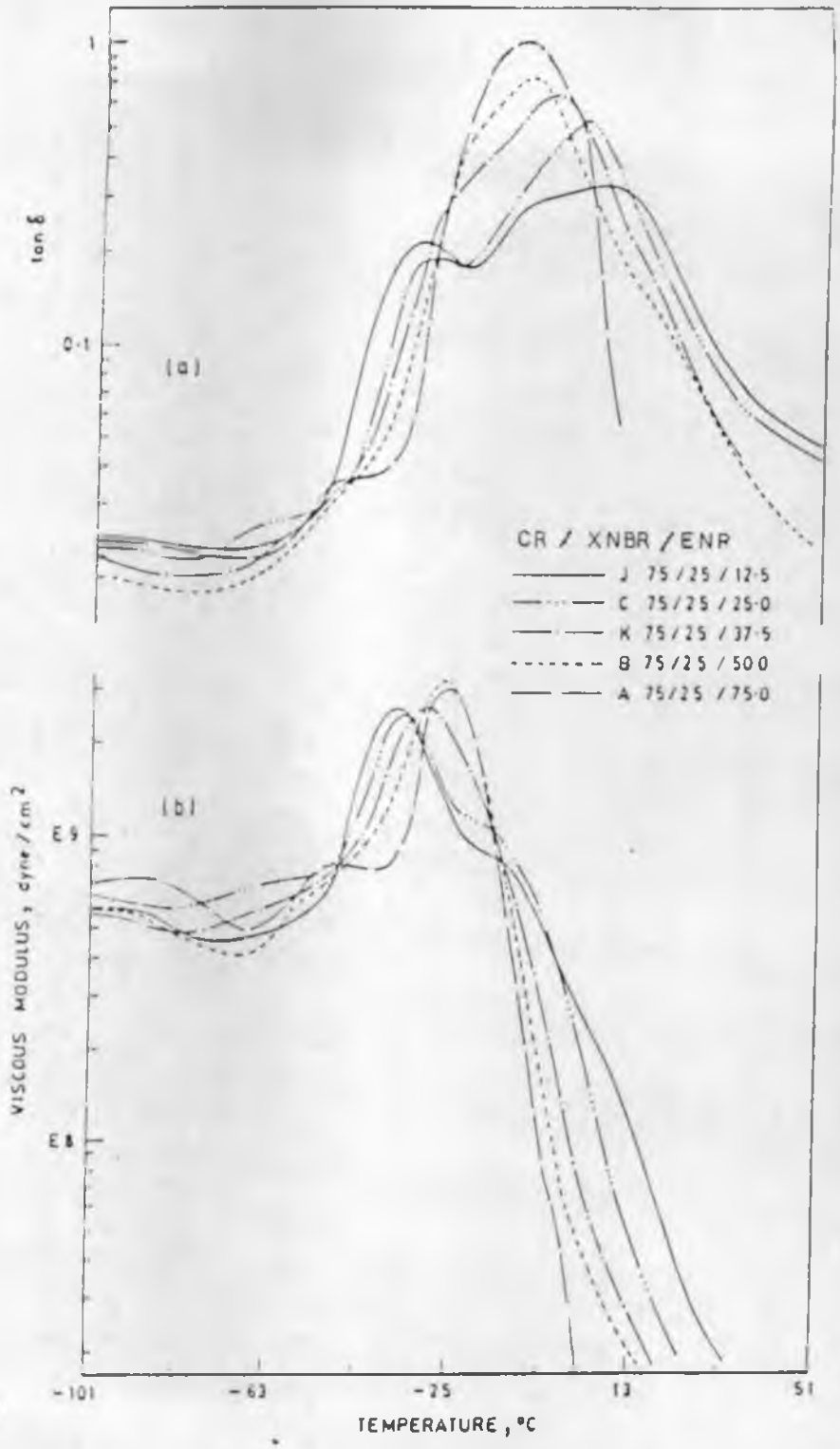

Fig. 5.1.1 : Dynamic mechanical spectra of the ternary blend showing the effect of ENR content on a fixed CR/XNBR ratio of 75/25.

(a) tan δ versus temperature
(b) viscous modulus versus temperature.

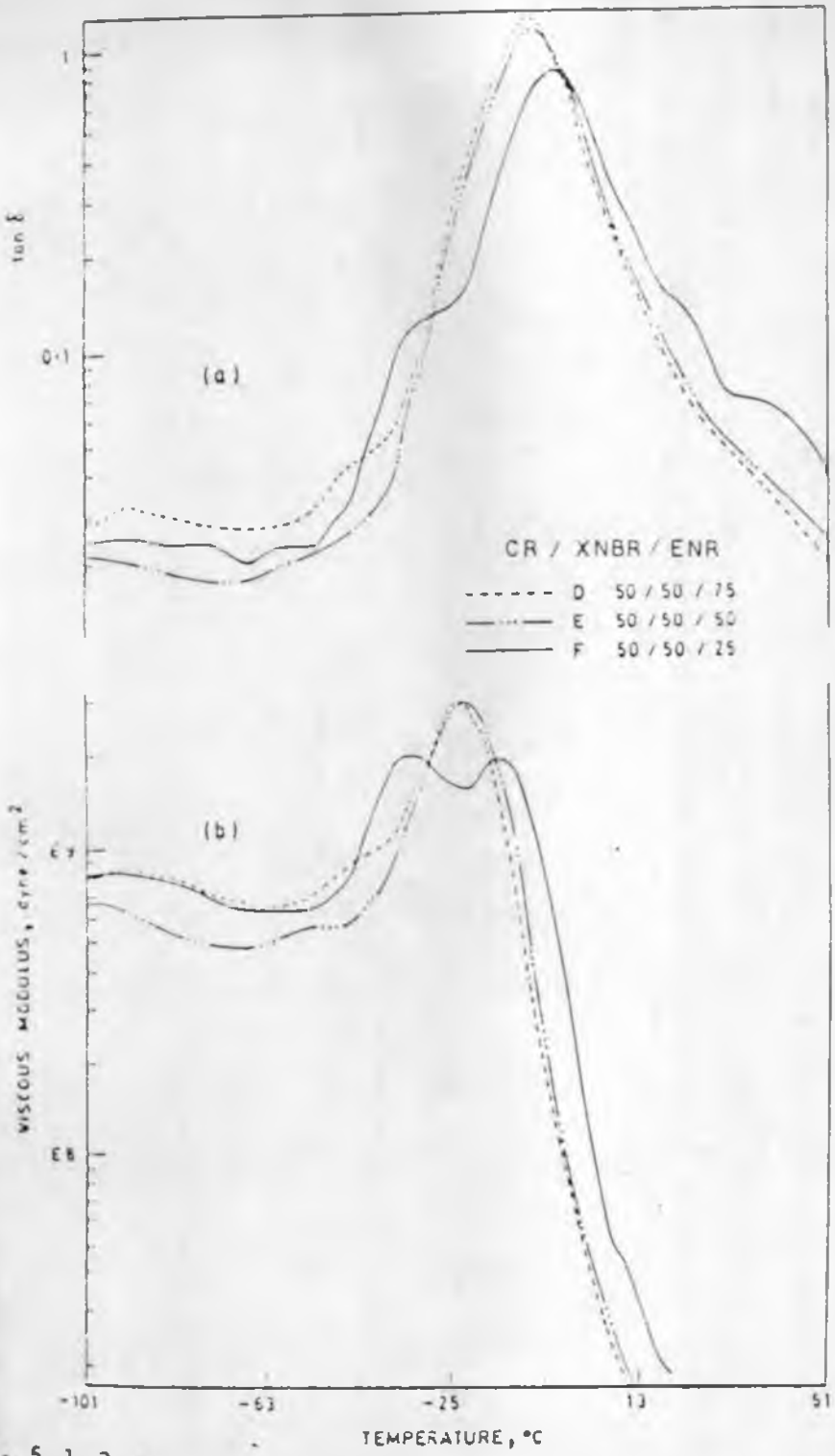

Fig. 5.1.2 : Dynamic mechanical spectra of the ternary blend showing the effect of ENR content on a fixed CR/XNBR ratio of 50/50.

(a) tan δ versus temperature.

(b) viscous modulus versus temperature.

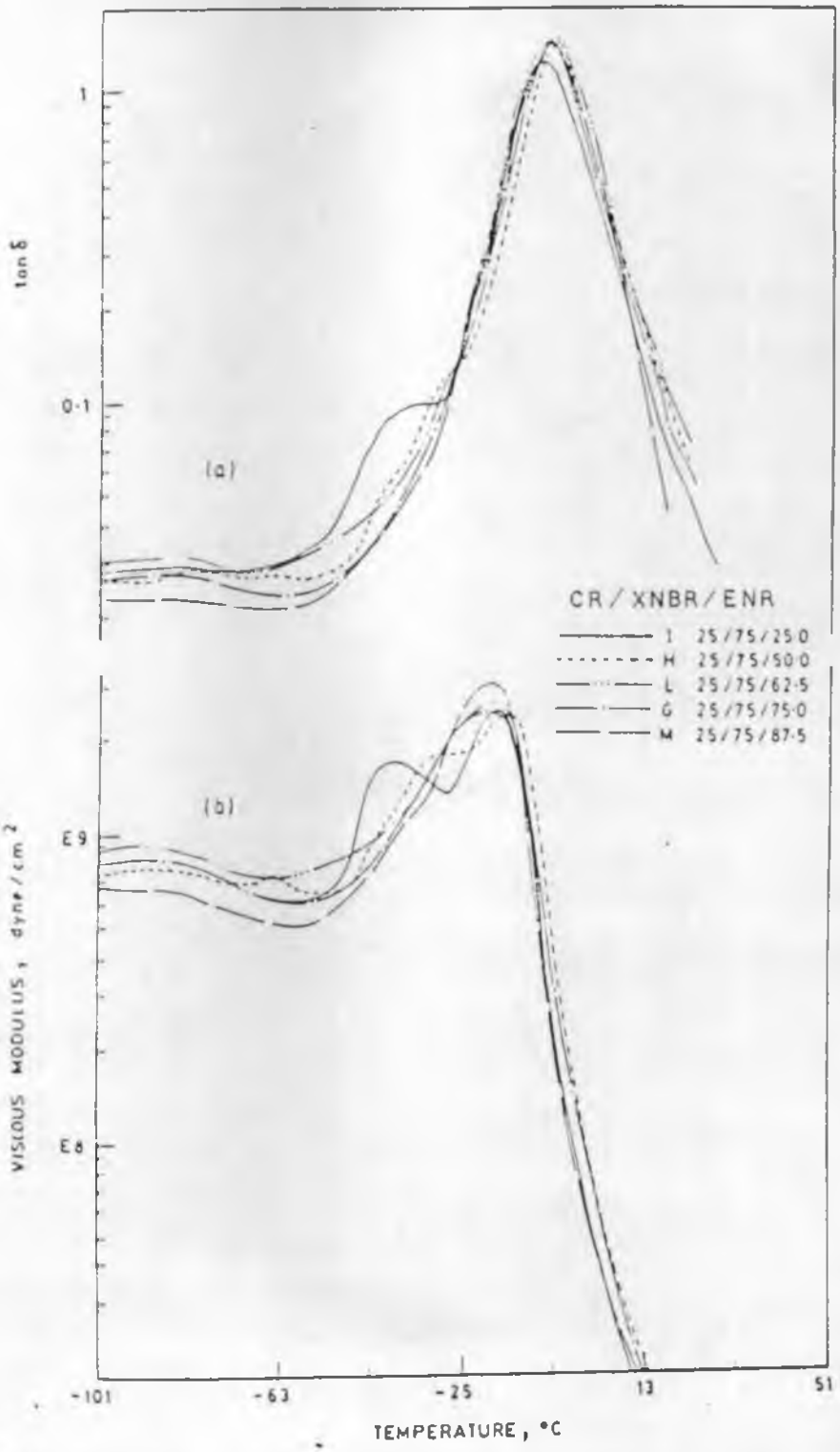

Fig. 5.1.3 Dynamic mechanical spectra of the ternary blend showing the effect of ENR content on a fixed CR/XNBR ratio of 25/75.

(a) tan δ versus temperature.
(b) viscous modulus versus temperature..

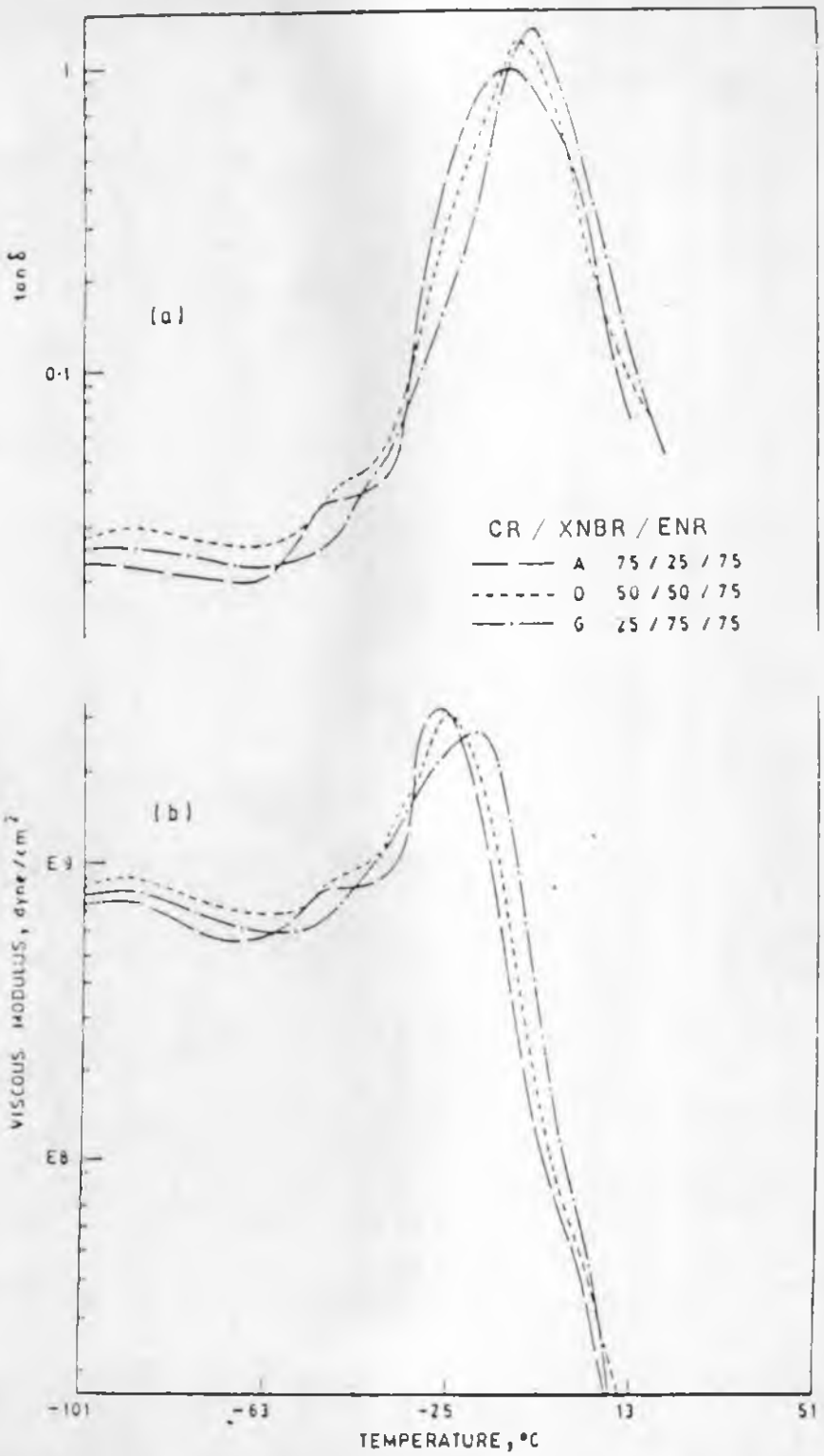

Fig. 5.1.4 : Dynamic mechanical spectra of ternary blend showing the effect of 75 phr of ENR on different CR/XNBR ratio of 75/25, 50/50, and 25/75.

(a) tan δ versus temperature.
(b) viscous modulus versus temperature.

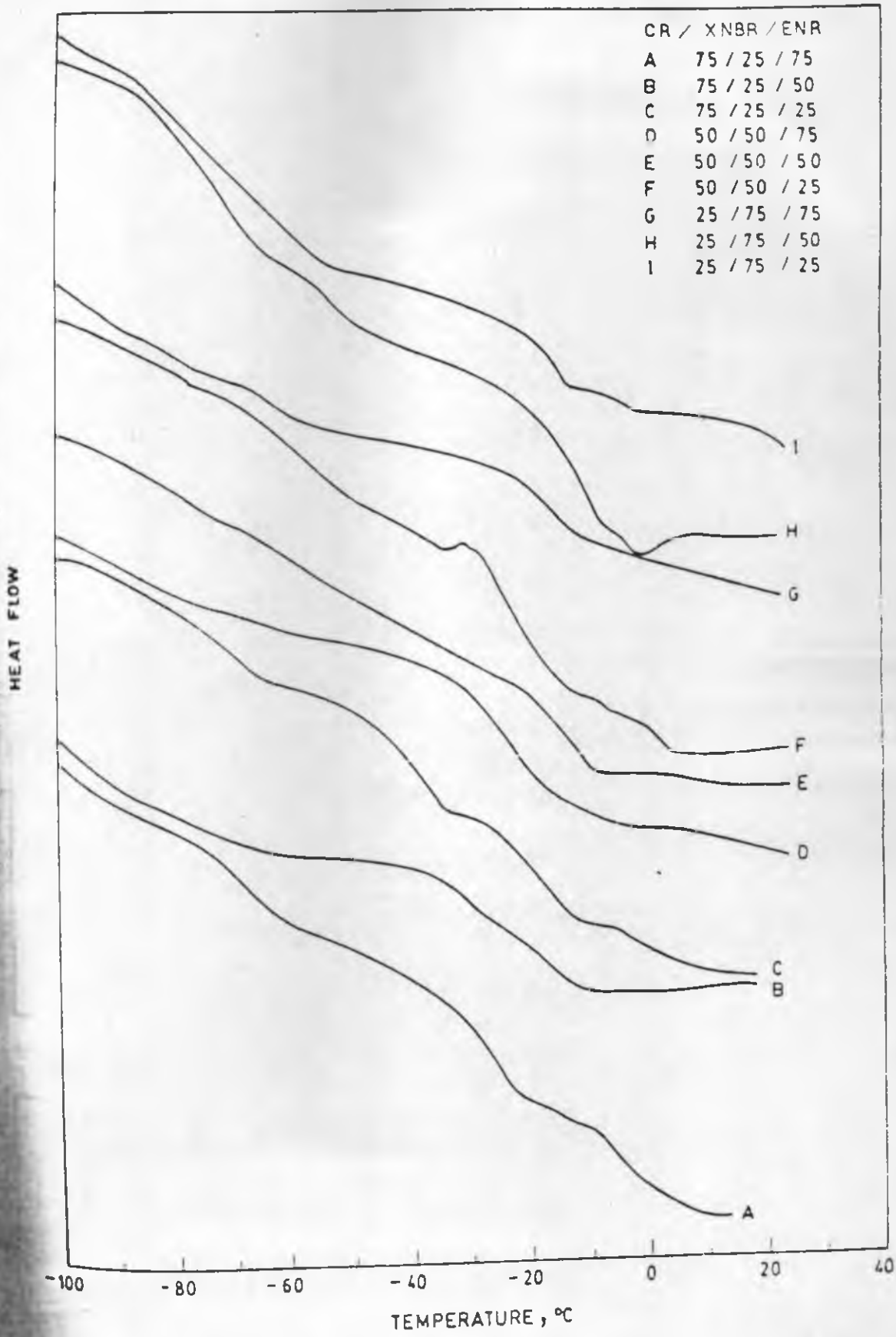

Fig. 5.1.5 : DSC thermograms for the ternary blends of ENR, XNBR and CR.

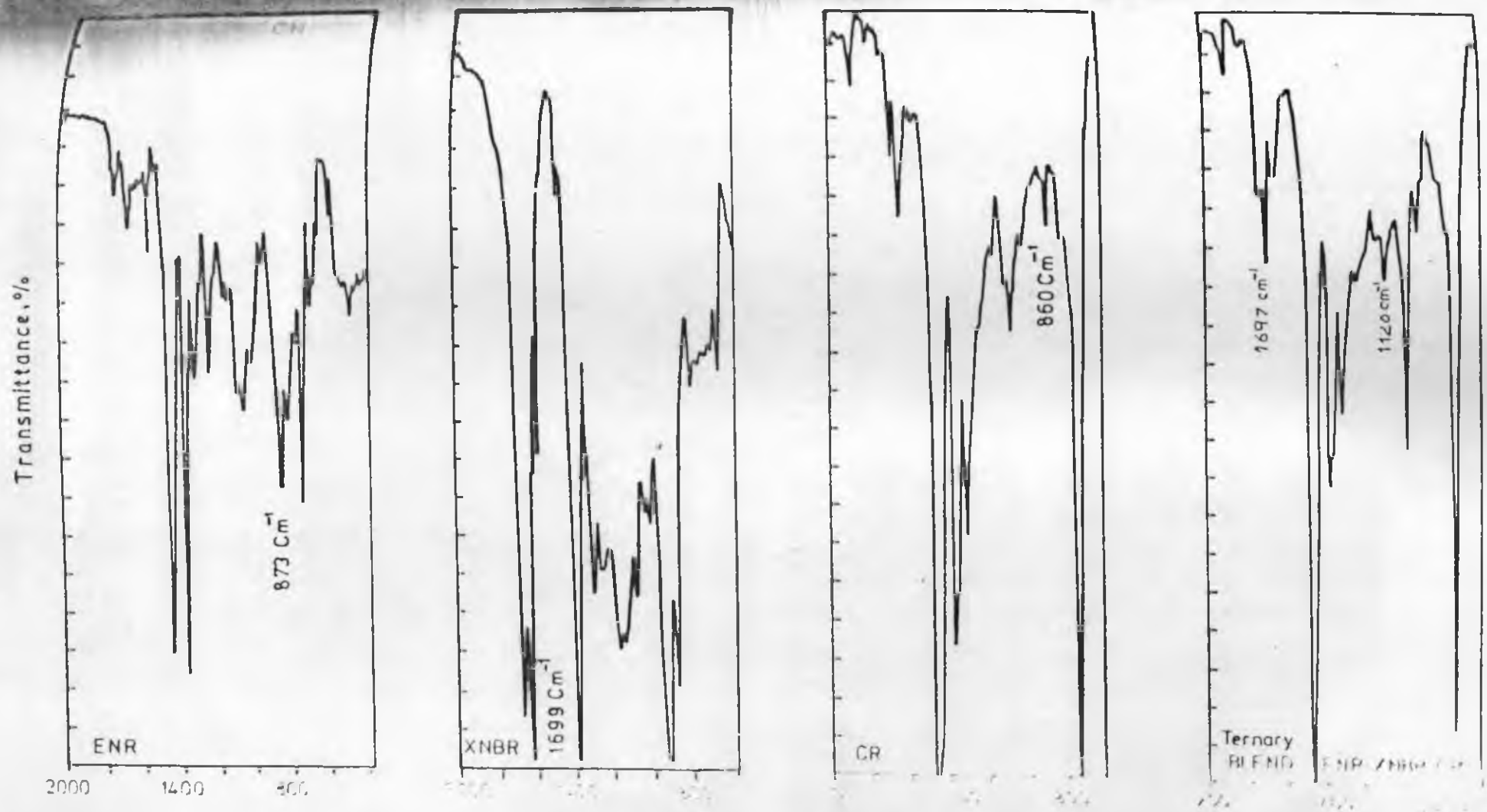

[illegible] ternary blend
ENR-XNBR-CR.

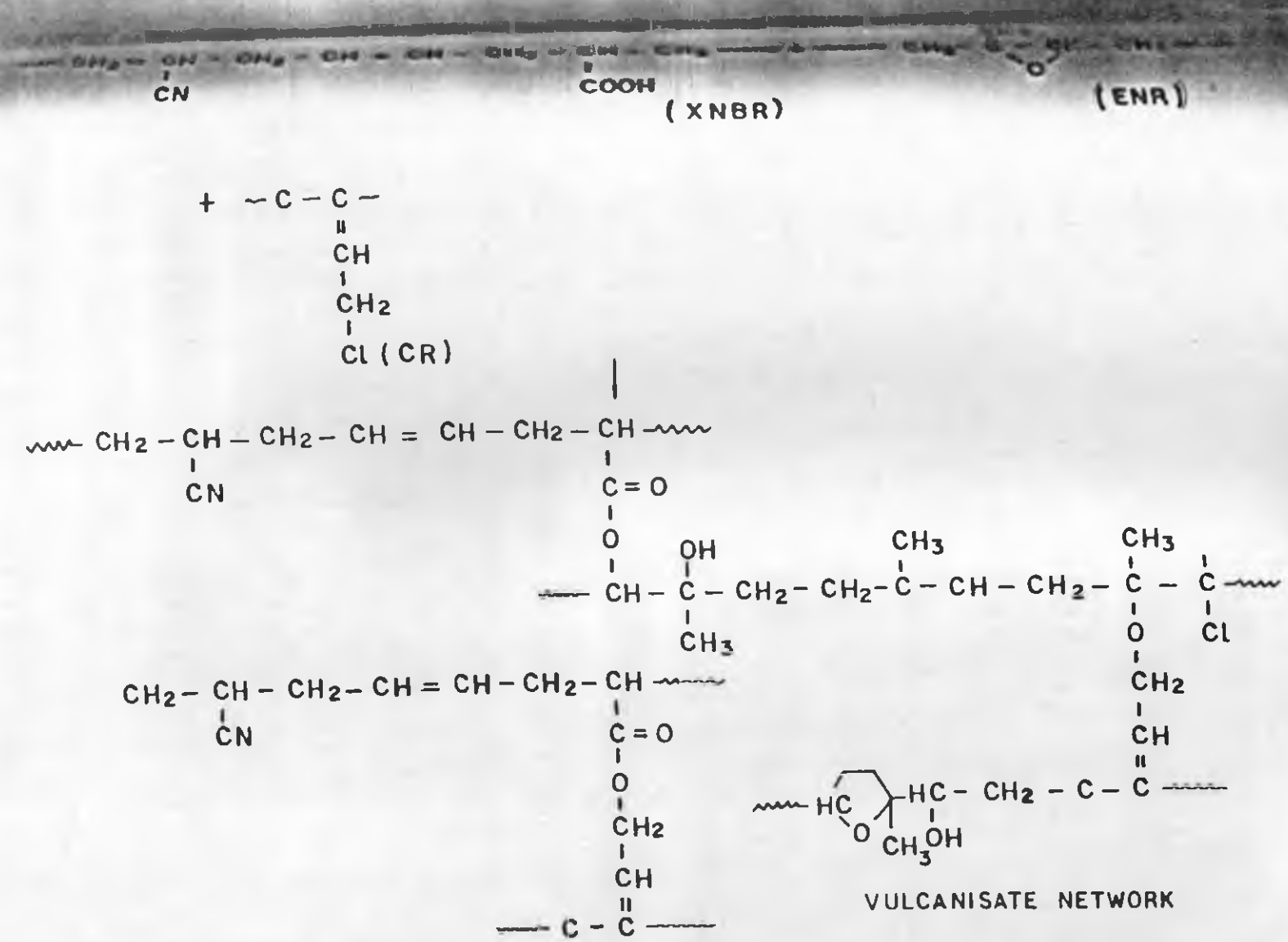

Fig. 5.1.7 : Possible mechanism of crosslinking in the ENR/XNBR/CR ternary blend.

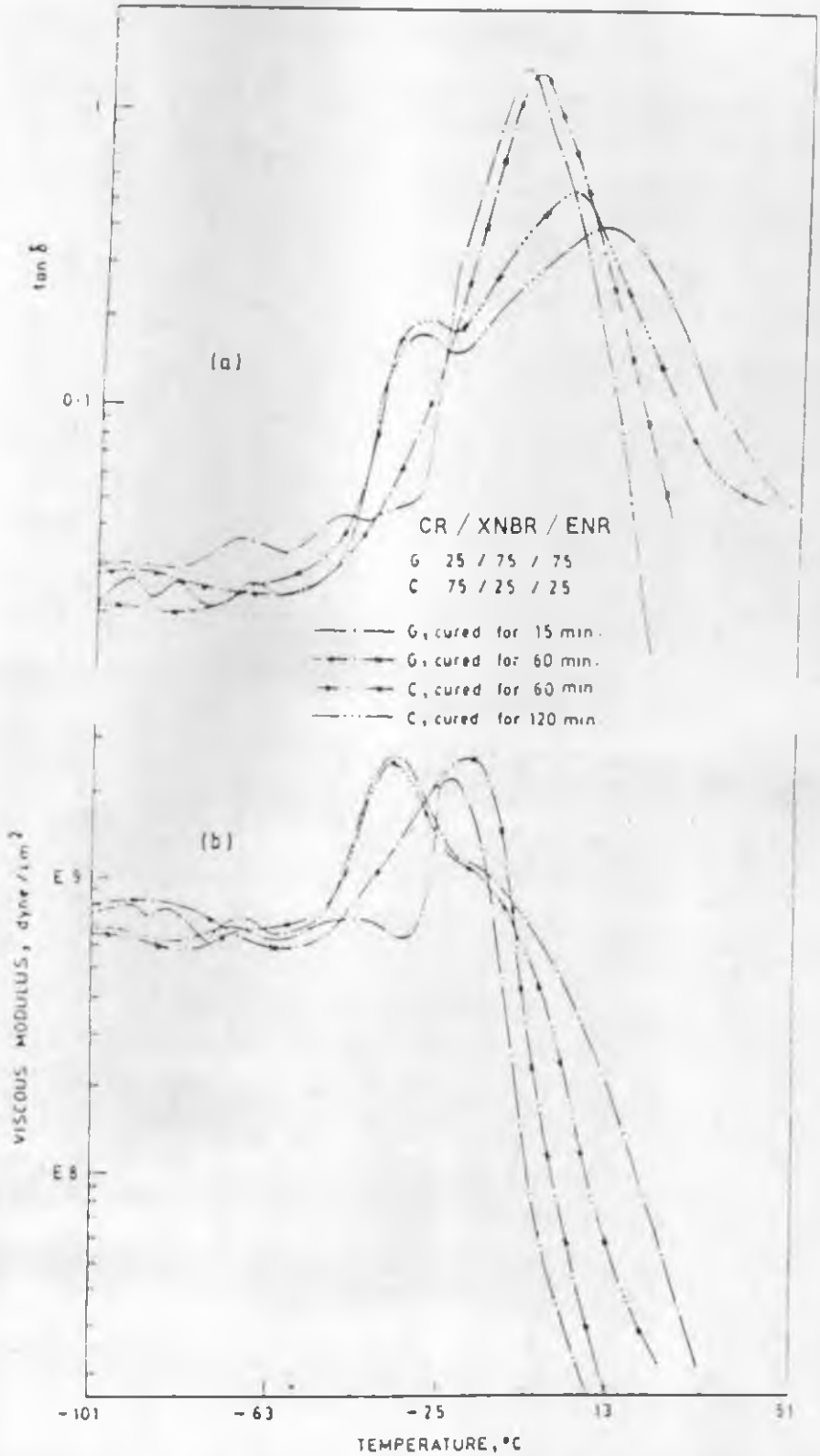

5.1.8 : Dynamic mechanical spectra of ternary blends (mix G and Mix (C) showing the effect of moulding time on Tg behaviour.

(a) tan δ versus temperature.
(b) viscous modulus versus temperature.

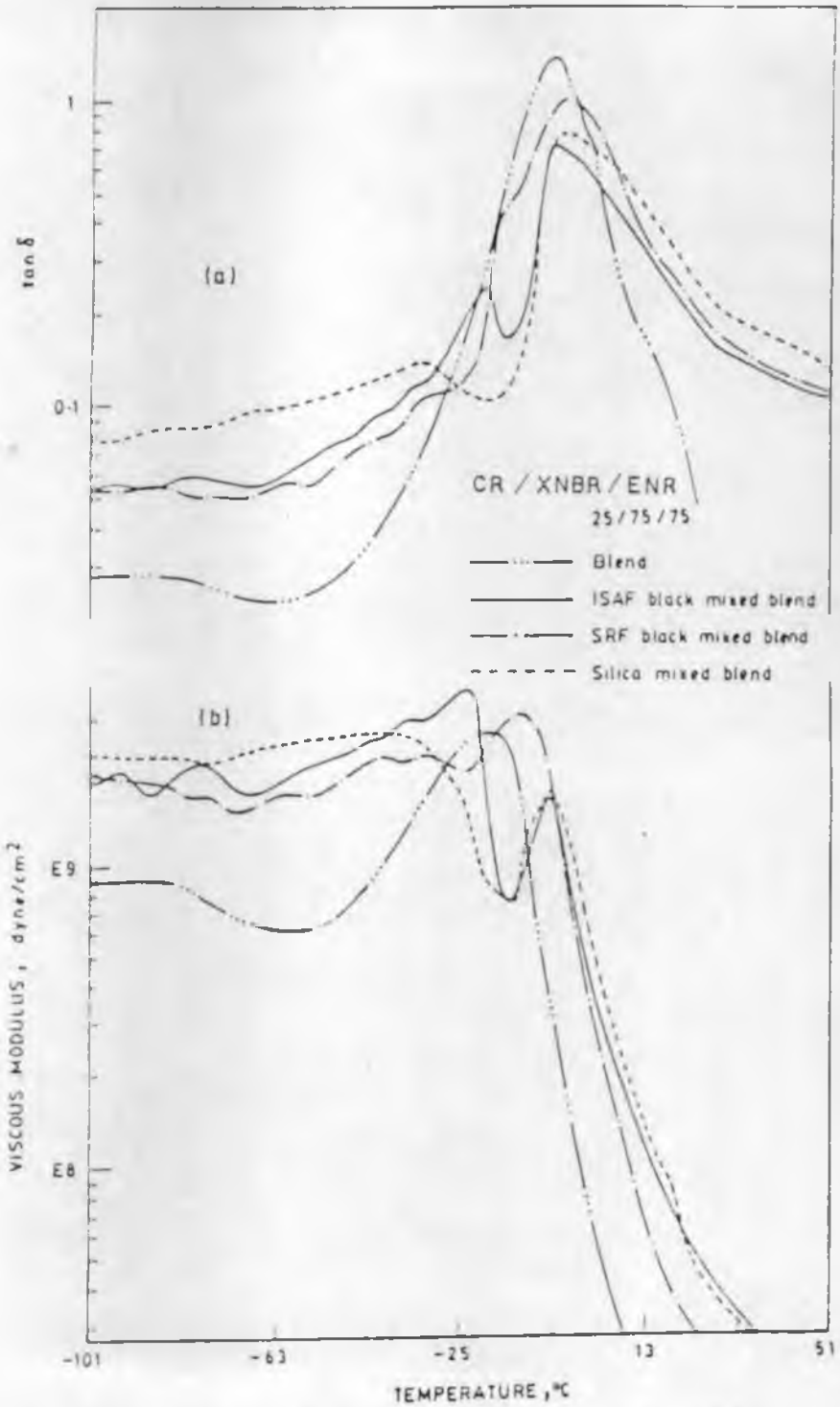

Fig. 5.1.9 : Dynamic mechanical spectra of the miscible tenary blend (mix G) filled with ISAF black, and precipitated silica. Filler loading was 40 parts per hundred of rubber in each case:

(a) tan δ versus temperature.

(b) viscous modulus versus temperature.

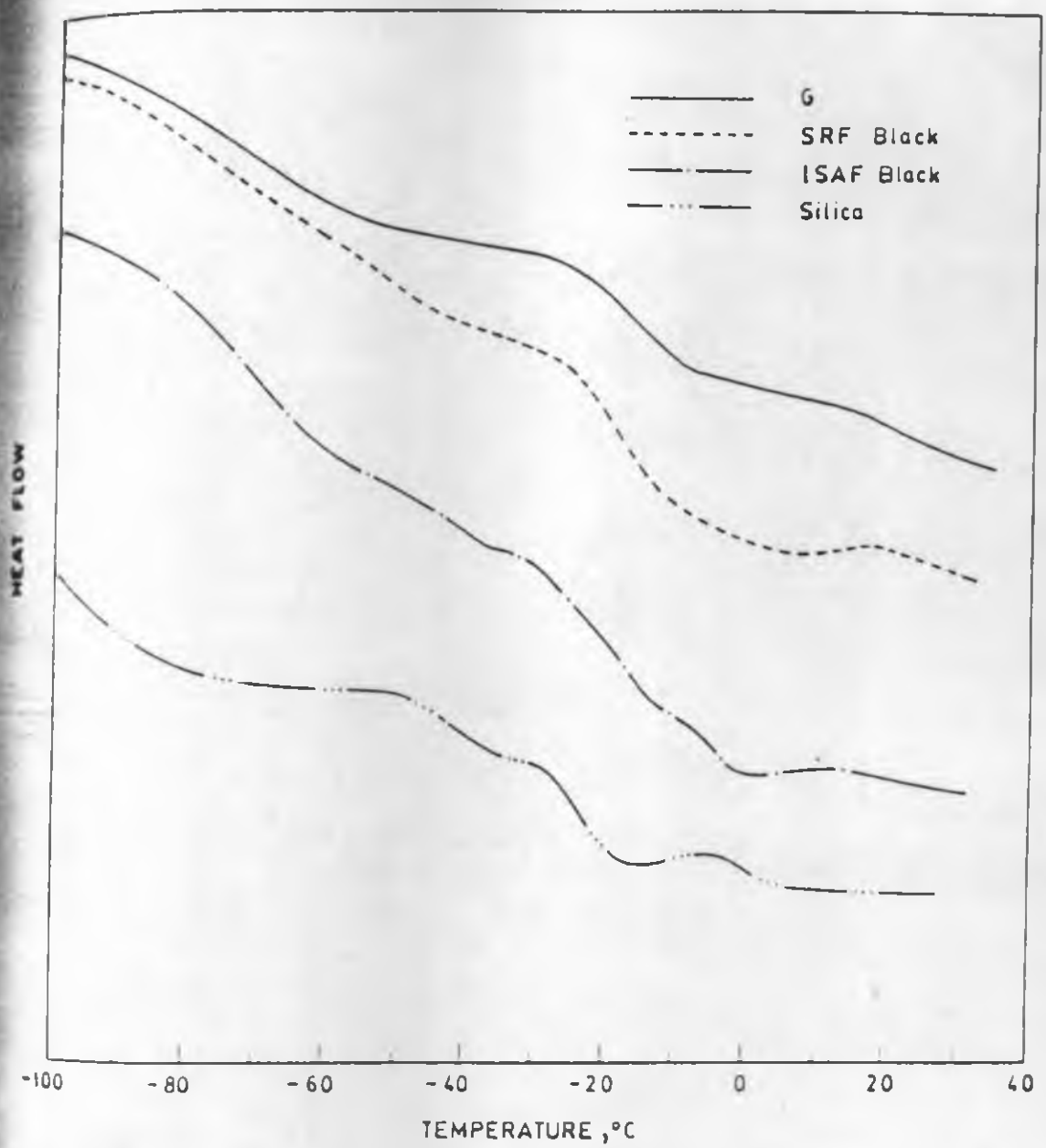

Fig. 5.1.10 :DSC thermograms of the miscible ternary blend (mix G) filled with ISAF black, SRF black and precipitated silica. Filler loading was 40 parts per hundred of rubber in each case.

CHAPTER 5 - PART II

VULCANISATION CHARACTERISTICS AND PHYSICAL PROPERTIES

• This part of the work has been published in Polymer 32 (1991) 2546

It has been reported that mill-mixed blend of [illegible]dised natural rubber (ENR), polychloroprene rubber and carboxylated nitrile rubber (XNBR), form a self-[illegible]ssible ternary rubber blend system upon moulding at [illegible]. It has been reported earlier in Part I of this chapter [illegible] miscibility of such systems depends on blend [illegible]ition, and incorporation of filler.

Part II of this chapter, deals with the results of the [illegible]ies on dependence of vulcanisation characteristics and [illegible]ical properties of the ternary blends on blend [illegible]ition and fillers like ISAF black, silica and SRF [illegible].

The formulation of different blends are shown in [illegible] 5.1.1and 5.2.1. The formulation of the control mixes [illegible] given in Table 5.2.2. For comparison between the blend [illegible] the single rubber in respect to properties, one blend [illegible], Mix. No. G is chosen. In the case of this blend the [illegible]ase in rheometric torque above the minimum torque was 26 [illegible] at 150°C. The control mixes of ENR and XNBR were cured [illegible] the time when the rheometric torque rise was the same as [illegible] of the blend, that was 26 units. The respective cure [illegible] at 150°C thus obtained were 30 min., 9 min. and 60 [illegible] respectively for ENR, XNBR and CR.

[illegible] Effect of blend ratio variation on cure characteristics

Results of cure characteristics of the blends are

Table 5.2.3. For a constant CR/XNBR ratio minimum iscosity and scorch time at 120°C showed progressive with ENR content. As the ENR content increased, the Mooney viscosity decreased and scorch time increased. XNBR in the CR/XNBR ratio increased, the scorch time eatly reduced and minimum Mooney viscosity was d. For instance, when 25 phr ENR was added to in the ratio 75/25, minimum Mooney viscosity was 33 rch time was 10.8 min., while in CR/XNBR ratio of imum Mooney viscosity was 45 and scorch time was 5.1 the ternary blend it was believed that carboxyl XNBR and epoxy group of ENR reacted to form ester and epoxy group of ENR and allylic chlorine of CR to form ether linkages. Further more -COOH group of been reported to interact with allylic chlorine of er to form a self-vulcanisable rubber blend[2]. Hence scorch time in ternary blends containing high XNBR to early onset of chemical reactions involving -COOH oxy group and allylic chlorine.

onsanto rheographs of the different blends at 150° C. n in Figure 5.2.1. All the blends showed marching c torque with time. Dependence of minimum c torque on blend ratio followed the same pattern as es in minimum Mooney viscosity. At a fixed CR/XNBR crease in ENR content lowered the Mooney viscosity. t of crosslinking as reflected from the rheometric pended on the composition of the blend. Maximum

tric torque was observed in blend G which conta ed R/ENR in the ratio 1/3/3. As shown in Part I of is r, the blend G has been found to be comple ly ble. It was believed that a homogeneous matrix of the was formed in the right composition where the ma mum ction between the constituents took place.

Effect of blend ratio variation on physical properties

The physical properties of different gum blends are in Table 5.2.4. Tensile stress - strain curves are in Figure 5.2.2. High tensile strength was observed in containing high proportion of CR. The systems which ined high proportion of CR was immiscible at the tal level (Part I of this chapter). However such were likely to be mechanically compatible due to linking between different phases. Immiscible systems are mechanically compatible are reported to have good al properties[27,28]. For CR/XNBR blends at 75/25 and blend ratios, increased incorporation of ENR caused in modulus, tensile strength, tear str gth, resilience and increase in compression s and loss. Vr values were found to decreas with in ENR content. Since Vr could be conside l as tional to crosslink density, the gradual char in ties could be understood on the basis of de e of ing. However, in CR/XNBR blend at 25/75 lend increased incorporation of ENR caused increas Vr

ccordingly the changes in properties with blend ratio ion followed a different pattern. In general, the s in properties with blend ratio variation were less able in this series.

Effect of fillers on cure characteristics

Minimum Mooney viscosities and Mooney scorch times for illed blends are given in Table 5.2.5. Expectedly, e of filler loading increased the minimum viscosity ecreased the scorch time. The increase in Mooney ity was very high in the case of silica filled mixes w in the case of SRF black filled mixes. For example, phr loading, Mooney viscosity at 120°C increased from the unfilled blend to 49 for SRF black filled mix, to ISAF black filled mix and to 98 for silica filled mix. gher Mooney viscosity of silica filled mix was probably strong interaction of silica with rubber during mixing oulding at higher temperatures[29]. The low scorch of the blends showed that crosslinking reaction started t a processing temperature of 120° C.

Rheographs of the gum blend at different temperatures control ENR,XNBR and CR mixes at 150°C are shown in 5.2.3. The gum blend showed marching rheometric torque ime and temperature of moulding. Figure 5.2.4 shows of ISAF black filled systems. It is evident that case of conventional rubbers ISAF black reinforced blend. The nature of rheographs with respect to

and temperature was similar to that of the gum blend. ease of filler loading increased rheometric torque. ure 5.2.5).

It has been reported that both CR and XNBR could be d by epoxy resins[30,31]. Furthermore CR and XNBR racted to form ester linkages. In the ternary blend of NR and XNBR it was likely that ether linkages and ester ages (Part I of this chapter) would be distributed domly in the matrix. Conventionally cured vulcanisates ing sulphur linkages showed tendency for reversion. The nary blend, on the other hand, due to the difference in type of crosslinks showed absence of cure reversion and a her degree of crosslinking at higher temperatures.

.0 Effect of fillers on physical properties

The tensile stress-strain behaviour of the filled s are shown in Figure 5.2.6. Effect of filler loading on ical properties are summarised in Table 5.2.6. rtedly, the following properties showed gradual increase increase in filler loading: modulus, tensile strength, strength, abrasion resistance and hardness. Resilience ased with filler loading. It was interesting to note that build-up was cosiderably reduced for filled mixes er loading of filler. It was believed that unequal ion of reinforcing filler occured between different the ternary blend. Unequal distribution of filler d is reported to show low hysteresis.[32,33].

Polymer-filler interaction was studied by swelling of blend vulcanisates in chloroform. The variation of V_{ro}/V_{rf} against $\phi/(1-\phi)$ according to Kraus equation[34] is shown in Figure 5.2.7.

$$\frac{V_{ro}}{V_{rf}} = 1 - \frac{m\,\emptyset}{(1-\emptyset)}$$

where, V_{ro} is the volume fraction of rubber in gum vulcanisate

V_{rf} is the volume fraction of rubber in the filled vulcanisate

$\emptyset$ is the volume concentration of filler in the filled vulcanisate

m is a constant characteristic of the filler rubber matrix.

It was evident that the linear relation according to Kraus plot was not obeyed in this system. This deviation from linearity could be due to two reasons. Firstly, as reported in Part I of this chapter, fillers could influence the miscibility of the ternary blend. Affinities of the fillers for the three different rubber systems were not likely to be same. Accordingly, fillers would not tend to distribute uniformly between different phases in a blend. It has been shown earlier that polymer filler interaction depended on the type of blend, vulcanisation temperature[35], curing system[36,37] and type of filler[30]. This could result

an accumlation of fillers at the interface[37] and quently some portion of fillers would not be available the rubber matrix for resisting solvent penetration. This cause a lower V_{rf} than expected, resulting in an ease in the ratio of V_{ro}/V_{rf}. Secondly, fillers selves take part in crosslinking reaction which might lt in increase in crosslink density of the network[38]. ingly, actual V_{ro} in the filled blend would be higher the measured V_{ro} of gum blend. As a result the ratio of V_{rf} would be higher than the value, if there were no ase in crosslink density due to filler incorporation.

The abrasion characteristics of the blends have been ied by Scanning Electron Microscope. Ridge formation in tomers has been reported earlier[39-41]. It is shown that spacing of ridges show high abrasion resistance[42]. ion resistance mainly depended on the strength of the ix. The gum ternary blend had poor matrix strength improved greatly by the addition of reinforcing ers. The SEM fractographs of the abraded surfaces of the ary blend showing the effect of reinforcing filler on ion resistance are shown in Figures 5.2.8-5.2.10. The ed surface of the gum mix (Figure 5.2.8) showed ontal ridges which were deformed and widely spaced poor abrasion resistance. With incorporation of 20 ISAF black the abraded surface showed tendency to form cal ridges (Figure 5.2.9). When the ISAF black loading aised to 40 phr closely spaced vertical ridges (Figure

.10) were formed showing that the abrasion resistance was roved. Vertical ridge formation was suggestive of rtional type of wear[43].

Cure characteristics of the ternary blend G and of trol ENR, XNBR and CR mixes are shown in Table 5.2.7. ney viscosity and scorch time of the blend were found to intermediate between the two control mixes of ENR and t, but the Monsanto rheometric torque values were close to

Physical properties of the ternary blend and of trol, ENR, XNBR and CR mixes are shown in Table 5.2.8. The ervations can be summarised as follows.

(i) Expectedly gum CR showed high strength, due to ain crystallisation. Addition of reinforcing ISAF black not change the physical properties significantly. However, ition of 20 phr ISAF black reduced the elongation at break aused reduction in the abrasion loss and compression

(ii) Gum XNBR showed good matrix strength, excellent sion resistance but high compression set due to ionic links[44]. Incorporation of 20 phr ISAF black caused vement in most of the physical properties.However, ion resistance remained unaffected by presence of ISAF

(iii) Gum ENR showed poor matrix strength, which, ever, could be reinforced on addition of 20 phr ISAF black ler

(iv) The self-vulcanised ternary blend in the gum e registered poor failure properties like gum ENR, but it ed high reslience and low compression set. Abrasion loss heat build-up of the blend was nearer to gum CR matrix. tion of 20 phr of reinforcing black caused improvement in physical properties.

.I Stress Relaxation

In the following section the results of studies on s-relaxation behaviour of the self-vulcanized ternary d of ENR, XNBR and CR are reported. For comparison, the relaxation behaviour of single CR vulcanisate is ded.The stress relaxation behaviour of gum and filled and XNBR are given in chapter 3 part 2.

Plots of (σ/σ_0) (σ_0 is obtained from the maximum ss at t = 0, when the desired strain is reached, is the ss at subsequent times) plotted against log(t) is shown ures 5.2.11 and 5.2.12. For comparison, results of ENR XNBR vulcanisates (Chapter 3) are shown in Figures 11 and 5.2.12. The stress relaxation parameters[45] of ternary blend and the polychloroprene rubber are rised in Table 5.2.9.

Gum polychloroprene vulcanisate showed linearity in relaxation change with time. The gum ternary blend

two relaxations as observed in case of other rubber vulcanisates[46-49]. The first relaxation which took place in less than 550 seconds could associated with small segments or domain of molecular chains[46], while the second could be due to rearrangement of molecular chains or aggregates[50]. As seen from Table 5.2.9, ternary blend had a lower stress relaxation than polychloroprene.

The slope of all mixes increased with addition of filler showing that stress relaxation increased with addition of filler. The filled polychloroprene vulcanisate showed linearity in stress relaxation with time, while the ternary blend showed two relaxations. The intercept on time axis was shifted to a higher time. The stress relaxation behaviour of ternary blend was close to the binary blend of CR and XNBR (Chapter 3, Part IV).

The stress relaxation behaviour of these vulcanisates showed that the ternary blend which contained ether and ester crosslinks, behaved similar to conventional rubber vulcanisates.

Formulations of filled ternary blends[a]

Blend designation	GIS10	GIS20	GIS30	GIS40	GSR10	GSR20	GSR30	GSR40	GSR50	GSI10	GSI20	GSI30	GSI40	GSI50
Neoprene AC	25	25	25	25	25	25	25	25	25	25	25	25	25	25
XNBR (Krynac221)	75	75	75	75	75	75	75	75	75	75	75	75	75	75
ENR	75	75	75	75	75	75	75	75	75	75	75	75	75	75
ISAF black	17.5	35.0	52.5	70.0	-	-	-	-	-	-	-	-	-	-
SRF black	-	-	-	-	17.5	35.0	52.5	70.0	87.5	-	-	-	-	-
Silica[b]	-	-	-	-	-	-	-	-	-	17.5	35.0	52.5	70.5	87.5

[a] Formulation is in parts by weight

[b] precipitated silica, Vulcasil S obtained from Bayer (India) Ltd.,Bombay.

3.2.2 : Formulations of control single rubber mixes[a]

	N	Nc	X	Xc	E	Ec
...ne AD	100	100	-	-	-	-
(Krynac 221)	-	-	100	100	-	-
	-	-	-	-	100	100
	-	-	-	-	0.25	0.25
	5	5	5	5	5	5
...ic acid	-	-	2	2	2	2
...black	-	20	-	20	-	20
...yl phthalate	-	2	-	2	-	-
...tic oil	-	-	-	-	-	2
	4	4	-	-	-	-
...rea	-	0.5	-	-	-	-
	-	-	-	-	1.6	-
	-	-	1.0	1.0	2.4	1.0
...ur	-	-	2.4	2.4	0.3	2.8

[a] Formulation is in parts by weight
[b] Tetramethylthiuram disulphide
[c] N-oxydiethylene benzothiazole-2-sulphenamide

Sample	A	B	X	C	J	D	E	F	H	G	L	K
Neoprene/XNBR/ENR	3/1/3	3/1/2	3/1/1.5	3/1/1	3/1/0.5	2/2/3	2/2/2	2/2/1	1/3/3.5	1/3/3	1/3/2.5	1/3/2
Mooney viscometry												
Minimum Mooney viscosity at 120° C.	31	31	32	33	38	31	32	38	26	30	33	36
Mooney scorch time at 120° C.,min.	20.8	11.1	11.0	10.8	6.0	10.0	8.3	6.3	8.3	8.0	8.0	6.5
Monsanto rheometry												
Minimum torque at 150° C.,dN.m	6	8	8	8	10	5	6	8	4	5	6	8
Maximum torque at 150° C. (at 60 min.)dN.m	15	22	23	21	26	24	25	31	12	31	28	31

[illegible] typical properties of gum ternary blends moulded for 60 min. at 150 °C.

	A	B	C	D	E	F	G	H	I
[illegible]	3/1/3	3/1/2	3/1/1	2/2/3	2/2/2	2/2/1	1/3/3	1/3/2	1/3/1
[illegible], MPa	2.5	2.8	6.4	3.5	3.5	6.1	-	5.0	4.8
[illegible] strength, MPa	9.3	8.6	15.5	5.0	5.8	9.7	4.7	5.3	5.4
[illegible] at break, %	550	510	440	380	370	370	270	310	330
[illegible], kN/m	33	29	39	23	26	27	18	18	23
[illegible] hardness	60	65	75	55	58	65	49	52	55
[illegible] at 60° C., %	57	62	62	63	65	67	68	66	65
[illegible] wt, 22 h at [illegible]	57	30	30	30	27	19	11	13	13
[illegible] loss, cc^{b}	4.6	4.6	4.2	4.6	4.6	1.6	4.2	2.8	1.2
[illegible] by Goodrich [illegible] with a load of [illegible] of 4.5 mm	a	a	a	a	a	a	38 b	a	a
	0.06	0.07	0.10	0.10	0.11	0.11	0.13	0.13	0.11

[illegible] blown out before 20 min.
[illegible] after 20 min.

[illegible] Cure characteristics of the filled ternary blend. (G)

	Filler	Loading					
		0	10	20	30	40	50
[illegible] viscosity	ISAF black		42	43	58	71	-
	SRF black	30	37	39	39	49	62
	Silica		45	49	67	98	170
[illegible] time at [illegible]	ISAF black		6.2	5.5	5.0	4.0	-
	SRF black	8.0	6.8	6.3	5.8	5.0	4.7
	Silica		6.2	5.5	5.0	3.2	2.5
[illegible]							
[illegible] at 150°C. [illegible]N.m	ISAF black		11	12	16	18	-
	SRF black	5	10	10	14	14	14
	Silica		11	12	17	31	34
[illegible] at 150° C. [illegible] dN.m	ISAF black		44	56	67	84	-
	SRF black	31	42	47	54	61	69
	Silica		51	66	67	91	96

[illegible] Physical properties of the filled ternary blend(G) moulded for 60 min.at 150 °C

	Filler	loading (parts per 100 of rubber)					
		0	10	20	30	40	50
[illegible]	ISAF black		5.5	7.3	10.0	15.4	-
	SRF black	2.8	6.5	7.0	7.5	9.9	11.8
	Silica		3.4	5.6	8.5	10.8	12.7
[illegible] strength, Mpa	ISAF black		7.4	8.0	16.0	17.0	-
	SRF black	4.7	7.2	8.0	9.7	11.9	15.0
	Silica		7.1	9.8	14.8	16.8	17.4
[illegible] break, %	ISAF black		240	290	280	220	-
	SRF black	270	210	220	250	250	270
	Silica		330	320	320	300	280
[illegible] strength, kN/m	ISAF black		30	39	50	48	-
	SRF black	18	34	40	45	47	54
	Silica		22	40	53	58	54
[illegible] Shore A	ISAF black		58	65	70	76	-
	SRF black	49	51	59	64	68	74
	Silica		60	65	75	82	89
[illegible] at 70° C., %	ISAF black		61	53	51	49	-
	SRF black	68	63	62	60	57	65
	Silica		64	62	60	53	49
[illegible] 22 h at 70° C., %	ISAF black		11	12	14	15	-
	SRF black	11	11	11	14	16	16
	Silica		14	14	14	16	16
[illegible] cc/hr	ISAF black		2.8	1.8	1.4	0.9	-
	SRF black	4.2	3.9	3.7	3.5	3.0	2.5
	Silica		2.8	2.1	1.2	0.5	0.5

	Filler	Loading(parts per hundred of rubber)					
		0	10	20	30	40	50
[illegible] by Goodrich [illegible] a load of 24 lb [illegible] 4.5 mm [illegible]	ISAF black		26	27	32	35	-
	SRF Black	38 [a]	30[b]	30	35	35	35
	Silica		[c]	30	33	31	26
[illegible] at. X	ISAF black		1.2	1.2	1.3	1.3	-
	SRF black	[d]	[d]	2.2	3.1	3.5	3.5
	Silica		[d]	0.4	3.3	1.4	1.4
	ISAF black		0.17	0.18	0.20	0.22	-
	SRF black	0.13	0.15	0.17	0.18	0.19	0.20
	Silica		0.15	0.17	0.18	0.20	0.22

[illegible] 20 min.

[illegible] 5 min.

[illegible] before 15 min.

[illegible] at.

[illegible] characteristics of control single rubber mixes.

	N	Nc	E	Ec	X	Xc	G[a]	GIS20[a]
[illegible]								
[illegible] viscosity at [illegible]	89	127	5	9	40	50	30	43
[illegible] time at [illegible]	5.0	3.0	10.0	6.5	3.8	2.0	8.0	5.5
[illegible]								
[illegible] at 150°.C, dN.m	18	25	2	3	11	12	5	12
[illegible] at 150° C., dN.m	39	87	33	80	87	115	31	56

[illegible] from Table 5.2.4

[illegible] Physical properties of the ternary blend and of control ENR and XNBR

	N	X	E	G	Nc	Xc	Ec	GIS20
[illegible] MPa	7.0	3.9	1.2	-	-	15.5	9.0	-
[illegible] MPa	17.0	18.7	4.2	4.7	9.0	24.0	23.0	8.0
[illegible] at break, %	900	470	650	270	170	380	595	290
[illegible], kN/m	70	34	18	18	68	70	49	39
[illegible] hore A	87	69	30	49	89	83	61	65
[illegible] at 40° C., %	61	62	26	68	60	54	49	53
[illegible] set, 22 h at 70° C., %	25	70	16	11	18	53	35	12
[illegible], cc/1000 rev.	1.00	0.05	8.40	1.80	0.77	0.05	0.42	0.80
[illegible] by Goodrich [illegible] with a load of 24 lb [illegible] of 4.5 mm								
[illegible]	38	b	20	38[a]	26	58	16	27
[illegible] wt	6.1	b	1.6	c	1.6	4.2	7.3	1.2
	0.09	0.05	0.09	0.13	0.23	0.10	0.12	0.18

[illegible] after 20 min.

[illegible] could not be tested

[illegible] not

Table 5.2.9 : Stress relaxation parameters for polychloroprene and the self-vulcanisate ENR-XNBR-CR blend

	Sample[a]	Slope		Interaction point on time axis
		Early	Later	
Raw polychloroprene	N	.06	-	-
Raw blend	G	.06	.04	500
Milled polychloroprene	Nc	.07	-	-
Milled blend	GIS20	.07	.04	2500

[a] reference Table Nos. 5.1.1, 5.2.1 and 5.2.2

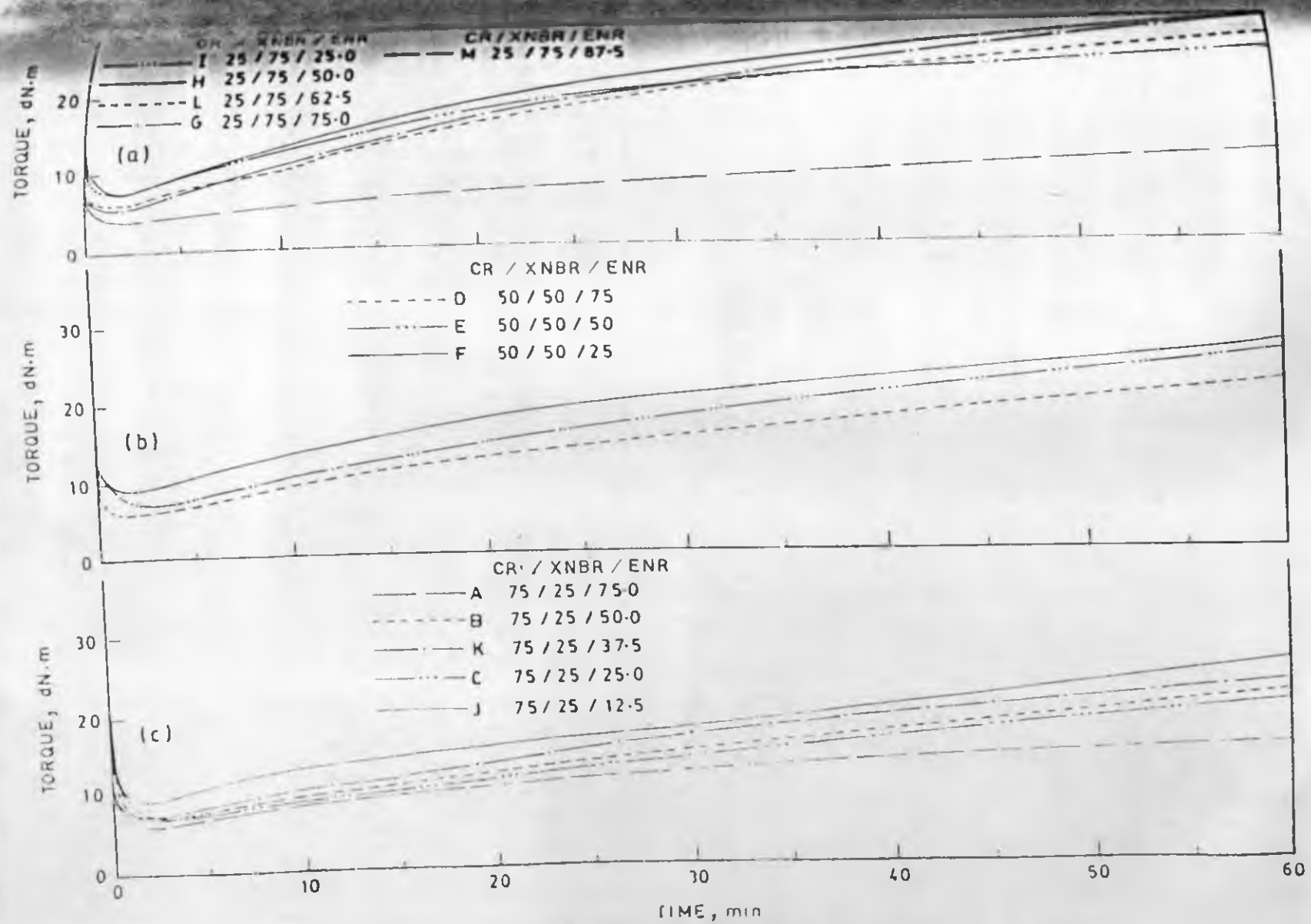

Fig. 5.2.1.:Monsanto rheographs of different gum ternary blends at 150°C.

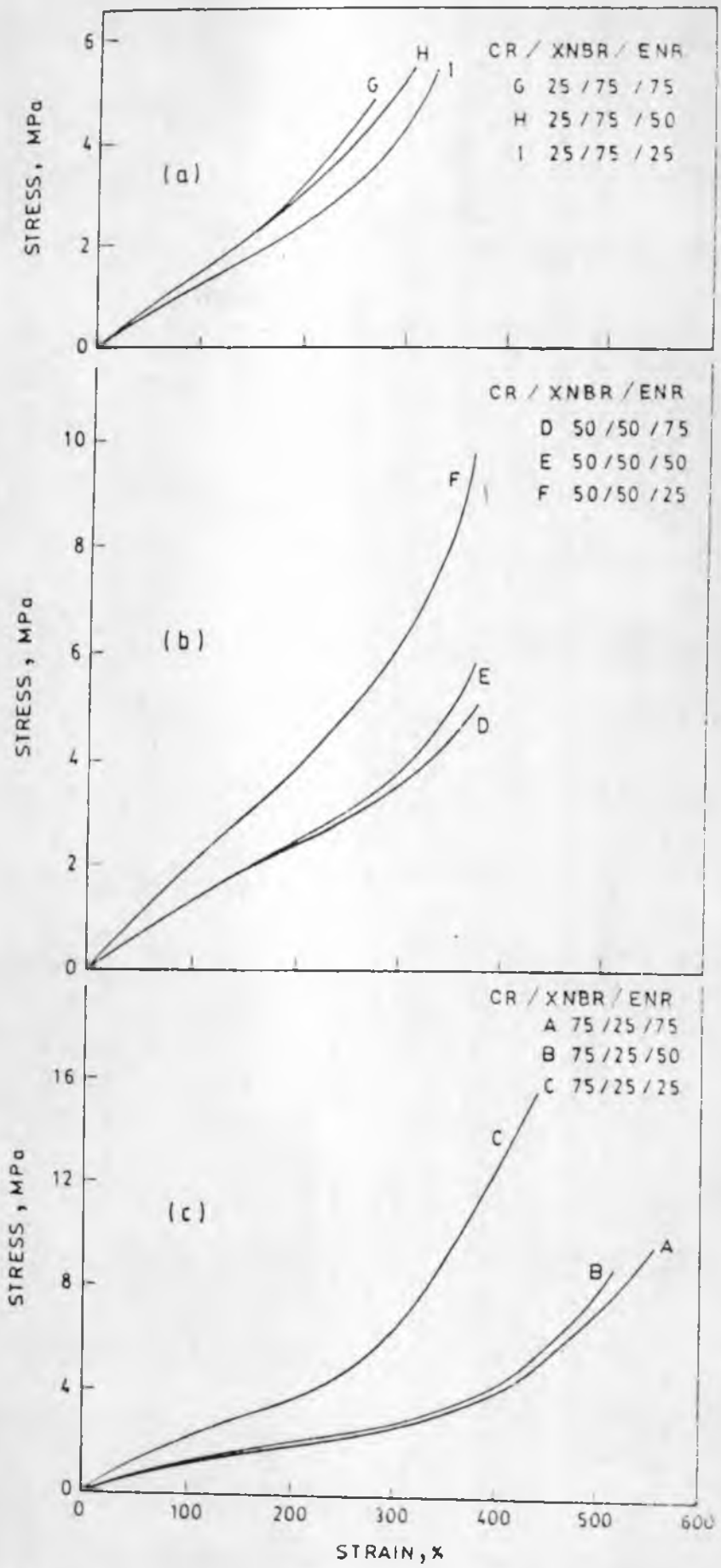

Fig. 5.2.2: Tensile stress - strain curves of ternary gum vulcanisates.

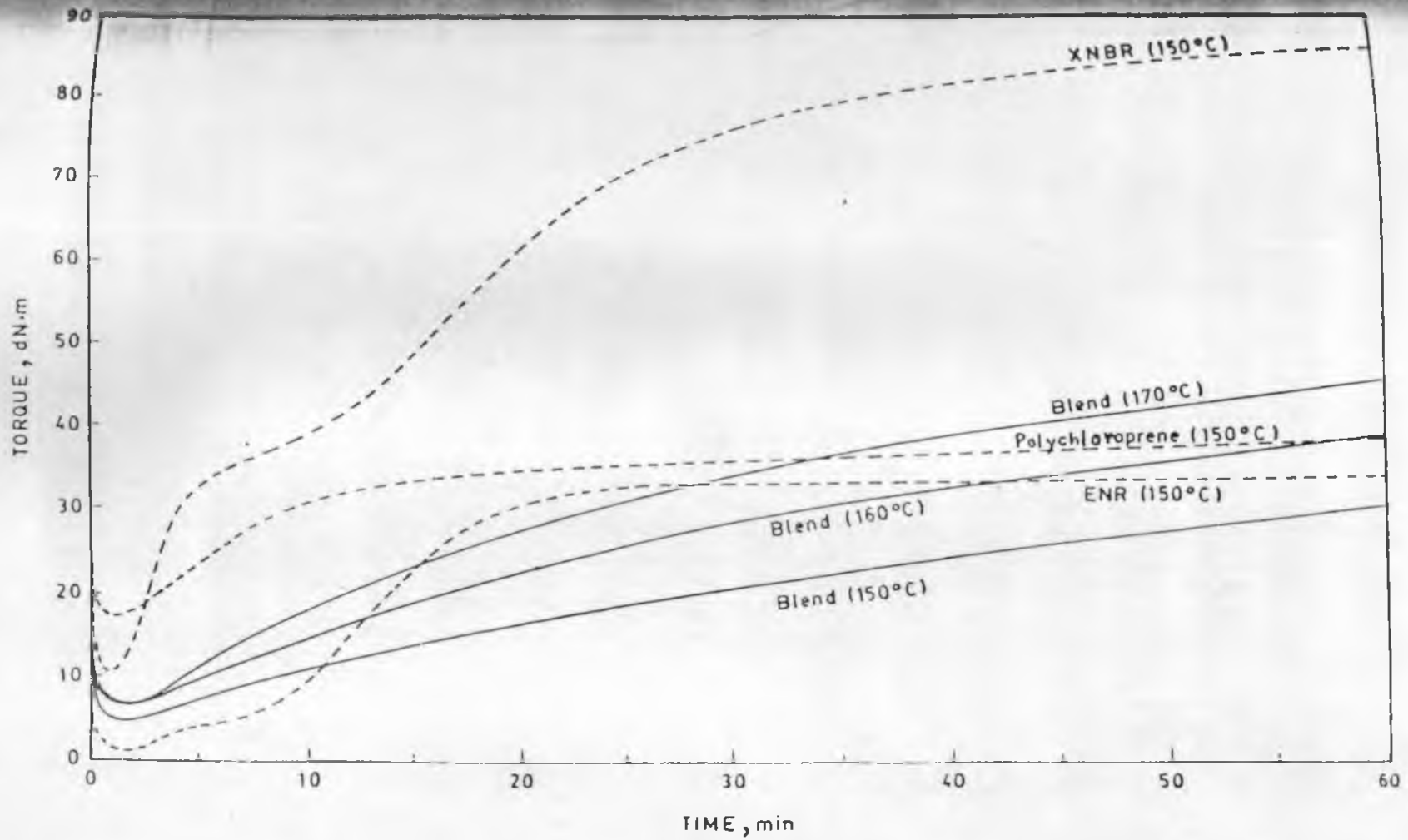

Fig. 5.2.3: Rheographs of gum blend at different temperatures and of control ENR, XNBR and polychloroprene mixes at 150°C.

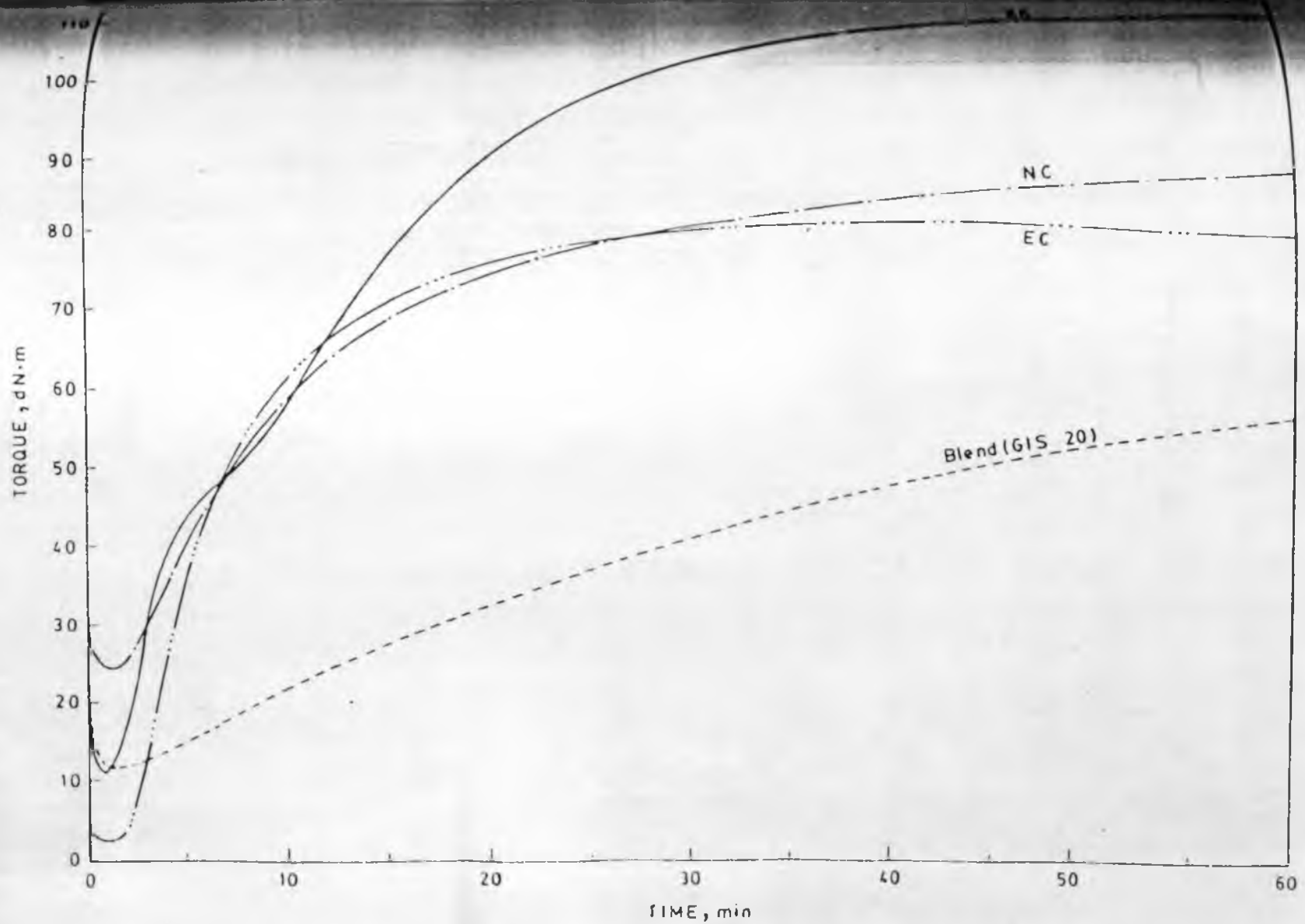

Fig. 5.2.4. Rheographs of ISAF black filled systems of single ENR, XNBR polychloroprene and the ternary

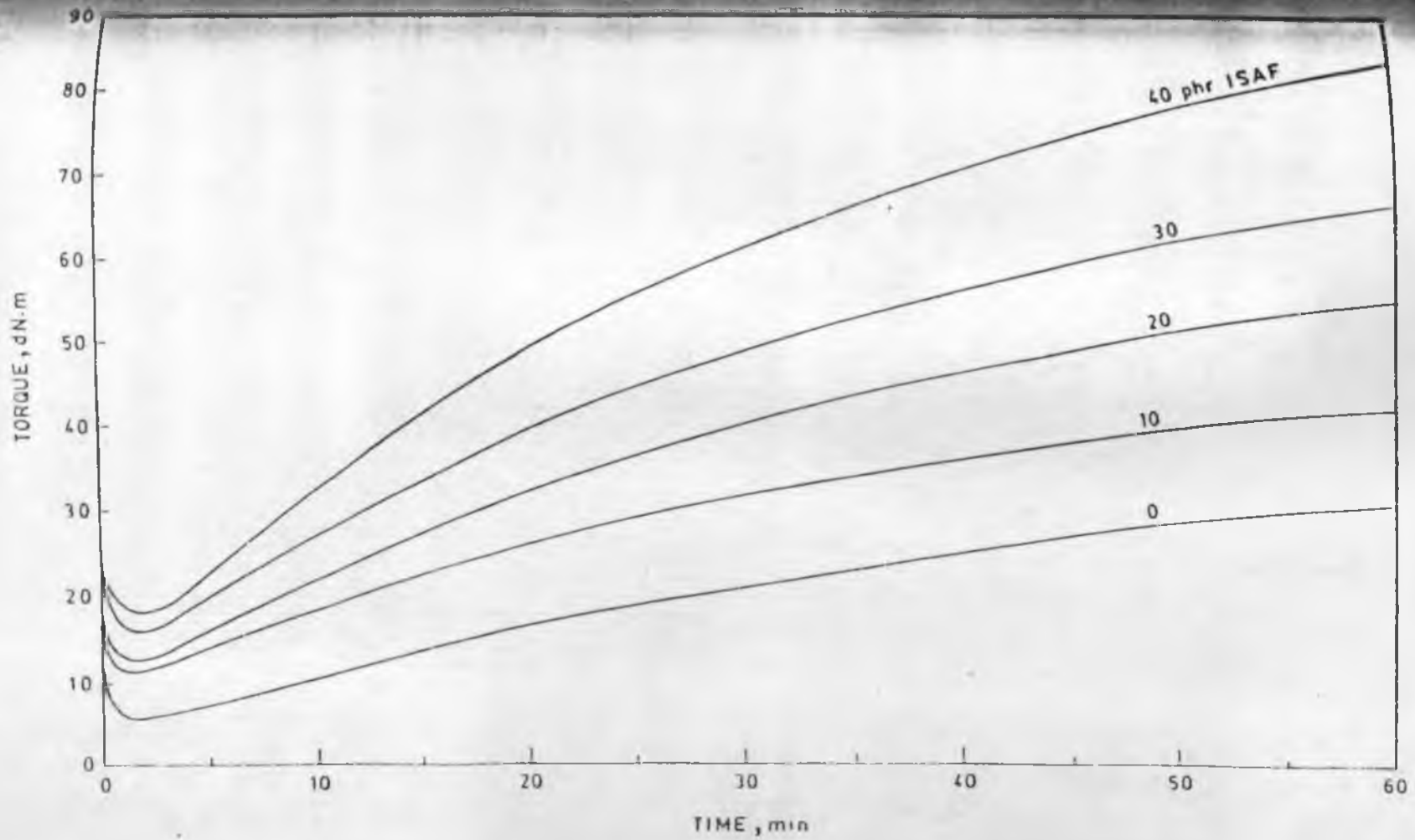

Fig. 5.2.5 : Rheographs at 150°C of the 25/75/75 CR/XNBR/ENR ternary blend filled with different loadings of ISAF black.

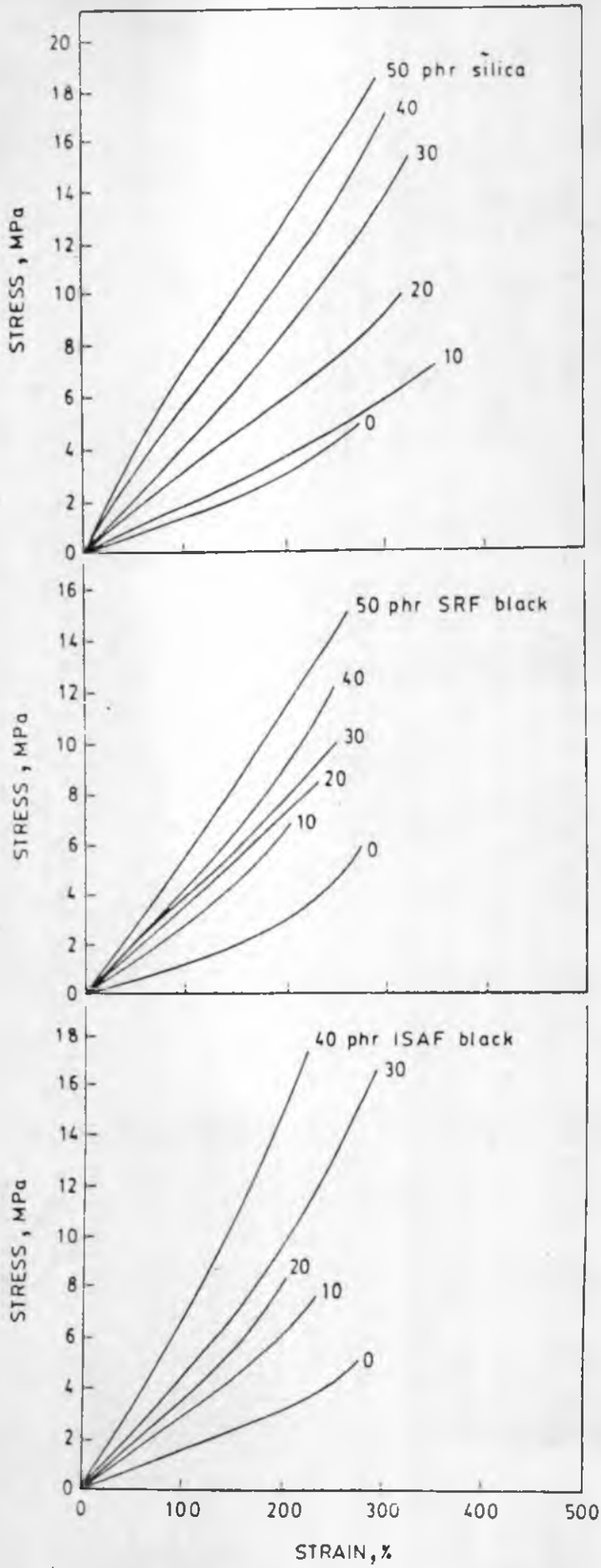

5.2.6: Tensile stress - strain curves of the miscible ternary blend (G) filled with different loadings of ISAF black, SRF black and silica.

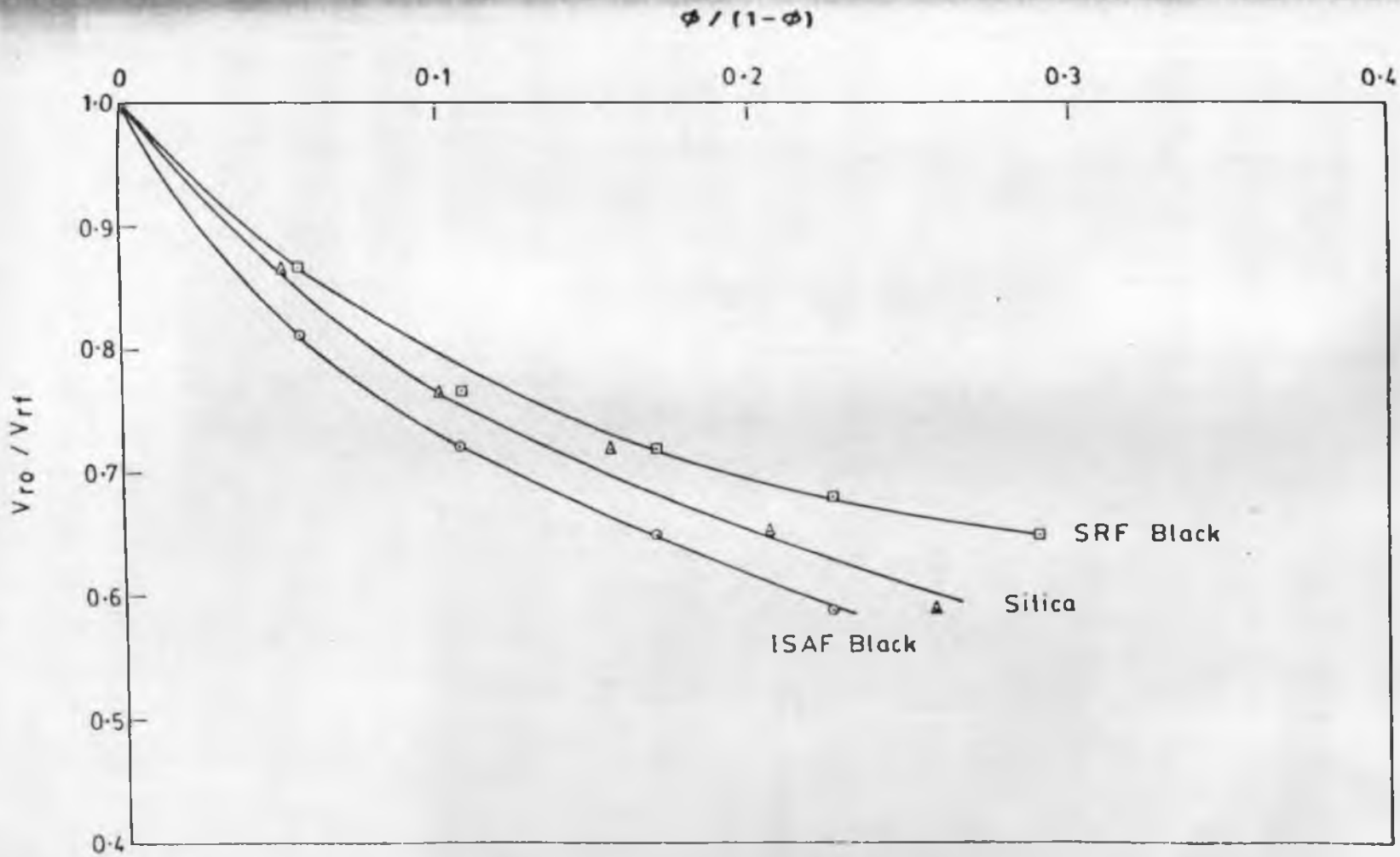

Fig. 5.2.7 :Kraus plots for ISAF black and silica filled (25/75/75 CR/XNBR/ENR) ternary blend.

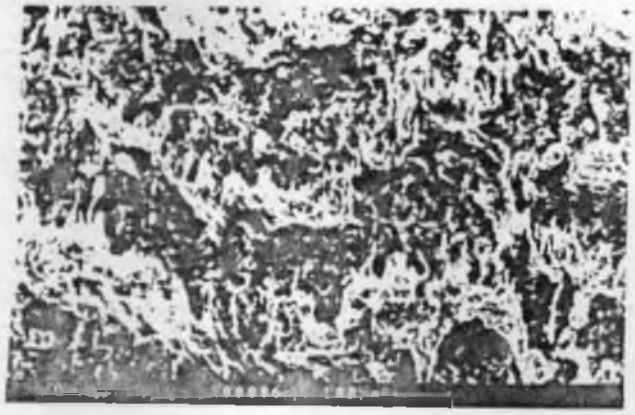

Fig. 5.2.8 : SEM fractograph of abraded surface of blend G.

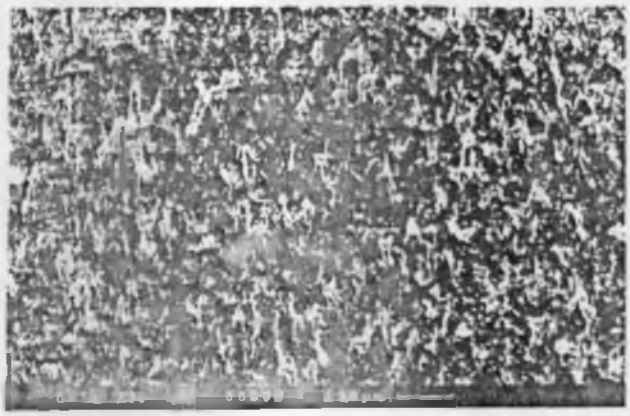

Fig. 5.2.9 : SEM fractograph of the abraded surface of blend G filled with 20 phr ISAF black.

Fig. 5.2.10 : SEM fractograph of abraded surface of blend G filled with 40 phr ISAF black.

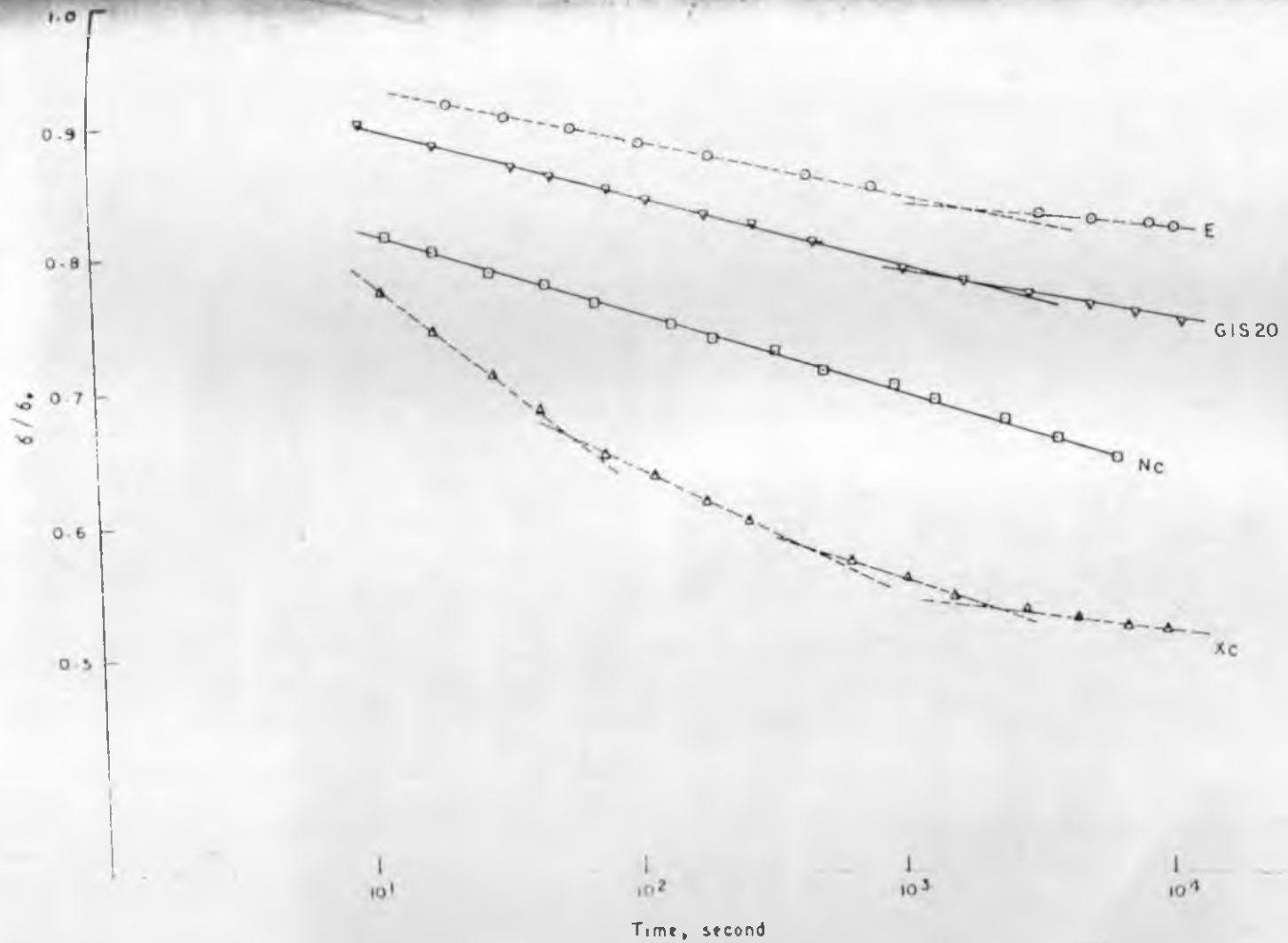

Fig. 5.2.11: Semilogarithmic plots of stress decay as a function of time for the 20 phr ISAF black filled ENR, XNBR CR and the ternary blend (GIS20) vulcanisates.

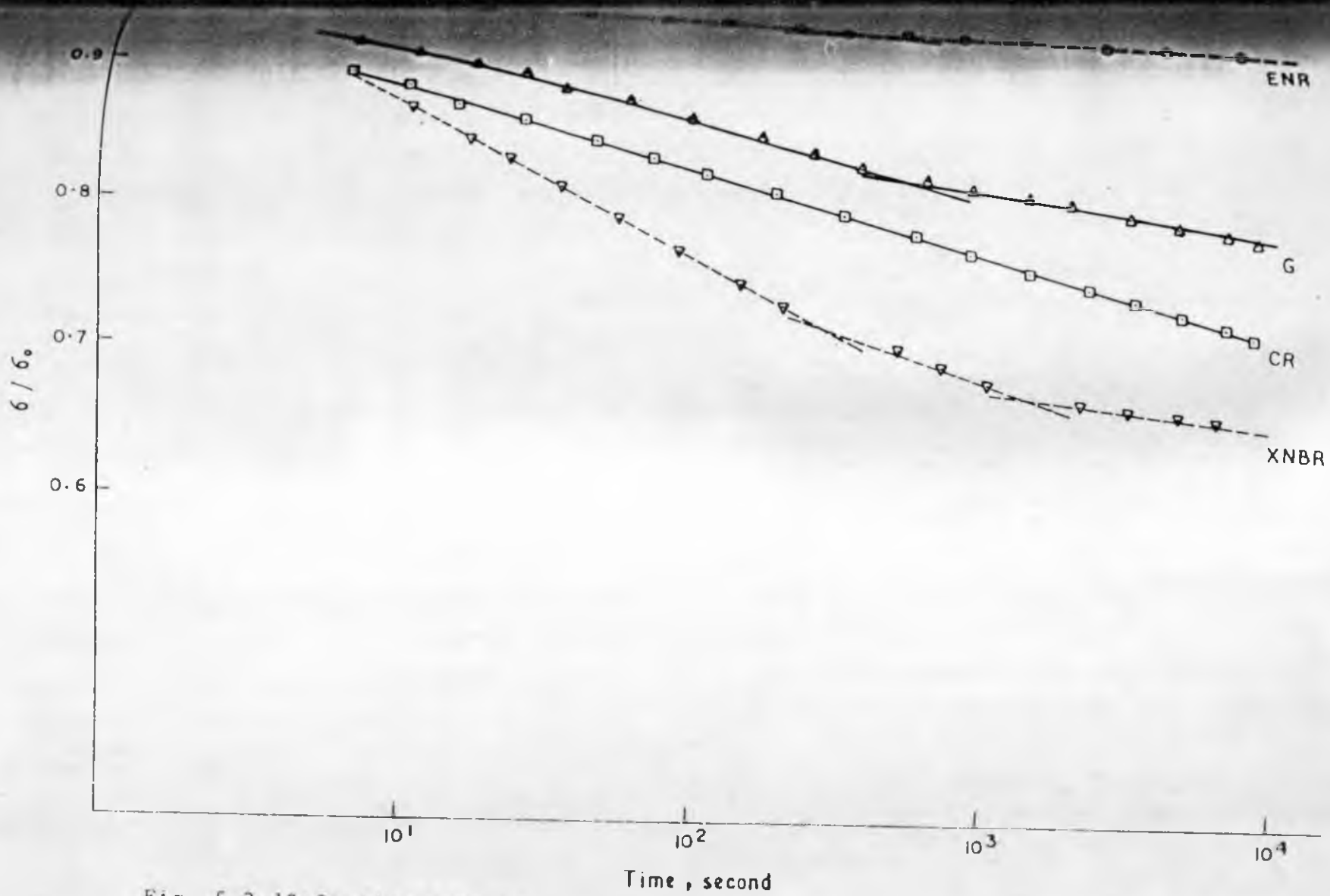

Fig. 5.2.12: Semilogarithmic plots of stress decay as a function of time, for, ENR, XNBR, CR and the ternary blend (G) vulcanizates.

CHAPTER 5 - PART III

AGEING STUDIES

In the following section, the results of studies on [illegible]ing of the self-vulcanised ternary blend of ENR, XNBR and [illegible] are reported. For comparison, single CR vulcanisate is [illegible]n.

[illegible] Ageing Studies

Ageing studies were done under the following different [illegible]ing conditions.

(a) Air at 70°C for 12 days

(b) Aqueous HCl, 25% at 70°C for 7 days

(c) Aqueous NaOH, 25% at 70°C for 7 days

(d) ASTM fuel C at 30°C for 7 days

The formulation of the mixes are given in Tables [illegible], 5.2.1 and 5.2.2. Tensile properties of aged and [illegible]ed gum and carbon black filled vulcanisates are given in [illegible]le 5.3.1. The percent retention of tensile strength [illegible] the gum and filled vulcanisates are given in Figures [illegible] and 5.3.2

[illegible] Air Ageing

On ageing both gum and filled polychloroprene [illegible]canisates showed a decrease in modulus and tensile [illegible]ngth, but constancy in elongation at break in gum [illegible]canisate and a decrease in filled vulcanisate.

The gum ternary blend showed constancy in modulus and

decrease in tensile strength and elongation at break, while the filled ternary blend showed an increase in modulus and tensile strength but decrease in elongation at break. In ternary blend, ageing might have similar effect of post vulcanization curing phenomenon.

4.3.B Acid Ageing

Polychloroprene vulcanisates, both gum and filled showed a decrease in modulus, tensile strength and elongation at break. This showed that polychloroprene vulcanisates had poor resistance towards acids.

The gum ternary blend showed constancy in modulus, tensile strength and elongation at break. The filled ternary blend, on the other hand, showed decrease in all tensile properties on ageing.

4.3.C Alkali Ageing

Both gum and filled polychloroprene vulcanisates showed considerable resistance to alkali ageing as compared to acid ageing. The aged vulcanisates showed a decrease in modulus and tensile strength and increase in elongation at break after alkali ageing.

The gum ternary blend, on the other hand, showed an increase in modulus and tensile strength and decrease in elongation at break. It was possible that in the ternary blend, there was crosslinking reaction in presence of NaOH as it is known that polymers containing ester groups crosslinked

hydrolysis in presence of basic oxides and hydroxides[51].

5.3.D Fuel Ageing

The polychloroprene vulcanisates (both gum and filled) showed a decrease in modulus and tensile strength, but an increase in elongation at break, after fuel ageing.

The gum ternary blend showed a decrease in modulus but increase in tensile strength and elongation at break after fuel ageing. The filled ternary blend showed a decrease in modulus, tensile strength and elongation at break. In retention of tensile properties, it showed a behaviour very close to that of ENR, as discussed earlier in Chapter 3.

Figure 5.3.1 and Fig. 5.3.2 show retention of properties of the self-vulcanised blends after ageing. For comparison retention properties of the single rubber vulcanisates are included. (Results of ENR and XNBR vulcanisates have been taken from Chapter 3).

As far as retention of properties in gum vulcanisates are concerned :

- In air-ageing the blend is close to XNBR and much better than ENR.
- In acid ageing the blend is superior to ENR, XNBR and CR.
- In alkali ageing the blend is superior to ENR, XNBR

and CR.

in fuel ageing the blend is superior to ENR, XNBR and CR.

As far as rentention of properties in filled vulcanlsates are concerned :

in air ageing the blend is closer to XNBR and CR, and much better than ENR.

in acid ageing, the blend is superior to ENR, XNBR and CR.

in alkali ageing, the blend is closer to CR and ENR,

in fuel ageing, the blend is nearer to ENR and CR, but inferior to XNBR.

5.3.1 : Tensile Properties of Aged and Unaged Vulcanisates

Ageing conditions	Modulus, MPa 100%	200%	300%	Tensile strength MPa	Elongation at break,
Original	3.5	4.4	3.9	17.3	750
Air 70°C/12d[b]	1.7	2.3	3.1	15.0	800
Acid 70°C/7d	1.8	2.3	3.0	7.7	690
Alkali 70°C/7d	2.8	3.3	4.1	16.0	950
Fuel 30°C/7d	1.3	1.7	2.1	13.6	1030
Original	1.2	2.3	-	2.6	250
Air 70°C/12d[b]	1.4	-	-	2.0	160
Acid 70°C/7d	1.3	2.4	-	2.7	230
Alkali 70°C/7d	1.8	3.5	-	3.8	215
Fuel 30°C/7d	1.1	1.90	2.9	3.1	320
Original	5.4	9.5	14.9	25.4	480
Air 70°C/12d[b]	2.7	5.8	11.2	22.0	5.65
Acid 70°C/7d	2.7	4.9	8.0	10.0	360
Alkali 70°C/7d	3.6	6.1	9.7	20.5	550
Fuel 30°C/7d	2.2	4.3	7.4	15.8	500
20[c] Original	2.3	5.5	10.2	11.4	320
Air 70°C/12d[b]	3.0	7.7	-	12.0	250
Acid 70°C/7d	3.8	-	-	6.5	160
Alkali 70°C/7d	3.6	8.0	-	9.0	230
Fuel 30°C/7d	2.0	4.3	-	5.8	250

erence;a Table No.5.2.2 b Table No 5.1.1 c Table No5.2.1

means days,

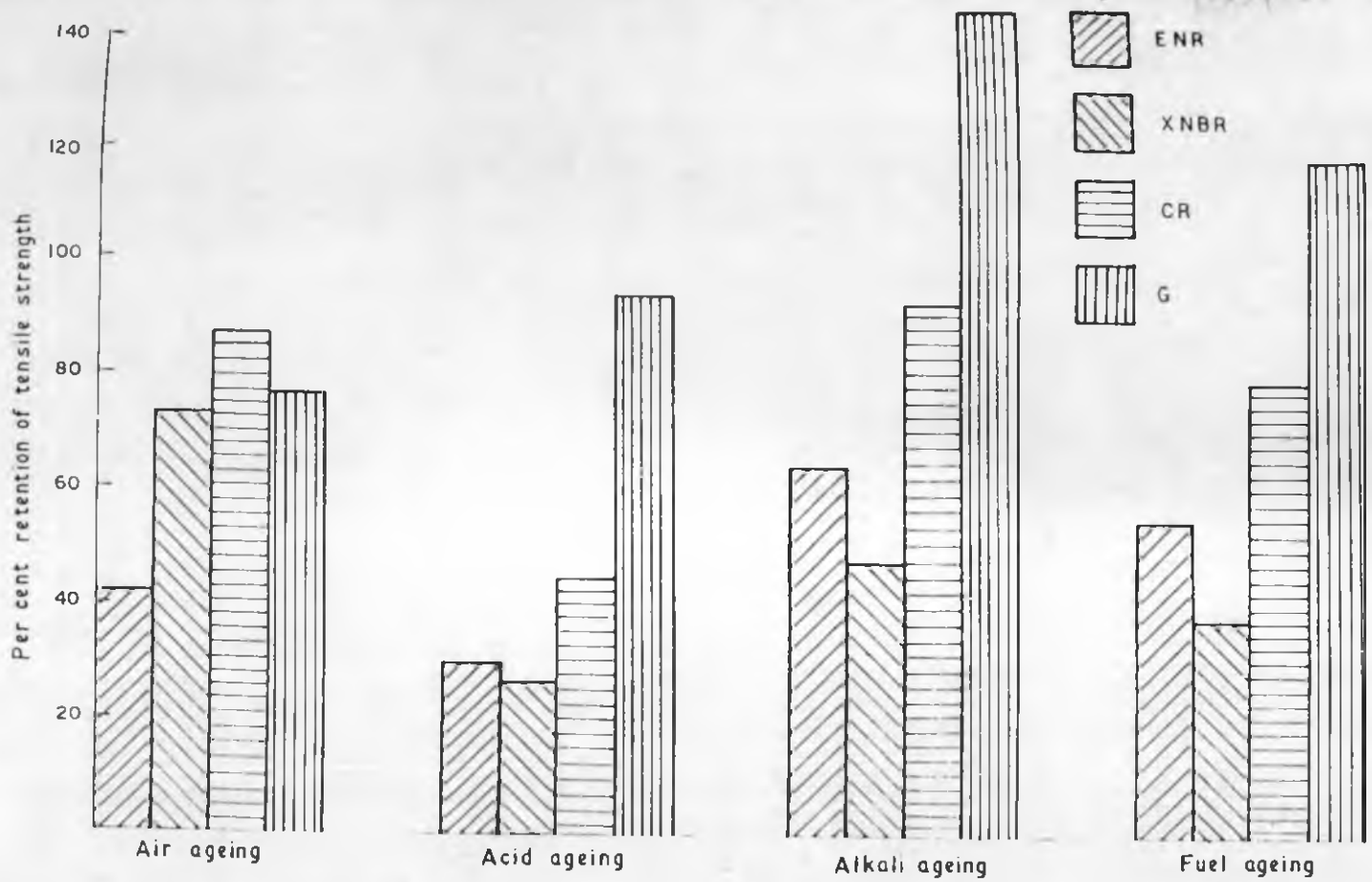

Fig. 5.3.1 : Percent retention of tensile strength for the gum ENR, XNBR, CR and the ternary blend vulcanisates

REFERENCES

S. Mukhopadhyay and S.K. De, Polymer 32(7) (1991) 1223.

S. Mukhopadhyay and S.K. De, J. Appl. Polym. Sci. (in press).

V.S. Shah, J.D. Keitz, D.R. Paul and J.W. Barlow, J. Appl. Polym. Sci., 32 (1986) 3863.

T.K. Kwei, H.L. Frisch, W. Radizan and S. Vogel, Macromolecules, 10 (1977) 157.

Y.Y. Wang, and S.A. Chen, Polym. Eng. Sci., 21 (1981) 47.

Yu-der Lee and Chi - Ming Chen J. Appl. Polym. Sci. 33 (1987) 1231.

C.E. Locke and D.R. Paul, Polym. Eng. Sci., 13(4) (1973) 308.

D.R. Paul, C.E. Locke and C.E. Vinson, Polym. Eng. Sci., 13(3) (1973) 2092.

Bruno Ameduri and Robert E. Prud homme, Polymer, 29 (1988) 1052.

K.E. Min, J.S. Chiou, J.W. Barlow and D.R. Paul, Polymer, 28 (1987) 1721.

G. Socrates, in Infrared Characteristic Group Frequencies, The Pitman Press Batch, John Wiley and Sons Ltd., New York, Chap. 10. .

R.A. Saunder and D.C. Smith, J. Appl. Phys., 20 (1949) 953.

C. Raux, R. Pautrat, R. Cheritat, F. Ledran and J.C. Danjard, J. Polym. Sci., Part C, 16 (1969) 468.

Annual Book of ASTM Standards, Part 37, 1981.

M.C.S. Perera, J.A. Elix and J.H. Bradbury, J. Polym. Sci., Part A : Polym. Chemistry, 26 (1988) 637.

R.E. Prudhomme, Polym. Eng., Sci., 22 (1982) 90.

A.I. Medalia, J. Colloid Interface Sci., 32 (1970) 115.

G. Kraus, J. Polym. Sci., Polym. Phys. Edn., 8 (1970) 601.

J.J. Brennan, T.E. Jermyn and B.B. Boonstra, J. Appl. Polym. Sci., 8 (1964) 2657.

A.M. Gesslar, Rubber Age, 101 (1969) 54.

K.A. Grosh, J. Appl. Polym. Sci., 12 (1968) 915.

H. Westlinning, Kautsch. Gummi. Kustst., 15 (1962) 475.

P.P.A. Smit, Rheol. Acta., 5 (1966) 277.

A.R. Payne and R.G. Whittaker, J. Composites, 1 (1970) 203.

J.A.C. Harwood, A.R. Payne and J.Z. Smith, Kautsch. Gummi. Kunstst., 22 (1969) 548.

T.G.F. Schoon and K. Adler, Kautsch. Gummi. Kunstst., 19 (1966) 414.

A. Siegmann, J.Appl. Polym. Sci., 24 (1979) 2333.

J.K. Kallitsis and N.K. Kalfoglou, J. Appl. Polym. Sci., 32 (1986) 5261.

D.C. Edwards and K. Sato, Rubber Chem. Technol., 52 (1979) 263.

S.K. Chakraborty and S.K.De, J. Appl. Polym. Sci. 27 (1982) 4561.

N.D. Zakharov and G.A. Maiorov, Sov. Rubber Technol. 22 (1963) 11.

C.M. Roland, Rubber Chem. Technol., 62 (1989) 456.

U.M. Hess and V.E. Chirico, Rubber Chem. Technol. 50 (1977) 301.

G. Kraus, J. Appl. Polym. Sci., 7 (1963) 861.

A.K. Bhowmick and S.K. De, Rubber Chem. & Technol., 53 (1980) 960.

S.K. Chrakraborty and S.K. De, Polymer, 24 (1983) 1055.

P.A. Marsh, A. Voet, L.O. Price, and T.J. Mullins, Rubber Chem. Technol. 1968, 41, 344

P.K. Pal and S.K. De, Rubber Chem. Technol., 55 (1982) 23.

A. Schallamach, Rubber Chem. Technol., 41 (1968) 209.

N.M. Mathew and S.K. De, J. Mat. Sci., 18 (1983) 515.

S.S. Bhagawan and D.K. Tripathy, Mat. Chem. and Phys. 17 (1987) 415.

A.N. Gent, and C.T.R. Pulford, Developments in Polymer Fracture -1, Andrews E. H. Ed., Applied Science, London, 1979, p.155

M.M. Reznikovskii and G.I. Brodskii, Abrasion of rubbers, James O.I. Ed,, MacLaren, London, 1967, p. 14 and p.81

S.K. Chakraborty, A.K. Bhowmick and S.K. De, J. Appl. Polym. Sci., 26 (1981) 4011.

C.I. MacKenzie and J. Scanlan, Polymer, 25 (1984) 559.

Per Flink and Bengt Stenberg, British Polymer Journal, 22 (1990) 193.

T. Kusano and K. Murakami, J. Polym. Sci., Polym. Chem. Ed., 10 (1972) 2823.

A.N. Gent, Rubber Chem. Technol.,36 (1963) 389.

S.S. Bhagwan, D.K. Tripathy and S.K. De, J. Appl. Polym. Sci., 33 (1987) 1623

A. Saha Deuri, P.P. De, A.K. Bhowmick and S.K. De, Polymer Degrn. Stability, 20 (988) 135.

S.T. Semegen and J.E. Wakelin, Rubber Age, 71 (1952) 57.

CHAPTER 6

RHEOLOGICAL BEHAVIOUR OF THE TERNARY BLEND OF EPOXIDISED NATURAL RUBBER (ENR) CARBOXYLATED NITRILE RUBBER (XNBR) AND POLYCHLOROPRENE RUBBER (CR)

CHAPTER 6 - PART I

VISCOSITY

• This part of the work has been communicated to Kautschuk Gummi Kunststoffe

A number of researchers have reported on rheology of polymer blends[1-7]. A comprehensive review on dependence of rheological properties on blend compositions has been given by Plochoki[8-9]. Generally viscosities of blends vary monotonically with the blend composition. The rheological properties are also affected by the method of preparation. The rheological behaviour of natural rubber (NR) with plastics[10,11] and cryoground rubber[12], epoxidised natural rubber with poly(vinylchloride)(PVC)[13] of other elastomers and elastomer blends[14,16] have been reported.

Viscosity of polymer blends as a function of blend composition has been described by different models[16-20]. The different blend additivity rules, like logarithmic rule[21], Hashin's upper control rule and Hashin's lower control rule[21], Heitmillers inverse additivity rule[19] and sheath-core rule[22] have been used for polymer melts[23].

In this chapter the rheological characteristics of the binary blend, ENR/XNBR/CR are reported and an effort is made to correlate the blend viscosities by additivity rules.

6.1 VISCOSITY

6.1.1 Variation of Shear Stress with Shear Rate

Formulation of the mixes are given in Table 6.1.1a and 6.1.1b.As evident from Fig. 6.1.1 all the mixes showed slope n to be less than one revealing that they were pseudoplastic in nature. Reasonable straight lines could be drawn for the polychloroprene mixes showing that it obeyed

power law model of flow in the range of shear rate from 10^0 to 10^4 s^{-1}. Close observation of flow curves showed that all mixes other than polychloroprene were not sufficiently linear and appeared to be concave. This means that `n' tended to decrease with rate of shear. Thus for these materials `n' was dependent on $\dot{\gamma}_{wa}$ and was not a unique material parameter. The experimental points of these rubbers could be fitted into two straight lines showing that the pattern of flow changed after a certain interval of shear rate.

6.1.B Shear Stress-Shear Rate Variation, Effect of Blend Ratio

The rate of deformation at a particular shear stress was very low and almost same except at very low shear rates for polychloroprene and XNBR while it was very high for ENR. The blends occupied a position which was a mean of that occupied by XNBR, CR and ENR. Mix C which contained a higher proportion of polychloroprene showed a lower rate of deformation than mix G which contained a lower proportion of polychloroprene, for a particular shear stress.

The flow parameters given in Table 6.1.2 showed that the value of n changed after two decades of shear rate and the slope of the second line was lower than slope of the first line at both 90°C and 100°C. Thus these mixes showed more deviation from parabolic flow, with a marked wall slip[24], which was more prominant after 2 decades of shear. The consistency parameter, which is the intercept on

cosity axis is also given in Table 6.1.2. This gives an of the initial viscosity and hence the susceptibility to kdown on mixing mill. As seen ENR had a lower value of compared to XNBR and CR, which showed that ENR was more eptible for breakdown on mixing mill. After filler ition, the control mixes of ENR and XNBR showed a lower e of k, while the other mixes showed higher values of k. showed that the viscosity of the mixes increased with ler addition.

1.C Shear Stress-Shear Rate Variation - Effect of Fillers

The addition of filler increased modulus of the mixes hence caused decrease in rate of deformation, as compared gum mixes. The silica filled mixes showed a lower rate eformation than the carbon black filled mixes. Straight could be drawn for the shear stress shear rate vlour, except at very low shear rates, for the filled ary mix.

1.D Variation of Viscosity with Shear Stress and Shear Rate

Viscosity as a function of shear stress at different eratures 90°C and 100°C for the gum mixes are shown in 6.1.2a and 6.1.2b. Variation of viscosity with shear for the gum and filled mixes are shown in Fig. 6.1.3a 1.3b. Viscosity of all mixes decreased with increasing rate and shear stress showing pseudoplastic flow

avior. Polychloroprene showed a higher shear sensitivity viscosity than XNBR in both filled and gum mixes.

4.3 Viscosity-Shear Stress, Shear Rate Variation - Effect of Blend Ratio

Polychloroprene and XNBR showed very high viscosity ile ENR showed a lower viscosity at a particular shear ress and shear rate. The blends occupied an intermediate ition. With increase in temperature ENR showed paratively lower viscosities, and due to this the flow ofiles were more spread, as the temperature increased. scosity of the ternary blend, decreases as the CR content creased.

4.4 Viscosity-Shear Stress Shear Rate Variation - Effect of Fillers

A higher viscosity was recorded for the filled mples. The viscosity change for the mixes was as follows : lica filler > ISAF black filler > SRF black filler. The fect of type of filler on the viscosity was noted ller[25,26], the smaller the particle size and greater the ructure the more is the viscosity increase and elasticity crease. Log-log plots of η versus shear rate were more near for the blend mixes than the gum mixes.

4.5 Application of Blending Rule for the Viscosity

The zero shear viscosity increased with the average

three component system equation could be written as

$$\log \frac{1}{\eta_b} = w_1 \log \frac{1}{\eta_1} + w_2 \log \frac{1}{\eta_2} + w_3 \log \frac{1}{\eta_3} \quad (7)$$

hide et al.[28] have presented the equation in the form in eqn. (8)

$$\frac{1}{\eta_b} = \frac{w_2}{\eta_1} + \frac{w_1}{\eta_2} \quad (8)$$

ternary blend component, equation (8) becomes

$$\frac{1}{\eta_b} = \frac{(w_2 + w_3)}{\eta_1} + \frac{(w_3 + w_1)}{\eta_2} + \frac{(w_1 + w_2)}{\eta_3} \quad \ldots(9)$$

we found that the blend viscosity fits the equation, if of the form in eqn. (10).

$$\frac{1}{\eta_b} = \frac{1}{2}\left[\frac{(w_2 + w_3)}{\eta_1} + \frac{(w_3 + w_1)}{\eta_2} + \frac{(w_1 + w_2)}{\eta_3}\right] \quad \ldots(10)$$

Equations (5), (7) and (10) have been applied to the viscosities of ternary blend for viscosities at shear 1 sec^{-1}, 10 sec^{-1}, 100 sec^{-1} and 1000 sec^{-1}. At all rates the viscosity behaviour fitted the models in ion (5) and (7), but at very high shear rate there was tion for the blend G. In blend C, there was deviation equation (10) at lower shear rates and blend G fitted odel at all shear rates. These are represented in Figs. 6.1.6. The viscosity additivity rule was valid only viscosities at constant shear rate and not for

viscosities at constant shear stress. Fig. 6.1.7 gives the behaviour of blends at two shear stresses of 2.9 MPa and [illegible] MPa. The deviation from equation (5) are larger than the observations in Figs. 6.1.4-6.1.6.

These ternary rubber blends had specific interaction causing a negative enthalpy change and as a result they were considered to be miscible. In the case of interacting polymers viscosity was very much dependent on residence time as shown by Kemblowski et al.[29], where the residence time functions were correlated with the kinetics of the polymer reactions. Hence viscosity in this tricomponent system depended on the residence time (t) in the capillary and temperature of test (T).

Mathematically,

$$\tau = \tau\,(\dot{\gamma},\ t,\ T) \qquad \ldots(11)$$

$$\eta = \frac{\tau}{\dot{\gamma}}\ (\dot{\gamma},\ t,\ T) \qquad \ldots(12)$$

Here, residence time was longer, in testing conditions at a shear rate of 1000 sec^{-1}, and there would be an increase in molecular weight during cure which was reflected from an increase in viscosity in blend G. However, in blend C, the interaction was lesser as ENR content was less.

Table 6.1.1(a) Formulations of Gum Mixes[a]

	E	X	N	G	C
NR	100	-	-	75	25
XNBR (Krynac 221)	-	100	-	75	25
Polychloroprene (Neoprene AD)	-	-	100	25	75

[a] Figures are in parts by weight

Table 6.1.1(b) Formulations of Filled Mixes[a]

	EIS20	XIS20	NIS20	GIS20	GSi20	GSR20
NR	100	-	-	75	75	75
XNBR (Krynac 221)	-	100	-	75	75	75
Polychloro-prene (Neoprene AD)	-	-	100	25	25	25
HAF black	20	20	20	35	-	-
SRF black	-	-	-	-	35	-
Silica[b]	-	-	-	-	-	35

[a] Figures are in parts by weight.
[b] Precipitated silica, Vulkasil S obtained from Bayer (India) Limited, Bombay.

Table 6.1.2 Flow Curve Characteristics

90℃			100℃			Consistency parameter K at 90℃
Slope of 1st line	Slope of 2nd line	Point of intersection (Seconds)	Slope of 1st line	Slope of 2nd line	Point of intersection (Seconds)	
0.33	0.19	58	0.36	0.24	58	0.57
0.47	0.13	58	0.44	0.13	116	1.06
0.17	only one line	–	0.16	only one line	–	2.31
0.35	0.18	116	0.35	0.18	58	0.97
0.39	0.23	116	0.44	0.27	58	0.46
0.49	0.25	116	0.38	0.31	116	0.50
0.17	only one line		0.17	only one line	–	3.14
0.35	0.20	58	0.41	0.21	29	1.46
0.37	0.20	58	0.45	0.14	29	1.64
0.37	0.22	58	0.37	0.18	29	1.35

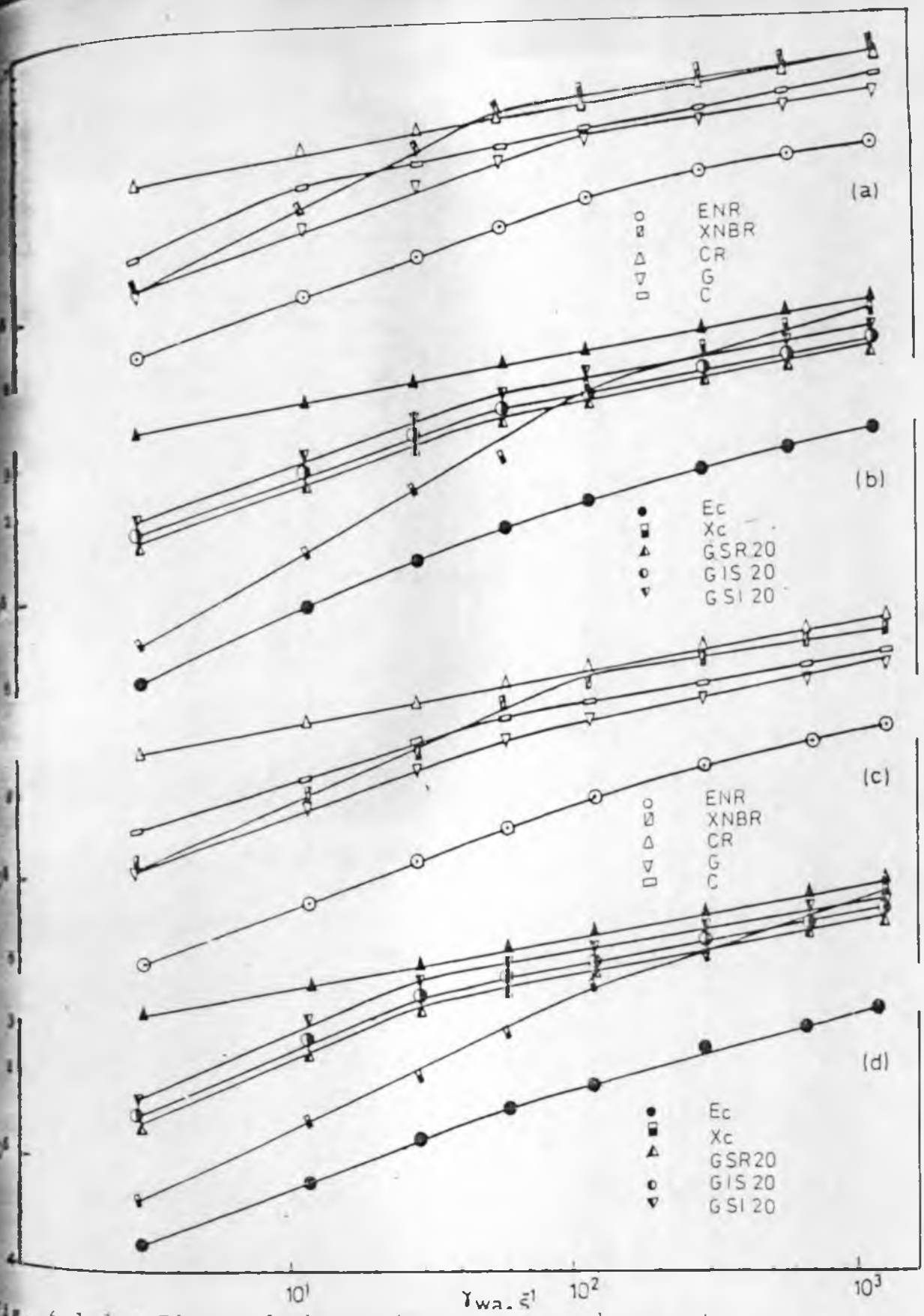

Fig. 6.1.1 : Plots of shear-stress versus shear rate for the gum and filled mixes at 90°C and 100°C.

(a) Gum mixes at 90°C; (b) Filled mixes at 90°C ;

(c) Gum mixes at 100°C ; (d) Filled mixes at 100°C.

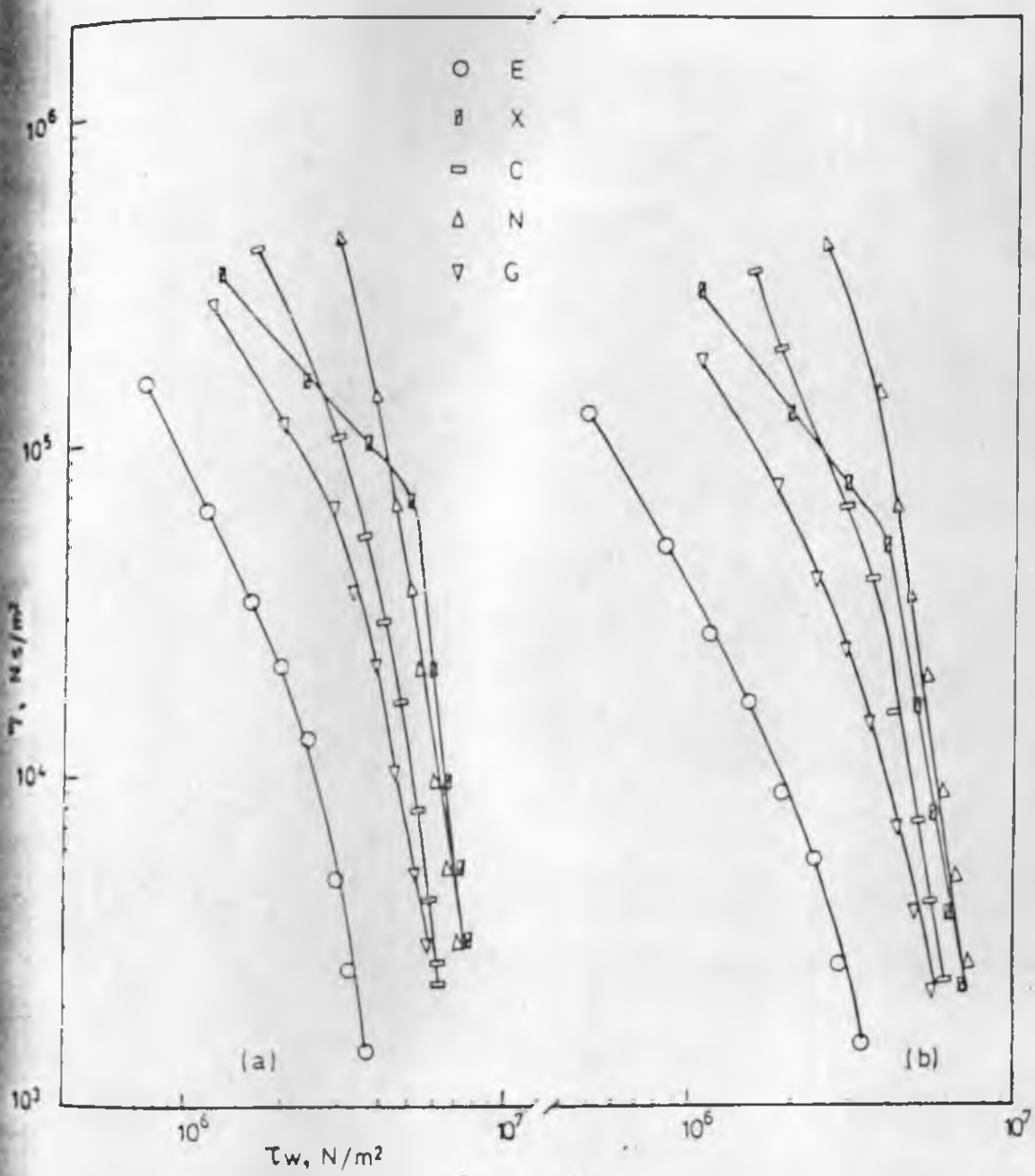

Fig 6.1.2 : Log-log plots of viscosity versus shear stress for the gum mixes showing effect of blend ratio.

(a) at 90°C ; (b) at 100°C.

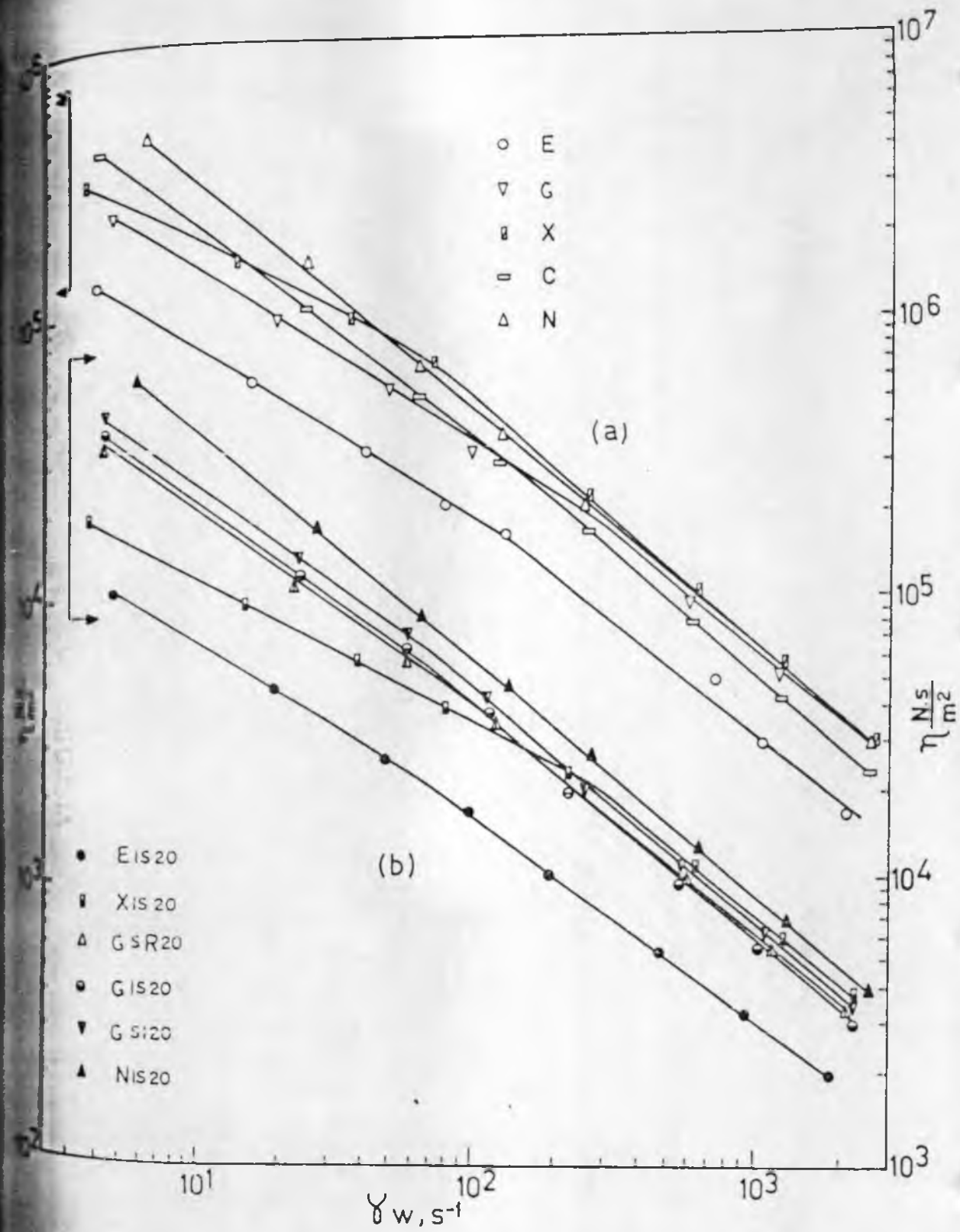

Fig. 6.1.3 : Log-log plots of viscosity versus shear rate for the gum and filled mixes at 90°C.

(a) Gum mixes (b) Filled mixes.

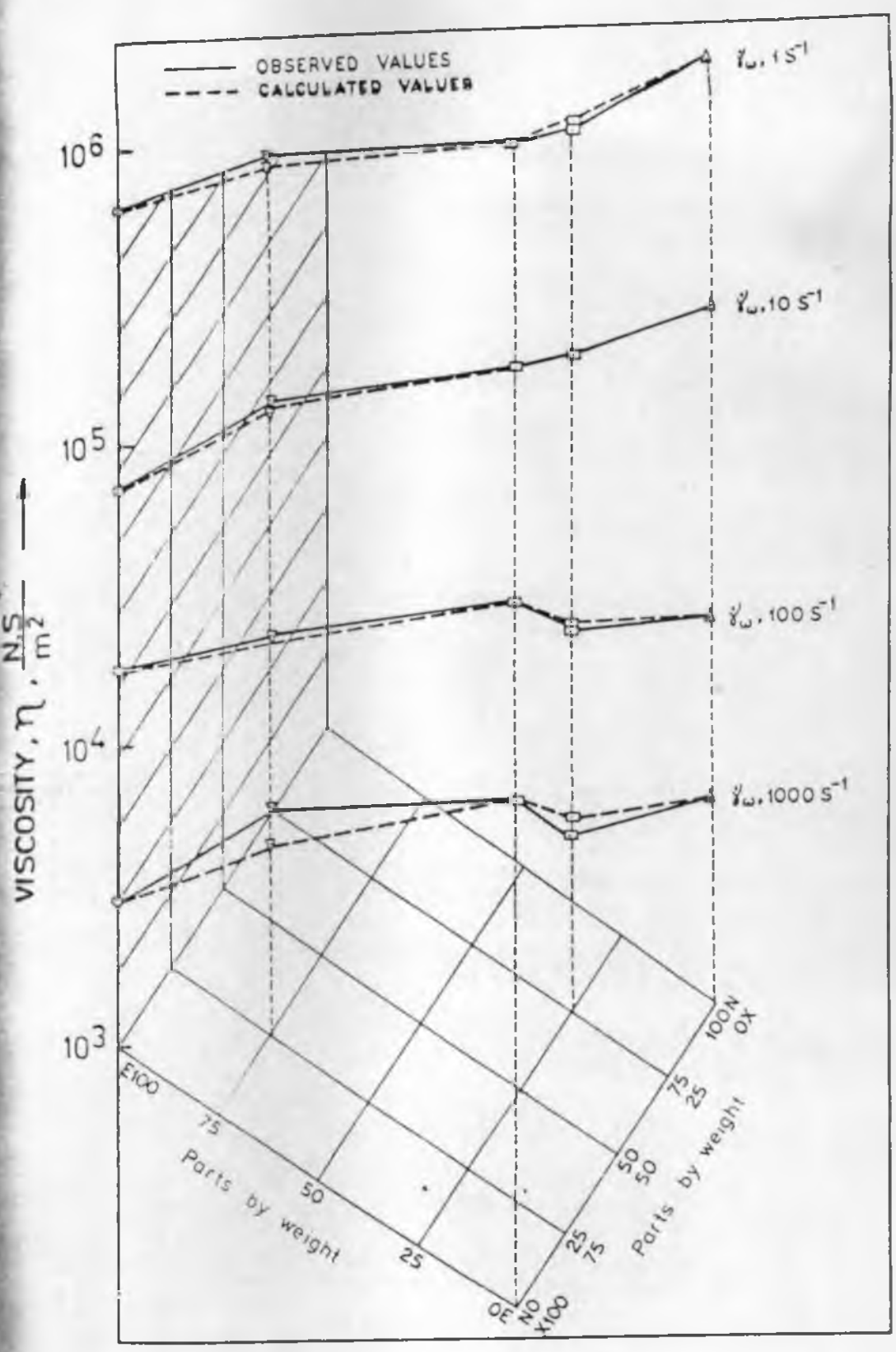

Fig. :6.1.4: Application of the additivity rule for the viscosity of blends at four different shear rates, 1 sec^{-1}, 10 sec^{-1}, 100 sec and 1000 sec .

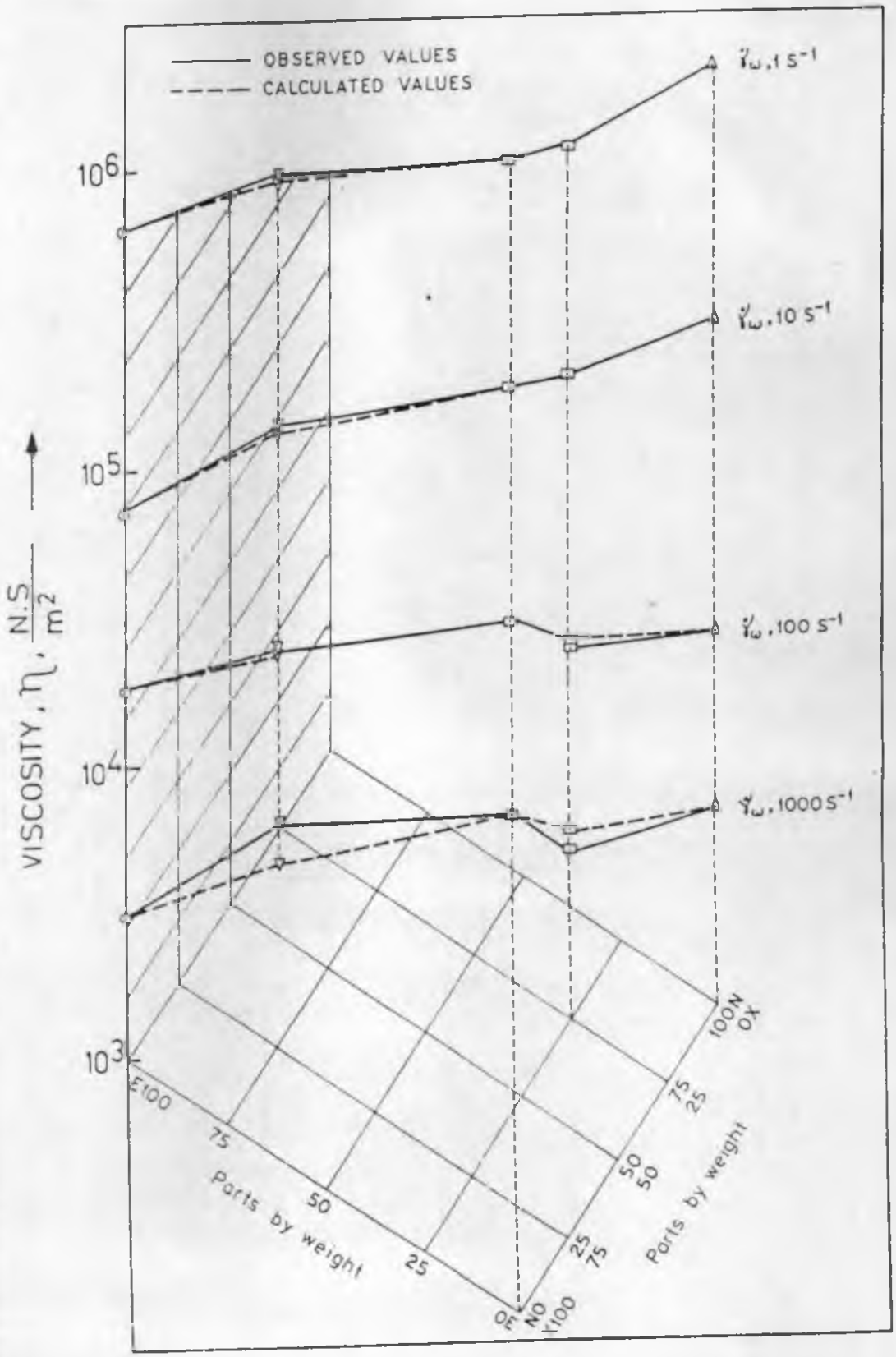

Fig.6.1.5 : Application of the Hietmillers model for viscosity of blends at four shear rate, 1 sec^{-1}, 10 sec^{-1}, 100 sec^{-1} and 1000 sec^{-1}.

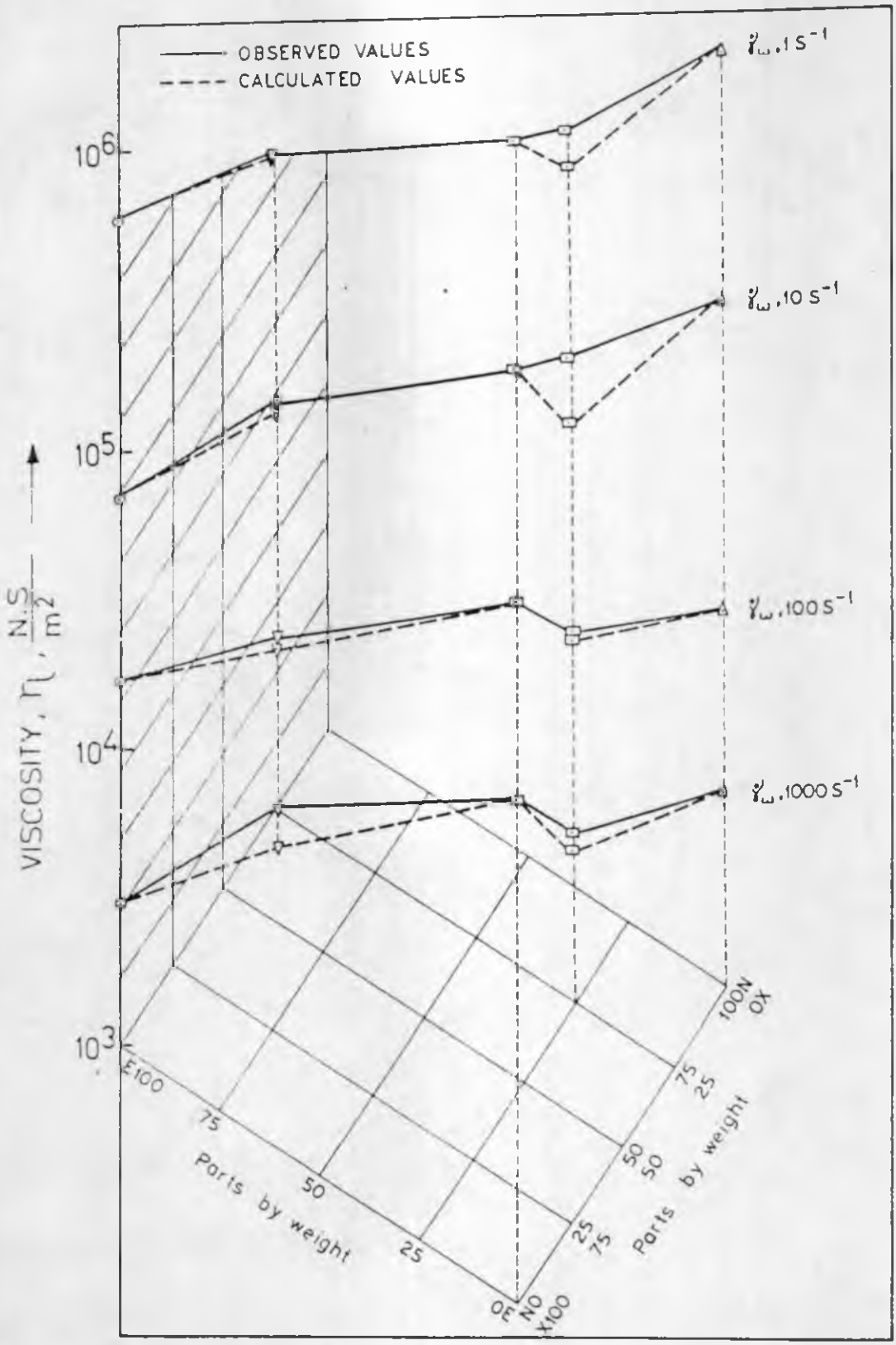

Fig.6.1.6 : Application of modified Hyashida's model for viscosity of blends at four different rates, 1 sec^{-1}, 10 sec^{-1} 100 sec^{-1} and 1000 sec^{-1}.

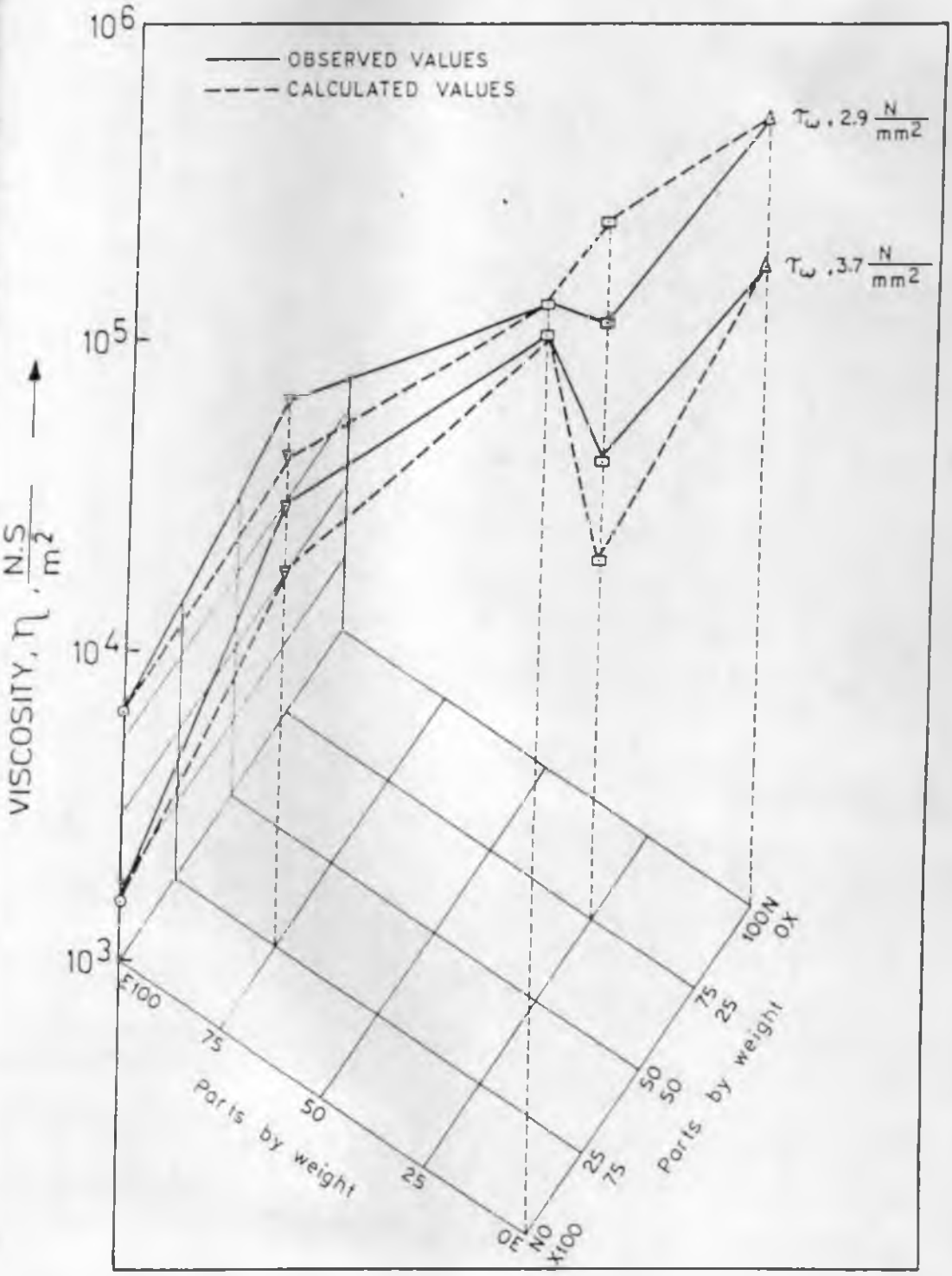

Fig. 6.1.7 : Application of additivity rule for the viscosity of blends at two different shear stresses of 2.9 MPa and 3.7 MPa

CHAPTER 6 - PART II

ELASTICITY

• This part of the work has been communicated to Kautschuk Gummi Kunstatoffe

Elastomeric materials, when they exit from a die, due their elasticity, get expanded and this is reported as die swell. The elasticity behaviour is characterised by the die swell ratio (D_e/D_c), the principal normal stress difference ($\tau_{11} - \tau_{22}$) recoverable shear stress, S_R and apparent shear modulus G. It is known that these factors are inter related and also that die swell increases with increasing shear rate and is independent of temperature at a constant shear stress. Die swell depends on fundamental properties of the polymers such as the molecular weight and its distribution, as well as on flow conditions such as temperature, shear rate, shear stress and L/D ratio of the capillary. Fillers generally reduce die swell in elastomers.

In this section, we report the results of studies on the die swell, principal normal stress difference, recoverable elastic strain and apparent shear modulus, using a capillary rheometer, for the tricomponent system of NR/XNBR/CR.

6.2.1.A Die Swell Ratio

Figures 6.2.1(a) and 6.2.1(b) are the photographs of the gum and filled mixes showing the effect of shear rate on die swell. Die swell increased as shear rate increased. It is seen that blending of rubbers and addition of filler reduced the die swell of the mixes. At shear rate of 594 s^{-1} surface smoothness of the filled blend was greater than the

control mixes of polychloroprene and XNBR. Polychloroprene showed a highly wrinkled surface probably due to the high crystallinity of the material. Fig. 6.2.2 is the plot of die swell as a function of shear stress. It showed that variation of die swell with shear stress is temperature dependent for the gum ternary mix, while the filled ternary mix showed temperature independence as noted earlier for several polymer melts[30,31].

According to the results in Fig. 6.2.3, the following relation existed between (D_e/D_c) and τ_w

$$\log (D_e/D_c) = B \log \tau_w + \log A \quad ....(13)$$

where, A and B are constants.

The values of A and B are given in Table 6.2.1. The change of die swell with shear stress (die swell index,B) was very low for XNBR and was high for CR. Blend C showed a much rapid change of die swell with shear stress and showed a very low intercept (A) on Y axis. This might be due to the presence of more CR, which was crystalline in nature.

The die swell is a mechanical property, and the additivity rule[32,33], could be applied to explain die swell of blends.

$$\log E = \sum \phi_r \log E_r \quad ....(14)$$

where, E designates the mechanical property and ϕ_r is the weight fraction of dispersed phase r.

The die swell of a tricomponent system could be written as

$$\alpha = \emptyset_1 \alpha_1 + \emptyset_2 \alpha_2 + \emptyset_3 \alpha_3 \qquad ....(15)$$

where, $\alpha = D_e/D_c$ and $\emptyset$ is the weight fraction of the components.

Values of die swell calculated on the basis of this equation at two constant shear stresses of 2.7 MPa and 3.5 MPa are given in Table 6.2.2.

The observed die swell for blend G was found to be lower than the calculated die swell, except at high temperature. In such cases the surface of G was not smooth and was wrinkled showing that there had been some interactions between the components at high temperature. As reported earlier, the ternary blend was miscible due to specific interactions between the components.The fact that blend C, showed a much lower die swell than the calculated values indicated the existence of miscibility in the system.

Theoretically it is known that swelling is contributed by two factors[34]. The first factor is due to change in parabolic velocity distribution of the melt in the die, to a constant velocity distribution, when it emerges from the die[35], and the second factor is due to randomization of polymer molecules which are oriented during their passage through the die[36]. The second factor depends on polymer

properties and dynamics of flow through the capillary. In the ternary blend ENR/XNBR/CR, there was specific interaction among the elastomers and as a result molecules mixed in the segmental level, and were more closely packed, compared with the individual rubbers. The blends oriented more in the direction of flow than the individual rubbers and the randomization of the molecules after emerging from the capillary was less due to the specific intermolecular interactions. Hence miscible blends were likely to have lower die swell than immiscible blends.

6.2.B Principal Normal Stress Difference

Values of the various elastic parameters at a shear rate of 2.9 sec^{-1} and 584 sec^{-1} are shown in Table 6.2.3. $(\tau_{11}-\tau_{22})$ as a function of shear stress at 100°C is given in Fig. 6.2.4. $(\tau_{11} - \tau_{22})$ was found to be sensitive to temperature as has been noted earlier[37] and also depended on molecular weight and molecular weight distribution[38].

(1) Effect of Blend Ratio

As observed from Table 6.2.3 the normal stress difference of XNBR was very low while that of polychloroprene is quite high and in all mixes $(\tau_{11} - \tau_{22})$ increased with shear rate. The blend showed a behaviour similar to ENR mix especially at lower shear rates. With blend ratio variation there was no much variation in normal stress.

(2) Effect of Fillers

Fillers both in control system and in blends decreased the principal normal stress difference, as it depended on the filler. The more reinforcing was the filler the greater was the reduction in principal normal stress difference (Table 6.2.3).

6.2.C Recoverable Elastic Shear Strain (S_R)

The surface distortion of the extrudate was observed when elastic shear strain energy stored in a polymer melt increases to a certain limit[39,40]. Figs. 6.2.5a and 6.2.5b are plots of S_R as a function of shear stress. The ternary blend G showed a higher value of S_R probably due to the onset of crosslinking reaction as scorch time was very low. The gum mixes showed a higher value of S_R and a more rapid change in S_R with shear stress than filled mixes.

6.2.D Elastic Shear Modulus

The elastic shear modulus as a function of shear stress is shown in Fig. 6.2.6. The elastic shear modulus of gum XNBR was quite high as compared to ENR and polychloroprene. Like principal normal stress differences elastic shear modulus did not vary much with blend ratio. The addition of fillers increased the shear modulus and the increase in shear modulus with shear rate was much lower than that of the gum mixes (Table 6.2.3). Shear modulus (G) showed temperature dependence.

6.2.E Dependence of Elastic Parameters on L/D Ratio

The elastic parameters depended strongly on the L/D ratio of the capillary used. The elastic parameters obtained by using two capillaries, one of shorter and other of longer length are summarised in Table 6.2.4. During the flow of a visco-elastic material through a capillary, the decay of pressure amplitude along the length of the capillary depended on the properties of the material[41]. The decay of pressure amplitude will be greater, if its residence time is longer which is achieved by reducing the flow rate or increasing the length of the capillary. Greater the elasticity of a material, lower will be its damping. It has been shown that severity of extrudate distortion decreased with increasing length of the capillary. Here it was observed that elasticity was considerably reduced by blending of the homopolymers and also by increasing the length of the capillary.

Table 6.2.1 : Constants A and B of eqn. $D_e/D_c = A\,\tau_w^{B}$, at two temperatures

Mix No.	Constant B (die swell index)		Constant A (Intercept on Y axis)	
	90°C	100°C	90°C	100°C
E	0.12	1.74	0.09	1.70
X	-0.04	1.36	0.07	1.20
N	0.12	1.64	0.22	1.24
G	0.14	1.42	0.09	1.75
C	0.26	1.13	0.36	0.90

Table 6.2.2: Experimental and calculated (additivity rule) values of die swell at two different temperatures (90°C and 100°C) and two shear stresses (2.7 MPa & 3.5 MPa)

Mix No.	90°C		100°C	
	2.7 MPa	3.5 MPa	2.7 MPa	3.5 MPa
E	2.0	2.05	1.90	1.90
X	1.30	1.30	1.30	1.30
N	1.85	1 90	1.65	1.55
G	1.55	1.75	1.95	1.95
	1.69*	1.12*	1.59*	1.60*
C	1.40	1.51	1.30	1.30
	1.78*	1.81*	1.57*	1.76*

* Calculated values from additivity rule

Table 6.2.3 : The Elastic Parameters of the Mixes at 90°C, at two Different Shear Rates

Mix No.	2.9 sec^{-1}			583.6 sec^{-1}		
	$(\sigma_{11}-\sigma_{22})$ N/mm^2	S_R	G N/mm^2	$(\sigma_{11}-\sigma_{22})$ N/mm^2	S_R	G N/mm^2
[illegible]	9.88	7.05	0.10	75.14	11.75	0.27
[illegible]	6.62	3.01	0.41	31.56	2.37	2.80
[illegible]	48.31	9.29	0.28	184.93	13.21	0.53
[illegible]	10.19	4.43	0.26	82.88	8.12	0.63
[illegible]	9.34	3.01	0.51	90.19	8.12	0.68
[illegible]IS 20	1.16	1.16	0.43	15.18	2.37	1.35
[illegible]IS 20	0.70	0.50	1.39	48.19	3.01	2.66
[illegible]IS 20	3.82	0.50	7.56	33.26	1.79	5.32
[illegible]IS 20	1.66	0.50	3.28	29.66	2.37	2.63
[illegible]SR 20	3.73	1.20	1.29	37.95	3.01	2.09
[illegible]SI 20	1.81	0.50	3.58	24.42	1.77	2.90

Table 6.2.4 : Elastic parameters of the mixes at a temperature of 90°C using two capillaries of different L/D ratios

Parameter	Die-swell		Shear stress N/mm^2		Normal stress difference N/mm^2		Elastic shear modulus N/mm^2		Recoverable shear strain	
L/D	40	67.5	40	67.5	40	67.5	40	67.5	40	67.5
Shear rate sec^{-1}	11.67	7.27	11.67	7.27	11.67	7.27	11.67	7.27	11.67	7.27
ENR	1.72	1.33	1.1	2.2	15.52	11.70	0.16	0.83	7.05	2.66
XNBR	1.33	1.19	2.2	3.3	13.25	12.66	0.73	1.72	3.01	1.92
N	1.88	1.39	3.7	5.0	68.52	43.70	0.40	1.76	9.26	3.53
G	1.57	1.47	1.9	2.6	20.09	22.17	0.36	0.61	5.29	4.26

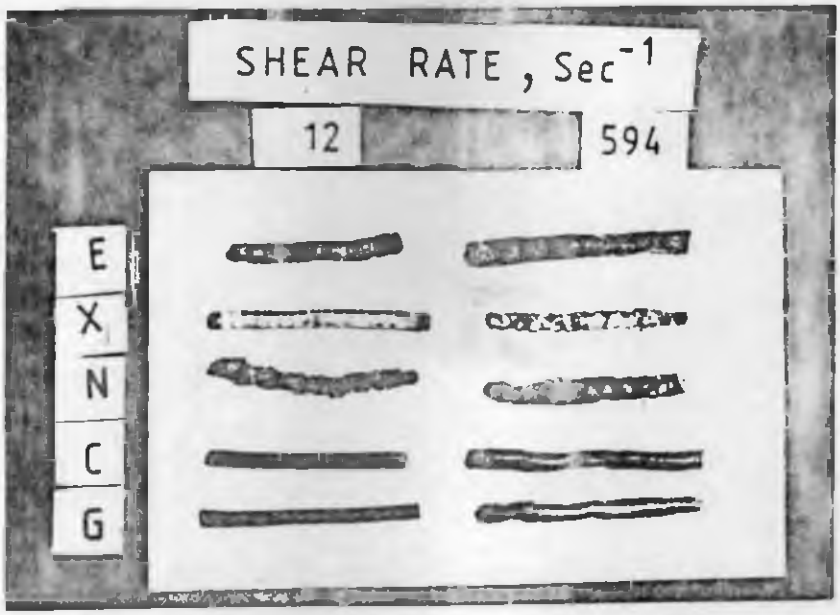

(a) Gum mixes

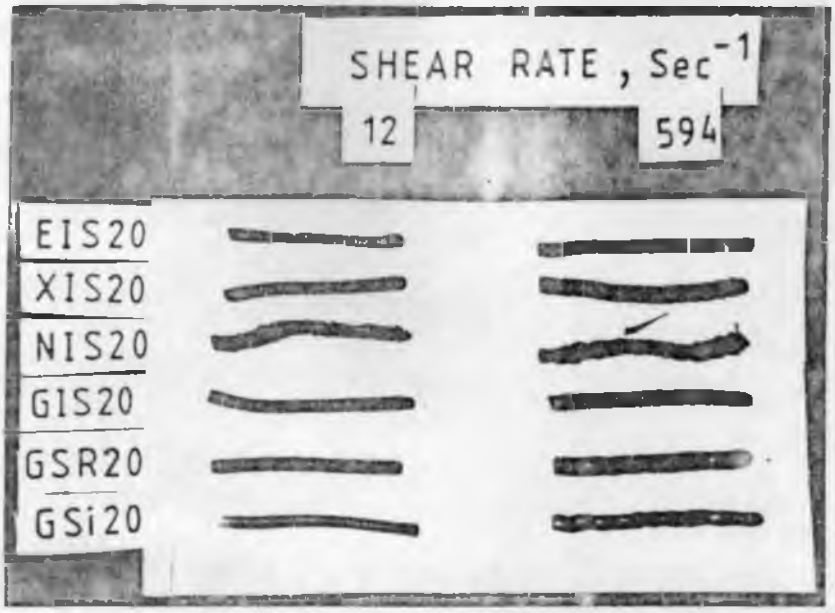

(b) Filled mixes

Fig. 6.2.1 : Photograph of the extrudates at two different shear rates of 2.92 s^{-1} and 594 s^{-1}.

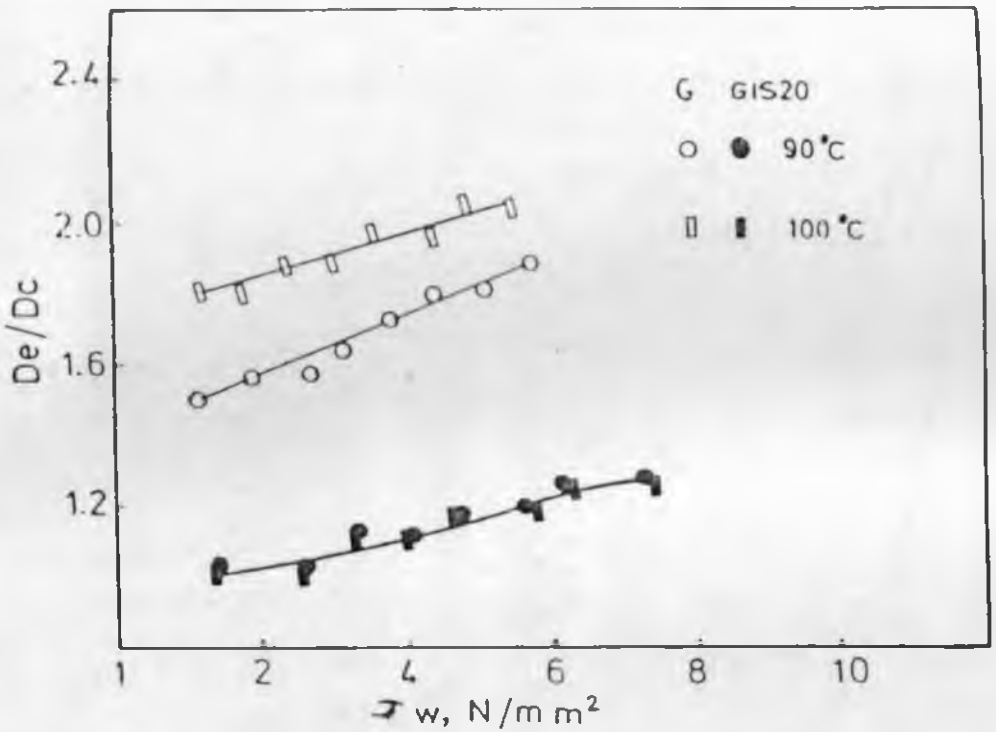

Fig. 6.2.2 : Plots of die-swell versus shear stress at two temperatures 90°C and 100°C for the gum and filled ternary mix.

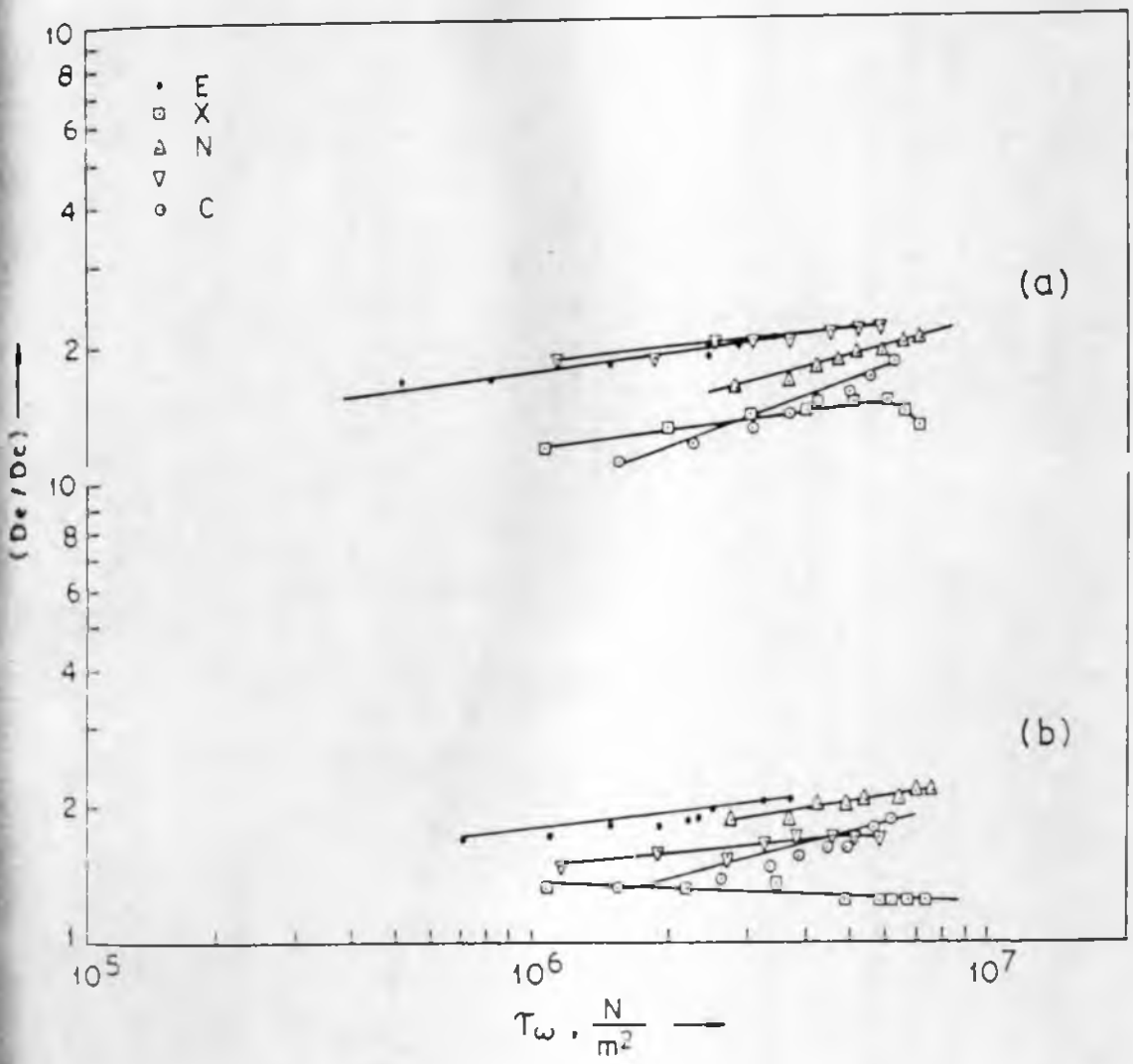

FIGURE : 6.2.3 : Log-log plots of die swell versus shear stress τ_w for the mixes at two temperatures (a) 100°C and (b) 90°C

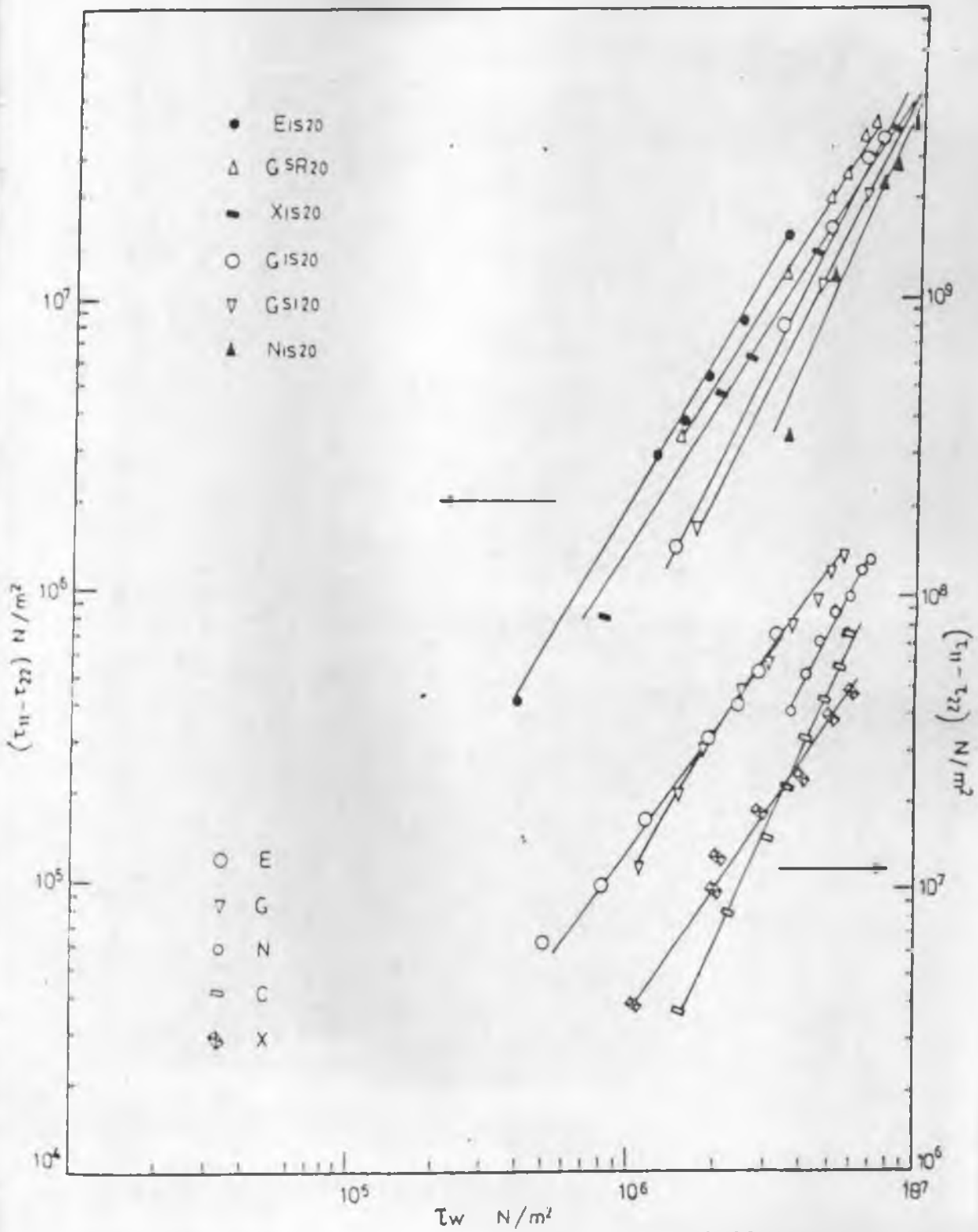

Fig. 6.2.4 : Plots of principal normal stress difference versus shear stress for the gum and filled mixes at 90°C.

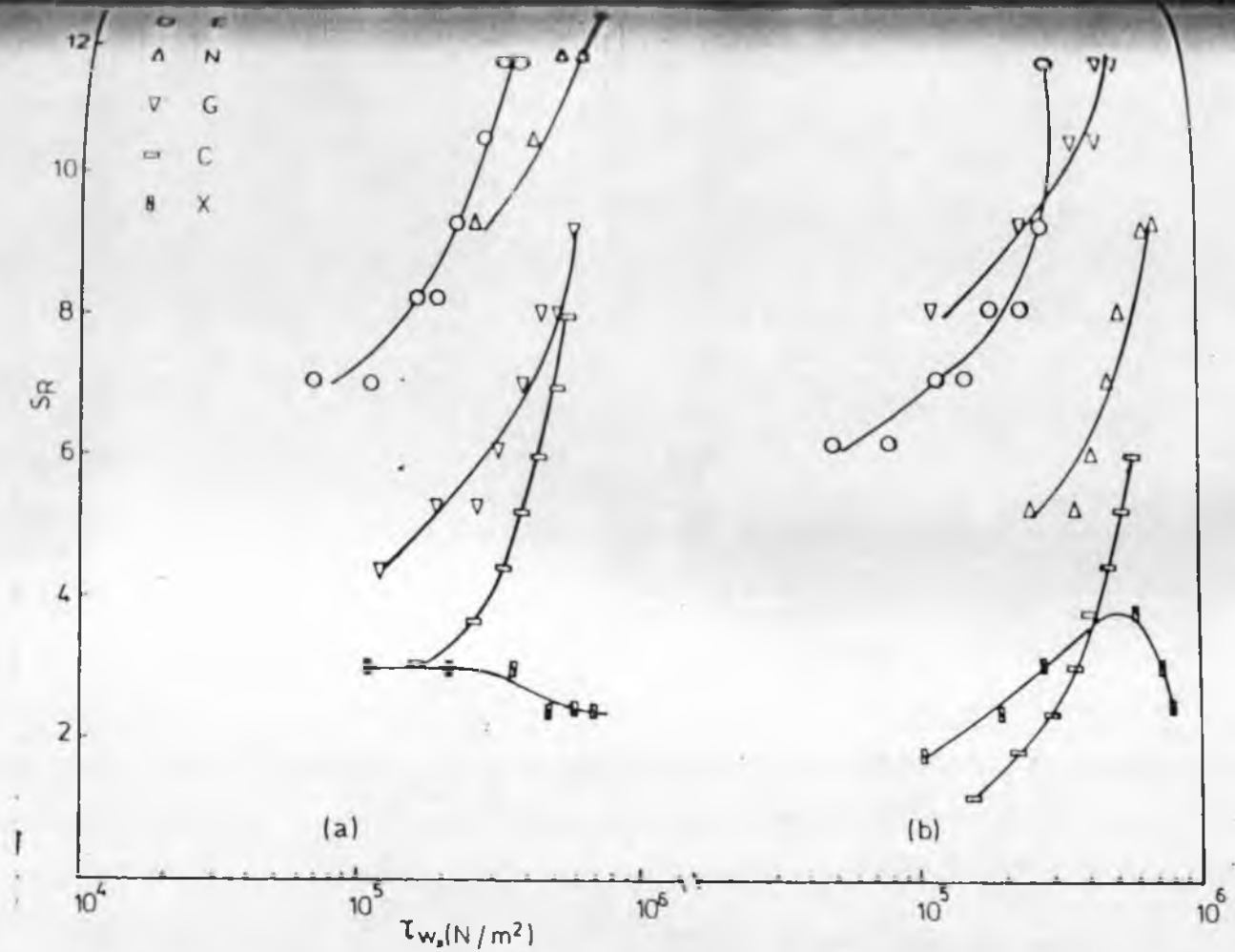

Fig. 6.2.5 : Plots of S_R versus shear stress for the gum mixes at two temperatures.
(a) at 90°C (b) at 100°C.

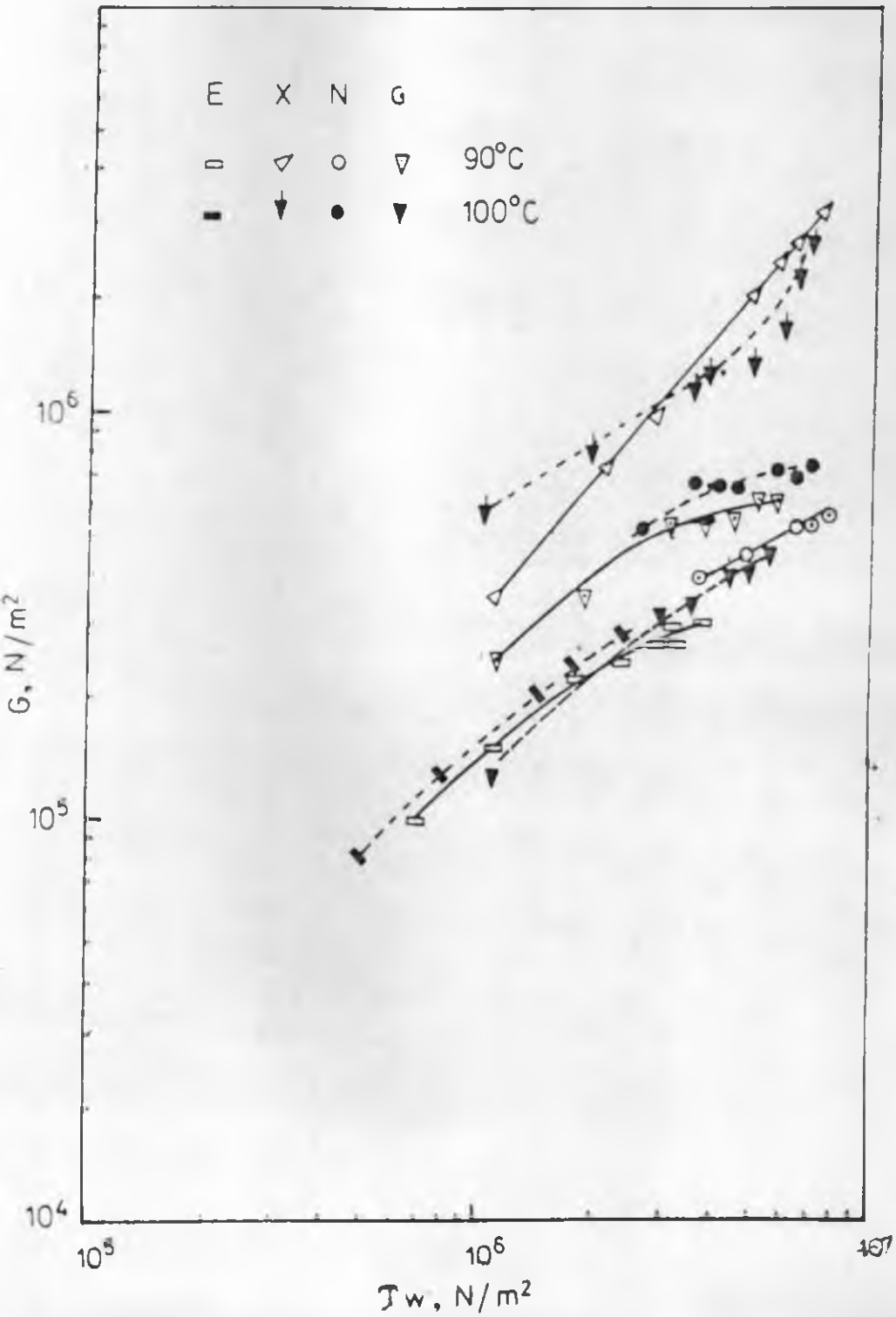

Fig. 6.2.6 : Plots of shear modulus versus shear stress for the gum mixes at two temperatures 90°C and 100°C

REFERENCES

1. D.R. Gregory, J. Appl. Polym. Sci., 16 (1972) 1479.
2. S. Daneshi and R.S. Porter, Polymer, 19 (1978) 448.
3. N. Alle and J. Lyngaae-Jorgensen, Rheol. Acta, 19 (1980) 104.
4. A.S. Hill and B. Maxwell, Polym. Eng. Sci., 10 (1970) 289.
5. C.L. Sieglaff, Polym. Eng. Sci., 9 (1969) 91.
6. H. Natov, P.L. Peera and E. Djagenora, J. Polym. Sci., C 16 (1968) 4497.
7. A.P. Plochoki, Trans. Soc. Rheol., 20 (1976) 287.
8. A. Plochocki in `Polymer Blend', eds. D.R. Paul and S.Newman, Academic Press, New York, Vol. 2, p. 319 (1978).
9. A. Plochocki, J. Appl. Polym. Sci., 16 (1972) 987.
10. Baby Kuriakose and S.K. De, Polym. Eng. Sci., 25(10) (1985) 630.
11. Sania Akhtar, Baby Kuriakose, Prajna P. De and Sadhan K. De, Plastics. Rubb. Procs. Appl., 7(1) (1987) 11.
12. A.A. Phadke and Baby Kuriakose, Kautschuk Gummi Kunststoffe, 38(8) (1985) 695.
13. K.T. Varughese, P.P. De, G.B. Nando and S.K. De, J. Vinyl. Technol., 9(4) (1987) 161.
14. T.K. Bhaumik, P.P. De, A.K. Bhowmick and B.R. Gupta, Kautschuk Gummi Kunststoffe., 42 (1989) 115.
15. B.L. Lee, Polym. Eng. Sci., 21 (1981) 294.
16. H. Munsteat, Polym. Eng. Sci., 21 (1981) 259.
17. J.F. Carley, Polym. Eng. Sci., 21 (1981) 249.

18. B.L. Lee and J.L. White, Trans. Soc. Rheol., 19 (1975) 481.

19. R.F. Heitmiller, R.Z. Naar and H.H. Zabusky, J. Appl. Polym. Sci., 8 (1964) 873.

20. S. Uemura and M. Takayanagi, J. Appl. Polym. Sci., 10 (1966) 113.

21. S.P. Mishra and B.L. Deopura, Rheol. Acta., 23 (1984) 189.

22. Van Oene in 'Polymer Blends', eds. D.R. Paul and S.Newman, Academic Press, New York, Vol. 1, p. 295.

23. T. Nishimura, Rheol. Acta., 23 (1984) 617.

24. D.M. Turner and M.D. Moore, Plast. Rubb. Procs. and Appl., 4 (1980) 81.

25. Jean L. Leblanc, Plast. Rubb. Procs. Appl., 1 (1981) 187.

26. Nobuhiko Minagawa and James L. White, J. Appl. Polym. Sci., 20 (1976) 501.

27. H. Schuch, Rheol. Acta., 27 (1988) 384.

28. K., Hayashida, J., Takahashi, M, Matsui, In Proc. Fifth Intern. Congr. Rheol. Ed. Onogys., University of Tokyo Press, Tokyo, Vol. 4, p. 525.

29. Z. Kemblowski and J. Torzecki, Rheol. Acta., 22(1) (1983) 34.

30. J.W.Teh, Alfred Rudin, and Henry P. Schreiber, Plast. Rubb. Procs. Appl., 4(2) (1984) 149.

31. D. Romanini and G. Pezzin, Rheol. Acta., 21 (1982) 699.

32. L.E. Nielsen, "Mechanical properties of polymers and composites", Marcel Dekker, New York. (1975)

33. T. Nishimura, Rheol. Acta., 23 (1984) 617.

34. L.L. Chapoy, Rheol. Acta., 8 (1969) 497.

35. S. Middleman and J. Gavis, Phys. Fluids., 4 (1961) 355.

36. R.S. Spencer and R.E. Dillon, J. Colloid. Sci., 3 (1948) 163.

37. K.T. Varughese, J. Appl. Polym. Sci., 39 (1990), p. 205.

38. G.V. Vinogradov and A. Ya Malkin, "Rheology of Polymers", Mir Publishers, Moscow (1980), Chap. 4, p 335-339.

39. J.P. Tordella, Rheol. Acta., 1(2-3) (1958) 216.

40. C.D. Han, "Rheology in polymer processing", Academic, New York (1976), Chap. 12.

41. A.K. Gupta and S.N. Purwar, J. Appl. Polym. Sci., 30 (1985) 1777.

SUMMARY AND CONCLUSIONS

SUMMARY AND CONCLUSIONS

The present thesis includes studies on self-vulcanisable rubber blends of epoxidised natural rubber (ENR) and carboxylated nitrile rubber (XNBR), ENR and polychloroprene rubber (CR) and their ternary self-vulcanisable rubber blend ENR-XNBR-CR. The primary objectives of the work included:

(1) Preparation of mill mixed binary blends of ENR and XNBR and studies on characterisation, technical properties, polymer-filler interaction, dynamic mechanical properties, failure envelope, stress relaxation and ageing behaviour of the blends.

(2) Preparation of mill mixed binary blends of ENR and CR and studies on characterisation, technical properties, and dynamic mechanical properties of the blends.

(3) Preparation of mill mixed ternary blends of ENR, XNBR and CR, and studies on characterisation, miscibility, technical properties, polymer-filler interaction, stress relaxation and ageing behaviour of the blends.

(4) Studies on capillary flow behaviour of the ternary blend of ENR, XNBR and CR.

The blends were prepared on laboratory size two-roll mixing mill. The fillers were added after blending the rubbers. The characterisation was made by Monsanto Rheometry, differential scanning calorimetry, infrared

spectrophotometry, solvent swelling (in chloroform) and by determination of physical properties.

Expectedly single rubbers showed increase in rheometric torque with time only in presence of vulcanising agents. In absence of vulcanising agents neat rubbers did not register any increase in torque. The blend, on the other hand, registered gradual increase in rheometric torque with time even in the absence of vulcanising agents. It is obvious that the increase in torque was due to the chemical reaction between the reactive group of one rubber (epoxy group of ENR) with the reactive group of another rubber (COOH group of XNBR). Single rubbers and the blend before moulding were soluble in a common solvent. But the moulded blend was insoluble in the same solvent and the degree of swelling decreased with increase in moulding time at a particular temperature. This phenomenon indicated occurrence of crosslinking during moulding. Individual rubbers and their blend before moulding showed characteristic infrared absorption peaks of single rubbers. But the moulded blend registered absorption peaks due to new bonds formed in the crosslinked structure. Furthermore single rubbers did not undergo any thermal change in differential scanning calorimeter when heated from room temperature upto the temperature before thermal degradation started. But the blend registered exothermic peak due to the crosslinking reaction. The exothermic peak occurred at a temperature much below the temperature at which thermal degradation of the

rubbers started.

The processing characteristics and technical properties of the blend depended on blend composition. During moulding at high temperature, binary blend of ENR and XNBR reacted to form ester crosslinks. There was thermal stability when the ENR content in the blend was high till 50/50 ratio and when the ENR content was lower as in 25/75 ratio, the crosslinking reaction reached a state of completion. The poor gum strength of the blend was improved by addition of reinforcing fillers. The processability and curing characteristics of the blend depended on type and amount of filler used. The blend vulcanisates showed lower compression set and higher resilience when compared with conventionally cured XNBR and ENR. Silica reinforcement in self-vulcanisable blend occurred in the absence of any coupling agent.

The polymer-filler interaction was estimated by Kraus equation by measurement of swelling of the vulcanisates in chloroform and it was observed that the slope was maximum in silica filled blend and minimum in the SRF black filled blend. The polymer-filler interaction in the self-vulcanisable ENR-XNBR blend was found to increase in the order, SRF black < ISAF black < silica. It was observed that the self-vulcanisable blend also yielded a failure envelope, similar to conventional rubber vulcanisates, when tensile strength obtained at different temperatures and test rates

were plotted against elongation at break on a logarithmic scale.

Increased polymer-filler interaction was manifested in the reduced tanδ value and broadness of the tanδ peak, in the glass-rubber transition (Tg) region of the filled vulcanisates.

The blend vulcanisates exhibited single Tg in the tanδ versus temperature plot. The miscibility of the system was ascribed to the specific interactions between the functional groups namely, epoxy and carboxyl of the two polymers. Furthermore, solubility parameters of the two polymers were found to be close to each other. The moulded blends were transparent.

Stress relaxation measurements showed that the blend vulcanisates showed two relaxations like the conventional rubber vulcanisates, in the time range studied. The first relaxation could be due to small segments or domains of molecular chains and the second due to rearrangement of molecular chains or aggregates.

Ageing studies under different ageing conditions like air ageing, acid ageing, alkali ageing and fuel ageing showed that the blend had better resistance to ageing than control single rubber vulcanisates.

Mill mixed blend of ENR and polychloroprene (CR) also formed self-vulcanisable rubber blend. Though the blend was

reported to be miscible due to specific chemical interactions, the vulcanisate was only partially miscible. The possible crosslinking reaction was by the interaction of the oxirane ring of ENR and allylic chlorine of CR. However, the vulcanised structure was believed to consist of many coexisting phases due to the following factors :

Polycholoroprene alone underwent thermovulcanisation by liberation of HCl. Secondly, ENR alone could form ether crosslinks in presence of HCl. Lastly ENR and CR formed ether crosslinks. The Tg of the vulcanisate consequently showed a broad maxima, particularly when CR content of the blend was high. The extent of crosslinking depended on the blend ratio. Higher proportion of polychloroprene in the blend showed higher crosslink density. The binary blend was reinforced by ISAF black. Dynamic mechanical studies showed that the broadening of the Tg zone increased after incorporation of filler. The carbon black filler was distributed unevenly in the two phases. The carbon black filled blend consists of the absorbed hard rubber and the bulk rubber. The absorbed, hard immobilized rubber caused perturbed relaxation response and the character of these layers shifted towards glassy state. As a result of these interactions the carbon black filled blend vulcanisate showed a broad maxima in Tg. Thus, it was possible to obtain rubber vulcanisates which showed damping over a wide temperature range by proper choice of blend constituents and fillers.

Since chemical interaction could take place between different functional groups in ENR, XNBR and CR, the ternary blend ENR/XNBR/CR also formed self-vulcanisable blend. Possible interactions among the different functional groups included, epoxy-carboxy, epoxy-allylic chlorine, and allylic chlorine-carboxyl. However, miscibility of the vulcanised blend depended on blend ratio and incorporation of filler. During moulding several reactions could take place : (a) interaction between epoxy group of ENR and allylic chlorine of CR to form ether linkages, (b) interaction between epoxy group of ENR and carboxyl group of XNBR to form ester crosslinks, (c) interaction between carboxyl group of XNBR and allylic chlorine of CR to form ester linkages,(d) thermo-vulcanisation of polychloroprene, (e) modification of ENR structure in presence of liberated acids from CR. As a result, depending on the blend composition, there was microheterogeniety in the blend vulcanisates. However, extent of the different reactions could be altered by varying blend ratio, thus affecting the miscibility of the ENR/CR/XNBR system. For example, miscibility was attained at an ENR content of 75 parts per 100 parts of CR/XNBR, irrespective of CR/XNBR ratio. At lower ENR content miscibility was found to depend on CR/XNBR ratio.

Increase in moulding time shifted the glass transition to a higher temperature due to increase in crosslink density without affecting the miscibility. Reinforcing fillers like ISAF black and silica caused phase separation in the miscible

ternary blend. Low reinforcing SRF black did not have any pronounced effect on miscibility.

Incorporation of reinforcing fillers like ISAF black, precipitated silica and SRF black caused changes in processing behaviour and physical properties of the ternary blend. The behaviour was similar to rubber mixes with conventional vulcanisation systems. Silica formed strong polymer-filler bonds during mixing in the ternary blend system, as was evident from the processing characteristics. Mooney viscosity and Mooney scorch time of the blend were found to be intermediate between the control mixes of ENR and XNBR but the Monsanto rheometric torque values were closer to ENR.

The blend in the gum state showed poor failure properties like gum-ENR but showed high resilience and low compression set. Abrasion loss and heat build-up properties of the blend were nearer to those of gum polychloroprene vulcanisate. The filled blends showed lower heat build-up due to non-uniform distribution of fillers in the miscible ternary blend.

Thus it is possible to develop rubber vulcanisates with low heat build-up, by the judicious choice of blend constituents, type and loading of filler.

The capillary flow behaviour of the tricomponent ENR/XNBR/CR system showed that polychloroprene and carboxylated nitrile rubber were less susceptible to

breakdown on mixing mill than the neat epoxidised natural rubber. All the mixes including the single rubbers and their ternary blends, showed psuedoplastic flow with the flow index decreasing after about two decades of shear.

The blends in general had a lower viscosity than that calculated by additivity rules. The Heitmiller's equation was reasonably accurate at constant shear rate. Hayashida's model was modified and applied to the blends (equation 1),

$$\frac{1}{\eta_b} = \frac{1}{2}\left(\frac{w_2 + w_3}{\eta_1} + \frac{w_3 + w_1}{\eta_2} + \frac{w_1 + w_2}{\eta_3}\right) \quad \ldots(1)$$

where η_b is the viscosity of the blend, η_1, η_2 and η_3 are the viscosities of the three components, and w_1, w_2 and w_3 are the corresponding weight fractions.

The die swell ratio of the blend was found to be lower than that calculated from the additivity rule which implied that the blends were miscible. The die swell ratio, (D_e/D_c) increased with shear stress (τ_w) and the system was found to follow the following equation,

$$\frac{D_e}{D_c} = A\ \tau_w^{\ B} \quad \ldots.(2)$$

where A and B are constants.

The elasticity parameters of ENR and CR decreased by blending with ENR.

It was found that self-vulcanisable rubber blends behaved like conventional rubber vulcanisates in respect to processing, curing and technical properties. In summary, mill mixed blends of functionally active rubbers crosslink by themselves during moulding without the aid of any vulcanising agent. Since no vulcanising agents are used, the problems of co-crosslinking and crosslink heterogeniety arising out of unequal distribution of vulcanising agents are minimised considerably.

It was observed that a few of the self-vulcanised blends, particularly in presence of fillers, showed a broad maxima in damping in the glass-rubber transition region (Tg) and beyond. The ternary self-vulcanised rubber blend showed deviation from Kraus plots, in polymer-filler interaction presumably due to non-uniform distribution of fillers in different phases. The heat build-up of the self-vulcanised ternary blends decreased in presence of filler.

Investigations on self-vulcanisable rubber blends with special reference to the effect of fillers on mechanical and dynamic mechanical behaviour open up a new area of research in the field of rubber blends in particular and in rubber technology in general.

LIST OF PUBLICATIONS

LIST OF PUBLICATIONS

1. R. Alex, P.P. De and S.K. De, `Self-vulcanisable rubber system based on epoxidised natural rubber and carboxylated nitrile rubber', J.Polym. Sci., Polym. Lett. Ed., 27 (1989) 361.
2. R. Alex, P.P. De and S.K. De, `Epoxidised natural rubber-carboxylated nitrile rubber blend : a self-vulcanisable miscible blend system', Polym. Commun., 31 (1990) 118.
3. R. Alex, P.P. De, N.M. Mathew and S.K. De, `Effect of fillers and moulding conditions on properties of self-vulcanisable blends of epoxidised natural rubber and carboxylated nitrile rubber', Plastics and Rubber Processing and Applications, 14(4) (1990) 223.
4. R. Alex, P.P. De and S.K. De, `Self-vulcanisable and miscible ternary rubber blend system based on epoxidised natural rubber,carboxylated nitrile rubber and polychloroprene', Polym. Commun., 31 (1990) 367.
5. R. Alex and P.P. De, `Characterisation of self-vulcanisable blends of epoxidised natural rubber and carboxylated nitrile rubber by Monsanto rheometry, Differential Scanning Calorimetry, Thermogravimetry, infrared spectrophotometry and swelling', Kautschuk + Gummi. Kunststoffe, 43(11) (1990) 1002.
6. R. Alex, P.P. De and S.K. De, `Self-vulcanisable rubber-rubber blends based on epoxidised natural rubber and polychloroprene', Kautschuk + Gummi. Kunststoffe, 44(4) (1991) 333.

7. R. Alex, P.P. De and S.K. De, `Self-vulcanisable ternary rubber blend based on epoxidised natural rubber, carboxylated nitrile rubber and polychloroprene rubber. Part I : Effect of blend ratio, moulding time and fillers on miscibility', Polymer, 32 (1991) 2345.

8. R. Alex, P.P. De and S.K. De, `Self-vulcanisable ternary rubber blend based on epoxidised natural rubber, carboxylated nitrile rubber and polychloroprene rubber. Part 2 : Effect of blend ratio and fillers on properties', Polymer, 32 (1991) 2546.

9. R. Alex, P.P. De and N.M. Mathew, `Capillary flow behaviour of tricomponent rubber blends of epoxidised natural rubber (ENR), carboxylated nitrile rubber (XNBR) and polychloroprene (CR) : Part I - Viscosity', Kautschuk + Gummi. Kunststoffe (communicated).

10. R. Alex, P.P. De and N.M. Mathew, `Capillary flow behaviour of tricomponent rubber blends of epoxidised natural rubber (ENR), carboxylated nitrile rubber (XNBR) and polychloroprene (CR) : Part 2 - Elasticity', Kautschuk + Gummi. Kunststoffe (communicated).

Radiat. Phys. Chem. Vol. 33, No. 2, pp. 91–95, 1989
Int. J. Radiat. Appl. Instrum. Part C
Printed in Great Britain.

0146-5724/89 $3.00 + 0.00

EFFECTS OF GAMMA-RADIATION ON NATURAL RUBBER VULCANIZATES UNDER TENSION

R. ALEX, N. M. MATHEW and S. K. DE

Rubber Research Institue of India, Kottayam 686 009 and Rubber Technology Centre, Indian Institue of Technology, Kharagpur 721 302, India

(*Received* 18 *March* 1988)

Abstract—The effect of γ-radiation on natural rubber vulcanizates under mechanical strain has been investigated with reference to the effect of antidegradants, fillers and vulanization system. Samples were irradiated in the dose range of 5–15 Mrad in air at room temperature (25°C) at a rate of 0.3 Mrad/h. Sol content and volume fraction of vulcanizates were also determined to gain insight into the network structure of the irradiated vulcanizates. Natural rubber vulcanizates undergo molecular scission which in effect cause a decrease in tensile strength. Generally the 300% modulus increases, the increment being more prominent at lower radiation dose. The fall in tensile strength is also high at higher doses of radiation. Carbon black and antidegradants protect rubber from γ-radiation.

INTRODUCTION

Application of rubber components in radiation therapy, nuclear plants, medical equipments etc. has been increasing and many of these components are used under mechanical strain. Although much work has been done on the effect of radiation on rubber[1–4] the influence of γ-radiation on rubber vulcanizates under mechanical strain has not been well studied. Neither has much work been done on the effect of fillers and additives like antidegradants, under the above conditions. Therefore an attempt has been made to study the influence of γ-radiation on NR vulcanizates under different levels of tensile strain.

EXPERIMENTAL

The composition of the mixes are given in Table 1 and their physical properties in Table 2. The mixes were prepared in a laboratory model two roll mixing mill and were vulcanized into thin sheets using a hydraulic press having steam heated platens maintained at a temperature of 150°C. Modulus, tensile strength and elongation of these vulcanizates were determined as per ASTM D 412-75 method A. Tear resistance of these vulcanizates was determined as per ASTM D 623-73.

Tensile dumbbells prepared from the vulcanizates were kept under tensile strain in a specially designed stretching device as shown in Fig. 7. The specimens were then exposed to γ-radiation in air in a γ-chamber (model N 900 supplied by the Bhabha Atomic Research Centre, Bombay) having a Co^{60} source. Irradiation doses of 5, 10 and 15 Mrad were given to the vulcanizates. The rate of irradiation was 0.3 Mrad/h. To give a radiation dose of 5 Mrad the samples were exposed for a period of 16 h. Correspondingly longer periods were given for higher doses. Samples were exposed under different levels of tensile strain ranging from 0 to 240%. After the required dose of irradiation the specimens were removed from the

Table 1. Composition of the mixes

	1	2	3	4	5	6	7	8
Natural rubber[a]	100	100	100	100	100	100	100	100
Zinc oxide	—	5	5	5	5	5	5	5
Stearic acid	—	2	2	2	2	2	2	2
HAF black	—	—	—	50	50	50	—	—
China clay	—	—	—	—	—	—	70	—
Graphite	—	—	—	—	—	—	—	50
Process oil	—	—	—	5	5	5	5	5
PBNA[b]	—	—	1	—	1	—	—	—
4010[c]	—	—	—	—	—	5	—	—
CBS[d]	—	0.6	0.6	0.6	0.6	0.6	0.6	0.6
Sulphur	—	2.5	2.5	2.5	2.5	2.5	2.5	2.5
DCP[e]	5	—	—	—	—	—	—	—

[a]Grade ISNR-5. [b]Phenyl-β-naphthylamme, commercial grade. [c]*N*-cyclohexyl *N'*-phenyl-*p*-phenylenediamine (Antioxidant 4010, Bayer (India) Ltd. [d]*N*-cyclohexyl benzothiazyl sulphenamide (Vulcacit CZ) Bayer (India) Ltd. [e]Dicumyl peroxide, 40% active, commerical grade.

Table 2. Properties of the mixes

Mix no.	1	2	3	4	5	6	7	8
Optimum cure time at 150°C, min	55.0	13.5	12.8	11.0	10.5	9.0	19.0	13.5
Cure rate index	1.9	14.8	15.4	12.9	12.9	16.1	8.3	14.8
300% Modulus (MPa)	2.3	1.6	1.6	11.8	10.8	12.0	4.0	4.1
Tensile strength (MPa)	10.6	23.8	24.0	25.3	26.0	22.0	14.4	18.9
Elongation at break (%)	705	1041	1045	555	589	503	693	711

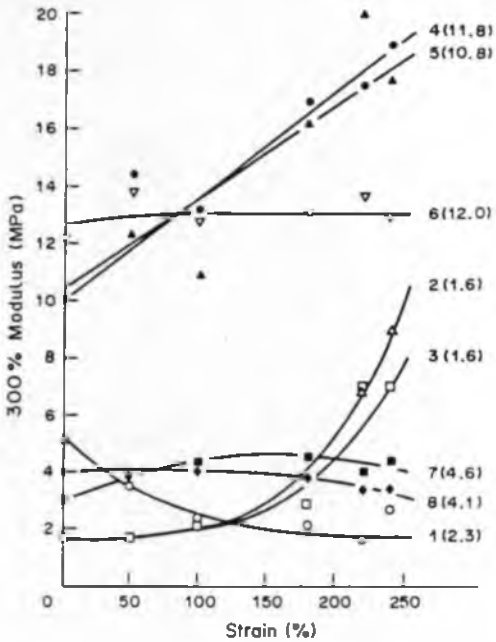

Fig. 1. Changes in tensile modulus of vulcanizates with respect to strain—radiation dose 5 Mrad. The figures in the parentheses indicate the original value of tensile modulus of vulcanizates.

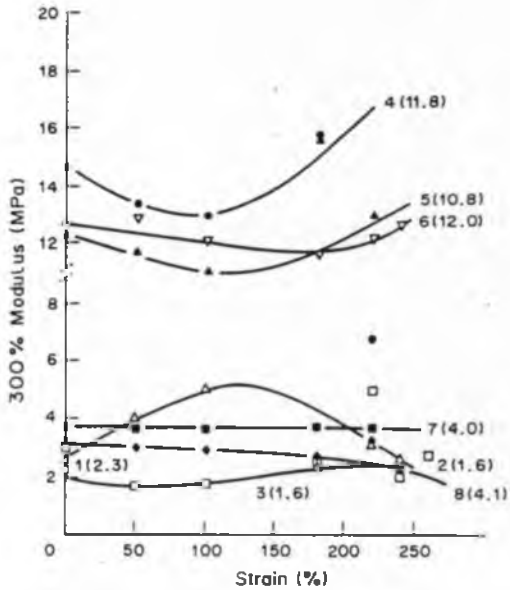

Fig. 3. Changes in tensile modulus of vulcanizates with respect to strain—radiation dose 15 Mrad. The figures in the parentheses indicate the original value of tensile modulus of vulcanizates.

stretching device and conditioned for 24 h, in the laboratory atmosphere and then tensile strength measured using a Zwick 1474 Universal Testing Machine.

Volume fraction of rubber in the benzene swollen vulcanizates, V_r, which is a measure of the crosslink density of the sample, was calculated from equilibrium swelling data using the method reported by Ellis and Welding.[5] Sol content was estimated by the method described by Bristow[6] according to which samples were extracted with cold acetone in the dark for 8–10 days, the acetone being replenished four times during the period. The samples were then dried to constant weight *in vacuo* at room temperature and from this, weighed portions were extracted with cold benzene in the dark for 8–10 days, the benzene being replenished four times during this period. After benzene extraction the samples were dried to constant weight *in vacuo*. The sol content was then calculated from the weight loss during benzene extraction.

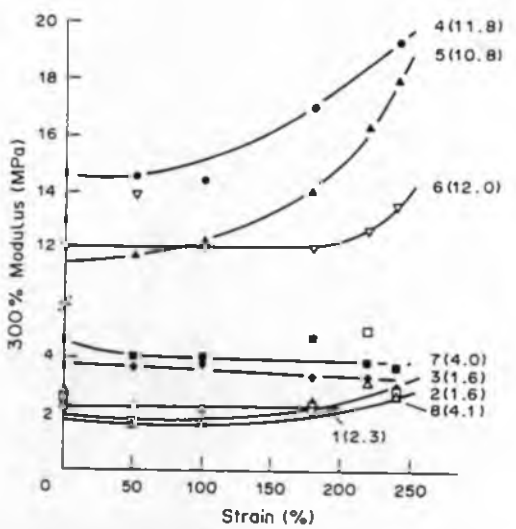

Fig. 2. Changes in tensile modulus of vulcanizates with respect to strain—radiation dose 10 Mrad. The figures in the parentheses indicate the original value of tensile modulus of vulcanizates.

RESULTS AND DISCUSSION

The properties of the mixes are given in Table 2. As expected the peroxide vulcanizates are poor in

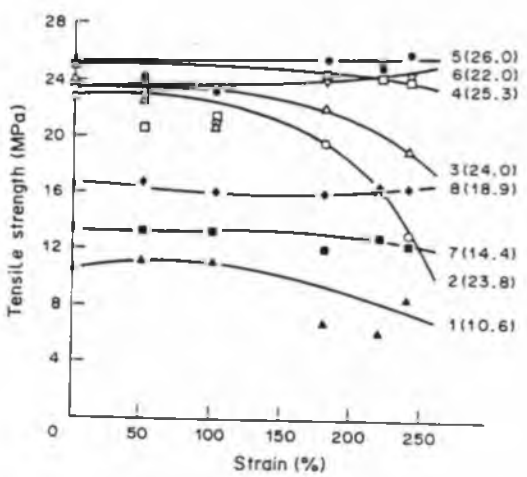

Fig. 4. Changes in tensile strength of vulcanizates with respect to strain—radiation dose 5 Mrad. The figures in the parentheses indicate the original value of tensile strength of vulcanizates.

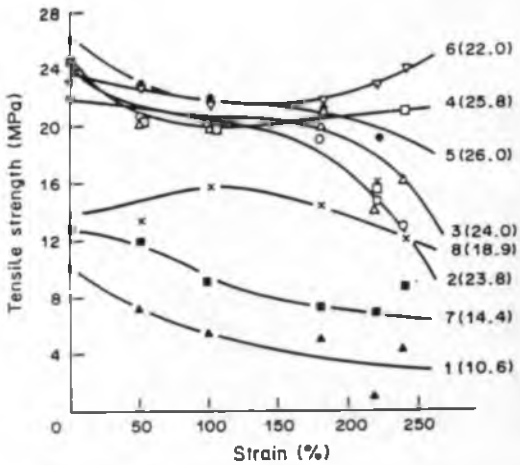

Fig. 5. Changes in tensile strength of vulcanizates with respect to strain—radiation dose 10 Mrad. The figures in the parentheses indicate the original value of tensile strength of vulcanizates.

stength compared to the sulphur cured ones. Addition of carbon black does not improve tensile stength, but there is an appreciable enhancement in modulus. But both china clay and graphite enhances modulus slightly, but reduces tensile strength. China clay is also found to influence the cure rate.

The effect of irradiation under tension on the tensile modulus of the vulcanizates is shown in Figs 1–3. In the case of the peroxide vulcanizate, the original modulus is 2.3 MPa, which increases to 5 after irradiation of 5 Mrad under zero strain and drops progressively as the strain in the specimen is raised. However, beyond 100% tensile strain the effect is rather slow possibly because the maximum damage has already taken place. When the radiation dose is raised to 10 Mrad modulus is found to remain rather constant irrespective of the tensile strain during irradiation. When the irradiation dose has been raised to 15 Mrad, the sample undergoes extensive degradation and the 300% modulus could not be measured.

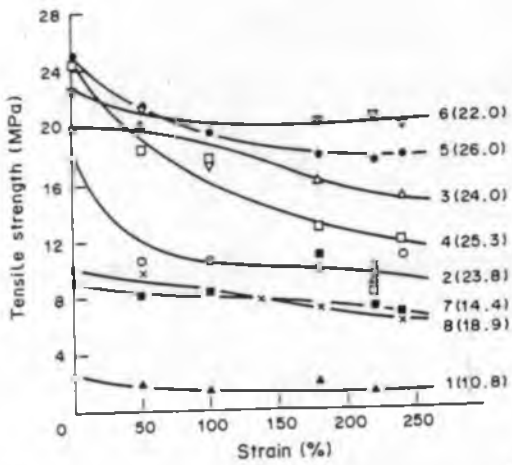

Fig. 6. Changes in tensile strength of vulcanizates with respect to strain—radiation dose 15 Mrad. The figures in the parentheses indicate the original value of tensile strength of vulcanizates.

In the case of the unfilled sulphur cured samples 300% modulus is found to remain constant up to a tensile strain of 100% beyond which it is found to increase rather abruptly when the irradiation dose has been limited to 5 Mrad. When the dose has been raised to 10 Mrad, the increase in modulus beyond 100% strain has been found to be only marginal as seen from Fig. 2. At 15 Mrad irradiation level the effects are much different especially in the case of Mix 2 which does not contain antioxidant. The maximum increase in modulus is observed when the tensile strain was around 150%.

Presence of carbon black in the sulphur cured samples is found to improve the radiation resistance. In the case of samples 4 and 5 at an irradiation dose of 5 Mrad modulus is found to increase almost linearly with increase in the strain level. The difference between the two samples is only marginal indicating that 1 phr of phenyl-β-naphthylamine (PBNA) does not influence the radiation resistance of black filled NR compounds. However, mix 6 which contain 5 phr *N*-cyclohexyl *N'*-phenyl *p*-phenylenediamine shows practically no change in modulus at 5 Mrad level. Even at 10 and 15 Mrad of irradiation dose changes in modulus are observed only when the strain in the specimens was above 180%. Influence of strain on radiation resistance is not significant in the case of china clay and graphite filled vulcanizates. In both cases modulus is found to remain rather constant irrespective of the strain in the sample.

Reduction in tensile stength is a better measure of irradiation damage in rubber vulcanizates. The effect of irradiation under different levels of tensile strain on the tensile strength of the vulcanizates at radiation doses of 5, 10 and 15 Mrad are shown in Figs 4–6 respectively. At 5 Mrad level, the tensile strength of peroxide cured vulcanizates is found unaffected up to 100% strain, beyond which it is found to drop. At 10 Mrad level and zero strain there is practically no drop in tensile strength. However, when the sample was under tensile strain, irradiation causes a significant drop in tensile strength and the drop increases with the increase in the strain. At 15 Mrad dose there is a drastic drop in tensile strength even when the sample was irradiated under zero strain. There is no significant further drop in tensile strength as the strain in the specimen was raised.

At 5 Mrad dose rate, the unfilled sulphur cured vulcanizates do not show any significant reduction in tensile strength up to about 50% strain. But beyond 50% the samples undergo degradation rapidly. However, the rate of degradation is less in the samples containing 1 phr of PBNA. The observations are the same at 10 Mrad dose. However, at 15 Mrad even at zero strain sample No. 3 containing no antioxidant shows a significant reduction in tensile strength,

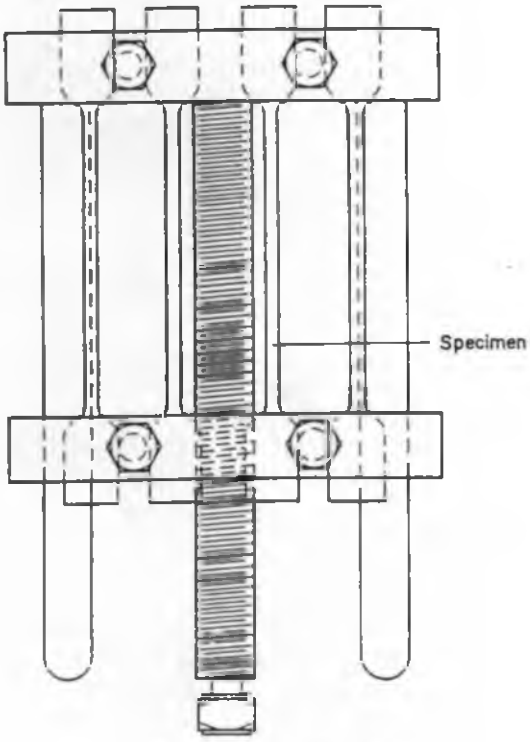

Fig. 7. Stretching device.

whereas sample No. 4 which contains 1 phr of PBNA does not show any reduction in tensile stength. But in both cases, when the irradiation was done under strain there is a fairly rapid degradation upto about 100% strain. Even under these conditions, it is found that antioxidant PBNA protects the rubber from radiation degradation although on a limited scale.

As observed earlier carbon black is found to protect rubber from radiation degradation but only at lower levels of radiation dose. At 5 Mrad there is no appreciable reduction in tensile strength even when samples were under 180% elongation. However, when the strain was larger, tensile strength was found to decrease. But the presence of 1 phr of PBNA is again found beneficial under these conditions as seen from Fig. 4. At 10 Mrad dose, when the specimens were irradiated under strain a limited extent of degradation is observed even in the samples containing PBNA. At 15 Mrad dose, when the specimens were under zero strain, no significant reduction in tensile strength was observed. However, when the irradiation was carried out under strain there is a fairly rapid degradation in the case of Mix 4 containing no antioxidant. But in the case of Mix 5 which contains 1 phr of PBNA the rate of degradation with respect to the degree of strain is less and at all levels of strain studied. Mix 5 was found to be significantly better than Mix 4 indicating again that antioxidant is effective in protecting rubber from irradiation damage. Mix 6 which contains 5 phr of *N* cyclohexyl-*N'* phenyl-*p*-phenylenediamine (Antioxidant 4010), is found to be resisting radiation at all levels of irradiation dose and at all levels of strain studied. In fact at 5 and 10 Mrad doses tensile strength is found to increase slightly when the sample was irradiated under tensile strain.

During irradiation of a rubber vulcanizate two types of reactions occur, crosslinking and chain scission. While the former causes an increase in modulus, the latter tends to reduce it. The data given in Table 3 show that generally crosslink density is not much affected by irradiation under strain except in peroxide vulcanizates at higher doses and at higher strains. The results also indicate that peroxide vulcanizates are more susceptible to radiation degradation than sulphur vulcanizates. The results of sol content determinations, as given in Tables 4–6, also indicate that chain scission under irradiation is also more predominant in the peroxide vulcanizates. It is also seen that as the strain in the sample is increased the degree of chain scission is increased. The sol content of sulphur cured vulcanizates, both unfilled and filled, increases as the strain in the sample is increased. It is also seen that antioxidant PBNA helps in preventing chain scission only slightly. However, the effect of

Table 3. Changes in volume fraction of rubber

Mix. no.	Dose rate (Mrad)	Strain (%) 50	100	180	220	240
1	5	0.21	0.21	0.21	0.21	0.20
2	5	0.22	0.22	0.22	0.23	0.22
3	5	0.22	0.23	0.23	0.23	0.22
1	10	0.21	0.21	0.21	0.21	0.20
2	10	0.22	0.22	0.22	0.22	0.22
3	10	0.22	0.24	0.22	0.24	0.25
1	15	0.21	0.20	0.21	0.17	0.18
2	15	0.22	0.23	0.23	0.23	0.22
3	15	0.22	0.22	0.23	0.24	0.25

Table 4. Changes in sol content of vulcanizates at radiation dose 5 Mrad

Mix no.	Strain (%) 50	100	180	220	240
1	1.0	1.5	1.8	4.1	3.0
2	0.4	0.6	1.0	1.5	1.8
3	0.5	0.5	0.7	1.0	1.8
4	1.1	1.7	2.0	2.5	1.8
5	1.9	2.0	2.3	2.5	1.8
6	0.23	0.27	0.29	0.22	0.27
7	0.66	0.76	0.90	1.53	1.54
8	0.71	0.63	0.92	0.52	0.58

Table 5. Changes in sol content of vulcanizates at radiation dose 10 Mrad

Mix no.	Strain (%) 50	100	180	220	240
1	1.0	1.5	1.8	4.5	3.7
2	0.5	0.5	0.6	1.9	1.7
3	0.5	0.5	0.5	1.9	1.8
4	1.6	1.7	2.0	2.7	1.8
5	2.0	2.0	3.0	2.5	1.8
6	0.3	0.27	0.35	0.31	0.39
7	1.10	0.96	0.95	2.64	2.00
8	0.98	0.76	1.11	0.86	1.17

Table 6. Change in sol content of vulcanizates at radiation dose 15 Mrad

Mix no.	Strain (%) 50	100	180	220	240
1	5.1	5.0	5.0	7.0	7.0
2	1.5	1.9	2.0	2.5	2.0
3	0.5	0.5	0.6	2.0	1.8
4	1.7	1.9	2.9	2.7	2.5
5	1.9	2.0	3.0	3.7	2.3
6	0.45	0.46	0.46	0.45	0.77
7	1.23	1.99	1.02	3.17	2.78
8	1.35	2.79	2.18	1.43	2.08

5 phr of anti-oxidant 4010 in preventing chain scission is very significant. It is also worth noting that china clay and graphite filled vulcanizates show fairly lower values for sol content at 5 Mrad indicating that both these fillers are contributing less towards chain scission than carbon black.

CONCLUSIONS

The following conclusions have been drawn.

(1) Exposure to radiation under tension causes decrease in tensile strength of NR vulcanizates.

(2) As the strain in the sample increases, the degradation is more rapid.

(3) The decrease in tensile strength is mainly due to molecular chain scission.

(4) Antioxidants and fillers like carbon black protect NR vulcanizates from radiation damage. Antioxidant 4010 at 5 phr is found to be a very effective protective system.

(5) For exposure to radiation, sulphur vulcanizing system is better than the peroxide system.

REFERENCES

1. H. R. Anderson, *Rubber Chem. Technol.* 1961, **34**, 228.
2. W. E. Shelberg and L. H. Gevantman, *Rubber Chem. Technol.* 1961, **34**, 250.
3. M. Ito, S. Odaka and I. Kuriyama, *J. Mater. Sci.* 1981, **16**, 10.
4. R. L. Zepp and A. A. Oswald, *Rubber Division Meeting*, Cleveland. Am. Chem. Soc. Paper No. 55, 1975.
5. B. Ellis and G. N. Welding, Technique of Polymer Science. *Soc. Chem. Ind.*, p. 46, 1964; *Rubber Chem. Technol.* 1964, **37**, 571.
6. G. M. Bristow, *J. Appl. Polym. Sci.* 1963, **7**, 1023.

Polymer POL/90/0214 filename: P21490.TXT

Sedhal 12

Self-vulcanizable ternary rubber blend based on epoxidized natural rubber, carboxylated nitrile rubber and polychloroprene rubber. Part 1: Effect of blend ratio, moulding time and fillers on miscibility

R. Alex, P. P. De and S. K. De
Rubber Technology Centre, Indian Institute of Technology, Kharagpur, 721 302, India
(Received 9 May 1990; revised 30 August 1990; accepted 30 August 1990)

Miscibility of the self-vulcanizable ternary blend based on epoxidized natural rubber (ENR), neoprene and carboxylated nitrile rubber (XNBR) depends on blend ratio. Miscibility is attained at an ENR content of 75 parts per 100 parts of neoprene/XNBR blend, irrespective of the neoprene/XNBR blend ratio. At lower ENR content, miscibility depends on neoprene/XNBR blend ratio. At a fixed ENR content, the higher the neoprene content in the neoprene/XNBR blend, the lower is the miscibility in the ternary blend system. Reinforcing fillers, such as silica and carbon black, cause phase separation in a miscible ternary blend. Variation in moulding time does not alter the miscibility, but shifts the glass transition temperature due to change in crosslink density.

(Keywords: epoxidized natural rubber; carboxylated nitrile rubber; polychloroprene rubber; ternary blend; miscible blend)

INTRODUCTION

De and co-workers[1–6] have developed novel self-vulcanizable rubber blends based on rubbers with appropriate reactive groups. Such blends are vulcanizable during moulding by the blend constituents themselves in the absence of any external vulcanizing agent. Examples are blends based on epoxidized natural rubber (ENR) and carboxylated nitrile rubber (XNBR)[1,2], polychloroprene (neoprene) and XNBR[3], chlorosulphonated polyethylene (hypalon) and XNBR[4], and ENR and hypalon[5]. It has also been observed that the miscibility of these binary blends depends on the blend ratio, concentration and nature of reactive groups and moulding conditions[6]. Three examples are worth mentioning in this context. The binary blend neoprene/XNBR is immiscible in all compositions[3]. On the other hand ENR/neoprene[7] is partially miscible and ENR/XNBR[2] blend is miscible at any composition. There are a few examples in which two of the binary pairs (A + B and A + C) are miscible but the third binary (B + C) is not[8–10]. It is of interest to investigate how to prepare a miscible blend on addition of A to the immiscible binary (B + C) blend. In the present series of rubber–rubber blends it is of interest to learn how much ENR needs to be added to the binary (neoprene/XNBR) blend to create a self-vulcanizable miscible ternary blend.

In an earlier communication[11] we have reported that epoxidized natural rubber acts as a compatibilizer when added to an immiscible blend of neoprene and XNBR to form a 1/1/1 miscible ternary blend. In the present paper we report the results of our investigations into the dependence of miscibility of such ternary blends on blend composition, moulding time and filler.

There are examples of a third component in a ternary blend acting as a polymeric compatibilizer for an incompatible or immiscible binary system. Lee and Chen[12] reported that chlorinated polyethylene, with ethylene segments similar to EPDM rubber and chlorinated sequences similar to poly(vinyl chloride) (PVC), serves as a compatibilizer for the binary blend of EPDM/PVC just like the effect of chlorinated polyethylene on PVC/polyethylene blends[13,14]. Blends of poly(caprolactone) (PCL) and PVC and PCL and chlorinated PVC (CPVC) are miscible at any composition[10]. However, PVC and CPVC are immiscible[15]. It has been shown by Ameduri and Prud'homme[15] that the addition of PCL to a PVC/CPVC mixture allows observation of a single glass transition temperature (T_g), at PCL contents >40% at high PVC/CPVC ratios and at PCL contents > ~26% at low PVC/CPVC ratio. Min *et al.*[16] have identified a ternary miscible system based on poly(methyl methacrylate)/poly(epichlorohydrine)/poly(ethylene oxide). There is no published report of a self-vulcanizable ternary rubber blend.

EXPERIMENTAL

Epoxidized natural rubber (ENR) with 50 mol% epoxidation was obtained from the Malaysian Rubber Producers' Research Association, UK. Carboxylated nitrile rubber, containing a high level of carboxylated monomer and a medium level of bound acrylonitrile

(Krynac 221) was obtained from Polysar Ltd, Canada. Neoprene AD was obtained from DuPont Ltd, UK. Vulcasil S (precipitated silica) was obtained from Bayer (India) Ltd, Bombay.

Formulations of the blends are shown in *Table 1*. ENR and XNBR were separately masticated for ~1 min each and neoprene for ~2 min, on a 14 × 16 in. two roll mixing mill. Neoprene and XNBR were blended first and then ENR was added and blended further. The total mixing time was about 8 min. The temperature rise during mixing was 2°C and the rolls were kept cool by circulation of cold water.

The blends were moulded for 60 min at 150°C in a laboratory-size moulding press.

Dynamic mechanical analyses (d.m.a.) were made using Toyo-Baldwin Rheovibron model DDV-III EP at a strain amplitude of 0.0025 cm and a frequency of 3.5 Hz. The procedure was to cool the sample to −100°C and record the measurements during the warm-up. The temperature rise was 1°C min^{-1}.

Differential scanning calorimetry (d.s.c.) studies were made on a DuPont thermal analyser model 910 in a nitrogen atmosphere. The T_g of the sample was taken as the mid-point of the step in the scan, run at a heating rate of 20°C min^{-1}.

RESULTS AND DISCUSSION

Miscibility of the ternary blend based on ENR/neoprene/XNBR depends on blend composition. At constant neoprene/XNBR ratio, an increase in ENR concentration increases the miscibility. *Figures 1–3* show the effect of

Table 1 Formulation of blends

Component	Blend designation												
	A	B	K	C	J	D	E	F	M	G	L	H	I
Neoprene AD (%)	75	75	75	75	75	50	50	50	25	25	25	25	25
XNBR (Krynac 221) (%)	25	25	25	25	25	50	50	50	75	75	75	75	75
ENR (phr)	75	50	37.5	25	12.5	75	50	25	87.5	75	62.5	50	25

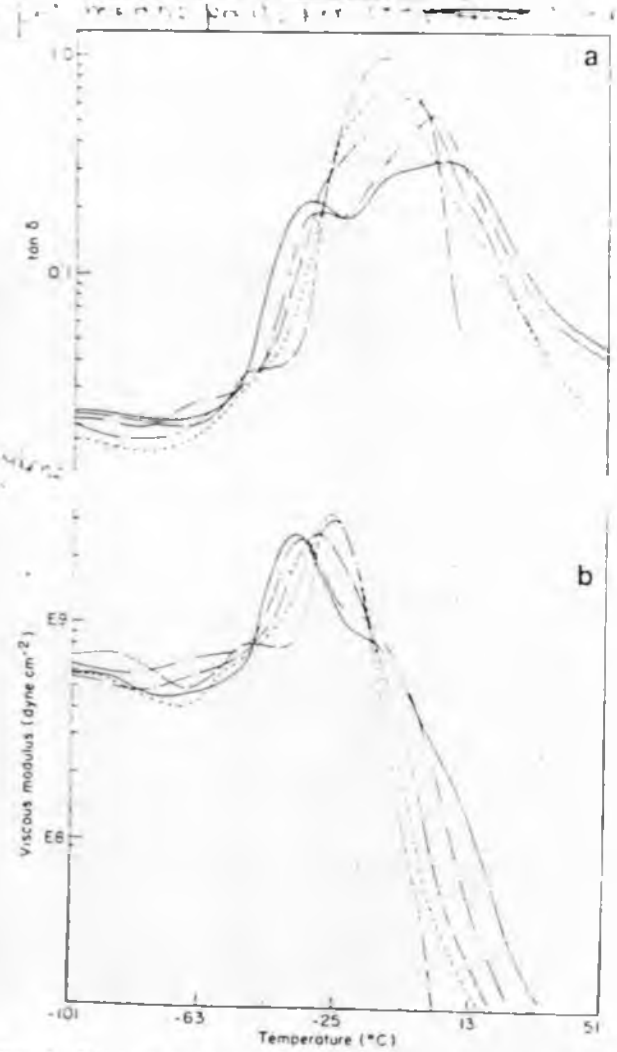

Figure 1 Dynamic mechanical spectra of the ternary blend showing the effect of ENR content on a fixed neoprene/XNBR ratio of 75/25. (a) tan δ *versus* temperature; (b) viscous modulus *versus* temperature. ENR content (blend designation): ——, 12.5 phr (J); ------, 25.0 phr (C); —·—, 37.5 phr (K); ····, 50.0 phr (B); —··—, 75.0 phr (A)

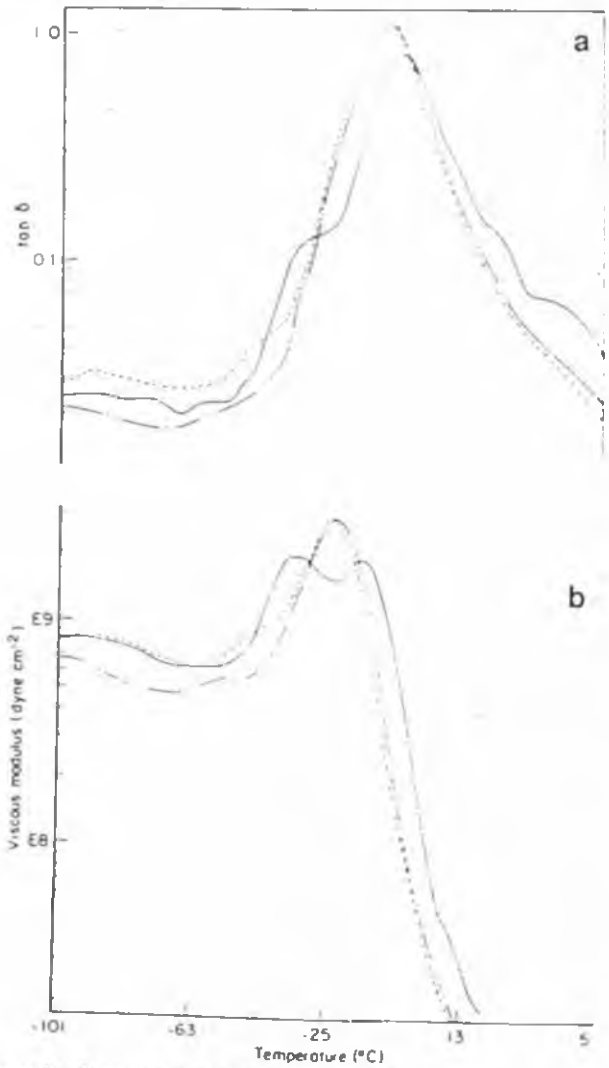

Figure 2 Dynamic mechanical spectra of the ternary blend showing the effect of ENR content on a fixed neoprene/XNBR ratio of 50/50. (a) tan δ *versus* temperature; (b) viscous modulus *versus* temperature. ENR content (blend designation): ····, 75 phr (O); ——, 50 phr (E); ------, 25 phr (F)

Table 2 Glass transition temperatures (T_g) of various ternary blends obtained from d.m.a. and d.s.c. studies

Blend designation	Blend composition	T_g (°C) from d.m.a. tan δ	Loss modulus	T_g (°C) from d.s.c.
A	75/25/75	11	27	26
B	75/25/50	11	27	*
K	75/25/37.5	−5	30	
C	75/25/25	−29, −1	−35, shoulder at −19	−40, −18
J	75/25/12.5	−33, +8	−38, shoulder at −19	
D	50/50/75	−10	−25	−19
E	50/50/50	−10	−24	−16
F	50/50/25	−29, −5	−37, −17	*
M	25/75/87.5	−9	−19	
G	25/75/75	−7	−19	−18
L	25/75/62.5	−9	−20	
H	25/75/50	−7	−30, shoulder at −17	*
I	25/75/25	−37 to −29, −10	−40, −20	*

*No clear-out transition

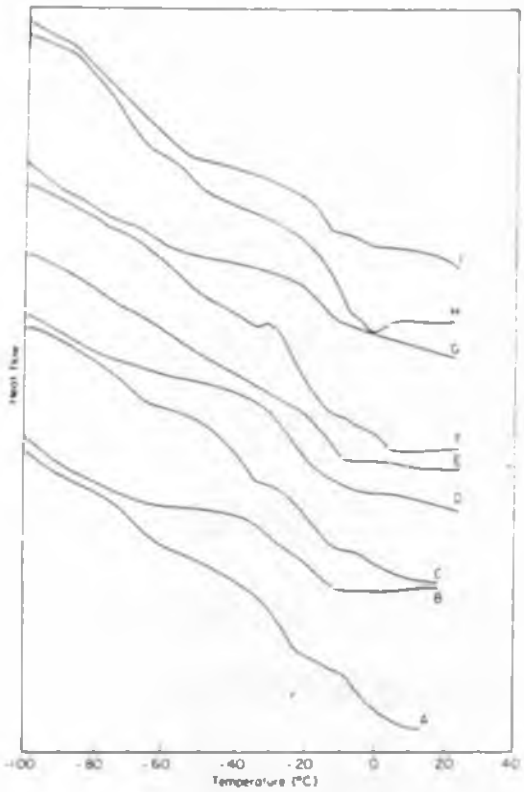

Figure 5 D.s.c. thermograms of ternary blends. Blend composition as given in *Table 1*

The effect of crosslink density on miscibility of such blends was then studied. In self-vulcanizable blends crosslink density can be varied by changing the moulding time[23]. The aim was to check whether miscibility of the immiscible blend could be improved by moulding for a longer time and similarly whether a miscible system could be made immiscible if moulded for a shorter time.

Figure 6 shows the effect of moulding time on variation of tan δ and viscous modulus with temperature for a miscible system (blend G) and an immiscible system (blend C). When the moulding time is reduced from 60 min to 15 min in a miscible system, miscibility is not affected. However, the tan δ peak is shifted to a lower

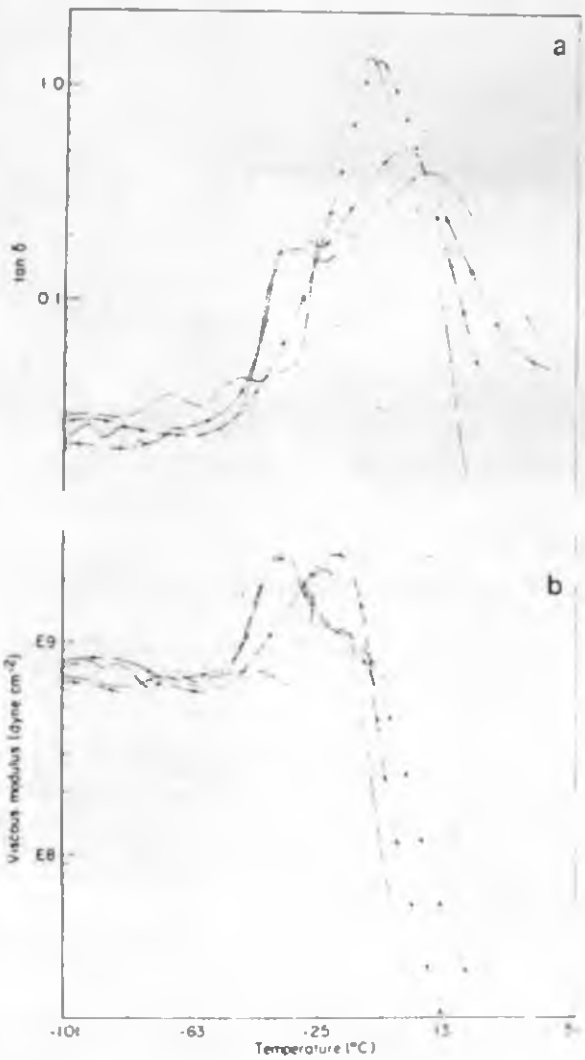

Figure 6 Dynamic mechanical spectra of ternary blends (G and C) showing the effect of moulding time on T_g behaviour: (a) tan δ *versus* temperature, (b) viscous modulus *versus* temperature. Curing time: blend G, ——, 15 min; ×—×, 60 min; blend C, ×—×, 60 min; ——, 120 min

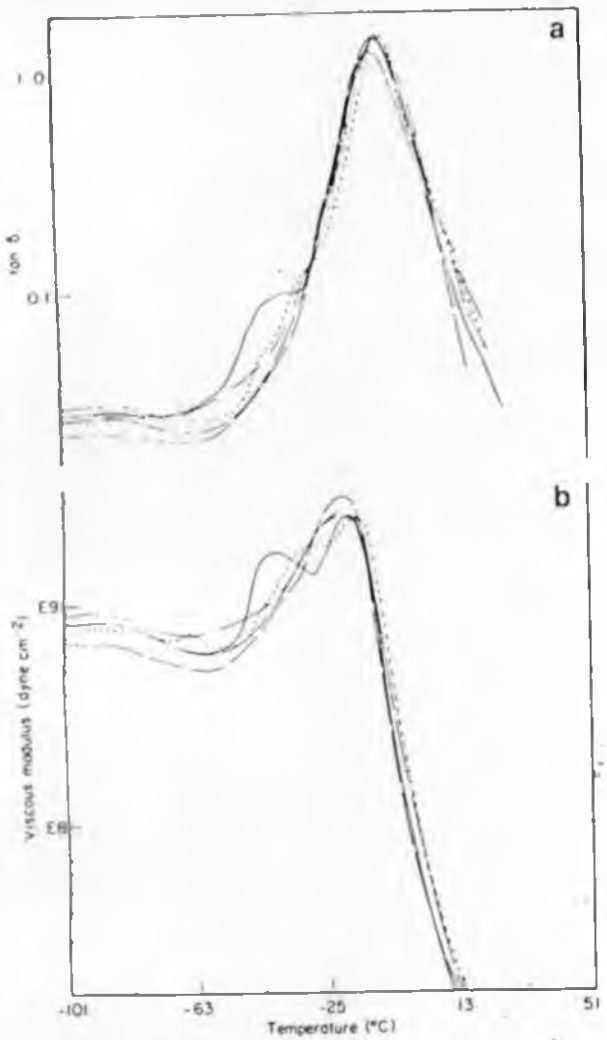

Figure 3 Dynamic mechanical spectra of the ternary blend showing the effect of ENR content on a fixed neoprene/XNBR ratio of 25/75: (a) tan δ *versus* temperature; (b) viscous modulus *versus* temperature. ENR content (blend designation): ———, 25.0 phr (I); ----, 50.0 phr (H); —·—·—, 62.5 phr (L); —·—, 75.0 phr (G); ——, 87.5 phr (H)

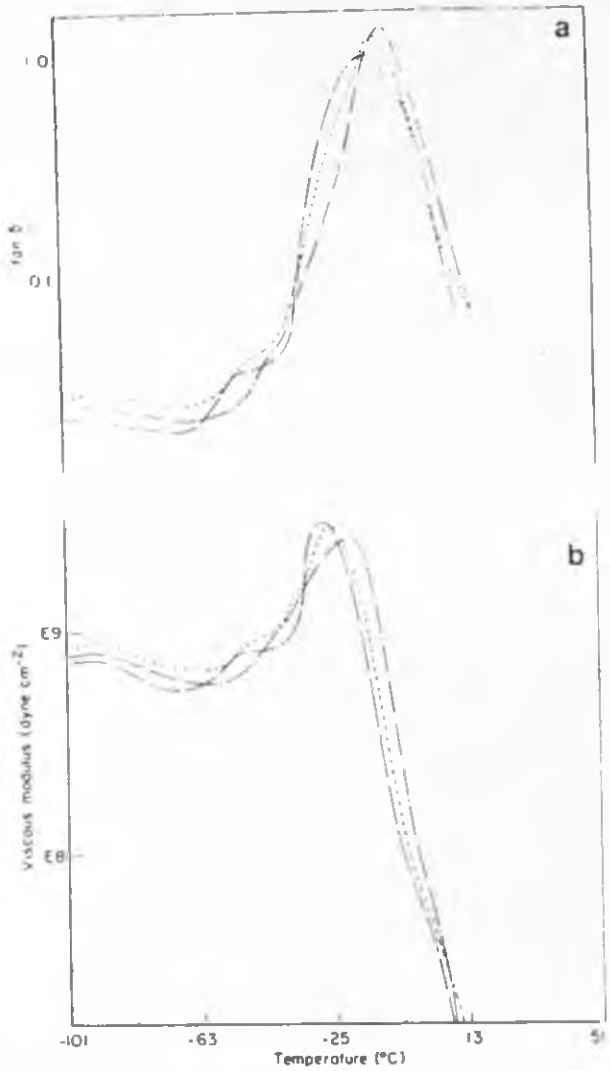

Figure 4 Dynamic mechanical spectra of ternary blend showing the effect of a 75 phr content of ENR on different neoprene/XNBR ratios of: ——, 75/25 (blend A); ---- 50/50 (blend D); and —·—, 25/75 (blend G): (a) tan δ *versus* temperature; (b) viscous modulus *versus* temperature

ENR content at constant neoprene/XNBR ratio on tan δ and viscous modulus plots of the ternary blends. At 75/25 ratio of neoprene/XNBR, an ENR concentration up to 25 parts per hundred parts neoprene/XNBR blend (phr) does not result in a miscible ternary blend. In fact two T_gs were observed, corresponding to two phases, i.e. neoprene/ENR and XNBR/ENR. When ENR content increases to 37.5 phr and above, the miscibility improves in the sense that instead of two peaks a single broad peak was observed. As ENR content in the blend increases from 50 to 75 phr the broad peak is replaced by a sharp peak, indicating enhanced miscibility.

Similar observations were made when neoprene content in the binary blend neoprene/XNBR decreases for example from blend composition 50/50 to 25/75. However, when neoprene content decreases in the blend, instead of a broad peak a sharp peak was observed, indicating enhanced miscibility.

Figure 4 shows that at an ENR content of 75 phr the ternary blend becomes a miscible system irrespective of the binary neoprene/XNBR composition. However, the miscibility is greater when the neoprene content is less in the binary neoprene/XNBR blend as evident from the sharp tan δ peak. Results are summarized in *Table 2*.

Results of d.s.c. studies (*Figure 5*) also provide supportive evidence for the conclusions drawn from d.m.a. studies. Results of d.s.c. studies are summarized in *Table 2*. It is evident that miscibility in a particular blend is manifested in the occurrence of sharp transition in the T_g zone. Accordingly, an immiscible system provided no clear-cut single transition, while a miscible system provides a single transition. For example, blend G is a miscible system showing a sharp T_g at $-18°C$, while blend C is an immiscible system showing two T_gs at $-40°C$ and $-18°C$ and blend H is an example of a partially miscible system wherein the two transitions merge with each other and no clear-cut transition is observed.

In the ternary blends, the broadening in the T_g is due to microlevel inhomogeneity. Microheterogeneity can be attributed to partial interpenetrating network formation involving thermovulcanized neoprene and crosslinked ENR/XNBR phases and also to density fluctuations[17]. The phase separation behaviour of interpenetrating polymer networks (IPNs) has been reported earlier[18–20]. It has been reported that due to microheterogeneity the glass transition of the IPN may be very broad, extending the range between the glass transitions of two homopolymers[21].

Table 3 Effect of fillers on glass transition temperature (T_g) of miscible ternary blend G of neoprene–XNBR–ENR

Blend designation	Filler type	T_g (°C) tan δ	Loss modulus	T_g (°C) from d.s.c.
G[a]	–	−7	−19	18
GISA40	ISAF black	−33, −5	−33, −7	[b]
GSi40	Silica	−21, −7	−23, −7	−40, −22
GSR40	SRF black	−5, shoulder at −16	−13	−19

[a]Unfilled; value from *Table 2*
[b]No clear-cut transition

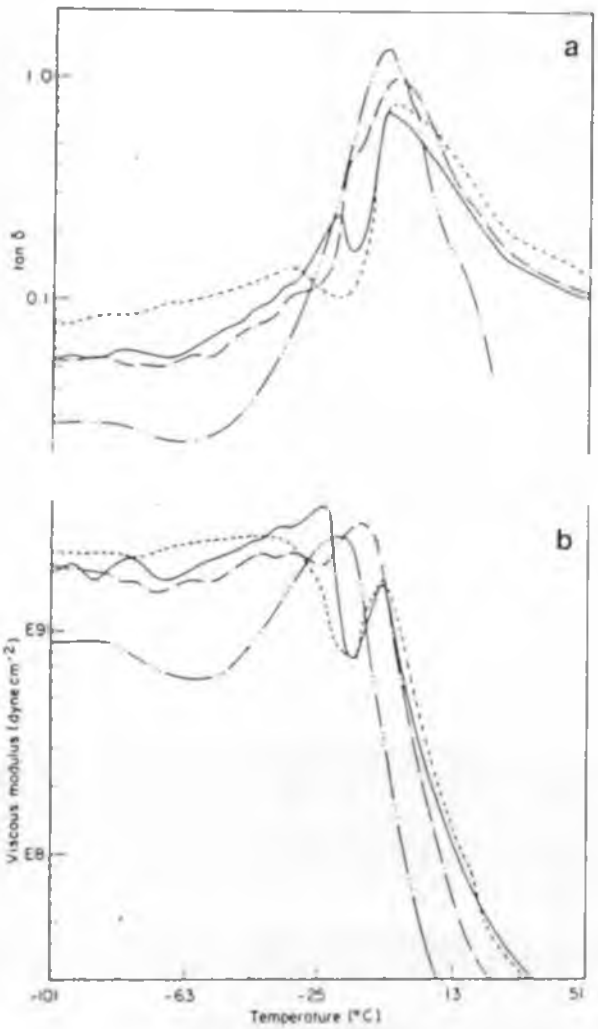

Figure 7 Dynamic mechanical spectra of the miscible ternary blend G filled with ISAF black, SRF black and precipitated silica. Filler loading was 40 parts per hundred parts of rubber in each case: (a) tan δ *versus* temperature; (b) viscous modulus *versus* temperature. —·—, Blend G; ———, ISAF black + G; —·—, SRF black + G; ----, silica + G

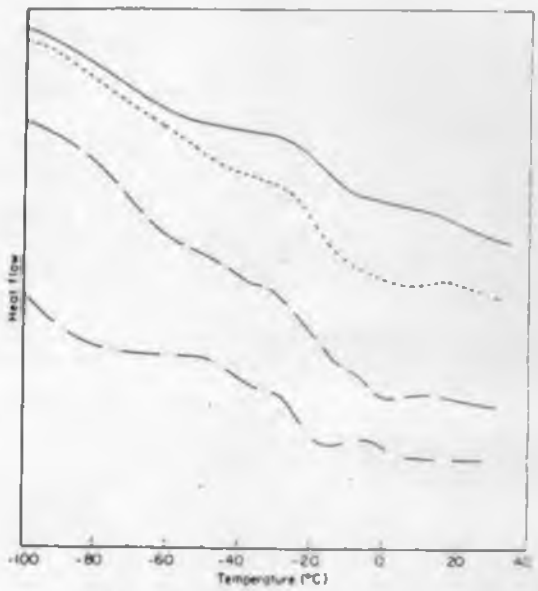

Figure 8 D.s.c. thermograms of the miscible ternary blend G filled with ISAF black, SRF black and precipitated silica. Filler leading was 40 parts per hundred parts of rubber in each case: ———, Blend G; ---, SRF black + G; —·—, ISAF black + G; —··—, silica + G

temperature due to lower crosslink density at 15 min moulding as compared to 60 min moulding. For the immiscible system, when the moulding time is increased to 120 min the miscibility does not change, but the tan δ peak is shifted to a higher temperature due to higher crosslink density at 120 min moulding as compared to 60 min moulding. The lowering of the damping level and broadening of the damping peak due to an increase of crosslinking has been reported previously[22].

Figure 7 shows the dynamic mechanical spectra of the miscible ternary blend system (blend G) filled with three fillers, namely silica, ISAF black and SRF black. The miscibility of the ternary blend was altered as is evident from the two peaks in both tan δ and viscous modulus plots in the case of blends with ISAF black (at −33°C and −5°C) and silica (at −21°C and −7°C). However, in the case of blends with SRF black a single peak at −5°C and a hump at −16°C were observed. It is evident that reinforcing fillers, such as ISAF black and silica, cause phase separation in a miscible ternary blend, presumably due to variations in the affinity of the filler to different rubbers. SRF black is less reinforcing and accordingly rubber–filler interaction will be less and the effect of the filler on miscibility will be less pronounced.

D.s.c. results showing the effect of different fillers on 25/75/75 neoprene–XNBR–ENR blend (blend G) are shown in *Figure 8*. It is evident that the addition of SRF black broadens the transition with no clear-cut glass transition. ISAF black also broadens the transition zone. Silica filler shows two transitions at −40°C and −22°C. It is evident that reinforcing fillers affect the miscibility of the self-vulcanizable ternary blend, as evidenced by the d.m.a. and thermal analysis studies (see *Table 3*). However, it is to be noted that transitions in d.s.c. studies are not as conclusive as those of d.m.a. results.

1991, 32, 1223

CONCLUSIONS

In the ternary blend of ENR/neoprene/XNBR, miscibility is attained at an ENR content of 75 parts per 100 parts of neoprene/XNBR blend, irrespective of neoprene/XNBR blend ratio. At lower ENR content miscibility depends on neoprene/XNBR blend ratio.

Reinforcing fillers like ISAF black and silica cause phase separation in a miscible ternary blend. SRF black does not have a pronounced effect on miscibility.

Increase in moulding time shifts the glass transition to a higher temperature due to increase in crosslink density without affecting the miscibility.

REFERENCES

1 Alex, R., De, P. P. and De, S. K. *J. Polym. Sci., Polym. Lett. Edn* 1989, **27**, 361
2 Alex, R., De, P. P. and De, S. K. *Polym. Commun.* 1990, **31**, 118
3 Mukhopadhyay, S. and De, S. K. *J. Appl. Polym. Sci.* in press
4 Mukhopadhyay, S., De, P. P. and De, S. K. *J. Appl. Polym. Sci.* in press
5 Mukhopadhyay, S., Chaki, T. K. and De, S. K. *J. Polym. Sci., Polym. Lett. Edn* 1990, **28**, 25
6 Mukhopadhyay, S. and De, S. K. *Polymer* ~~in press~~
7 Alex, R., De, P. P. and De, S. K. *Kautsch. Gummi Kunst.* in press
8 Shah, V. S., Keitz, J. D., Paul, D. R. and Barlow, J. W. *J. Appl. Polym. Sci.* 1986, **32**, 3863
9 Kwei, T. K., Frisch, H. L., Radizan, W. and Vogel, S. *Macromolecules* 1977, **10**, 157
10 Wang, Y. Y. and Chen, S. A. *Polym. Eng. Sci.* 1981, **21**, 47
11 Alex, R., De, P. P. and De, S. K. *Polym. Commun.* ~~in press~~ 1990, 31
12 Lee, Y.-O. and Chen, C.-M. *J. Appl. Polym. Sci.* 1987, **33**, 1231
13 Locke, C. E. and Paul, D. R. *Polym. Eng. Sci.* 1973, **13** (4), 308
14 Paul, D. R., Locke, C. E. and Vinson, C. E. *Polym. Eng. Sci.* 1973, **13** (3), 2092
15 Ameduri, B. and Prud'homme, R. E. *Polymer* 1988, **29**, 1052
16 Min, K. E., Chiou, J. S., Barlow, J. W. and Paul, D. R. *Polymer* 1987, **28**, 1721
17 Mackright, W. J., Karasz, F. E. and Fried, J. R. in 'Polymer Blends' (Eds D. R. Paul and S. Newman), Academic Press, New York, 1975, Ch. 5
18 Houston, D. J. and Zia, Y. *J. Appl. Polym. Sci.* 1983, **28**, 3849
19 Sperling, L. H. *Polym. Eng. Sci.* 1985, **25** (9), 517
20 Nielsen, L. E. 'Mechanical Properties of Polymers and Composites', Marcel Dekker, New York, 1974
21 Sperling, L. H. 'Interpenetrating Polymer Networks and Related Materials', Plenum Press, New York, 1981
22 Prud'homme, R. E. *Polym. Eng. Sci.* 1982, **22**, 90
23 Alex, R., De, P. P., Mathew, N. M. and De, S. K. *Plast. Rubber Process. Applic.* in press

1990, 14, 223

Super Abrasion Furnace

Semi Reinforcing Furnace

Polymer POL/90/0215

Self-vulcanizable ternary rubber blend based on epoxidized natural rubber, carboxylated nitrile rubber and polychloroprene rubber. Part 2: Effect of blend ratio and fillers on properties

R. Alex, P. P. De and S. K. De
Rubber Technology Centre, Indian Institute of Technology, Kharagpur, 721 302, India
(Received 9 May 1990; revised 30 August 1990; accepted 30 August 1990)

Mill-mixed blends of epoxidized natural rubber (ENR), carboxylated nitrile rubber (XNBR) and neoprene form a self-vulcanizable ternary blend system which can be reinforced by fillers such as carbon black and silica. The effect of fillers on processing characteristics and physical properties of self-vulcanizable blends is similar to that of conventional rubbers. The properties depend on blend ratio and type of filler. The blend in the gum state shows poor failure properties like gum ENR, but shows high resilience and low compression set. Abrasion loss and heat build-up properties of the blend are nearer to those of gum neoprene vulcanizate. The filled blends show lower heat build-up due to non-uniform distribution of fillers in the miscible ternary blend. Mooney viscosity and Mooney scorch time of the blend are found to be intermediate between the control mixes of ENR and XNBR, but the Monsanto rheometric torque values are closer to ENR.

(Keywords: ternary blends; miscibility; mechanical properties)

INTRODUCTION

In earlier papers[1,2] it has been reported that a mill-mixed blend of epoxidized natural rubber (ENR), polychloroprene rubber (neoprene) and carboxylated nitrile rubber (XNBR), forms a self-vulcanizable ternary rubber blend system upon moulding at 150°C. It has been observed that miscibility of such systems depends on blend composition and incorporation of filler[2]. The processing and physical properties of these blends have not been studied with respect to blend ratio variation and effect of filler. In this paper we report the results of studies on dependence of vulcanization characteristics and physical properties of the ternary blends on blend composition and fillers such as ISAF black, silica and SRF black. Similar studies have previously been made on the self-vulcanizable binary blend system of ENR/XNBR[3].

EXPERIMENTAL

Epoxidized natural rubber (ENR) with 50 mol% epoxidation was obtained from Malaysian Rubber Producers' Research Association, UK. Carboxylated nitrile rubber containing a high level of carboxylated monomer and a medium level of bound acrylonitrile (Krynac 221) was obtained from Polysar Ltd, Canada. Neoprene AD was obtained from DuPont Ltd, UK. Vulcasil S (precipitated silica) was obtained from Bayer (India) Ltd, Bombay. ENR and XNBR were separately masticated for ~1 min and neoprene for ~2 min on a 14 × 6 in. two roll mixing mill. Masticated samples of neoprene and XNBR were blended for ~2 min and after addition of ENR were blended for a further 2 min. The mill temperature for the initial mastication was 25°C. The temperature rise during the mixing of gum rubbers was only 2°C. The fillers were added after blending the rubbers. The total mixing time for the filled blends was ~12 min. The temperature rise during mixing in the case of filled blends was 7°C. The rolls were kept cool by the circulation of cold water.

Formulations of different blends are shown in *Tables 1* and *2*. Formulations of the control mixes are given in *Table 3*. In the case of the blend the increase in rheometric torque above the minimum torque was 26 units. The control mixes of ENR and XNBR were cured until the rise in rheometric torque was the same as that of the blend, i.e. 26 units. The cure times thus obtained were 30 min, 9 min and 60 min for ENR, XNBR and neoprene respectively.

Rheographs of the mixes were taken on a Monsanto Rheometer R-100 at 150, 160, 170 and 180°C. Scorch time and minimum Mooney viscosity at 120°C were determined using Mooney viscometer MK III (Negretti Automation Ltd), according to ISO 667. The properties determined by standard test methods were: tensile strength, (ISO 37) using dumbbell specimens by Instron 1195 Universal Testing Machine; tear resistance (ASTM D624-84) using an unnicked 90° angle specimen die C by Instron 1195 Universal Testing Machine; hardness, shore A (ISO 7619); and resilience (BS 903, part A8: method A: 1963) by Dunlop tripsometer. Samples for compression set (ISO 815) were cylindrical discs 29 mm diameter and 13 mm thickness, subjected to compressive deformation at constant strain for 22 h at 70°C. While determining heat build-up (ASTM D623-75) by Goodrich flexometer the samples were subjected to cyclic deformation for 25 min at an ambient temperature of

Table 1 Formulation of blends

Component	A	B	K	C	J	D	E	F	M	G	L	H	I
	Blend designation												
Neoprene AD (%)	75	75	75	75	75	50	50	50	25	25	25	25	25
XNBR (Krynac 221) (%)	25	25	25	25	25	50	50	50	75	75	75	75	75
ENR (phr)[c]	75	50	37.5	25	12.5	75	50	25	87.5	75	62.5	50	25

Table 2 Formulations of filled ternary blends

Component	GIS10	GIS20	GIS30	GIS40	GSR10	GSR20	GSR30	GSR40	GSR50	GSi10	GSi20	GSi30	GSi40	GSi50
	Blend designation													
Neoprene AD	25	25	25	25	25	25	25	25	25	25	25	25	25	25
XNBR (Krynac 221)	75	75	75	75	75	75	75	75	75	75	75	75	75	75
ENR	75	75	75	75	75	75	75	75	75	75	75	75	75	75
ISAF black	17.5	35.0	52.5	70.0	–	–	–	–	–	–	–	–	–	–
SRF black	–	–	–	–	17.5	35.0	52.5	70.0	87.5	–	–	–	–	–
Silica[a]	–	–	–	–	–	–	–	–	–	17.5	35.0	52.5	70.5	87.5

[a]Precipitated silica, Vulcasil S obtained from Bayer (India) Ltd, Bombay

Table 3 Formulations of control single rubber mixes

Component	N	Nc	X	Xc	E	Ec
	Blend designation					
Neoprene AD	100	100	–	–	–	–
XNBR (Krynac 221)	–	–	100	100	–	–
ENR	–	–	–	–	100	100
Na_2CO_3	–	–	–	–	0.25	0.25
ZnO	5	5	5	5	5	5
Stearic acid	–	–	2	2	2	2
ISAF black	–	20	–	20	–	20
Dioctyl phthalate	–	2	–	2	–	–
Aromatic oil	–	–	–	–	–	2
MgO	4	4	–	–	–	–
Thiourea	–	0.5	–	–	–	–
TMTD[a]	–	–	–	–	1.6	–
NBS[b]	–	–	1.0	1.0	2.4	1.0
Sulphur	–	–	2.4	2.4	0.3	2.8

[a]TMTO = Tetramethylthiuram disulphide
[b]NBS = *N*-oxydiethylene benzothiazole-2-sulphenamide

50°C with a load of 24 lb (≈10.8 kg) and stroke of 4.5 mm. Abrasion resistance (BS 903: part A9: method A: 1957) was determined using a DuPont abrader. Samples were abraded for 10 min with the abrasive paper rotating at a speed of 40 rev min^{-1}. The volume (in cm^3) lost from a specified test specimen for 1000 revolutions of the abrasive wheel was then calculated.

Scanning electron microscope (SEM) studies of the abraded surfaces were made on a scanning electron microscope model Camscan series 2 DV. The size, shape and direction of abrasion of specimens are shown in *Figure 1*. The abraded surfaces were sputter-coated with gold for SEM studies.

Volume fraction (V_r) of the rubber in the swollen vulcanizate was calculated from equilibrium swelling data by the method reported by Ellis and Welding[4]:

$$V_r = \frac{(D - FT)/\rho_r}{[(D - FT)/\rho_r] + (A_0/\rho_s)} \quad (1)$$

where T is the weight of the specimen, D is the swollen weight, F is the weight fraction of insoluble components and A_0 is the weight of absorbed solvent corrected for swelling increment. ρ_r and ρ_s are the densities of the rubber and solvent respectively. Chloroform was used as the solvent in this study.

RESULTS AND DISCUSSION

Effect of blend ratio variation

Cure characteristics. Results of cure characteristics are

shown in *Table 4*. For a constant neoprene/XNBR ratio, minimum Mooney viscosity and scorch time at 120°C show progressive change with ENR content. As the ENR content increases, the minimum Mooney viscosity decreases and scorch time increases. As the XNBR in the neoprene/XNBR ratio increases, the scorch time is greatly reduced and minimum Mooney viscosity is increased. For instance at a neoprene/XNBR ratio of 75/25 when ENR at 25 parts per hundred parts neoprene/XNBR blend (phr) is added, minimum Mooney viscosity is 33 and scorch time is 10.8 min. However, at a neoprene/XNBR ratio of 25/75 with 25 phr ENR, minimum Mooney viscosity is 45 and scorch time is 5.1 min. In the ternary blend it is believed that the carboxyl group of XNBR and the epoxy group of ENR react to form ester linkages[5,6] and the epoxy group of ENR and allylic chlorine of neoprene react to form ether linkages[7]. Furthermore –COOH group of XNBR has been reported to interact with allylic chlorine of neoprene in order to form a self-vulcanizable rubber blend[8]. Hence the low scorch time in ternary blends containing high XNBR is due to early onset of chemical reactions involving –COOH group, epoxy group and allylic chlorine.

Monsanto rheographs of the different blends at 150°C are shown in *Figure 2*. All the blends show increasing rheometric torque with time. The dependence of minimum rheometric torque on the blend ratio follows the same pattern as the changes in minimum Mooney viscosity. At a fixed neoprene/XNBR ratio, increase in ENR content lowers the Mooney viscosity. The extent of crosslinking, as reflected from the rheometric torque, depends on the composition of the blend. Maximum rheometric torque was observed in blend G which contains neoprene/XNBR/ENR in the ratio 1/3/3. Blend G has been found to be completely miscible and a homogeneous matrix is formed at the composition at which maximum interaction between the constituents takes place.

Physical properties. The physical properties of different gum blends are shown in *Table 5*. Tensile stress *versus* strain curves are shown in *Figure 3*. High tensile strength is observed in blends containing a high proportion of neoprene. The systems which contain a high proportion of neoprene are immiscible at the segmental level, but are mechanically compatible. Immiscible systems which are mechanically compatible are reported to have good physical properties[9,10]. For neoprene/XNBR blends at 75/25 and 50/50 ratios, increased incorporation of ENR causes a decrease in modulus, tensile strength, tear strength, hardness and resilience and an increase in compression set and abrasion loss. Values of V_r were found to decrease with increased ENR content. Since V_r

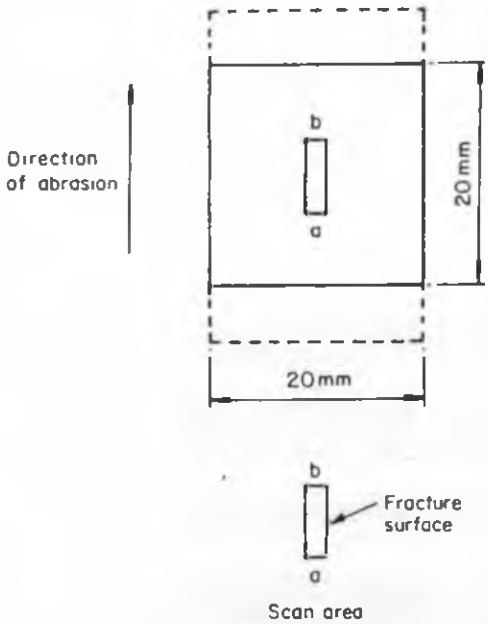

Figure 1 Abrasion sample showing direction of abrasion and scan area

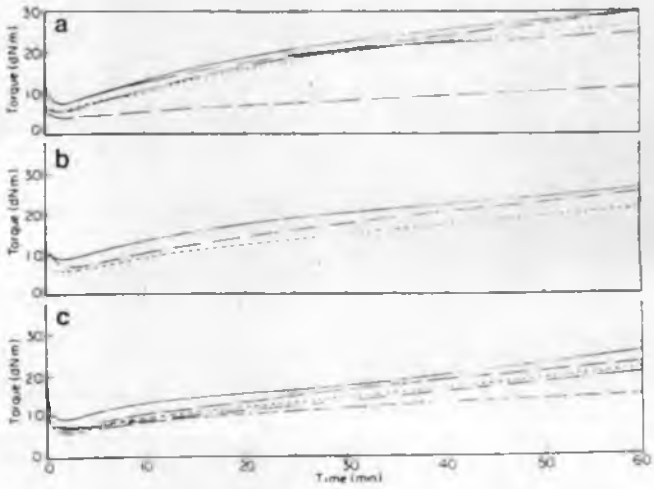

Figure 2 Monsanto rheographs of different gum ternary blends at 150°C. (a) Blends: —·—·—, I; ——, H; ----, L; —·—, G; —·—, M. (b) Blends: ----, D; —·—·—, E; ——, F. (c) Blends: —·—, A; ----, B; —·—, K; —·—·—, C; ——, J. Compositions of blends as given in *Table 1*

Table 4 Cure characteristics of ternary blends

Property	A (3/1/3)	B (3/1/2)	K (3/1/1.5)	C (3/1/1)	J (3/1/0.5)	D (2/2/3)	E (2/2/2)	F (2/2/1)	M (1/3/3.5)	G (1/3/3)	L (1/3/2.5)	H (1/3/2)	I (1/3/1)
	Blend (neoprene/XNBR/ENR ratio)												
Mooney viscometry													
Minimum Mooney viscosity at 120°C	31	31	32	33	38	31	32	38	26	30	33	36	45
Mooney scorch time at 120°C (min)	20.8	11.1	11.0	10.8	6.0	10.0	8.3	6.3	8.3	8.0	8.0	6.5	5.1
Monsanto rheometry													
Minimum torque at 150°C (min)	6	8	8	8	10	5	6	8	4	5	6	8	8
Maximum torque at 150°C (at 60 min) (dN. m)	15	22	23	21	26	24	25	31	12	31	28	31	26

Table 5 Physical properties of gum ternary blends moulded for 60 min at 150 C

Property	A (3/1/3)	B (3/1/2)	C (3/1/1)	D (2/2/3)	E (2/2/2)	F (2/2/1)	G (1/3/3)	H (1/3/2)	I (1/3/1)
	Blend (neoprene/XNBR/ENR ratio)								
Modulus 300% (MPa)	2.5	2.8	6.4	3.5	3.5	6.1		5.0	4.8
Tensile strength (MPa)	9.3	8.6	15.5	5.0	5.8	9.7	4.7	5.3	5.4
Elongation at break (%)	550	510	440	380	370	370	270	310	330
Tear strength (kN m^{-1})	33	29	39	23	26	27	18	18	23
Hardness (Shore A)	60	65	75	55	58	65	49	52	55
Resilience at 40°C (%)	57	62	62	63	65	67	68	66	65
Compression set, 22 h at 70°C (%)	57	30	30	30	27	19	11	13	13
Abrasion loss (cm^3 10^{-3} rev)	2.0	2.0	1.8	2.0	2.0	0.7	1.8	1.2	0.5
Heat build-up by Goodrich flexometer with a load of 24 lb and stroke of 4.5 mm, ΔT (°C)	*	*	*	*	*	*	38[b]	*	*
V_r	0.06	0.07	0.10	0.10	0.11	0.11	0.13	0.13	0.11

*Sample blown out before 20 min
[b]Value after 20 min

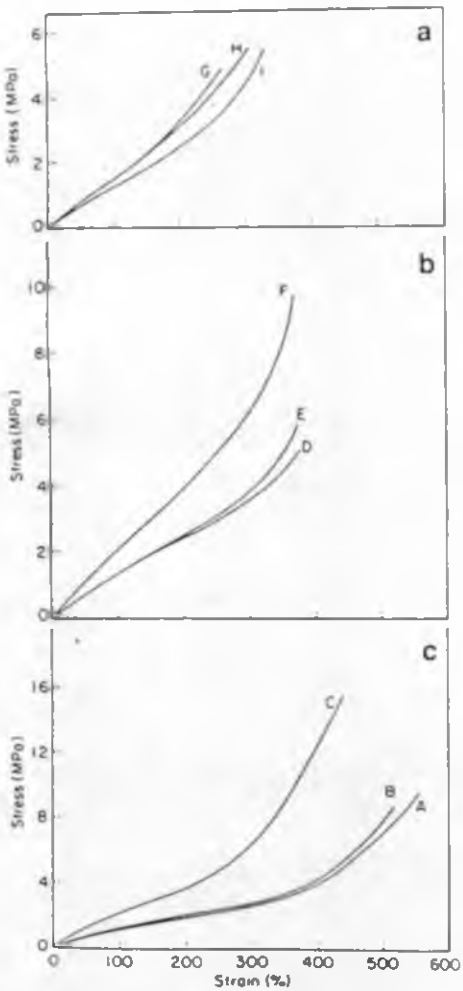

Figure 3 Tensile stress *versus* strain curves of ternary gum vulcanizates. Blend compositions as given in *Table 1*

can be considered as proportional to crosslink density, the gradual changes in properties could be understood on the basis of degree of crosslinking. However, in neoprene/XNBR blend at 25/75 ratio, increased incorporation of ENR causes an increase in V_r and accordingly the changes in properties with blend ratio variation follow a different pattern. In general, the changes in properties with blend ratio variation are less remarkable in this series.

Effect of fillers

Cure characteristics. Minimum Mooney viscosities and Mooney scorch times for the filled blend[9] are given in *Table 6*. As expected, an increase of filler loading increases the minimum viscosity and decreases the scorch time. The increase in Mooney viscosity is very high in the caseof silica-filled mixes and low in the case of SRF black-filled mixes. For example, at a loading of 40 parts filler (er hundred parts rubber (phr), Mooney viscosity at 120°C increases from 30 for the unfilled blend to 49 for SRF black-filled mix, to 71 for ISAF black-filled mix and to 98 for silica-filled mix. The higher Mooney viscosity of silica-filled mix is probably due to the strong interaction of silica with rubber during mixing and moulding at higher temperatures[11,12]. The low scorch times of the blends show that the crosslinking reaction starts even at a processing temperature of 120°C.

Rheographs of the gum blend at different temperatures and of control ENR, XNBR and neoprene mixes at 150°C are shown in *Figure 4*. The gum blend shows increasing rheometric torque with time and temperature of moulding. *Figure 5* shows rheographs of ISAF black-filled systems. It is evident that, as in the case of conventional rubbers, ISAF black reinforces the ternary blend. The nature of rheographs with respect to time and temperature is similar to that of gum blend. Increase of filler loading increases the rheometric torque (*Figure 6*).

It has been reported that both neoprene and XNBR can be cured by epoxy resins[12,13]. Furthermore neoprene and XNBR interact to form ester linkages. In the ternary blend of neoprene/ENR/XNBR it is likely that ether linkages and ester linkages will be distributed randomly in the matrix. Conventionally cured vulcanizates with sulphur linkages show a tendency for reversion. On the other hand, due to the difference in the type of crosslinks, the ternary blend shows an absence of cure reversion and a higher degree of crosslinking at higher temperatures

Table 6 Cure characteristics of the filled ternary blend G

Property	Filler	Loading (phr) 0	10	20	30	40	50
Mooney viscometry							
Minimum Mooney viscosity at 120°C	ISAF black		42	43	58	71	
	SRF black	30	37	39	39	49	62
	Silica		45	49	67	98	170
Mooney scorch time at 120°C (min)	ISAF black		6.2	5.5	5.0	4.0	
	SRF black	8.0	6.8	6.3	5.8	5.0	4.7
	Silica		6.2	5.5	5.0	3.2	2.5
Monsanto rheometry							
Minimum torque at 150°C (dN m)	ISAF black		11	12	16	18	-
	SRF black	5	10	10	14	14	14
	Silica		11	12	17	31	34
Maximum torque at 150°C	ISAF black		44	56	67	84	-
(at 60 min) (dN m)	SRF black	31	42	47	54	61	69
	Silica		51	66	67	91	96

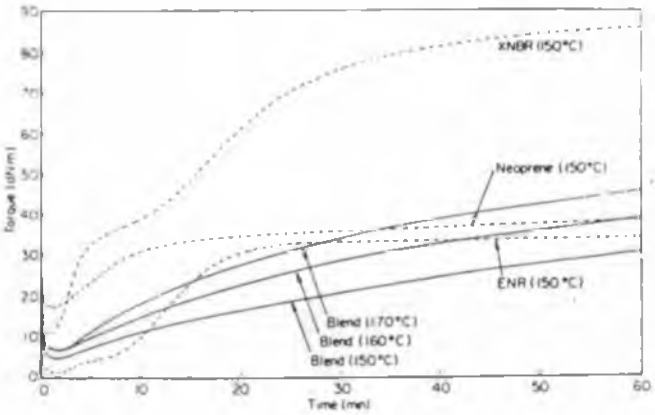

Figure 4 Rheographs of gum blend at different temperatures and of control ENR, XNBR and neoprene mixes at 150°C

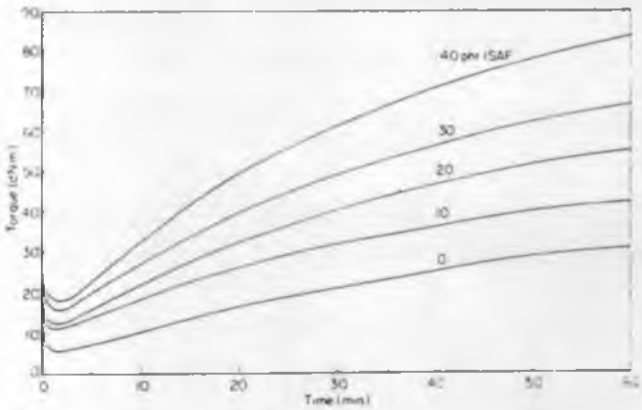

Figure 6 Rheographs at 150°C of ternary blend G filled with different loadings of ISAF black

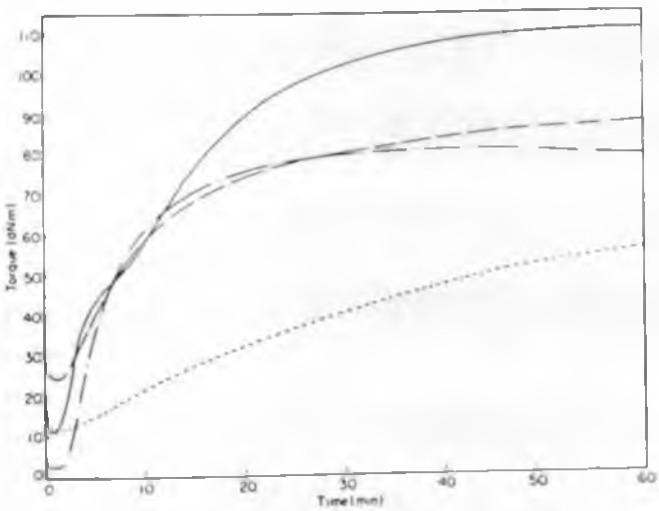

Figure 5 Rheographs at 150°C of ISAF black-filled systems of: —·—·—, single ENR; ———, XNBR; —·—, neoprene; ----, ternary blend G

Physical properties. The tensile stress *versus* strain behaviour of the filled mixes is shown in *Figure 7*. The effect of filler loading on the physical properties is summarized in *Table 7*. As expected, the following properties show gradual increase with increase in filler loading: modulus, tensile strength, tear strength, abrasion resistance and hardness. Resilience decreases with filler loading. It is interesting to note that heat build-up is considerably reduced for filled mixes at higher loading of filler. There is believed to be an unequal distribution of reinforcing filler in the ternary blend and this has been reported to result in low hysteresis[14,15].

Polymer–filler interaction was studied by swelling of the blend vulcanizates in chloroform. *Figure 8* shows the variation of V_{ro}/V_{rf} against $\phi/(1-\phi)$ according to the Kraus plot[16]:

$$V_{ro}/V_{rf} = 1 - (m\phi/1-\phi) \qquad (2)$$

where ϕ is the volume concentration of filler in the filled vulcanizate, V_{ro} is the volume fraction of rubber phase in swollen gel of gum rubber vulcanizate and V_{rf} is the volume fraction of rubber phase in swollen gel of filled rubber vulcanizate, assuming that filler does not swell. Both V_{ro} and V_{rf} are determined by equation (1). m is a constant characteristic of the filler–rubber matrix.

It is evident that the linear relation according to the Kraus plot is not obeyed in this system. This deviation from linearity may be due to two reasons. Firstly, fillers

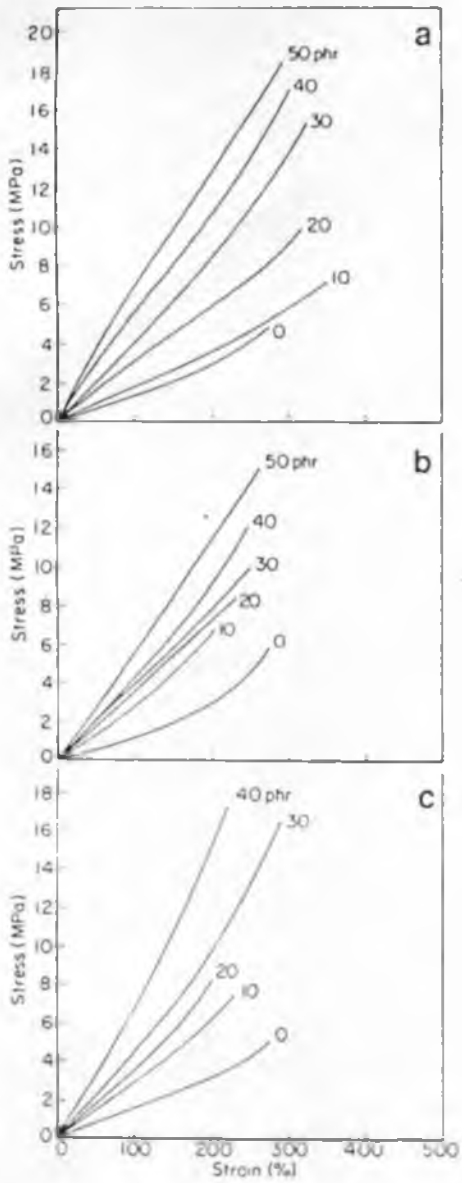

Figure 7 Tensile stress *versus* strain curves of the miscible ternary blend G filled with different loadings of (a) silica, (b) SRF black and (c) ISAF black

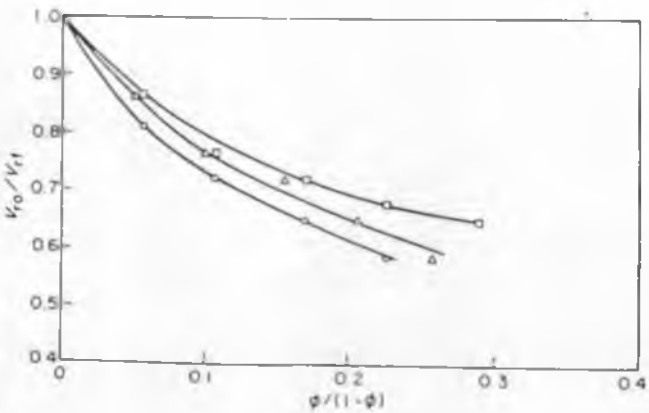

Figure 8 Kraus plots for ternary blend G filled with ISAF black (○), SRF black (□) and silica (△)

have been reported to influence the miscibility of the ternary blend[5]. Affinities of the three rubbers for the fillers are not the same and therefore fillers will tend to redistribute when mixed into a blend. This can result in an accumulation of fillers at the interface[17] and consequently some portion of fillers will not be available in the rubber matrix for resisting solvent penetration. This would cause a lower V_{rf} than expected, resulting in an increase in the ratio of V_{ro}/V_{rf}. Secondly, fillers themselves take part in crosslinking reactions which may result in an increase in crosslink density of the network. Accordingly the actual V_{ro} value in the filled blend will be higher than the measured V_{ro} value of the gum blend. As a result the ratio of V_{ro}/V_{rf} will be higher than the value obtained if there were no increase in crosslink density due to filler incorporation.

The abrasion characteristics of the blends have been studied by SEM. Ridge formation in elastomers has been reported previously[18–20]. It has been shown that close spacing of ridges results in high abrasion resistance[21]. Abrasion resistance depends mainly on the strength of the matrix. The gum ternary blend has poor matrix strength which is greatly improved by the addition of reinforcing fillers. The SEM fractographs of the abraded surfaces of the ternary blend, showing the effect of reinforcing filler on abrasion resistance, are shown in *Figures 9–11*. The abraded surface of the gum mix (*Figure 9*) shows horizontal ridges which are deformed and widely spaced showing poor abrasion resistance. With incorporation of 20 phr ISAF black the abraded surface shows a tendency to form vertical ridges (*Figure 10*). When the ISAF black loading is raised to 40 phr closely spaced vertical ridges (*Figure 11*) are formed showing that the

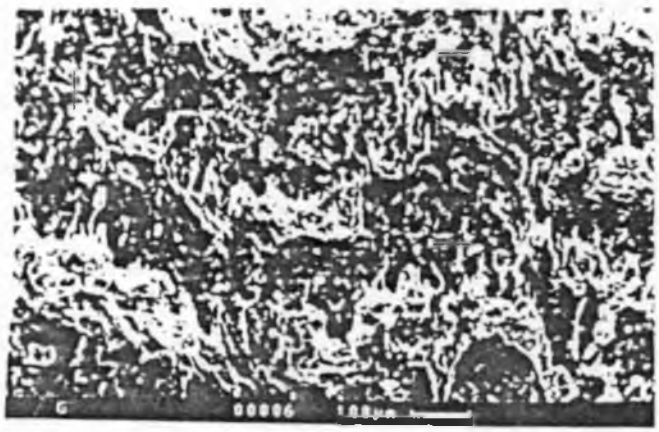

Figure 9 SEM fractograph of abraded surface of blend G

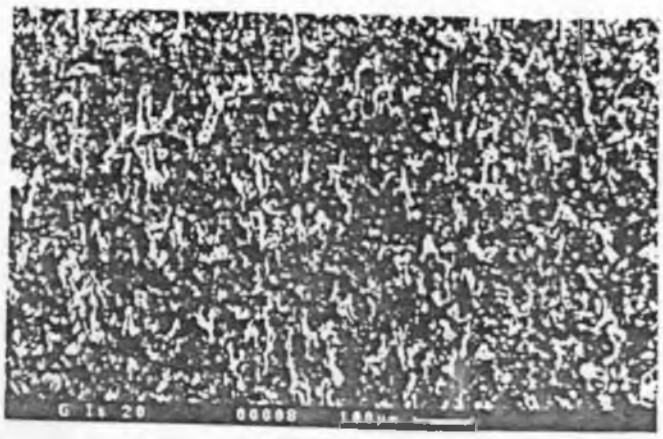

Figure 10 SEM fractograph of the abraded surface of blend G filled with 20 phr ISAF black

Table 7 Physical properties of the filled ternary blend G moulded for 60 min at 150°C

Property	Filler	Loading (phr) 0	10	20	30	40	50
Modulus 200% (MPa)	ISAF black		5.5	7.3	10.0	15.4	–
	SRF black	2.8	6.5	7.0	7.5	9.9	11.8
	Silica		3.4	5.6	8.5	10.8	12.7
Tensile strength (MPa)	ISAF black		7.4	8.0	16.0	17.0	
	SRF black	4.7	7.2	8.0	9.7	11.9	15.0
	Silica		7.1	9.8	14.8	16.8	17.4
Elongation at break (%)	ISAF black		240	290	280	220	
	SRF black	270	210	220	250	250	270
	Silica		330	320	320	300	280
Tear strength (kN m^{-1})	ISAF black		30	39	50	48	
	SRF black	18	34	40	45	47	54
	Silica		22	40	53	58	54
Hardness (Shore A)	ISAF black		58	65	70	76	
	SRF black	49	51	59	64	68	74
	Silica		60	65	75	82	89
Resilience at 40°C (%)	ISAF black		61	53	51	49	–
	SRF black	68	63	62	60	57	65
	Silica		64	62	60	53	49
Compression set, 22 h at 70°C (%)	ISAF black		11	12	14	15	–
	SRF black	11	11	11	14	16	16
	Silica		14	14	14	16	16
Abrasion loss (cm^3 10^{-3} rev)	ISAF black		1.2	0.8	0.6	0.4	–
	SRF black	1.8	1.7	1.6	1.5	1.3	1.1
	Silica		1.2	0.9	0.5	0.2	0.2
Heat build-up by Goodrich flexometer at a load of 24 lb and stroke of 4.5 mm							
ΔT (°C)	ISAF black		26	27	32	35	–
	SRF black	38	30	30	35	35	35
	Silica		[c]	30	33	31	26
dynamic set (%)	ISAF black		1.2	1.2	1.3	1.3	–
	SRF black	[d]	[d]	2.2	3.1	3.5	3.5
	Silica		[d]	0.4	3.3	1.4	1.4
V_r	ISAF black		0.17	0.18	0.20	0.22	–
	SRF black	0.13	0.15	0.17	0.18	0.19	0.20
	Silica		0.15	0.17	0.18	0.20	0.22

[a] Reading after 20 min
[b] Reading after 15 min
[c] Sample blown out before 15 min
[d] Sample blown out

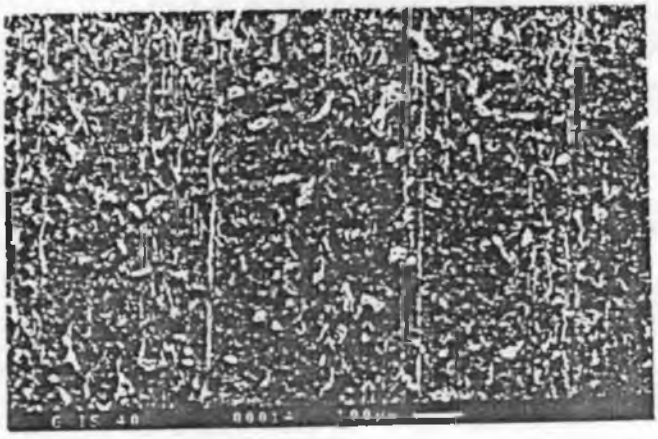

Figure 11 SEM fractograph of abraded surface of blend G filled with 40 phr ISAF black

abrasion resistance is improved. Vertical ridge formation suggests frictional type wear[22].

Physical properties of the ternary blend and of control ENR, XNBR and neoprene mixes are shown in *Table 8*. The observations can be summarized as follows.

1. As expected gum neoprene shows high strength, due to strain crystallization. Addition of reinforcing ISAF black does not change the physical properties significantly. However, addition of 20 phr ISAF black reduces the elongation at break and causes reduction in the abrasion loss and compression set.
2. Gum XNBR shows good matrix strength, excellent abrasion resistance but high compression set due to ionic crosslinks. Incorporation of 20 phr ISAF black causes improvement in most of the physical properties. However, abrasion resistance remains unaffected by the presence of ISAF black.

Table 8 Physical properties of the ternary blend and of control ENR, XNBR and neoprene mixes

Property	Blend							
	N	X	E	G	Nc	Xc	Ec	GIS20
Modulus 300% (MPa)	7.0	3.9	1.2			15.5	9.0	
Tensile strength (MPa)	17.0	18.7	4.2	4.7	9.0	24.0	23.0	8.0
Elongation at break (%)	900	470	650	270	170	380	595	290
Tear strength (kN m^{-1})	70	34	18	18	68	70	49	39
Hardness (Shore A)	87	69	30	49	89	83	61	65
Resilience at 40 C (%)	61	62	26	68	60	54	49	53
Compression set, 22 h at 70 C (%)	25	70	16	11	18	53	35	12
Abrasion loss (cm^3 10^{-3} rev)	1.00	0.05	8.40	1.80	0.77	0.05	0.42	0.80
Heat build-up by Goodrich flexometer with a load of 24 lb and stroke of 4.5 mm								
ΔT (°C)	38	[a]	20	38[b]	26	58	16	27
dynamic set	6.1	[a]	1.6	[c]	1.6	4.2	7.3	1.2
V_r	0.09	0.05	0.09	0.13	0.23	0.10	0.12	0.18

[a]Reading after 20 min
[b]Sample could not be tested
[c]Sample blown out

Table 9 Cure characteristics of control single rubber mixes and blend G

Property	Blend							
	N	Nc	E	Ec	X	Xc	G[a]	GIS20[a]
Mooney viscometry								
Minimum Mooney viscosity at 120°C	89	127	5	9	40	50	30	43
Mooney scorch time at 120°C (min)	5.0	3.0	10.0	6.5	3.8	2.0	8.0	5.5
Monsanto rheometry								
Minimum torque at 150 C (dN m)	18	25	2	3	11	12	5	12
Maximum torque at 150 C (dN m)	39	87	33	80	87	115	31	56

[a]Values from *Table 4*

3. Gum ENR shows poor matrix strength which, however, is reinforced on addition of 20 phr ISAF black filler.
4. The self-vulcanizable ternary blend in the gum state registers poor failure properties, as does gum ENR, but it shows high resilience and low compression set. Abrasion loss and heat build-up properties of the blend are nearer to those of gum neoprene matrix. Addition of 20 phr reinforcing black causes improvement in all physical properties.

Cure characteristics of the ternary blend G and of control ENR, XNBR and neoprene mixes are shown in *Table 9*. Mooney viscosity and scorch time of the blend were found to be intermediate between the two control mixes of ENR and XNBR, but the Monsanto rheometric torque values are close to ENR.

CONCLUSIONS

Mill-mixed blend of ENR, XNBR and neoprene forms a self-vulcanizable ternary blend system. Processing characteristics, crosslink density and physical properties of this blend depend upon blend ratio. Incorporation of reinforcing fillers, such as ISAF black, precipitated silica and SRF black, causes changes in processing behaviour and physical properties which are similar to conventional rubber mixes.

Silica forms strong polymer–filler bonds during mixing in the ternary blend system as is evident from processing characteristics.

Due to non-uniform distribution of fillers in the blend components Goodrich heat build-up of filled composites is less than the unfilled blend.

REFERENCES

1 Alex, R., De, P. P. and De, S. K. *Polym. Commun.* 1990, 31, 118
2 Alex, R., De, P. P. and De, S. K. *Polymer* POL/90/0214
3 Alex, R., De, P. P., Mathew, N. M. and De, S. K. *Plast. Rubber Process Applic.* in press
4 Ellis, B. and Welding, G. N. *Rubber Chem. Technol.* 1964, 37, 92
5 Alex, R., De, P. P. and De, S. K. *J. Polym. Sci., Polym. Lett. Edn* 1989, 30, 361
6 Chakraborty, S. K., Bhowmick, A. K. and De, S. K. *J. App. Polym. Sci.* 1981, 26, 4011
7 Alex, R., De, P. P. and De, S. K. *Kautsch. Gummi Kunst.* in press
8 Mukhopadhyay, S. and De, S. K. *J. Appl. Polym. Sci.* in press
9 Siegmann, A. *J. Appl. Polym. Sci.* 1979, 24, 2333
10 Kallitsis, J. K. and Kalfoglou, N. K. *J. Appl. Polym. Sci.* 1986, 32, 5261
11 Edwards, D. C. and Sato, K. *Rubber Chem. Technol.* 1979, 52, 263
12 Chakraborty, S. K. and De, S. K. *J. Appl. Polym. Sci.* 1982, 27, 4561

13 Zakharov, N. D. and Maiorov, G. A. *Sov. Rubber Technol* 1963, 22, 11
14 Roland, M. C. *Rubber Chem. Technol.* 1989, 62, 456
15 Hess, W. M. and Chiroco, V. E. *Rubber Chem. Technol.* 1977, 50, 301
16 Marsh, P. A., Voet, A., Price, L. O. and Mullins, T. J. *Rubber Chem. Technol.* 1968, 41, 344
17 Kraus, G. *J. Appl. Polym. Sci.* 1963, 7, 861
18 Schallamach, A. *Rubber Chem. Technol.* 1968, 41, 209
19 Mathew, N. M. and De, S. K. *J. Mater. Sci.* 1983, 18, 515
20 Bhagwan, S. S. and Tripathy, D. K. *Mater. Chem. Phys.* 1987, 17, 415
21 Gent, A. N. and Pulford, C. T. R. in 'Developments in Polymer Fracture', Vol. 1 (Ed. E. H. Andrews), Applied Science, London, 1979, p. 155
22 Reznikovskii, M. M. and Brodskii, G. I. in 'Abrasion of Rubbers' (Ed. O. I. James), MacLaren, London, 1967, pp. 14, 81

Self-vulcanizable ternary rubber blend. 2: R. Alex et al.
Self-vulcanizable ternary rubber blend. 2: R. Alex et al.
Self-vulcanizable ternary rubber blend. 2: R. Alex et al.
Self-vulcanizable ternary rubber blend. 2: R. Alex et al.
Self-vulcanizable ternary rubber blend. 2: R. Alex et al.
Self-vulcanizable ternary rubber blend. 2: R. Alex et al.
Self-vulcanizable ternary rubber blend. 2: R. Alex et al.
Self-vulcanizable ternary rubber blend. 2: R. Alex et al.

The rate is not linearly influenced by the initiator concentration, $[I]_0$, throughout (*Figure 5*). At values of $[I]_0$ below c. 1.5 wt% ln $r_{p,0}$ shows a linear relation with $[I]_0$ leading to an order of 0.6 in $[I]_0$. The small deviation from the classical 0.5 order indicates a small tendency towards a monomolecular termination along with a bimolecular termination mechanism. Monomolecular termination could occur by entrapment of isolated living radicals in the polymer network during polymerization[2,3,10,11,15] which may be expected to increase in the low region. Trapped radicals have been detected by e.s.r. in the case of several multifunctional acrylic monomers[3,4,15].

In contrast there is no influence on $r_{p,0}$ when $[I]_0$ is exceed c. 1.5 wt%. This may be rationalized as follows. Applying Beer's law Joshi[18] derived the following equation for the initial rate:

$$r_{p,0}=k_p/k_t^{1/2}[\phi J_0(1-e^{-\varepsilon[I]_0 l})]^{1/2}[M]_0$$

where: k_p = propagation constant; k_t = termination constant; ϕ = quantum yield; J_0 = intensity of incident light; ε = molar extinction coefficient; l = sample thickness; $[M]_0$ = initial monomer concentration.

For small values of $\varepsilon[I]_0 l$ this simplifies to

$$r_{p,0}=k_p/k_t^{1/2}[\phi J_0\varepsilon[I]_0 l]^{1/2}[M]_0$$

the (initial) rate is proportional to the square root of $[I]_0$. For large values of $\varepsilon[I]_0 l$ which may be caused by high $[I]_0$ as in the present case:

$$r_{p,0}=k_p/k_t^{1/2}(\phi J_0)^{1/2}[M]_0$$

$r_{p,0}$ is independent of $[I]_0$.

From these considerations one may anticipate a gradual change in the order of $[I]_0$ from 0.5 to 0 by varying the $[I]_0$ from low to high values. The apparent sharpness in *Figure 3* has no physical meaning and is due to logarithmic scales on the axes.

Finally *Table 1* shows the total conversion as a function of temperature and initiator concentration (wt%) after 5 min of reaction time, i.e. after the d.s.c. curves had practically returned to the base line. Above a change-over temperature of 330 K these conversions varied only little between 80 and 90% for all initiator concentrations, except for the lowest one, which averaged 58%. There is a possibility that the actual end conversions are higher than those given in *Table 1* because of a very slow prolonged polymerization reaction, which cannot be detected by d.s.c.[10].

Incomplete conversions may be expected, especially in network formation during bulk polymerization because this leads to rapid vitrification of the system immobilizing double bonds and polymeric radicals rendering them unavailable for further polymerization.

Table 1 Total conversion after 15 min for less depending on wt% initiator and temperature as a function of temperature and initiator concentration for the photopolymerization of PUA

	Temperature (K)								
$[I]_0$ (wt%)	293	308	323	328	330	333	336	343	353
0.1	–	47	60	–	–	68	–	68	62
0.18	–	48	53	–	–	–	69	69	76
0.4	37	63	71	–	75	–	76	80	86
0.8	–	48	53	–	70	–	65	70	85
2.7	–	75	80	–	88	–	–	90	92
5.0	58	76	78	83	–	89	–	90	91

ACKNOWLEDGEMENTS

The authors are grateful to the European Community and Philips Research Laboratories Eindhoven for financially supporting this research in a BRITE project, no. RI 1B-0070-NL. They also thank D. J. Broer, R. G. Gossink, J. G. Kloosterboer (Philips Research Laboratories, Eindhoven) and G. O. R. Alberda van Ekenstein (State University Groningen) for their stimulating and useful discussions.

REFERENCES

1 Roffey, C. G. 'Photopolymerization of Surface Coatings', Wiley, New York (1982)
2 Tryson, G. R. and Schultz, A. R. *J. Polym. Sci., Polym. Phys. Edn.* 1979, **17**, 2059
3 Decker, C. and Moussa, K. *J. Appl. Polym. Sci.* 1987, **34**, 1603
4 Decker, C. and Moussa, K. *J. Polym. Sci., Polym. Chem. Edn* 1987, **25**, 739
5 Bellobono, I. R., Selli, E., Marcandalli, B. *J. Appl. Polym. Sci.* 1986, **32**, 4323
6 Furst, W. and Heusinger, H. *Angew. Makromol. Chem.* 1986, **143**, 131
7 Hoyle, Ch. and Kim, K. J. *J. Appl. Polym. Sci.* 1987, **33**, 2985
8 Hoyle, Ch. and Kim, K. J. *Polymer* 1988, **29**, 18
9 Nakanishi, F., Morishita, N. and Shoji, S. *Polym. Comm.* 1988, **29**, 52
10 Kloosterboer, J. G. *Adv. Polym. Sci.* 1988, **84**, 1–61
11 Nicolais, L., Apicella, A. and Grimaldi, P. *J. Appl. Polym. Sci.* 1987, **33**, 2077
12 Kloosterboer, J. G. V. and Lijten, G. F. C. M. *Polymer* 1987, **28**, 1149
13 Broer, D. and Mol, G. N. *ACS Polym. Mater. Sci. Eng.* 1986, **55**, 540
14 Broer, D. and Mol, G. N. 'Polymers for High Technology: Electronics and Photonics' (Eds. M. J. Bowden and S. R. Turner), American Chemical Society: Washington DC (1987), ACS Symp. Ser. No. 346, p. 417
15 Kloosterboer, J. G., v. d. Hei, G. M. M., Gossink, R. G. and Dortant, G. C. M. *Polym. Commun.* 1984, **25**, 322
16 Alberda van Ekenstein, G. O. R. and Tan, Y. Y. *Eur. Polym. J.* 1988, **24**, 1073
17 Brandrup, J. and Immergut, E. H., eds. Polymer Handbook, 2nd edn., Wiley, New York (1975)
18 Joshi, M. *J. Appl. Polym. Sci.* 1981, **26**, 3945

Self-vulcanizable and miscible ternary rubber blend system based on epoxidized natural rubber, carboxylated nitrile rubber and polychloroprene

Rosamma Alex, Prajna P. De and Sadhan K. De
Rubber Technology Centre, Indian Institute of Technology, Kharagpur 721 302, India
(Received 21 July 1989; revised 24 January 1990)

Incorporation of epoxidized natural rubber (ENR) into the immiscible blend of carboxylated nitrile rubber (XNBR) and polychloroprene rubber (Neoprene) results in a miscible ternary blend which is self-vulcanizable in the absence of any vulcanizing agent. The moulded blend registers properties similar to that of conventional rubber vulcanizates.

(Keywords: epoxidized natural rubber; carboxylated nitrile rubber; polychloroprene rubber; self-vulcanizable rubber blend; miscible rubber blend)

INTRODUCTION

Blends of carboxylated nitrile rubber (XNBR) and polychloroprene rubber (Neoprene) have been reported to be self-vulcanizable but immiscible[1]. However, epoxidized natural rubber (ENR) was found to form miscible self-vulcanizable binary blends with XNBR and with Neoprene[2,3]. Accordingly, it was thought that if ENR is blended with the XNBR–Neoprene binary system to form a ternary blend, it could result in a miscible ternary blend system which is self-crosslinkable in the absence of any vulcanizing agent. There are no published reports of self-vulcanizable and miscible ternary rubber blend systems. In the present communication, we report the results of our preliminary studies on the XNBR–ENR–Neoprene ternary blend.

EXPERIMENTAL

Neoprene AC was procured from Du Pont Limited, USA. The ENR used was ENR-50 (Malaysian Rubber Producers' Research Association, UK) with 50 mol% epoxidation. The XNBR used was Krynac-221 (Polysar Limited, Canada) containing high level of carboxylated monomer and medium high bound acrylonitrile level. Neoprene, ENR and XNBR were masticated in a 14 × 6 inch, two-roll mill for about 2 min each. Masticated samples of Neoprene and XNBR were blended in the mill for about 2 min. Masticated ENR was added to this blend and further mixed for about 4 min. A rheograph of the blend was taken at 150°C on a Monsanto Rheometer R-100. The scorch time was determined using Mooney shearing disc viscometer, model MK-III (Negretti Automation, UK) according to ASTM D1646-1963. The following physical properties of the vulcanizates were determined as per standard test methods: tensile strength (Instron 1195 universal testing machine, ASTM D 412-87 method A); tear resistance (Instron 1195 universal testing machine, ASTM D 624-86), using an unnicked 90° angle specimen (Die C); hardness (Shore A, ASTM D 2240-86); resilience (Dunlop Tripsometer BS: 903: Part A8: 1963-method A); compression set (ASTM D 395-85 method A and method B), where the samples were subjected to compressive deformation at 70°C for 22 h; heat build-up (Goodrich Flexometer, ASTM D 623-78) with a load of 10.9 kg and stroke of 4.45 mm; and abrasion res (Du Pont Abrasion Tester BS: 903: Part A9 - method C) expressed as abrasion loss, is the volume in cubic centimetres abraded f specified test specimen for 1000 revolutions o abrasive wheel. Volume fraction of the rubber i solvent swollen vulcanizate was determined by equil swelling in chloroform. The method is the same a reported by Ellis and Welding[4].

Dynamic mechanical properties were measured Toyo Baldwin Rheovibron, model DDV-III-EP strain amplitude of 0.0025 cm and frequency of 3 The procedure was to cool the sample to −100°C record the measurements during the warm up temperature rise was 1°C min^{-1}.

Differential scanning calorimeter measurements run on a Du Pont differential scanning calorim model 910 in nitrogen atmosphere. The glass trans temperature (T_g) of the samples was taken as the mid of the step in the scan, run at a heating ra 20°C min^{-1}.

RESULTS AND DISCUSSION

Formulation and processing characteristics are show *Table 1*. A rheograph of the blend is shown in Fig The increase in rheometric torque with time ind progressive crosslinking of the system. Although E Neoprene and XNBR are soluble in chloroform vulcanized blend is insoluble in chloroform; this ind that a crosslinking reaction has taken place. The vo fraction of the rubber in the swollen vulcanizate is The stress–strain curve of the blend is shown in Fig *Table 2* gives the physical properties of the blen registers poor physical properties like non-crystall rubbers.

Table 1 Formulation and processing characteristics of the blend

ENR-50
Neoprene AC
XNBR (Krynac-221)
Minimum Mooney viscosity, at 120°C
Mooney score time at 120°C (min)

0263–6476 90/090366–03

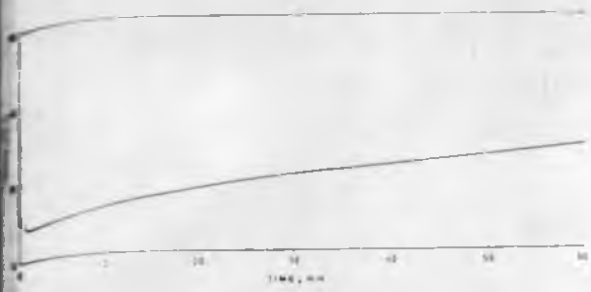

1 Rheograph of ENR–XNBR–Neoprene ternary blend at C

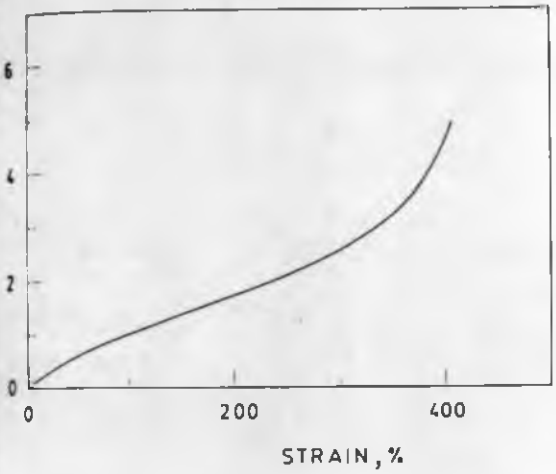

2 Stress–strain curve of ENR–XNBR–Neoprene blend

2 Physical properties of ENR–XNBR–Neoprene ternary blend moulded at 150 C for 60 min

100% modulus (MPa)	2.9
Tensile strength (MPa)	4.6
Elongation at break (%)	400
Tear strength (kN m^{-1})	16.0
Compression set at constant stress (%)	19
Compression set at constant strain (%)	27
Hardness, Shore A	55
Heat build-up (Goodrich Flexometer)	
ΔT at 50 C (C)	29
Dynamic set after 25 min (%)	2.8
Abrasion loss (cc per 1000 rev)	5
Resilience at 40 C (%)	66
Volume fraction	0.10

Differential scanning calorimeter thermograms of Neoprene, XNBR, ENR and the ternary blend are shown in *Figure 3*. The blend shows a single T_g at a temperature of $-30°C$, indicating that the polymers are miscible. The results of dynamic mechanical studies (*Figures 4, 5* and *6*) further substantiate this observation. The glass transition temperatures as determined by d.s.c. and Rheovibron studies are summarized in *Table 3*. The occurrence of a single T_g does not correspond to the coexistence of two binary XNBR–ENR and ENR–Neoprene phases because the binary phases do not have close T_g values[2,3]. Accordingly, it is believed that the three polymers in XNBR–ENR–Neoprene system form a homogeneous phase in the 100:100:100 blend composition studied.

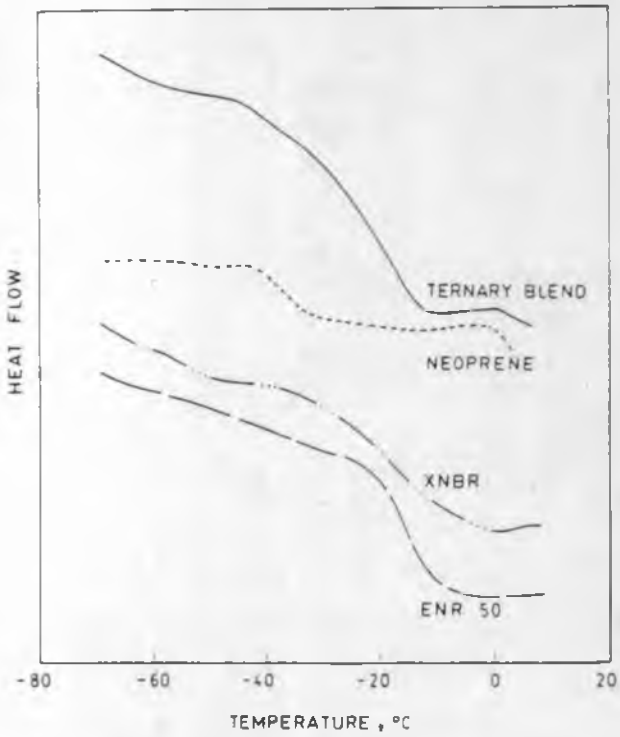

Figure 3 D.s.c. thermograms of Neoprene, ENR, XNBR and the ternary blend

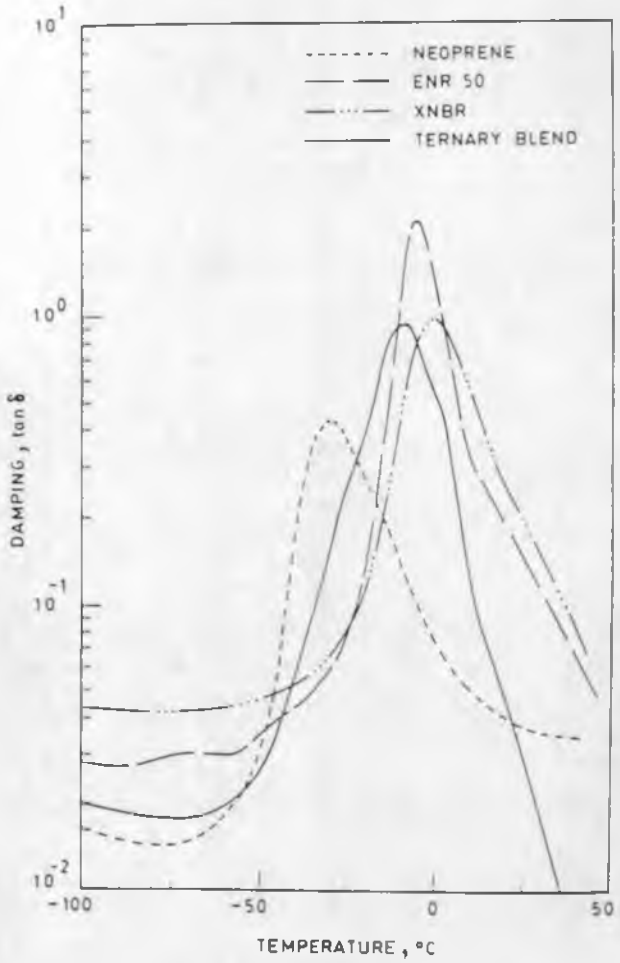

Figure 4 Damping (tan δ) plots of neoprene, ENR, XNBR and the ternary blend

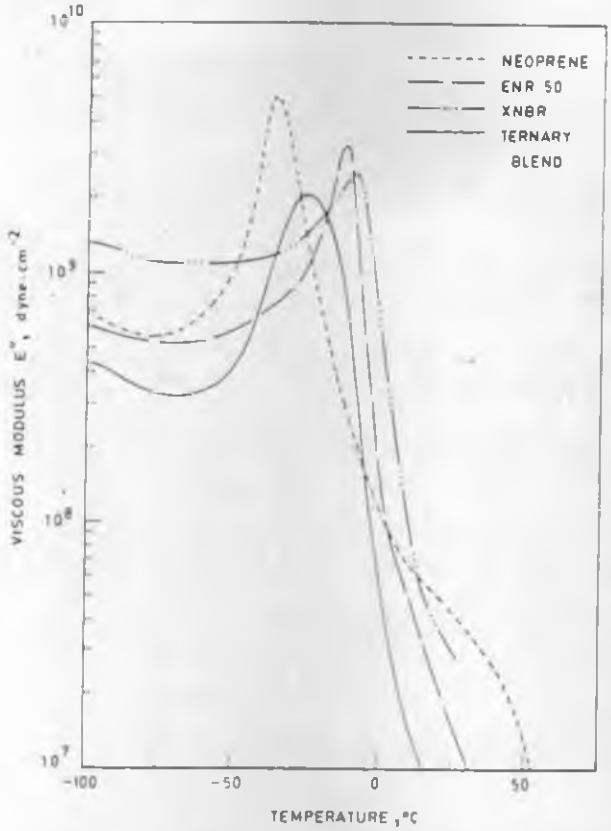

Figure 5 Loss modulus (E'') plots of Neoprene, ENR, XNBR and the ternary blend

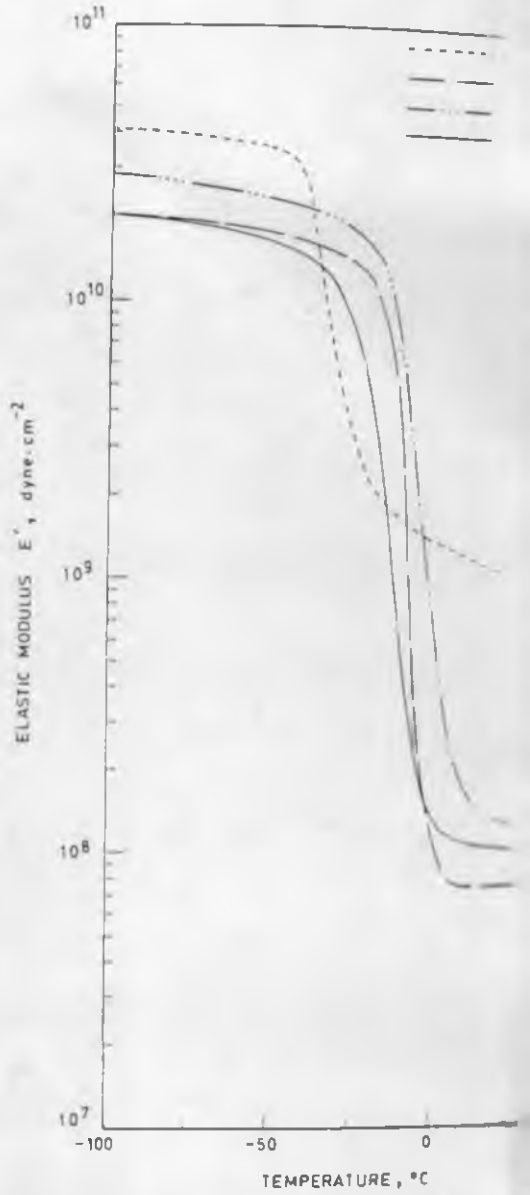

Figure 6 Elastic modulus (E') plots of Neoprene, ENR, X the ternary blend

Examination of the literature reveals recent interest in studies on the thermodynamic phase behaviour of ternary blends where two of the binary pairs, (A + B) and (A + C), are miscible, but the third binary (B + C) is not[5–9]. It is of interest to study how much of A is to be added to the immiscible blend B–C to create a miscible ternary blend A–B–C. The ternary system in the present investigation belongs to the same category. Moreover, the present system is self-crosslinkable in the absence of any vulcanizing agent. Further work on such novel ternary blends is in progress.

Table 3 Glass transition temperatures as obtained from d scanning calorimeter and Rheovibron studies

	Glass transition temperature T_g		
		Dynamic mechanical	
Sample	D.s.c.	Tan δ (max)	
XNBR	−25	0	
ENR-50	−15	−5	
Neoprene AC	−37	−29	
Ternary blend	−30	−9	

REFERENCES

1 Mukhopadhyay, Sujata and De, S. K. submitted to *J. Appl. Polym. Sci.*
2 Alex, R., De, P. P. and De, S. K. *Polym. Commun.* in press
3 Alex, R., De, P. P. and De, S. K. submitted to *J. Polym. Sci., Polym. Phys. Edn.*
4 Ellis, B. and Welding, G. N *Rubber Chem. Technol.* 1964, **37**, 571
5 Shah, V. S., Keitz, J. D., Paul, D. R. and Barlow, J. W. *J. Appl. Polym. Sci.* 1986, **32**, 3863
6 Kwei, T. K., Frisch, H. L., Radizan, W. and Vogel, S. *Macromolecules* 1977, **10**, 157
7 Wang, Y. Y. and Chen, S. A. *Polym. Eng. Sci.* 1981, **21**, 47
8 Ameduri, B. and Prudhomme, R. E. *Polymer* 1988, **29**, 1052
9 Belaribi, C., Marin, G. and Monge, Ph. *Eur. Polym. J.* 1986, **22**, 487

Filmset by Mid-County Press, London
Printed by Cambridge University Press, Ca

Thermal properties of PHP PEO blends[a]

PEO	T_g (K)	T_m (K)	ΔH_f (blend) (J g^{-1} blend)	ΔH_f (PEO) (J g^{-1} PEO)	Blend Cryst. (%)	PEO Cryst (%)
	212	338	152.6	152.6	74	74
	254	337	136.4	151.5	67	74
	240	336.5	120.4	150.5	59	73
	225	335	113.7	151.6	56	74
	238	334	81.0	124.6	40	61
	260	333	45.7	91.4	22	45
	340					
	452					

[a] example is for PEO of molecular weight 21 500

the melting point depression of PEO has not been rated out[5,10]. At most, the value of χ is small and roximates to zero around 333 K suggesting that ific interactions between the components is not ng, presumably due to poorer hydrogen bonding ability of PHP.

PHP/PVME blends. THF cast films of PHP/PVME ds were not homogeneous and brittle despite the fact the PVME did not crystallize. These films did not come transparent on heating to any temperature. The ds showed two T_gs close to those of pure PHP and PVME. It is concluded that PHP is immiscible with ME.

PHP/PCL blends. PHP/PCL blends were quite aque at room temperature and did not become clear ve the T_m of PCL. Some of the previously mentioned PEO blends exhibited haze at low temperatures, ing to PEO crystallinity, but all became fully nsparent above T_m. D.s.c. showed the existence of two It is quite evident that these blends were immiscible.

Conclusions

In summary, PHP has miscibility with PEO. mogeneous films were obtained for temperatures ween the melting temperature of the PEO in the blends the cloud point curve. The existence of a single, mposition dependent T_g reveals that the blend presents homogeneous single amorphous phase. Adding PHP PEO greatly lowers the crystallinity owing to the increasing T_g of the system. The minimum in the cloud curve for PHP/PEO systems would appear to occur around 75 wt% PHP. However, PVME and PCL do not exhibit miscibility with PHP. It has been established that PEO, PVME, and PCL are all miscible with phenoxy, phase separation of the PEO/phenoxy blends and the PCL/phenoxy blends could not be induced by heating up to 300 C[15]. Thus, it can be concluded that the hydrogen-bonding capability with proton-acceptable polymers for PHP is poorer than that for phenoxy.

References

1 Zhang, H., Chen, T. and Yuan, Y. Chinese Patent No. 85108751, 1985
2 Liu, K. and Zhang, H. Chinese Patent No. 85101721, 1985
3 Chen, T. in preparation
4 Guo, Q., Huang, J. and Chen, T. Polym. Bull. 1988, **20**, 517
5 Guo, Q., Huang, J. and Chen, T. *J. Appl. Polym. Sci.* submitted for publication
6 McMaster, L. P. *Macromolecules* 1973, **6**, 760
7 Olabisi, O. *Macromolecules* 1975, **8**, 316
8 Walsh, D. J. and Singh, V. B. *Makromol. Chem.* 1984, **185**, 1978
9 Walsh, D. J., Rostami, S. and Singh, V. B. *Makromol. Chem.* 1985, **186**, 145
10 Swinyard, B. T., Barrie, J. A. and Walsh, D. J. *Polym. Commun.* 1987, **28**, 331
11 Vdotto, G., Levy, D. L. and Kovacs, A. J. *Kolloid. Z. Z. Polym.* 1969, **230**, 289
12 Nishi, T. and Wang, T. T. *Macromolecules* 1975, **8**, 909
13 Imken, R. L., Paul, D. R. and Barlow, J. W. *Polym. Eng. Sci.* 1976, **16**, 593
14 Guo, Q., Xu, H., Ma, D. and Wang, S. *Eur. Polym. J.* in press
15 Robeson, L. M., Hale, W. F. and Merriam, C. N. *Macromolecules* 1981, **14**, 1644

polymer reports

Epoxidized natural rubber–carboxylated nitrile rubber blend: a self-vulcanizable miscible blend system

R. Alex, P. P. De and S. K. De*
Rubber Technology Centre, Indian Institute of Technology, Kharagpur 721302, India
(Received 24 February 1989; revised 24 June 1989)

Epoxidized natural rubber and carboxylated nitrile rubber can be blended and vulcanized during moulding without addition of any curative. Such a blend system of self-vulcanizable rubber is completely miscible as is evident from differential scanning calorimetry and dynamic mechanical studies. Physical properties of the blends are comparable to those of conventional rubber vulcanizates. The blends are reinforced on addition of reinforcing carbon black filler.

(Keywords: epoxidized natural rubber; carboxylated nitrile rubber; self-vulcanizable rubber blend; miscible rubber blend)

INTRODUCTION

It has been reported earlier that carboxylated nitrile rubber (XNBR) is vulcanizable by epoxy resin[1] and epoxidized natural rubber (ENR) can be vulcanized by dibasic acids[2]. Accordingly the blend of carboxylated nitrile rubber and epoxidized natural rubber was studied to examine the vulcanizing ability of one rubber by the functional group of another rubber. In the present communication we report the results of our studies on XNBR–ENR blend. We designate such a system as a self-vulcanizable rubber blend. No curative was used.

EXPERIMENTAL

XNBR used was Krynac-221 (Polysar Limited, Ontario, Canada), containing high level of carboxylated monomer and medium high bound acrylonitrile level. ENR used was ENR-50 (Malaysian Rubber Producers' Research Association, UK), with 50 mol% epoxidation. Both ENR and XNBR were first masticated in the 14 × 6 in 2-roll mixing mill for 6 min each. Masticated samples were blended on the mill for a further period of 10 min. Rheographs were taken at 140°C on a Monsanto Rheometer R-100. The blends were vulcanized during moulding for 45 min at 140°C. The following physical properties of the vulcanizates were determined according to standard methods: stress–strain (Zwick UTM, ASTM D412-87); tear (Zwick UTM, ASTM D624-86); hardness (Shore A, ASTM D2240-86); resilience (Dunlop tripsometer, BS 903: Part A8: 1963, method A); compression set (ASTM D395-85, method A and method B); heat build-up (Goodrich flexometer, ASTM D623-78); abrasion resistance (Cryodon-Akron Dupont abrader, BS 903: Part A9: 1957, method C). For swelling studies the vulcanizates were swollen in chloroform for 48 h and the percent increase in weight due to solvent swelling was noted.

Dynamic mechanical properties (damping) were measured using a Rheovibron model DDV III-EP at a strain amplitude of 0.0025 cm and a frequency of 3.5 Hz. The procedure was to cool the sample to −100°C record the measurements during the warm up. temperature rise was 1°C min^{-1}.

D.s.c. measurements were run on a Dupont differe scanning calorimeter model 910 in nitrogen atmosph Glass–rubber transition temperatures (T_gs) of the sam were taken as the midpoint of the step in the scan, at a heating rate of 10°C min^{-1}.

RESULTS AND DISCUSSION

Formulation of the two blends and the phys properties of the moulded blends are shown in *Table* Blend A contains XNBR:ENR in the ratio 100:50. Bl A_c is similar to blend A, but contains 45 parts by wei of ISAF carbon black.

Rheographs of the two blends at 140°C are shown *Figure 1*. Increase in rheometer torque with vulcanizati time indicates progressive crosslinking of the system. we shall discuss later, one blend constituent p vulcanized at 140°C by the other component. The hig

Table 1 Composition and properties of ENR–XNBR blend mixt at 140°C for 45 min

	Blend designati	
	A	A_c
Composition (parts by weight)		
ENR	50	50
XNBR	100	100
ISAF carbon black	–	45
Properties		
100% modulus (MPa)	1.02	[illegible]
Tensile strength (MPa)	3.70	30
Elongation at break (%)	396	530
Tear strength (kN m^{-1})	14.40	30
Compression set at constant stress (%)	11	14
Compression set at constant strain (%)	20	32
Heat build up (ΔT) at 50°C (°C)	24	40
Resilience (%)	62	47
Hardness (Shore A)	43	55
Swelling in chloroform (percent increase in weight)	672	517

* To whom correspondence should be addressed

0263–6476/90/030118–03

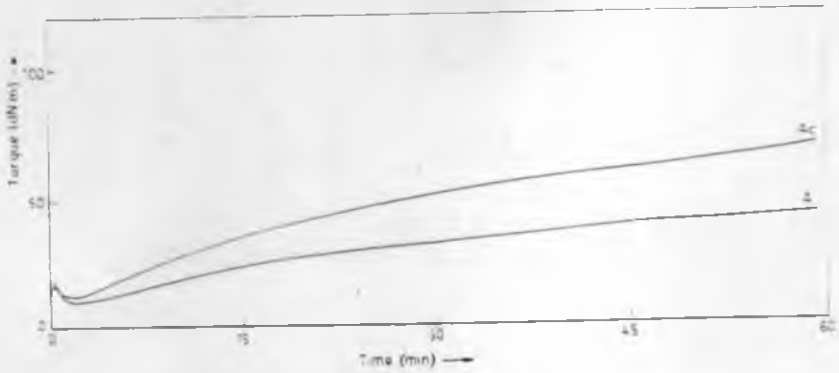

Figure 1 Rheographs of blends A and A_c at 140 C

Table 2 Effect of moulding vulcanization time on physical properties of black-filled XNBR–ENR blend (A_c)

Physical property	Moulding vulcanizing time (min)		
	30	45[a]	90
Modulus at 100% strain (MPa)	1.15	1.57	3.57
Tensile strength (MPa)	20.17	20.56	19.28
Elongation at break (%)	737	538	374
Tear resistance (kN m^{-1})	41.75	38.00	33.02
Heat build-up at 50 C (ΔT) (°C)	44	40	30
Permanent set (%)	9.3	3.6	0.76
Resilience (%)	44	47	48
Swelling in chloroform (percent increase in weight)	652	517	426

[a] Values also reported in *Table 1*

Torque value in the case of blend A_c is similar to that of a conventional rubber system in the sense that reinforcing carbon black increases the torque value due to high polymer–filler interaction. Results of physical properties and swelling studies, as discussed later in the paper, further substantiate these findings. Marching increase in modulus with cure time as shown in the rheographs implies that the cure reversion is absent and the vulcanizate network is thermally stable.

Physical properties of the blend vulcanizate, as summarized in *Table 1*, shows that gum blend vulcanizate shows poor physical properties. However, addition of reinforcing carbon black filler increases the tensile strength more than 5 times, tear resistance more than 3 times and abrasion resistance about 4 times. As expected, addition of reinforcing carbon black increases modulus and hardness and causes reduction in resilience. High hysteresis of the filled system causes an increase in heat build-up and compression set. Reduction in percent swelling in solvent (chloroform), from 872% for the gum system to 527% for the filled system, shows increased restriction to solvent swelling due to polymer–filler interaction.

The degree of crosslinking can be changed by varying the curing or moulding time. *Table 2* shows that with increase of cure time, percent swelling decreases due to increase in crosslink density, which causes formation of a tighter network resulting in low dynamic set, low heat build-up in Goodrich flexometer test, lower elongation at break, higher modulus and higher resilience. However, tensile strength was not greatly affected. Tear strength decreased at higher curing time. It has been reported that undercuring results in higher tear resistance[3].

D.s.c. thermograms of ENR, XNBR and blends of ENR and XNBR are shown in *Figure 2*. Glass transition temperatures of the systems are summarized in *Table 3*. The T_gs of ENR and XNBR were detected at −14.5 and −25 C and the blends A and A_c showed T_g values at −19 C. The occurrence of single T_g in the blend and the transparent nature of the gum blend indicate complete miscibility of ENR and XNBR. This is also evident from the dynamic mechanical analysis. *Figure 3* shows the plot of damping (tan δ) at different temperatures. Both single

Table 3 Glass transition temperatures (T_gs) as obtained from differential scanning calorimetry studies

Rubber blend	T_g (°C)
XNBR	−25
ENR	−15
Blend A	−19
Blend A_c	−19

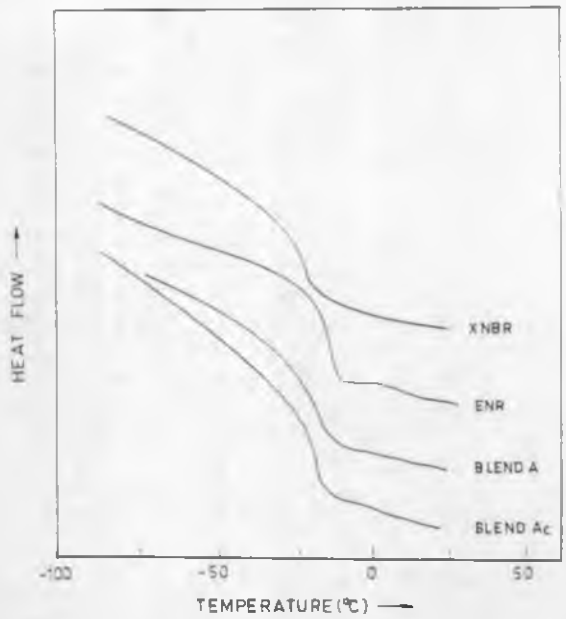

Figure 2 D.s.c. thermograms of XNBR, ENR and XNBR–ENR blends (A and A_c)

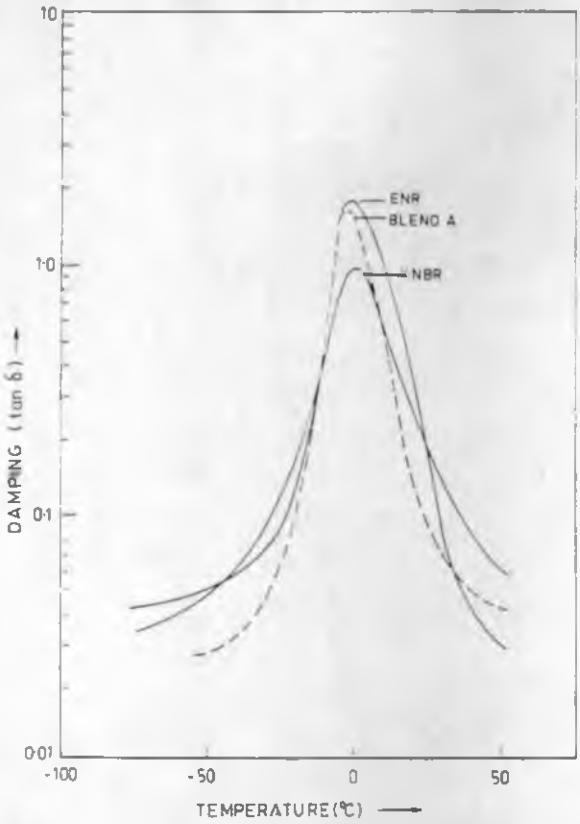

Figure 3 Damping (tan δ) plots for XNBR, ENR and ENR–XNBR blend

components and the blend A register maxima in the tan δ value almost at the same temperature varying between -1 and -2.5 C. However, the damping peak of the blend occurred in between the individual components and the peak width or broadening is smaller in the case of the blend as compared to XNBR and ENR. This indicates that blends of XNBR and ENR form a miscible system.

The present investigation shows that carboxylated nitrile rubber and epoxidized natural rubber form a miscible blend system which is self-vulcanizable in the absence of curatives and the black-filled system exhibits reinforcement similar to conventional rubbers. During vulcanization, carboxyl groups of XNBR react with epoxy groups of ENR to form ester crosslinks.

ACKNOWLEDGEMENT

Thanks are due to Sri K. L. Saha, R. Banerjee and [illegible] Mitra for assistance in experimental work.

REFERENCES

1 Chakraborty, S. K. and De, S. K. *J. Appl. Polym. Sci.* 1982, [illegible]
2 Tiek, L. C. in 'Proceedings of the International Rubber Conference 1985, Kuala Lumpur', International Rubber Conference Committee 1985, p. 1
3 Coran, A. Y. in 'Science and Technology of Rubber' (Ed. F. R. Eirich), Academic Press, New York (1978), p. 291

Filmset by Mid-County Press, London SW[illegible]
Printed by Cambridge University Press, Cambridge

Reprint from Kautschuk + Gummi · Kunststoffe, Vol. 43, (1990), No. 11, pages 1002–1005, Dr. Alfred Hüthig Verlag, Heidelberg

Characterization of Self-Vulcanizable Blends of Epoxidized Natural Rubber and Carboxylated Nitrile Rubber by Monsanto Rheometry, Differential Scanning Calorimetry, Thermogravimetry, Infrared Spectrophotometry and Swelling

R. Alex and P. P. De, Kharagpur (India)

Still mixed blends of epoxidized NR (with 50 mol % epoxidation) and carboxylated nitrile rubber undergo self-vulcanization during moulding at elevated temperature (150 °C) in absence of any vulcanizing agent. The self-vulcanization characteristics are evident from studies on Monsanto rheometer, infrared spectrophotometer, differential scanning calorimeter, thermogravimetric analyses and solvent swelling. The extent of vulcanization depends on blend ratio, the maximum occurring at 50:50 blend. Both processing behaviour and physical properties are found to depend on blend composition.

Charakterisierung selbstvulkanisierbarer Verschnitte aus epoxidiertem Naturkautschuk mit carboxyliertem Nitrilkautschuk durch Monsanto-Rheometrie, dynamische Differenzkalorimetrie, Thermogravimetrie, Infrarotspektrometrie und Quellungsmessungen

Auf der Walze hergestellte Verschnitte aus epoxidiertem NR (zu 50 % epoxidiert) und carboxyliertem Nitrilkautschuk erfahren während der Formgebung bei höheren Temperaturen (150 °C) eine Selbstvulkanisation ohne jegliches Vulkanisationsmittel. Die Selbstvulkanisation gibt sich in ihrer Charakteristik in Untersuchungen mit dem Monsanto-Rheometer, dem Infrarotspektrometer, dem dynamischen Differenzkalorimeter, dem Thermogravimeter sowie durch Quellungsmessungen in Lösungsmitteln zu erkennen. Das Ausmaß der Vulkanisation wird durch das Verschnittverhältnis bestimmt und erreicht bei einem Verhältnis 1:1 sein Maximum. Das Verarbeitungsverhalten und ebenso die physikalischen Endeigenschaften hängen von der Zusammensetzung des Verschnittes ab.

1 Introduction

Recent publications [1 – 5] report self-vulcanizable rubber blends which get crosslinked at high temperatures by the functional groups of two rubbers without any curatives. In this self-vulcanizable blend of epoxidized NR (ENR) and carboxylated nitrile rubber (XNBR), it is observed that crosslinking depends on the time and temperature of moulding, and that fillers enhance the gum strength of the blend [6]. In this communication, we report the results of our studies on characterization of the self-vulcanizable blend of ENR und XNBR by Monsanto rheometry, differential scanning calorimetry, thermogravimetry, infrared spectrophotometry and solvent swelling with respect to blend ratio variation.

2 Experimental

ENR (with 50 mol % epoxidation) was obtained from Malaysian Rubber Producers' Research Association, UK. XNBR, Krynac-221, containing high level of carboxylated monomer and medium high bound acrylonitrile level was obtained from Polysar Limited, Canada.

The formulations of the blends are given in *Table 1*. Both ENR and XNBR were separately masticated for about 1 min on a 14" x 6" two roll mixing mill. The masticated samples of the two rubbers were blended together for a period of about 6 min. Cold water was circulated through the rolls to keep the temperature low in order to avoid sticking of the rubber on the rolls. The mill temperature for the initial mastication was 25 °C. The temperature rise during the mixing of gum rubbers was only 2 °C.

Table 1. **Formulation of the mixes**

Blend	EXa	EXb	EXc
ENR	75	50	25
XNBR(Krynac-221)[a]	25	50	75

[a]High level of carboxylated monomer and medium high bound acrylonitrile content

Rheographs of the mixes were taken on Monsanto rheometer R-100 at 150 and 180 °C. Scorch time and Mooney viscosity at 120 °C were determined by using Mooney viscometer MK-III (Negretti Automation Ltd., UK) according to ISO 667. The properties determined as per standard test methods were tensile strength (ISO 37), using dumb-bell specimens by Instron 1195 universal testing machine; tear resistance (ASTM D624-84), using an unnicked 90° angle specimen (die C) by same Instron machine; hardness, Shore A (ISO 7619) and resilience (BS:903:Part A 8:1963, method A) by Dunlop tripsometer. Samples for compression set (ISO 815) were cylindrical discs (29 mm dia and 13 mm thickness) and subjected to compressive deformation at constant strain for 22 h at 70 °C. While determining heat build-up according to ASTM (D623-75) by a Goodrich flexometer, the samples were subjected to cyclic deformation for 25 min with a load of 10,9 kg (24 lb) and a stroke of 4,5 mm. Abrasion resistance (BS:903:Part A 9, method A-1957) was determined by using a DuPont abrader, by calculating the volume loss in cm^3 from a specified test specimen for 1000 revolutions of the abrasive wheel.

DSC measurements and thermogravimetric analysis (TGA) were run on a DuPont differential scanning calorimeter, model 910, and DuPont thermal analyser model 900 in nitrogen atmosphere at a heating rate of 10 °C/min.

IR spectra were recorded by 843 Perkin Elmer spectrophotometer. The thin films of ENR and XNBR were prepared by pressing the neat samples between aluminium foils for 2 min with a pressure of 50 kg/cm^2 at 100 °C, using a Labo press. Thin films of blends were prepared in a similar way, by moulding for 60 min at 150 °C.

Volume fraction of the rubber (V_r) in the solvent swollen vulcanizate was determined by equilibrium swelling in chloroform. The method is the same as that reported by *Ellis* and *Welding* [7].

$$V_r = \frac{(D\text{-}FT/\varrho_r)}{[(D\text{-}FT/\varrho_r) + (A_o/\varrho_s)]}$$

where T is the weight of the specimen, D is its deswollen weight, F is the weight fraction of insoluble components, A_o is the weight of absorbed solvent corrected for swelling increment and ϱ_r and ϱ_s are the densities of the rubber and solvent respectively.

3 Results and discussion

3.1 Mooney viscosity

The cure characteristics of the blends are shown in *Table 2*. In all the three blends of ENR and XNBR, increase in XNBR content in the blend increases the minimum Mooney viscosity and decreases the scorch time. As oxirane rings open readily in presence of acids [8, 9] the reactions involving carboxyl groups are reported to start earlier and such mixes become very scorchy [10]. Due to the early onset of reaction, with increase in XNBR content in the blends, the scorch times decreases.

Table 2. **Cure characteristics of the blends obtained from Mooney viscometer and Monsanto rheometer studies**

	EXa	EXb	EXc
Mooney viscometry			
Minimum Mooney viscosity at 120 °C	23	35	45
Mooney scorch time at 120 °C, min	14.5	7.0	5.7
Monsanto rheometry			
Minimum torque at 150 °C, dN · m	5	6	8
Maximum torque at 150 °C, dN · m (in 60 min)	13	36	36
Minimum torque at 180 °C, dN · m	4	5	6
Maximum torque at 180 °C, dN · m (in 60 min)	[illegible]	[illegible]	[illegible]

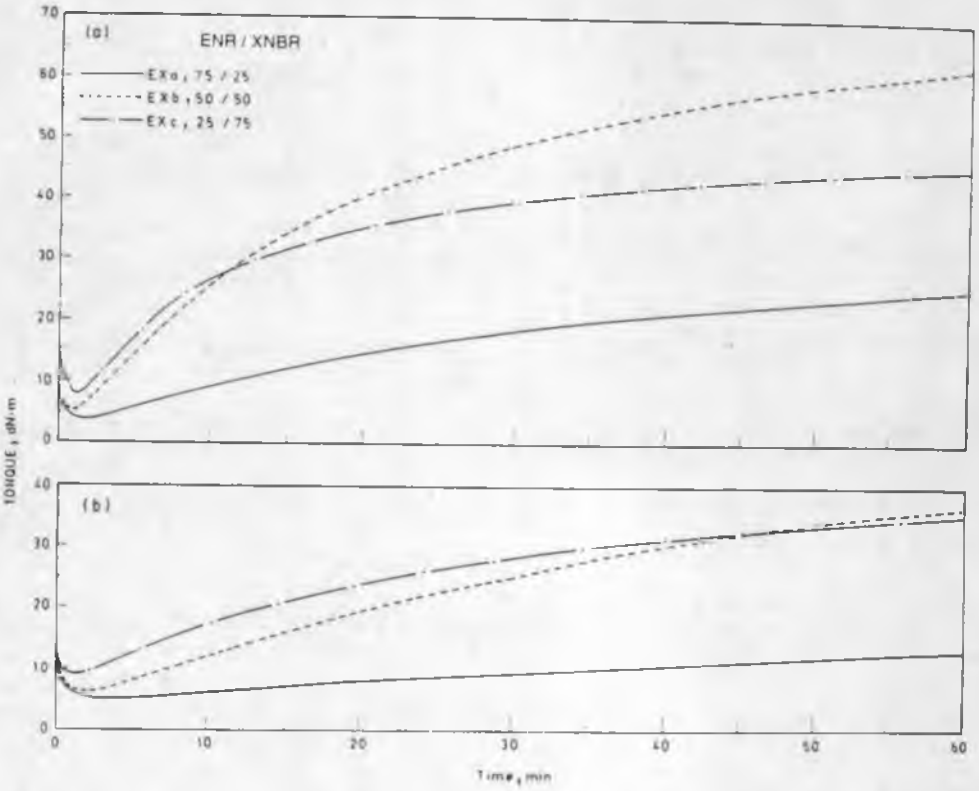

Figure 1. Rheographs of blends of EXa and XNBR – (a) at 180 °C, (b) at 150 °C

3.2 Monsanto rheometry

The Monsanto rheographs of the blend are shown in *Figure 1*. The blends show marching increase in rheometric torque both at 150 and 180 °C. Blend EXa (ENR/XNBR in the ratio 75/25) shows comparatively low crosslinking at both temperatures. Blend EXb (50:50 blend of ENR/XNBR) shows maximum rise in torque both at 150 and 180 °C.

In EXa, the concentration of carboxyl groups may not be sufficient to cause enough crosslinking and as the XNBR content increases the availability of carboxyl groups increases resulting in higher extent of crosslinking as in EXb. In EXc, however, the concentration of epoxide groups available for crosslinking is less. Epoxidation is a random process [11, 12] and *Davey* et al. [8] have shown that when a reaction between an acid and epoxy group is initiated at one epoxide group of a block, the remaining epoxide groups undergo furanization and are destroyed before other reactions can occur. In EXc, even though there may be sufficient epoxide groups, the number of epoxide groups available for reaction is likely to be less due to furanization or follow-up reactions. Due to the nonavailability of epoxide groups, crosslinking in EXc reaches a state of completion.

3.3 DSC and TGA

Figure 2 illustrates the DSC profiles for cure of blends of ENR and XNBR and also control single ENR and XNBR. It is evident that there is no change in enthalpy in the temperature range from 170 to 300 °C for the two neat polymers, while blends register an exothermic enthalpy [13] due to self-vulcanization. TGA plots (*Figure 3*) indicate that the thermal degradation of neat polymers and the blend occur at sufficiently high temperatures, above 300 °C, resulting in main chain scission and loss of volatile fragments. The magnitude of exothermic enthalpy was calculated using the equation [14].

$$E = \frac{Hv \cdot m}{60\,A \cdot B \cdot \Delta qs}$$

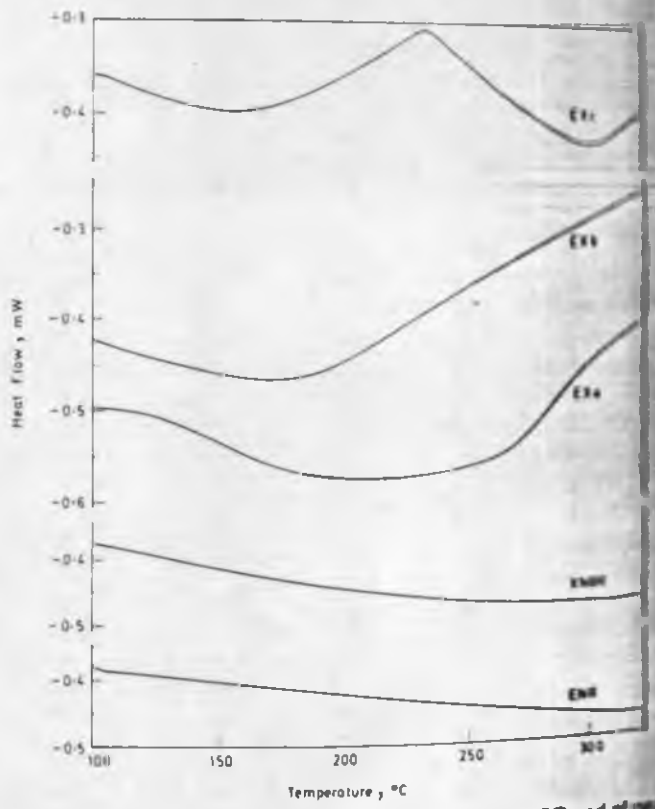

Figure 2. DSC profiles for cure of blends of ENR and XNBR and of neat ENR and XNBR

where, Hv = enthalpy change in J/g
m = mass of the sample in mg
A = exothermic peak area in cm^2
B = time base scaling in min/cm
Δqs = y axis scaling in mW/cm
E = 1, calibration coefficient

The enthalpy changes occurring during crosslinking between ENR and XNBR are shown in *Table 3*. The enthalpy change is maximum in the 50/50 blend of ENR and XNBR. In EXa, where

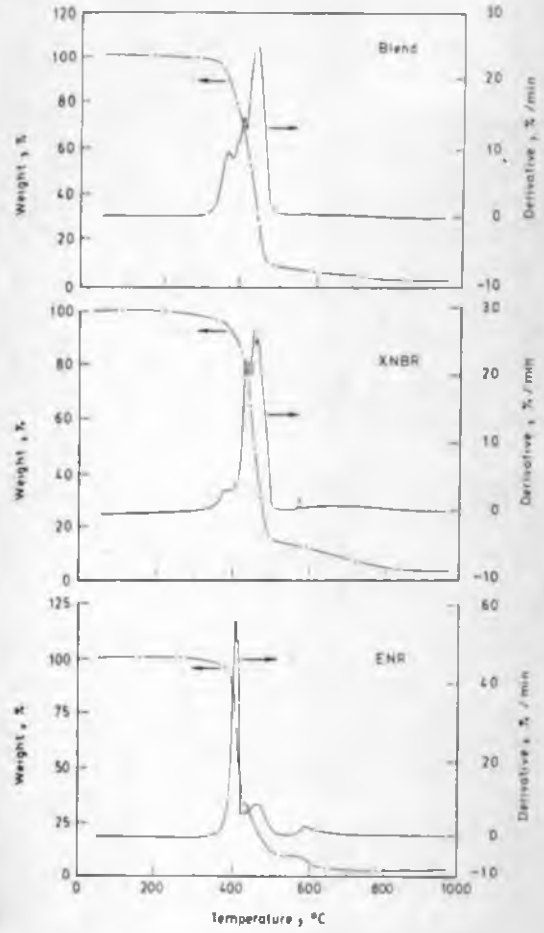

ure 3. TG curves of neat ENR, XNBR and 50:50 ENR-XNBR blend

ble 3. Cure characteristics of the blends obtained from thermal analysis

ple	Cure initiation temperature °C	Cure termination temperature °C	Degradation temperature, °C[b]	Hv, J/g
	213	[a]	300	3,25
	186	[a]	300	13,75
	171	300	300	12,18

[a] Cure termination overlapped by degradation of polymer
[b] Obtained from thermogravimetric analyses

e state of cure is low, cure initiation starts at a higher tempera-re. As the XNBR content in the blend increases the cure initia-n starts at lower temperatures. This is in agreement with the ooney scorch times of the blend. The plot of Mooney scorch es versus cure initiation temperature (obtained from DSC dies) as shown in *Figure 4* reveals that as the ENR content in

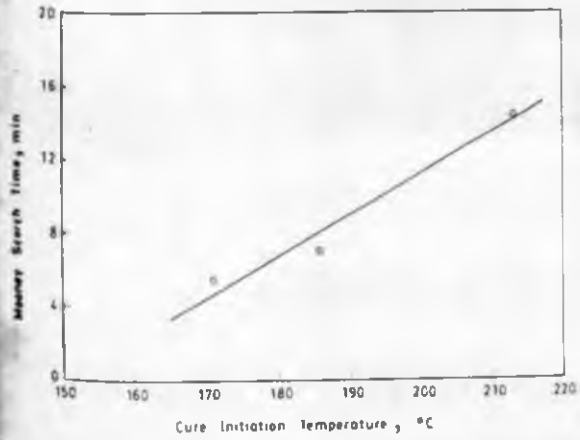

ure 4. Plot of Mooney scorch time versus cure initiation temperature ained from DSC thermograms

the blend increases both cure initiation temperature and scorch time increase. The vulcanization reaction as observed from the exotherms, show completion only when XNBR content in ENR/XNBR blend is high as in EXc. At a lower XNBR content as in EXa and EXb, the crosslinking proceeds till degradation and crosslinking reaction is overlapped by degradation reaction.

3.4 Infrared spectrophotometry (IR)

The IR spectra of the three blends, and that of neat ENR and XNBR are shown in *Figures 5 A and B* (see next page). The epoxide group shows a characteristic band at 870 cm^{-1} due to ring vibration, together with absorption at 1240 cm^{-1} due to C-O stretching. The cis 1,4 double bond (C = C cis) stretching absorption is at 840 cm^{-1}. The carboxyl group of XNBR shows absorption due to C = O stretching at 1696 cm^{-1}.

In all the three blends of ENR and XNBR, there is a strong absorption peak at 1660 cm^{-1}, which is absent in both neat ENR and neat XNBR.

Esters absorb strongly in the region 1725 to 1720 cm^{-1}, and this absorption is reported to be shifted to a lower frequency around 1650 cm^{-1}, when C = O group of ester is hydrogen bonded [15]. The absorption peak in the blend at 1660 cm^{-1} shows that during vulcanization epoxy group of ENR and carboxyl group of XNBR react to form ester linkages and that the C = O of ester is hydrogen bonded with adjacent – OH group [4].

In EXa, since epoxy groups are large in number in addition to the ester groups, the characteristic peak due to epoxy groups are retained and the absorption in the range of 1680 to 1750 cm^{-1} (due to C = O group of acids) is greatly reduced. In EXc, there is strong absorption due to carboxyl group in the range of 1680 to 1750 cm^{-1} (as in neat XNBR) showing that there are unreacted carboxyl groups. Compared to EXa and EXc, in EXb the absorption due to epoxy group and C = O of acids is greatly reduced. These results are in agreement with the results of Monsanto rheometry and DSC.

3.5 Solvent swelling

Both ENR and XNBR were found to be soluble in chloroform while the vulcanized blends were insoluble in the same solvent, showing that during vulcanization ENR and XNBR get crosslinked. The volume fraction of rubber in the swollen vulancizate calculated from equilibrium swelling data shown in *Table 4* (see next page) reveals that in EXa degree of crosslinking is less than that in EXb and EXc.

3.6 Physical properties

The physical properties of blends of ENR and XNBR are summarised in Table 4. As the XNBR content increases, tensile strength, modulus, tear strength and abrasion resistance increase whereas elongation at break decreases. This is also evident from the stress-strain curve (*Figure 6*) (see next page). This change in properties can be attributed to the high XNBR content in the blend, as XNBR mixes are reported to have very good gum strength. However, in the 50/50 blend (EXb) the Goodrich heat build-up is lower and resilience is higher than EXc.

4 Conclusions

Mill mixed blend of ENR and XNBR forms a self-vulcanizable rubber blend system. The processing characteristics and technical properties depend on the blend composition. During moulding at high temperature epoxy group of ENR and carboxyl

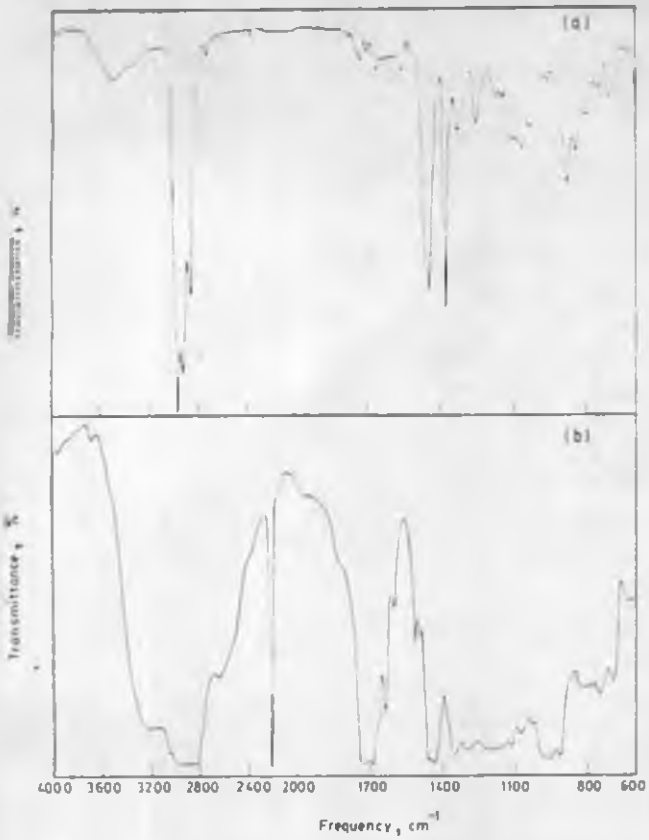

Figure 5 (A). Infrared spectra of thin films of (a) ENR and (b) XNBR

Table 4 **Physical properties of the blends**

	EXa	EXb	EXc
Modulus 300 %, MPa	1.9	3.2	–
Tensile strength, MPa	2.2	3.2	3.6
Elongation at break, %	380	300	220
Tear strength, kN/m	11.0	12.6	16.8
Hardness, Shore A	30	47	50
Resilience at 40 °C, %	55	69	58
Compression set for 22 h at 70 °C, %	27	12	12
Abrasion loss, cm³ / 1000 rev.	–	1.97	0.80
Heat build-up by Goodrich Flexometer with a load of 10.9 kg (24 lb) and stroke of 4.5 min			
ΔT, °C	[a]	17	30[b]
V,	0.07	0.12	0.12

[a]Sample blown out before 20 min
[b]Value after 20 min

group of XNBR react to form ester linkages. There is thermal stability, when the ENR content in the blend is high till 50/50 ratio and when the ENR content is lower as in 25/75 ratio of ENR/XNBR the crosslinking reaction reaches a state of completion.

References

[1] S. Mukhopadhyay, T. K. Chaki and S. K. De, J. Polym. Sci., Polym. Lett. **28** (1990) 25.
[2] S. Mukhopadhyay, P. P. De and S. K. De, J. Appl. Polym. Sci. (communicated).
[3] S. Mukhopadhyay and S. K. De, J. Mat. Sci. (in press).
[4] R. Alex, P. P. De and S. K. De, J. Polym. Sci., Polym. Lett. **27** (1989) 361.
[5] P. Ramesh and S. K. De, Polym. Commun. (in press).
[6] R. Alex, P. P. De and N.M. Mathew and S. K. De, Plast. Rubber Proc. Appl. (in press).
[7] B. Ellis and G. N. Welding, Rubber Chem. Technol. **37** (1964) 571.
[8] John E. Davey and M. John R. Loadman, Polymer **16** (1984) 134.
[9] S. C. Ng and L. H. Gan, Eur. Polym. J. **17** (1981) 1073.
[10] S. K. Chakroborty, A. K. Bhowmick and S. K. De, J. Appl. Polym. Sci. **26** (1981) 4011.

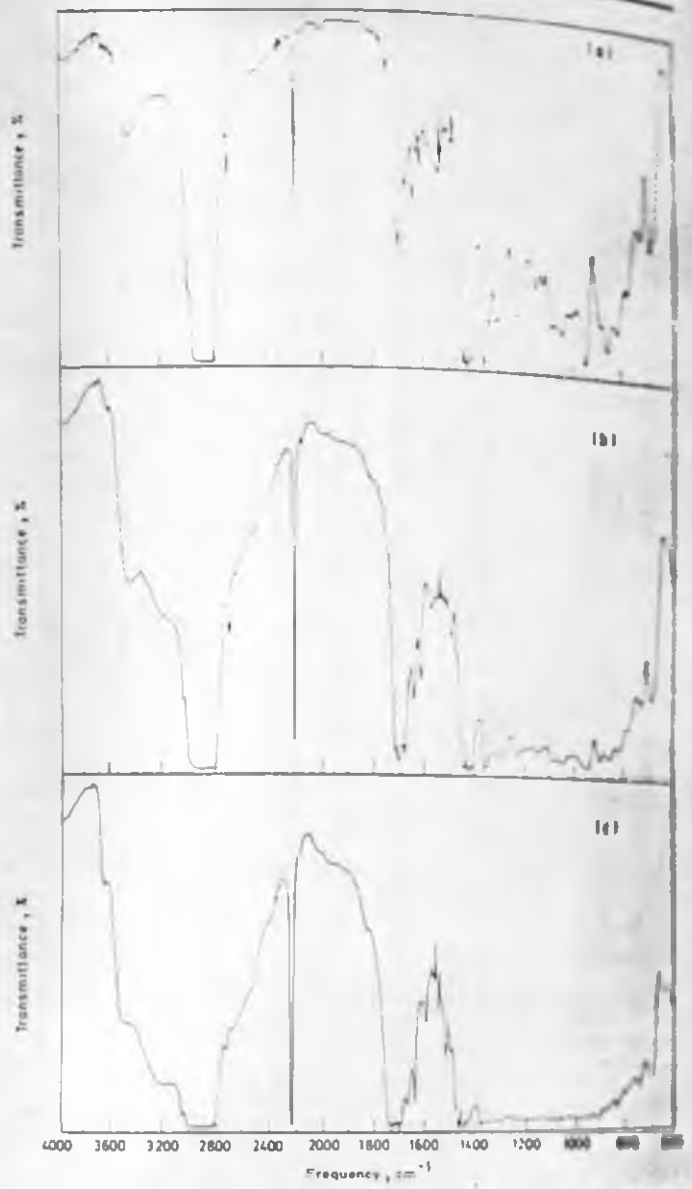

Figure 5 (B). Infrared spectra of thin films of blends of ENR and XNBR – (a) EXa; (b) EXb; and (c) EXc

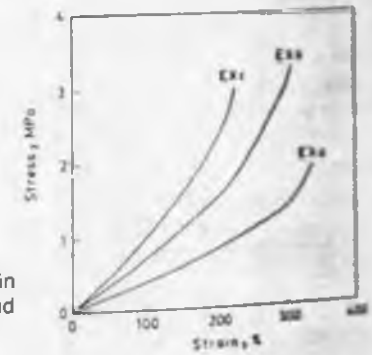

Figure 6. Tensile stress-strain curves of blends of ENR and XNBR

[11] J. H. Bradbury and M. C. S. Perera, J. Appl. Polym. Sci. **30** (1985) 3347.
[12] D. R. Burfield, K. L. Kim and K. S. Law, J. Appl. Polym. Sci. **29** (1984) 1661.
[13] D. W. Brazier, Rubber Chem. Technol. **53** (1980) 437.
[14] 910 Differential Scanning Calorimeter. DuPont Company, Operator's Manual, January, 1985, p. 71.
[15] G. Socrates: In: "Infrared Characteristic Group Frequencies". The Pitman Press, Bath, John Wiley & Sons Ltd., New York, Chap. 10, p. 69.

Dr. R. Alex is research scholar and Dr. (Mrs.) Prajna P. De is lecturer in the Rubber Technology Centre of the Indian Institute of Technology (ITT).

Reprint from Kautschuk + Gummi · Kunststoffe, Vol. 44, (1991), No. 4, pages 333–335, Dr. Alfred Hüthig Verlag, Heidelberg

Self-Vulcanisable Rubber-Rubber Blends Based on Epoxidised Natural Rubber and Polychloroprene

R. Alex, P. P. De and S. K. De, Kharagpur (India)

[illegible] mixed blends of polychloroprene (Neoprene AC) and epoxidised NR (ENR) have been found to be self-vulcanisable in the absence of any vulcanising agent. This is found to be a partially miscible system. Crosslink density and physical properties of the system depend on the blend ratio.

Selbstvulkanisierbare Kautschuk/Kautschuk-Verschnitte auf Basis von epoxidiertem Naturkautschuk und Polychloropren

[illegible] der Walze hergestellte Verschnitte aus epoxidiertem NR (ENR) und Polychloropren (CR) (Neoprene AC) zeigten in Abwesenheit jeglichen Vulkanisationsmittels die Fähigkeit zur Selbstvulkanisation. Es wurde festgestellt, daß es sich um ein teilweise mischbares System handelt. Die Netzwerkdichte und die physikalischen Eigenschaften sind vom Verschnittverhältnis abhängig.

1 Introduction

[illegible] and co-workers have developed self-vulcanisable blends based on rubbers with reactive groups. Examples are blends based on Hypalon (CSM)-epoxidised NR (ENR) [1, 2], CSM-carboxylated nitrile rubber (XNBR) [3], XNBR-ENR [4, 5] and polychloroprene (CR)-XNBR [6]. These rubbers get crosslinked during moulding in the absence of any vulcanising agent and can be reinforced with fillers like carbon black and silica. While making further investigations on blends based on ENR, we observed that CR (Neoprene AC)-ENR system gets vulcanised during moulding in the absence of any crosslinking agent. Saharov and *Mairov* have reported that Neoprene can be vulcanised by epoxy resin [7].

In the present communication we report the results of our preliminary studies on self-vulcanisable Neoprene AC-ENR blends. According to preliminary studies other forms of CR also undergo similar reaction like Neoprene AC grade. But we have not studied details. This paper therefore deals with only Neoprene AC type.

2 Experimental

[illegible] polychloroprene type Neoprene AC was procured from Du Pont, U.S.A. ENR used was ENR-50 with 50 mol% epoxidation, obtained from Malaysian Rubber Producers' Research Association (MRPRA), [illegible]. The Mooney viscosities of the samples ML (1 + 4) at 120 °C were [illegible] for Neoprene AC and 46 for ENR-50. The formulation of the blends [illegible] given in *Table 1*. Both CR and ENR-50 were mastificated on a 14×6 in [illegible] roll mixing mill to the same Mooney viscosity and were blended on [illegible] mill for about 6 min. Minimum Mooney viscosity and scorch time [illegible] determined as per ASTM D 1646-1963 by using Negretti automatic Mooney shearing disc viscometer model MK III. Rheographs of the [illegible] were taken at 180 °C on a Monsanto rheometer R-100. The [illegible] were cured at 180 °C for 60 min. The following physical properties of the vulcanisates were determined according to standard test methods: Tensile strength (Instron 1195 universal testing machine [illegible] D 412-75 method A), tear strength (Instron 1195 universal testing [illegible] ASTM D 624-65) using an unnicked 90° angle specimen (Die [illegible]), Shore A hardness (ASTM D 2240-68), resilience (Dunlop tripsometer [illegible] 903 Part A 8 1963 method A), compression set (ASTM D 395-61 [illegible] B) where the specimens were subjected to 25% compressive deformation at 70 °C for 22 h, heat build up (Goodrich flexometer ASTM D 623-83) with a load of 24 lb and stroke of 4.87 in [illegible] ambient temperature of 50 °C, abrasion resistance (expressed as abrasion loss which is the volume in cm³ abraded from a specified test specimen in 1000 revolutions of the abrasive wheel (Du Pont abrasion tester BS 903 Part A 9 – 1957 method A).

Dynamic Mechanical Analysis (DMA) was done by Toyo Baldwin Rheovibron model DDV III EP at a strain amplitude of 0.0025 cm and frequency of 3.5 Hz. The procedure was to cool the sample to [illegible] and to record the measurements during the warm up. The temperature rise was 1 °C/min.

Differential Scanning Calorimeter (DSC) studies were done on a Du Pont thermal analyser model 910 in nitrogen atmosphere. Glass transition temperature (T_g) of the sample was taken as the midpoint of the step in the scan run at a heating rate of 20 °C/min.

The volume fraction of rubber (V_r) in solvent swollen blend was calculated from equilibrium swelling data by the method reported by [illegible] and *Welding* [8]:

$$V_r = \frac{(D-FT)/\rho_r}{(D-FT)/\rho_r + A_0/\rho_s}$$

[illegible] is the weight of the specimen, [illegible] weight fraction of insoluble components, [illegible] weight of polymer, [illegible] solvent corrected for swelling increment, [illegible] densities of the rubber and solvent respectively. Chloroform was used as the solvent for the present study.

3 Results and discussion

The rheographs of the blends of Neoprene AC and ENR are shown in *Figure 1*. CR alone is reported to undergo thermovulcanisation [9]. It is not known whether thermovulcanisation of Neoprene AC will take place in the presence of functionally active rubbers like ENR. In a blend of Neoprene AC and a rubber which does not contain active functional groups (for example NR), rise in rheometric torque, if any, in the blend, will be due to thermovulcanisation of Neoprene AC only. According to comparison we have taken rheographs of blends of Neoprene AC and NR. The blend compositions of Neoprene AC-ENR system were chosen to be the same as the Neoprene AC-NR system. It is believed that in the same blend composition rheometric torque in the Neoprene AC-NR system corresponds to thermovulcanisation alone while in the case of the Neoprene AC-ENR system the torque rise corresponds to thermovulcanisation of Neoprene AC as well as self-vulcanisation between Neoprene AC and ENR. At a particular curing time the difference in the two torque values will correspond to the torque due to self-vulcanisation. The calculated rheographs thus obtained are shown in *Figure 2*. Although both ENR and Neoprene AC are soluble in chloroform, the moulded blend is insoluble in the same solvent showing thereby that each blend constituent is crosslinked by the other during moulding. The weight loss after 48 h of immersion in chloroform is less than 15% for the blends showing that during vulcanisation both ENR and Neoprene AC gets crosslinked to a large extent. This is also evident from the volume fraction of rubber in the swollen vulcanisate, shown in *Table 2*. The crosslink density which can be regarded as proportional to V_r is high when the Neoprene AC content is high. A plausible mechanism of self-vulcanisation between Neoprene AC and ENR is shown in *Figure 3*.

The very long scorch time for the blends of Neoprene AC and ENR shows good processing safety. The processing characteristics are shown in Table 1.

Table 1 Formulation and processing characteristics of the blend

	Blend designation	
	N-E 25 75	N-E 50 50
Neoprene AC	75	50
ENR	25	50
Minimum Mooney viscosity at 120 °C	18	31
Mooney scorch time at 120 °C [illegible]	36	135

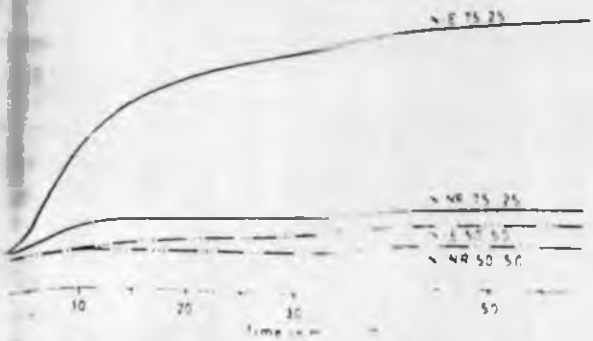

Rheographs of Neoprene AC [illegible] Neoprene AC-NR [illegible] 180 °C

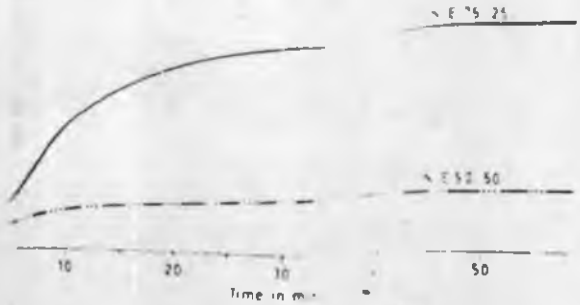

alculated rheographs of the self-[illegible] Neoprene AC-[illegible]s after deducting the effect due [illegible] vulcanisation of [illegible]C

[illegible] Physical properties of the blends [illegible] at 180 °C for 60 min

	[illegible]	N E 50 50
[illegible] 300% in MPa		[illegible]
Strength in MPa		[illegible]
[illegible]on at break in [illegible]		[illegible]
[illegible]ngth in kN/m		[illegible]
[illegible]s. Shore A		[illegible]
[illegible]e at 40 °C in [illegible]		[illegible]
[illegible]ssion set at constant strain in [illegible]		[illegible]
[illegible]d up by Goodrich flexometer [illegible] °C		
[illegible]amic set after 2[illegible] min [illegible]		
[illegible] loss in cm³/1000 [illegible]		[illegible]
[illegible]action, V		[illegible]

[illegible]lown out in the [illegible] min

[illegible]king reaction between ENR and Neoprene AC in the [illegible]

The physical properties of blends are shown in Table 2. Higher proportion of Neoprene AC in the blend results in improved physical properties. The stress-strain curves are shown in *Figure 4*. As the proportion of Neoprene AC in the blend increases compression set, abrasion loss and heat build-up decreases. However, resilience values do not show any change.

Figure 4 (right) Stress-strain curves of blends of Neoprene AC and ENR

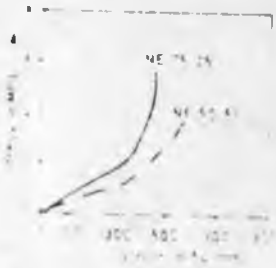

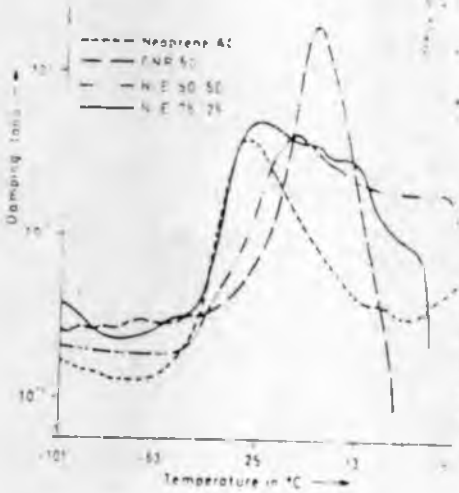

Figure 5. Plots of damping (tan δ) versus temperature for Neoprene AC, ENR and blends of Neoprene AC and ENR

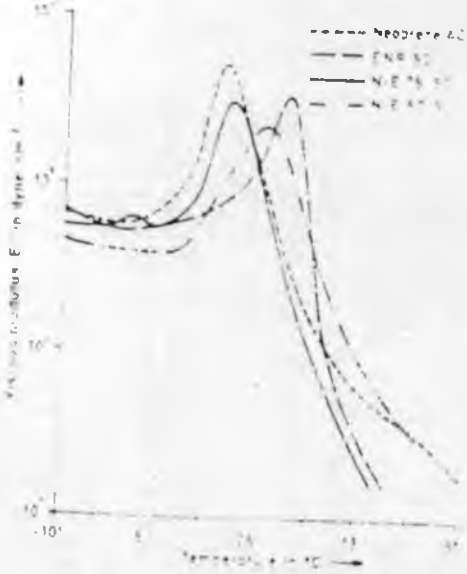

Figure 6. Plots of viscous modulus versus temperature for Neoprene AC, ENR and blends of Neoprene AC and ENR

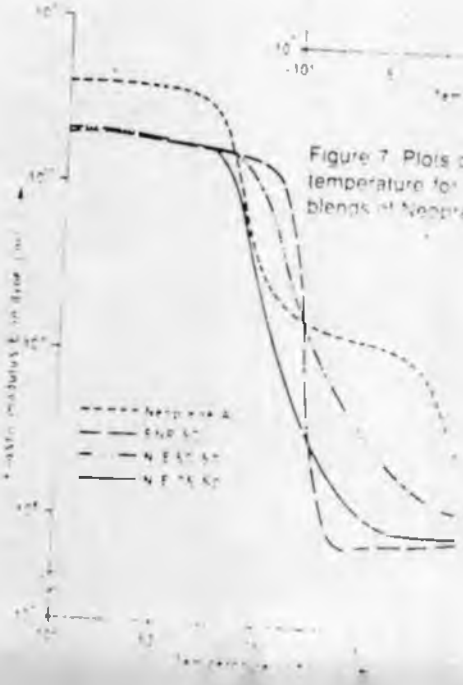

Figure 7. Plots of elastic modulus versus temperature for Neoprene AC, ENR and blends of Neoprene AC and ENR

Dynamic storage modulus or elastic modulus (E'), dynamic viscous modulus or loss modulus (E'') and damping (tan δ) at different compositions are shown in *Figures 5 to 7*. The temperatures corresponding to maximum damping and maximum viscous modulus, were as taken as T_gs. The T_gs of the samples thus obtained are shown in *Table 3*. Pure ENR shows a main relaxation at T_g and a relaxation corresponding to motion of side groups in the glassy region as seen from plots of viscous modulus and damping versus temperature [10]. Neoprene AC in the glassy region does not show any transition other than T_g. In the T_g region as a general trend loss modulus and damping increase until they attain their maxima and then fall with increase in temperature whereas the dynamic storage modulus falls rapidly to the level in the rubber elastic region. Pure ENR shows single transition in the T_g region. Pure Neoprene AC is observed to show two transitions in the rubbery region as reflected from plots of damping and elastic modulus. For Neoprene AC there is a sharp transition in elastic modulus around −46 °C and a slow second transition around −13 to +36 °C. In the plots of damping versus temperature the maximum damping occurs at −29 °C.

Table 3 T_g and width of T_g zone in Neoprene-ENR blends

	T_g in °C			Width of T_g zone in DSC thermogram
	DMA		DSC	
	tan δ	E		ΔT in °C
Neoprene AC	−29	−37	−37	9
N-E 75:25	−27	−33	−36	17
N-E 50:50	−13	−22	−33	24
ENR-50	−6	−13	−15	12

In Neoprene AC the first sharp transition observed in damping and elastic modulus is due to transition from the glassy to the rubbery state, and the second transition is due to the melting of the crystallites in the polymer as it contains about 90 % trans 1,4 configuration of the chloroprene unit in CR [11]. Development of crystallinity at low temperatures for elastomers which are substantially amorphous at room temperature have been reported earlier [12, 13].

The β relaxation shown by pure ENR is absent in the case of blends of Neoprene AC and ENR. This shows that there is interaction between the blend components. Absence of secondary relaxation in blends, due to the interaction between blend components have been reported earlier [14, 15]. In blends of Neoprene AC and ENR there is considerable broadening of the T_g zone. This shows that there is microlevel inhomogeneity i.e. partial miscibility for the blends. When the Neoprene AC content increased the transition to rubbery region starts at a lower temperature. In Neoprene AC-ENR 75:25 blend the damping is high in the region −27 to +9 °C. However, maximum damping observed at −27 °C. In Neoprene AC-ENR 50:50 blend the maximum damping is observed at −13 °C and the damping is high in the region −13 to +50 °C. The transition in elastic modulus occurs in a wider range of temperature, −43 to −6 °C for Neoprene AC-ENR 75:25 blend and −38 to +50 °C for Neoprene AC-ENR 50:50 blend. This wide temperature range transition in the T_g region is also observed in the loss modulus of the blends. Thus the blends show high damping over a wide range of temperature depending on the blend ratio.

DSC thermograms as shown in *Figure 8* gives additional support to the partial miscibility of ENR-Neoprene AC blends. Blends show a single T_g which is shifted to a higher temperature as ENR content decreases. As observed in the case of DMA results there also the T_g zone becomes broadened in the case of blends.

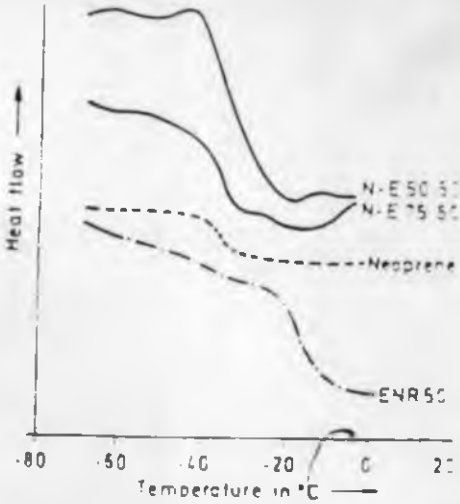

Figure 8. DSC thermograms of Neoprene AC, ENR and blends of Neoprene AC and ENR

This broadening shows partial miscibility of the components in the blend. *Vukovic* et al. [16] while studying compatibility of poly(2,6 dimethyl 1,4-phenylene oxide)/poly(fluorostyrene-co-chlorostyrene) have observed that there is increase in T_g width of DSC thermogram with blend composition till there is phase separation. In an immiscible system the T_g width of the DSC thermograms in the blends is the same as the T_g width of DSC thermograms of individual components. The magnitude of this broadening and the transition width temperature (ΔT) is shown in Table 3. The difference in transition temperature obtained from DMA and DSC results, is due to different nature of response in molecular segments of samples in the two techniques of analysis.

4 Conclusions

It is concluded that mill mixed blends of ENR and Neoprene AC form a self-vulcanisable system when moulded at 180 °C. These blends are partially miscible. The system shows high damping in a wide range of temperature depending on the blend ratio. The extent of self-vulcanisation also depends on the blend ratio. Higher proportion of Neoprene AC in the blend shows higher crosslink density and improved physical properties.

References

[1] S. Mukhopadhyay, T. K. Chaki, and S. K. De, J. Polym. Sci. Polym. Lett. 28 (1990) 25
[2] S. Mukhopadhyay and S. K. De, J. Mat. Sci. (in press)
[3] S. Mukhopadhyay and S. K. De, J. Polym. Sci. (communicated)
[4] R. Alex., P. P. De, and S. K. De, J. Polym. Sci. Polym. Lett. 27 (1989) 361
[5] R. Alex, P. P. De, and S. K. De, Polym. Commun. 31 (1990) 118
[6] S. Mukhopadhyay and S. K. De, J. Appl. Polym. Sci. (communicated).
[7] N. D. Zakharov, G. A. Mairov, Sov. Rubber Technol. 22 (1963) 1
[8] B. Ellis and G. N. Welding, Rubber Chem. Technol. 37 (1964) 57
[9] M. Behal and V. Duchacek, J. Appl. Polym. Sci. 35 (1988) 507
[10] K. T. Varughese, G. B. Nando, P. P. De, and S. K. De, J. Mat. Sci. 23 (1988) 3894
[11] M. Steinfink, "Handbook of Adhesives", Irving Skeist, Ed. 2nd Ed. Van Nostrand Reinhold Comoany, Inc. New York 1977, Chap. 21, p. 346
[12] F. P. Baldwin, G. Verstrate, Rubber Chem. Technol. 45 (1972) 709
[13] M. A. Mohsen, J. P. Berry, and L. R. G. Treloar, Polymer 26 (1985) 1463
[14] J. V. Koleska and R. D. Lundberg, J. Polym. Sci. Polym. Phys. 7 (1969) 795
[15] J. J. Hickman and R. N. Ikeda, J. Polym. Sci. Polym. Phys. 11 (1973) 1713
[16] R. Vukovic, V. Kuresevic, N. Segudovic, F. E. Karasz, and W. J. Macknight, J. Appl. Polym. Sci. 28 (1983) 1379

The authors are co-workers of the Rubber Technology Centre, Indian Institute of Technology

Effect of fillers and moulding conditions on properties of self-vulcanisable blends of epoxidised natural rubber and carboxylated nitrile rubber

R. Alex, P. P. De, N. M. Mathew* & S. K. De‡
Rubber Technology Centre, Indian Institute of Technology, Kharagpur 721302, India

Received 18 September 1989; revised version received and accepted 2 April 1990

Abstract: A mill mixed blend of epoxidised natural rubber (ENR) and carboxylated nitrile rubber (XNBR) forms a self-vulcanisable rubber blend on moulding at high temperatures, when a crosslinking reaction occurs between the epoxy group of ENR and the carboxyl group of XNBR. Such a vulcanisate is reinforced by fillers like silica and carbon black.

1 Introduction

Mill mixed blends of functionally active rubbers can be vulcanised at high temperatures to form self vulcanisable rubber blends. De and co-workers have developed such blends based on epoxidised natural rubber, hypalon, carboxylated nitrile rubber, neoprene, halobutyl rubber and polyvinyl chloride.[1-5] It has been shown that a mill mixed blend of epoxidised natural rubber (ENR) and carboxylated nitrile rubber (XNBR) forms a self-vulcanisable and miscible rubber blend system during moulding at 140°C.[6-7] The crosslinking mechanism in such a self-vulcanisable rubber blend system is based on the reaction between the epoxy group of ENR and the carboxyl group of XNBR (Fig. 1). It has been reported earlier by Chakraborty and De[8] that carboxylated nitrile rubber can be vulcanised by epoxy resin.

*Present address: Rubber Research Institute of India, Rubber Board, Kottayam 686009, India.
‡To whom all correspondence should be addressed.

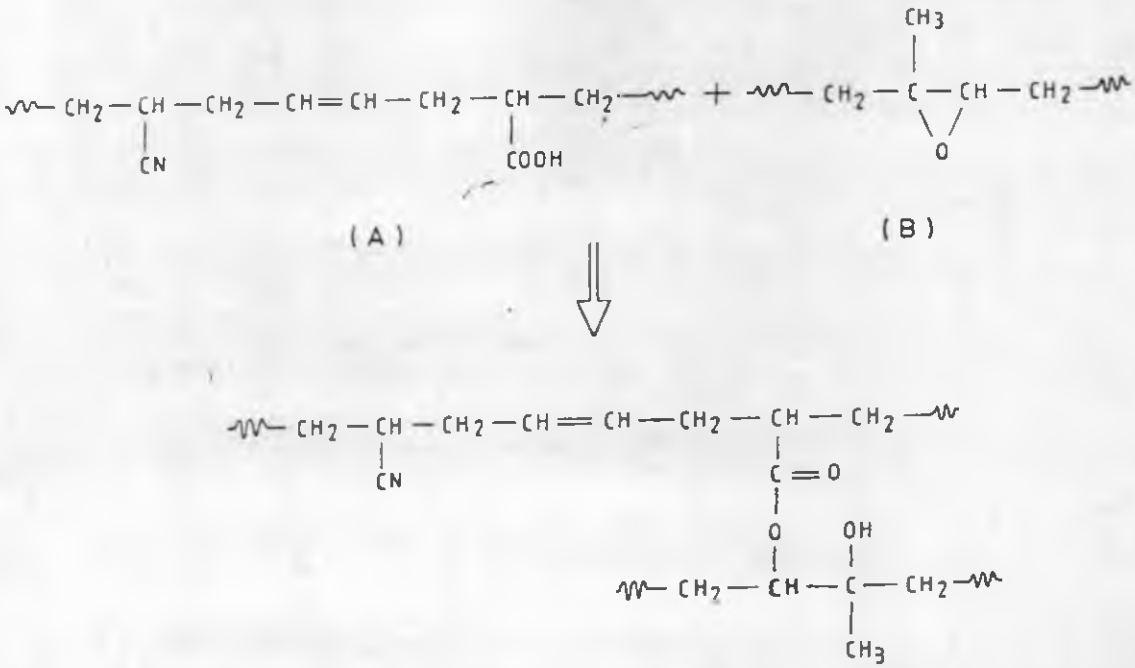

Fig. 1 The possible mechanism of crosslinking between carboxylated nitrile rubber (A) and epoxidised natural rubber (B).

Plastics and Rubber Processing and Applications 0144-6045/90/$03.50

In the present paper we report the results of our tudies on the effects of moulding temperature, noulding time and fillers on the properties of such elf-vulcanisable rubber blends.

Experimental

Epoxidised natural rubber with 50 mol% epoxidation (ENR-50) was obtained from the Malaysian Rubber Producers Research Association, UK. Carboxylated nitrile rubber, containing a high level of carboxylated monomer and a medium high bound acrylonitrile level (Krynac 221) was obtained from Polysar Ltd. Canada. The silica filler used was Vulkasil S (precipitated silica) obtained from Bayer (India) Ltd. Thane.

Both ENR and XNBR were first individually masticated on a 0·356 m×0·152 m (14 in ×6 in) two roll mixing mill for about 1 min each. The Mooney viscosities (ML_{1+4} at 120°C) of ENR and XNBR before blending were 33 and 24 respectively. Masticated samples of the two rubbers were blended together in equal amounts on the mill for a further period of 6 min. Cold water was circulated through the rolls to keep the temperature low in order to avoid the rubber sticking on the rolls. The mill temperature for the initial mastication step was 25°C. The temperature rise during the mixing of gum rubber was only 2°C. The fillers were added after blending the two rubbers. The total mixing time for the filled blend was 10 min. The temperature rise during mixing in the case of filled blend was 7°C.

The formulation of the different blends is given in Tables 1 and 2. The formulation for the control mixes is given in Table 3.

In the case of blend, the increase in rheometric torque above the minimum torque was 30 units. The control mixes of ENR and XNBR were cured to the time when the rheometric torque rise was the same as that of the blend (that is 30 units). For ENR and XNBR these times were 18 and 12 min respectively, at 150°C. This was thought likely to eliminate the effect of curing time or crosslink density on the comparison of properties of blend and control vulcanisates.

Rheographs of the mixes were taken on Monsanto rheometer R-100 at 150, 160, 170 and 180°C. Scorch time and Mooney viscosity at 120°C were determined by using Mooney viscometer MK III (Negretti Automation Ltd) according to ISO 667. The properties determined as per standard test methods were tensile strength (ISO 37) using dumb bell specimens and an Instron 1195 universal testing machine; tear resistance (ASTM D624-84) using an unnicked 90° angle specimen (die C) and an Instron 1195 universal testing machine; hardness, shore A (ISO 7619), and resilience (BS: 903, part AB: 1963 method A) and a Dunlop tripsometer. Samples for compression set (ISO 815) were cylindrical discs 29 mm diameter and 13 mm thickness which were subjected to compressive deformation at constant strain for 22 h at 70°C. While determining heat build-up (ASTM D623-75), using a Goodrich flexometer, the samples were subjected to cyclic deformation for 25 min with a load of 10·89 kg (24 lb) and a stroke of 4·5 mm. Abrasion resistance (BS: 903, part A9, method A-1957) was determined by using a Du Pont abrader. In the Du Pont machine two test specimens were abraded simultaneously against an abrasive paper (silicon carbide paper with grain size 325). The specimens were held under a load of 3·62 kg and the abrasive paper rotated at a speed of 40 RPM. The samples were abraded for 10 min and then the volume lost (in m^3 from a specified test

Table 1. Formulation of XNBR–ENR blend mixes (in parts by weight)

Mix no.	Exb	Si10	Si20	Si30	Si40
ENR-50	50	50	50	50	50
XNBR (Krynac 221)	50	50	50	50	50
Silica (Vulkasil S)	—	10	20	30	40

Table 3. Formulation of control mixes (in parts by weight)

Mix no.	E	Ec	Es	X	Xc	Xs
XNBR (Krynac 221)	—	—	—	100	100	100
ENR-50	100	100	100	—	—	—
Na_2CO_3	0·25	0·25	0·25	—	—	—
ZnO	5	5	5	5	5	5
Stearic acid	2	2	2	2	2	2
ISAF black	—	20	—	—	20	—
Silica	—	—	20	—	—	20
Aromatic oil	—	2	2	—	—	—
Dioctyl phthalate	—	—	—	—	2	2
TMTD[a]	1·6	—	—	—	—	—
MBS[b]	2·4	1	1	1	1	1
Sulphur	0·3	2·8	2·8	2·4	2·4	2·4

[a] Tetramethylthiuram disulphide.
[b] *N*-Oxydiethylenebenzothiazole-2-sulphenamide.

Table 2. Formulation of XNBR–ENR blend mixes (in parts by weight)

Mix no.	IS5	IS10	IS15	IS20	IS30	IS40	SR5	SR10	SR15	SR20	SR30	SR40
ENR-50	50	50	50	50	50	50	50	50	50	50	50	50
XNBR (Krynac 221)	50	50	50	50	50	50	50	50	50	50	50	50
ISAF black	5	10	15	20	30	40	—	—	—	—	—	—
SRF black	—	—	—	—	—	—	5	10	15	20	30	40

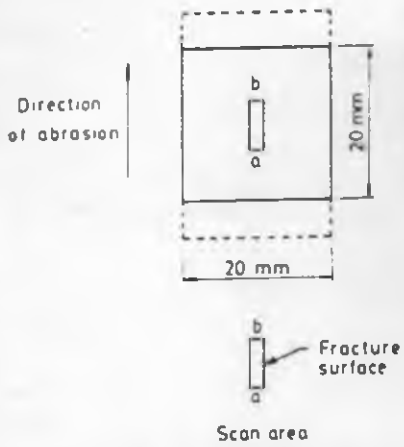

Fig. 2 Sample for abrasion tests showing fracture surface and scan area.

specimen for 1000 revolutions of the abrasive wheel) was calculated.

Scanning electron microscope (SEM) studies of the abraded surfaces were done on a SEM, model CAN SCAN series 2DV. The shape, size and direction of abrasion of specimens are given in Fig. 2. After abrasion for 10 min the abraded surfaces were sputter coated with gold for SEM studies.

Table 4(a). Cure characteristics of different blends

Mix no.	Exb	Si10	Si20	Si30	Si40
Minimum Mooney viscosity at 120°C	35	43	59	66	100
Mooney scorch time at 120°C (min)	7·0	6·1	5·0	4·3	3·0
Monsanto rheometry					
Minimum torque at 150°C (dN m)	6	9	10	17	25
Maximum torque at 150°C (in 60 min) (dN m)	37	53	58	76	96
Minimum torque at 180°C (dN m)	6	8	9	12	20
Maximum torque at 180°C (in 60 min) (dN m)	62	74	91	100	118

Volume fraction of the rubber in the swollen vulcanisate was calculated from equilibrium swelling data by the method reported by Ellis and Welding[9]

$$Vr = \frac{[D - FT/\rho_r]}{[(D - FT/\rho_r) + (Ao/\rho_s)]} \quad (1)$$

where T is the weight of the specimen, D is its deswollen weight, F is the weight fraction of insoluble components and Ao is the weight of absorbed solvent corrected for swelling increment. ρ_r and ρ_s are the densities of rubber and solvent respectively. Chloroform was used as the solvent in the present study.

3 Results and discussion

Minimum Mooney viscosities and Mooney scorch times for the gum and filled blends are given in Tables 4(a) and (b). It is evident that an increase of filler loading increases the minimum viscosity and decreases the scorch time. Also, the increase in Mooney viscosity and decrease in scorch time is most prominent in the case of silica-filled mixes and least prominent in the case of SRF black-filled mixes, while the ISAF black-filled mixes occupy an intermediate position. For example, at 40 PHR loading, Mooney viscosity at 120°C increases from 35 for the unfilled blend to 49 for SRF black, to 63 for ISAF black and to 100 for silica-filled blend. The higher Mooney viscosity of the silica-filled mix is probably due to strong interaction of the silica with the rubber during mixing. It is well known that ISAF black is more reinforcing than SRF black, hence the higher viscosity in the case of ISAF black-filled mix.[10]

Samples of neat ENR and neat XNBR were masticated for 8 min, which is also the blending time for the two rubbers, and the Mooney viscosity values, $ML_{(1+4)}$ at 120°C were determined. The values are as follows: ENR, 10; XNBR, 30, and blend, 35. It is evident that reaction between ENR

Table 4(b). Cure characteristics of different blends

Mix no.	IS5	IS10	IS15	IS20	IS30	IS40	SR5	SR10	SR15	SR20	SR30	SR40
Minimum Mooney viscosity at 120°C	35	39	43	43	58	63	36	39	39	39	41	49
Mooney scorch time at 120°C (min)	6·8	6·7	6·0	5·0	4·8	4·5	6·7	5·8	5·7	5·3	5·2	5·1
Monsanto rheometry												
Minimum torque at 150°C (dN m)	8	8	9	10	13	13	9	9	10	10	10	11
Maximum torque at 150°C (in 60 min) (dN m)	44	48	54	62	76	86	48	50	52	57	60	69
Minimum torque at 180°C (dN m)	8	8	8	8	10	10	7	7	8	8	8	8
Maximum torque at 180°C (in 60 min) (dN m)	75	87	92	92	113	130	69	75	84	88	106	109

Table 5. Cure characteristics of control mixes

Mix no.	E	Ec[a]	Es[b]	X	Xc[a]	Xs[b]
Minimum Mooney viscosity at 120°C	5	9	6	40	50	53
Mooney scorch time at 120°C (min)	10·0	6·5	20·0	3·8	2·0	2·5
Monsanto rheometry						
Minimum torque at 150°C (dN m)	2	3	2	11	12	12
Maximum torque at 150°C (dN m)	33	80	63	87	115	118

[a] 20 PHR ISAF black-filled.
[b] 20 PHR silica-filled.

and XNBR takes place to limited extent at 120°C during Mooney viscosity determination. The minimum Mooney viscosity and scorch time for the control mixes of ENR and XNBR are shown in Table 5. The mixes of XNBR are very scorchy compared to ENR mixes. It is reported that mixes of XNBR containing ZnO have a low scorch time and a high Mooney viscosity, where metal carboxylate crosslinks are formed.[11] In such mixes the low scorch time is due to the early onset of the reaction of the carboxyl group. The epoxy group of ENR permits effective crosslinking with chemicals like dibasic acids and polyamines.[12,13] Hence, the low scorch time of the blend mix of ENR and XNBR is due to the early onset of the reaction of the carboxyl group of XNBR with the epoxy group of ENR.

Rheographs of the gum blend (formulation Exb) at different temperatures 150, 160, 170 and 180°C are shown in Fig. 3. For comparison rheographs of one control XNBR mix and one control ENR mix (Table 3) were taken. It is evident that the rheometric torque of the blend progressively increases with moulding time and with moulding temperature. This shows that in the blend both XNBR and ENR crosslink each other during moulding and that both time

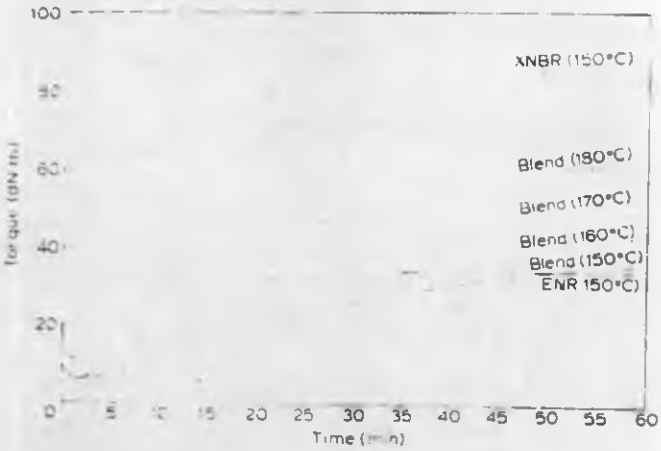

Fig. 3 Rheographs of a gum 1:1 ENR–XNBR blend at different temperatures and of control gum XNBR and ENR mixes at 150°C.

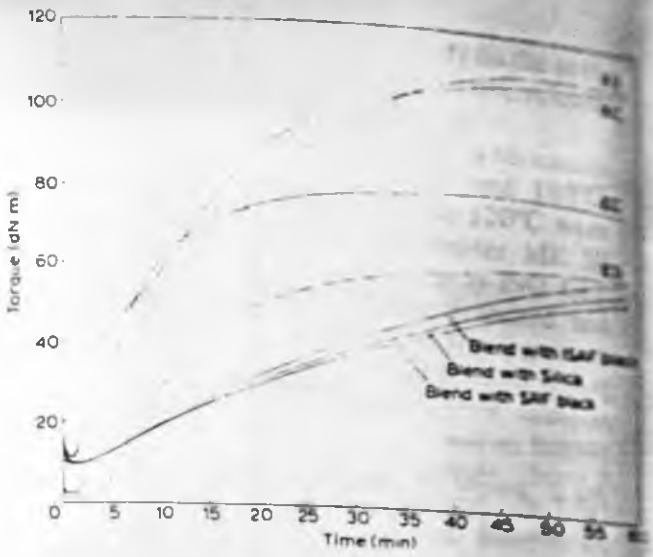

Fig. 4 Rheographs, at 150°C, of ENR, XNBR and 1:1 ENR–XNBR blend filled with 20 PHR loading of ISAF black, SRF black and silica filler.

and temperature cause progressive increase in crosslinking. At 150°C the self-vulcanisable blend registers marching rheometric torque like that of control XNBR compounds, while the ENR compounds show reversion. Crosslinking of ENR with dibasic acids has been reported to show a marching increase in modulus with cure time.[14] The XNBR system at 150°C shows much higher rheometric torque than the blend. Figure 4 shows the rheographs of the filled systems at 150°C. It is evident that addition of filler increases the rheometric torque as in the case of conventional rubber systems. The nature of rheographs with respect to moulding time and temperature is similar to that of gum blend. Increase of filler loading increases the rheometric torque.

It has been reported that the gum strength of dibasic acid cured ENR is greatly improved by the addition of reinforcing black.[14] In blend, the chemistry of vulcanisation and nature of crosslinks is different from conventionally cured ENR or XNBR.

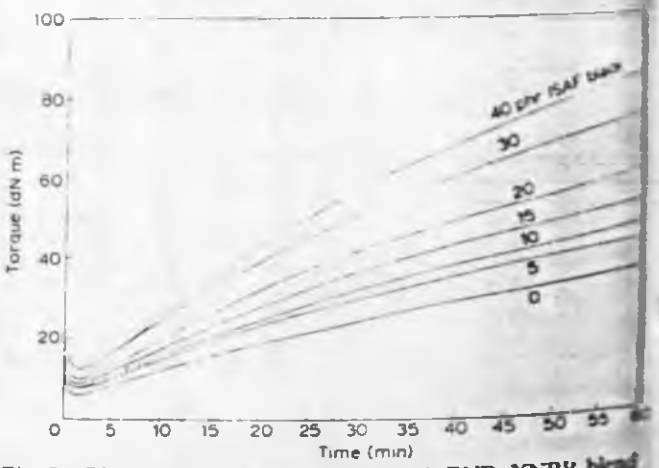

Fig. 5 Rheographs at 150°C of the 1:1 ENR–XNBR blend filled with different loadings of ISAF black filler.

in conventionally cured ENR crosslinking is by sulphur linkages[15] and in XNBR crosslinking is by sulphur linkages and metal carboxyl linkages.[11] In blends of ENR and XNBR the crosslinking reaction is by epoxy and carboxyl groups forming ester linkages which are distributed randomly in the matrix. Due to this difference in the mechanism of vulcanisation, the rheographs of blends show an absence of cure reversion, thermal stability of the crosslinked structure and a high cure rate.

Figure 5 shows the effect of ISAF black loading at 150°C. The cure characteristics of these mixes at temperatures 150 and 180°C are shown in Table 4. Enhancement of torque occurs in the following order: silica ≥ ISAF > SRF. As we shall see later, polymer–filler interaction also follows the same order.

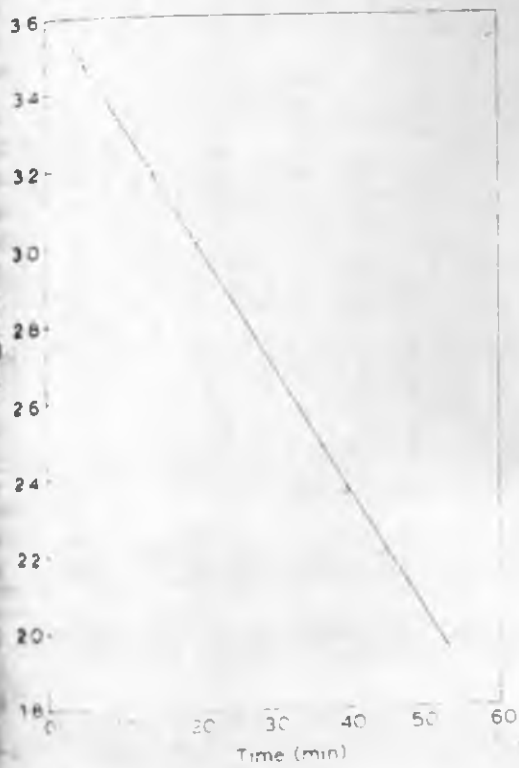

Fig. 6. Plot of ln $(M_\infty - M)$ versus time for the gum 1:1 ENR–XNBR blend at 150°C.

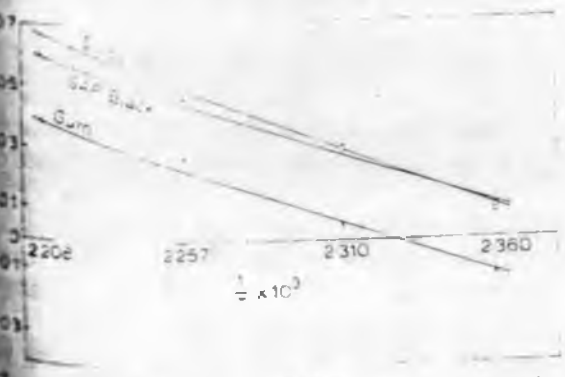

Fig. 7. Plot of log cure rate, log k, versus reciprocal of absolute temperature for the 1:1 ENR–XNBR blend and for the blend filled with 20 PHR ISAF black and silica filler.

The kinetics of a crosslinking reaction can be followed from the changes in rheometric maximum torque with time. For the first order reaction,[16,17]

$$\ln(M_\infty - M) = -kt + \ln(M_\infty - M_0) \qquad (2)$$

where M is the torque at time t, M_0 is the torque at zero time, and M_∞ is the maximum torque. For cure curves showing marching modulus, M_∞ was taken as the torque when the rise in torque is less than one unit in 5 min; at this stage it is assumed that the reaction has almost come to an end. From the linear plot

Table 6. Rate constant (k) of vulcanisation of the blend and control mixes at 150 and 180°C

	Rate constant, k (min^{-1} × 10^2)					
	E		X		Blend	
	150°C	180°C	150°C	180°C	150°C	180°C
Gum[a]	12·34	72·34	7·0	23·50	3·31	3·84
ISAF black-filled[a]	21·07	194·60	7·0	26·27	3·20	4·68
Silica-filled[a]	—	—	—	—	3·70	5·87

[a]Mix number Exb, IS20 and Si20 (Table 1).

Table 7. Activation energy for vulcanisation

	Activation energy, E (kJ/mol)		
	E	X	Blend
Gum[a]	77	34	65
ISAF black-filled[a]	86	43	65
Silica-filled[a]	—	—	70

[a]Mix number Exb, IS20 and Si20 (Table 1).

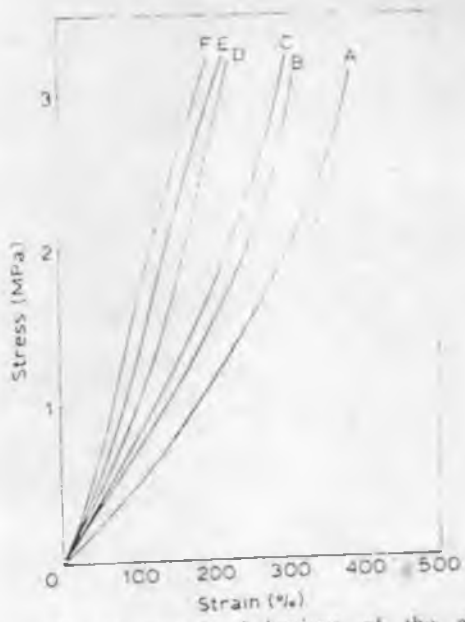

Fig. 8. Tensile stress–strain behaviour of the gum 1:1 ENR–XNBR blend moulded under different conditions of moulding time and temperature. (A) 150°C/30 min; (B) 150°C/45 min; (C) 150°C/60 min; (D) 160°C/60 min; (E) 170°C/60 min; (F) 180°C/60 min.

of $\ln(M_\infty - M)$ versus time the rate constant of the first order crosslinking reaction can be determined. The activation energy for the initial vulcanisation reaction was calculated by using an Arrhenius equation. Figures 6 and 7 show typical plots for the calculation of rate constants and activation energies. Table 6 summarises the rate constants of blend and control mixes at two temperatures and Table 7 gives the values of the activation energy for vulcanisation. The activation energy for self vulcanisation is found to lie between 65 and 70 kJ/mol. This is of the same order of magnitude as reported by other workers for conventional rubbers.[18]

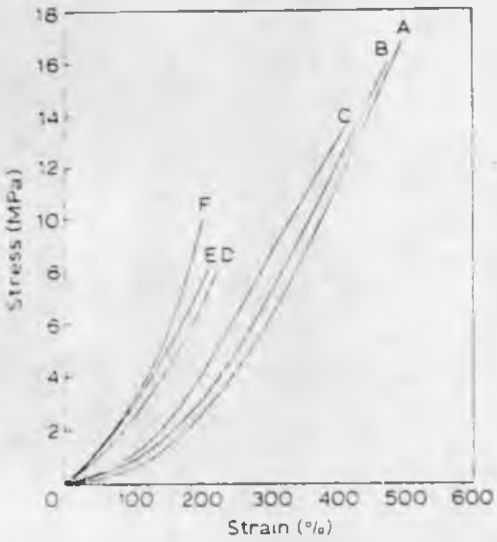

Fig. 9 Tensile stress–strain behaviour of the 1:1 ENR–XNBR blend filled with 20 PHR ISAF black and moulded under different conditions of time and temperature. (A) 150°C/30 min; (B) 150°C/45 min; (C) 150°C/60 min; (D) 160°C/60 min; (E) 170°C/60 min; (F) 180°C/60 min.

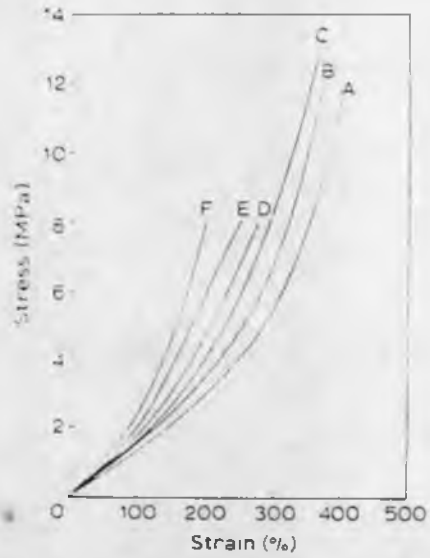

Fig. 10 Tensile stress–strain behaviour of the 1:1 ENR–XNBR blend filled with 20 PHR silica and moulded under different conditions of time and temperature. (A) 150°C/30 min; (B) 150°C/45 min; (C) 150°C/60 min; (D) 160°C/60 min; (E) 170°C/60 min; (F) 180°C/60 min.

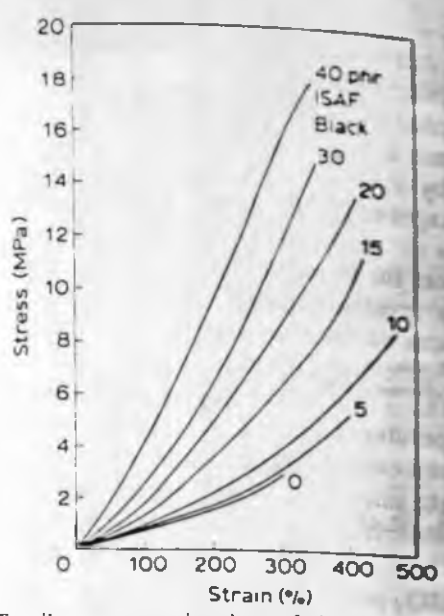

Fig. 11 Tensile stress–strain plots of the 1:1 ENR–XNBR blend filled with different loadings of ISAF black, moulded at 150°C for 60 min.

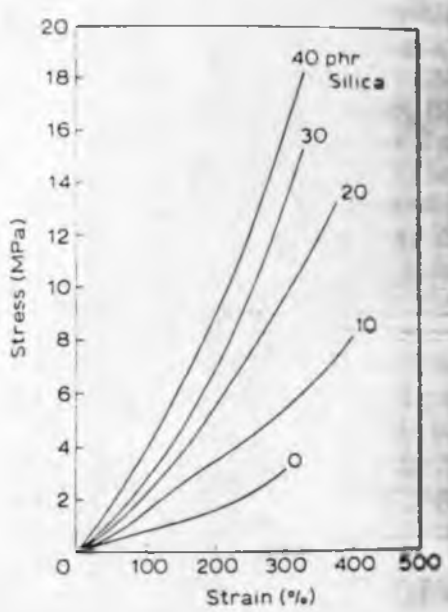

Fig. 12 Tensile stress–strain plots of the 1:1 ENR–XNBR blend filled with different loadings of silica moulded at 150°C for 60 min.

3.1 Physical properties

Tensile stress–strain behaviour of the gum blend moulded under different conditions is shown in Fig. 8. Similar plots for ISAF black and silica-filled compositions are shown in Figs 9 and 10. It is evident that both moulding time and temperature alter the stress–strain behaviour and the effect is prominent in filled systems. The effect of filler loading on stress–strain behaviour is shown in Figs 11–13. Energy at rupture increases with increasing filler loading and the trend continues up to the highest filler loading studied. The variation of rupture energy with filler loading is given in Fig. 14.

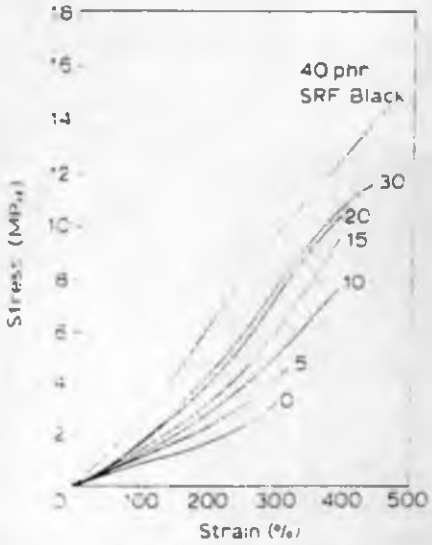

Fig 13 Tensile stress–strain plots of the 1:1 ENR–XNBR blend filled with different loadings of SRF black, moulded at 150°C for 60 min.

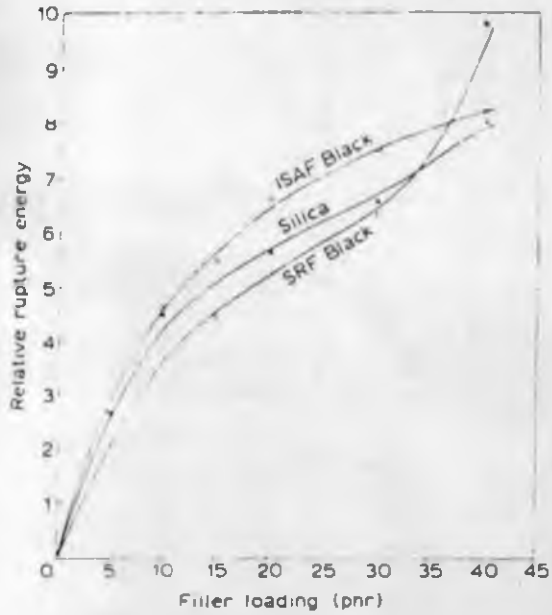

Fig. 14 Plots of relative rupture energy versus filler loading for ISAF black, SRF black and silica-filled 1:1 ENR–XNBR blend.

Table 8 summarises the results of the effect of moulding time at 150°C on some physical properties like modulus, tensile strength, elongation at break and tear resistance. It is evident that increasing moulding time at a constant temperature causes lowering of both tensile strength and tear resistance. However, as modulus increases, elongation at break decreases. Table 9 shows the results of the variation of moulding temperature at a constant moulding

Table 8. Effect of moulding time at 150°C on physical properties of the 1:1 XNBR–ENR blend

Time of moulding (min)	Gum			ISAF black[a]			Silica[a]		
	30	45	60	30	45	60	30	45	60
Modulus 100% (MPa)	0·5	0·8	0·8	0·6	0·7	1·1	1·3	1·4	1·5
Modulus 200% (MPa)	1·0	1·5	1·5	2·9	3·3	4·3	2·7	3·6	4·2
Modulus 300% (MPa)	2·0	2·8	3·2	6·2	7·0	8·9	5·3	7·1	9·2
Tensile strength (MPa)	3·0	3·1	3·2	17·0	16·0	13·5	12·0	12·0	13·0
Elongation at break (%)	340	310	300	500	470	410	400	370	370
Tear strength (kN/m)	17·0	16·0	12·6	53·0	47·0	38·0	33·0	29·0	29·0

[a] At 20 PHR loading.

Table 9. Effect of moulding temperature at constant moulding time (60 min) on physical properties of the 1:1 XNBR–ENR blend

	Gum		ISAF black[a]		Silica[a]	
	150°C	180°C	150°C	180°C	150°C	180°C
Modulus 300% (MPa)	3·2	—	8·9	—	9·2	—
Tensile strength (MPa)	3·2	3·2	13·5	10·0	13·0	8·0
Elongation at break (%)	300	200	410	200	370	200
Tear strength (kN/m)	12·6	11·8	38·0	27·0	29·0	23·0
Hardness, shore A	47	50	58	60	57	74
Resilience at 40°C (%)	69	74	61	67	64	70
Abrasion loss ($\times 10^{-6}$ m^3/1000 rev)	1·97	1·61	0·69	0·46	0·61	0·37
Compression set at 70°C for 22 h (%)	12	4	14	6	12	7
Heat build-up by Goodrich flexometer with a load of 10·89 kg and stroke of 4·5 mm						
ΔT^b (°C)	17	11	26	21	22	18
Dynamic set (%)	0·6	0·5	1·3	0·5	1·0	0·5
V_r	0·12	0·18	0·17	0·24	0·15	0·19

[a] At 20 PHR loading.
[b] Ambient temperature, 50°C.

Table 10. Physical properties of ISAF black filled 1 : 1 XNBR–ENR blend moulded at 150°C for 60 min

	Filler loading (parts per 100 of rubber)						
	0	5	10	15	20	30	40
Modulus 300% (MPa)	3·2	3·3	4·0	6·4	8·9	11·6	15·9
Tensile strength (MPa)	3·2	5·2	8·6	10·7	13·5	15·0	17·8
Elongation at break (%)	300	395	460	410	410	350	340
Tear strength (kN/m)	12·6	25·8	28·4	29·0	38·0	46·7	55·0
Hardness, shore A	47	49	53	55	58	67	76
Resilience at 40°C (%)	69	65	63	62	61	52	48
Abrasion loss ($\times 10^{-6}$ m³/1000 rev)	1·97	1·54	0·80	0·72	0·69	0·46	0·3[illegible]
Compression set at 70°C for 22 h (%)	12	13	14	14	14	15	17
Heat build-up by Goodrich flexometer with a load of 10·89 kg and stroke of 4·5 mm							
ΔT* (°C)	17	19	21	25	26	30	33
Dynamic set (%)	0·6	1·1	1·2	1·3	1·3	1·6	1·6
Vr	0·12	0·13	0·14	0·15	0·17	0·19	0·20

*Ambient temperature, 50°C.

Table 11. Physical properties of SRF black filled 1 : 1 XNBR–ENR blend moulded at 150°C for 60 min

	Filler loading (parts per 100 of rubber)						
	0	5	10	15	20	30	40
Modulus 300% (MPa)	3·2	3·7	4·9	6·3	7·3	7·6	9·8
Tensile strength (MPa)	3·2	5·2	7·6	9·2	10·5	11·5	14·5
Elongation at break (%)	300	310	385	390	390	440	460
Tear strength (kN/m)	12·6	26·0	28·0	29·5	30·9	36·0	47·0
Hardness, shore A	47	48	49	51	55	60	65
Resilience at 40°C (%)	69	69	68	68	66	59	57
Abrasion loss ($\times 10^{-6}$ m³/1000 rev)	1·97	1·15	0·89	0·80	0·69	0·63	0·43
Compression set at 70°C for 22 h (%)	12	13	14	15	16	16	16
Heat build-up by Goodrich flexometer with a load of 10·89 kg and stroke of 4·5 mm							
ΔT* (°C)	17	18	19	20	21	23	30
Dynamic set (%)	0·6	0·6	0·6	0·7	0·7	0·7	1·0
Vr	0·12	0·13	0·13	0·14	0·15	0·16	0·18

*Ambient temperature, 50°C.

Table 12. Physical properties of silica-filled 1 : 1 XNBR–ENR blend moulded at 150°C for 60 min

	Filler loading (parts per 100 of rubber)				
	0	10	20	30	40
Modulus 300% (MPa)	3·2	5·0	9·2	13·4	16·0
Tensile strength (MPa)	3·2	8·0	13·0	15·3	18·0
Elongation at break (%)	300	400	370	330	330
Tear strength (kN/m)	12·6	26·0	29·0	40·0	49·7
Hardness, shore A	47	51	57	67	76
Resilience at 40°C (%)	69	64	64	60	55
Abrasion loss ($\times 10^{-6}$ m³/1000 rev)	1·97	0·82	0·60	0·48	0·33
Compression set at 70°C for 22 h (%)	12	12	12	15	16
Heat build-up by Goodrich flexometer with a load of 10·89 kg and stroke of 4·5 mm					
ΔT* (°C)	17	19	22	24	30
Dynamic set (%)	0·6	1·0	1·0	1·1	1·4
Vr	0·12	0·13	0·15	0·19	0·20

*Ambient temperature, 50°C.

time on physical properties. It is observed that increase of moulding temperature from 150 to 180°C causes increasing hardness and resilience and decreasing abrasion loss, compression set, heat build-up and dynamic set. On the evidence of V_r values, these changes are ascribed to the formation of additional crosslinks at elevated temperatures.

Effects of filler loading on the physical properties are summarised in Tables 10–12. As expected, the following properties show a gradual increase with increasing filler loading: modulus, tensile strength, tear strength, abrasion resistance hardness, heat build-up and dynamic set. Resilience decreases gradually and compression set increases with filler loading.

In order to understand abrasion mechanism we have analysed SEM fractographs of the abraded surfaces. In abrasion, mechanical, chemical and thermal processes are involved.[19] Reznikoiskii and Broskii have described different types of wear in elastomers.[20] High abrasion resistance is observed in vulcanisates with high hardness, modulus, tensile strength, tear strength, resistance to thermo-oxidative degradation and crack growth resistance under dynamic conditions.[21] Such elastomeric vulcanisates show ridge formation during abrasion.[22,23] Figures 15 and 16 show the failure surfaces of E and EIS 20 (formulations in Table 3). In ENR the abrasion resistance is very poor and the material seems to be chipped by the abrasive. This is due to low matrix strength as seen from tensile properties and hardness. The cut growth resistance is also poor as rubber is removed in lumps by the abrasive. When filler is added, the abrasion resistance is improved due to high matrix strength. There is ridge formation in XNBR vulcanisates and blends as seen from Figs 17–21. Gum XNBR and ISAF black-filled XNBR show high abrasion resistance and follow frictional type wear (Figs 17 and 18).

The gum blend shows abrasive type wear (Fig. 19). Here the abrasion resistance is better than pure ENR due to a higher matrix strength. At low ISAF black loading (20 PHR) the blend shows the abrasive type wear, and at higher ISAF black loading (40 PHR) the mechanism of wear changes from an abrasive to a frictional type (Figs 20 and 21). It has been reported that low ridge height and close spacing of ridges, as noted in the present case of black-filled blend and XNBR, are indicative of high abrasion resistance.[24]

Although the self-vulcanisable rubber blend system is similar to conventional rubber vulcanisates

Fig. 15 SEM micrograph of the gum ENR vulcanisate showing a coarse abrasion pattern.

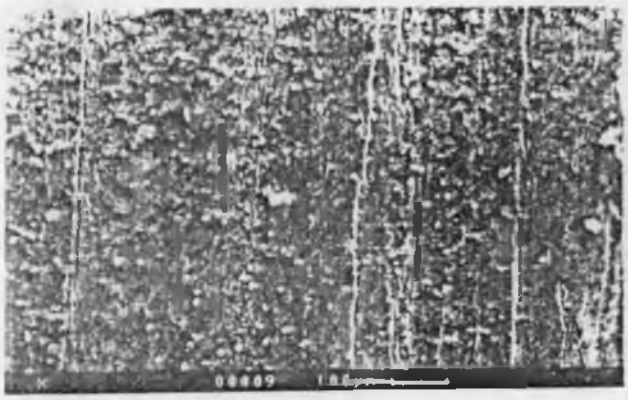

Fig. 17 Abraded surface of the gum XNBR vulcanisate showing clear surface.

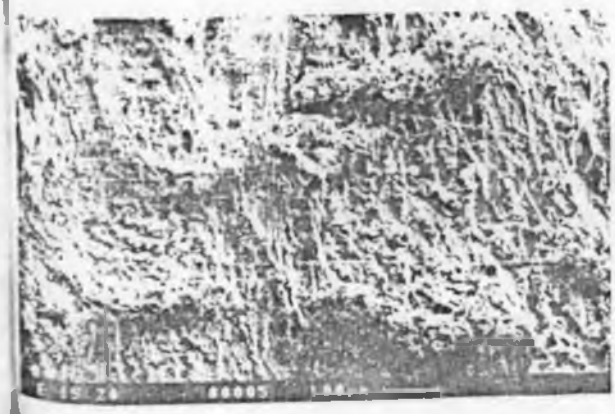

Fig. 16 SEM micrograph of a filled (20 PHR ISAF black) ENR vulcanisate showing material removal.

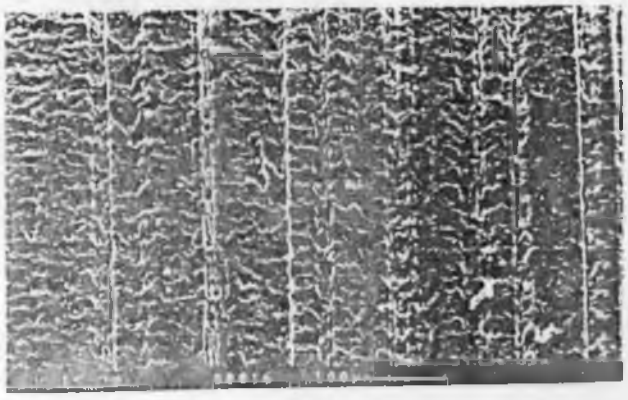

Fig. 18 Abraded surface of the 20 PHR ISAF black-filled XNR vulcanisate showing fine and closely spaced ridges.

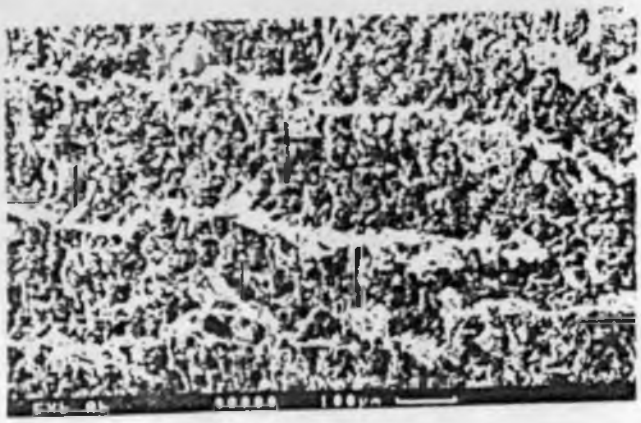

Fig. 19 Abraded surface of the 1:1 ENR-XNBR blend showing abrasive type of wear.

Fig. 20 Abraded surface of the 1:1 ENR-XNBR blend filled with 20 PHR ISAF black showing ridges which are not closely spaced.

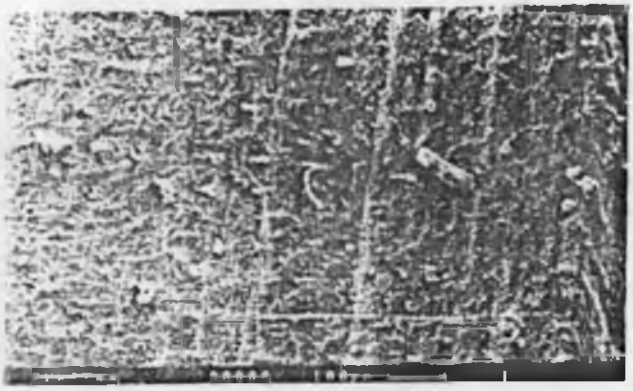

Fig. 21 Abraded surface of the 1:1 ENR-XNBR blend filled with 40 PHR ISAF black showing closely packed fine ridges.

as regards the influence of filler, silica reinforcement in such blend occurs even in the absence of a coupling agent and the extent of silica reinforcement is similar to the ISAF black reinforcement. The degree of reinforcement occurs in the following order: SRF < ISAF = silica. Reinforcement can be related with the polymer-filler interaction. An indication of polymer-filler interaction can be obtained from the Kraus plot.[25] It has been shown elsewhere that both ENR and XNBR vulcanisates can be reinforced by silica in the absence of coupling agent.[26,27]

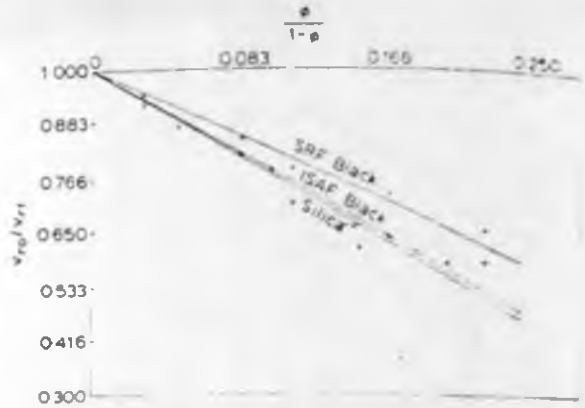

Fig. 22 Kraus plots for ISAF black, SRF black and silica-filled 1:1 ENR-XNBR blend.

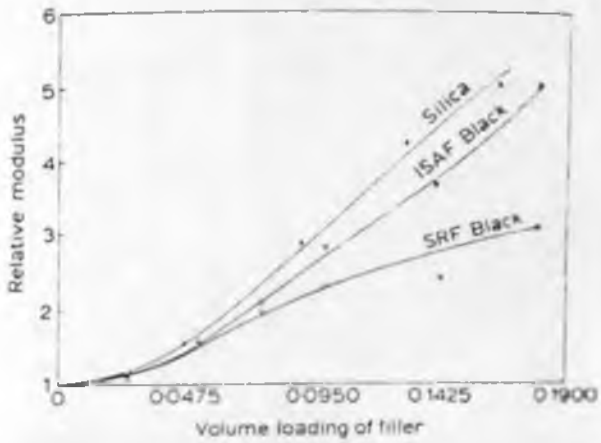

Fig. 23 Variation of relative modulus with volume fraction of filler for a 1:1 ENR-XNBR blend filled with silica, ISAF black and SRF black and moulded at 150°C for 60 min.

The plot of $V_{ro}/\nu V_{rf}$ against $\phi/(1-\phi)$ is shown in Fig. 22. The slope of the plot is maximum for the silica-filled blend and minimum for the SRF black-filled blend. The slope of the ISAF black-filled blend is close to the silica-filled blend. Accordingly, we observe that polymer-filler interaction increases in the order: SRF < ISAF ≤ silica. It has been noted earlier in this paper that reinforcement in physical properties also follows the same order. The plot of relative modulus versus volume fraction of filler is shown in Fig. 23. The increase in relative modulus with filler loading also follows the same trend. Accordingly, we conclude that filler reinforcement of the self-vulcanisable rubber blend system is similar to the filler reinforcement of conventional rubber vulcanisates.

For comparison, we have included in our studies two control systems based on XNBR alone and ENR alone. These mixes were cured to a rheometric torque rise similar to the corresponding blend mixes.

Table 13 shows properties of the XNBR-ENR blend and the control vulcanisates, for both gum and filled systems. The blend shows higher resilience and lower compression set than the corresponding control ENR and XNBR vulcanisates. The difference in

Table 13. Physical properties of the XNBR–ENR blend with control XNBR and ENR systems

Mix no.	E	X	Exb	Ec	Xc	IS20	Es	Xs	Si20
Modulus 300% (MPa)	1·2	3·9	3·2	9·0	15·5	8·9	6·9	13·0	9·2
Tensile strength (MPa)	4·2	18·7	3·2	23·0	24·0	13·5	18·0	25·1	13·0
Elongation at break (%)	650	470	300	595	380	410	500	400	370
Tear strength (kN/m)	18·4	34·2	12·6	49·0	69·7	38·0	39·0	60·7	29·0
Hardness, shore A	30	69	47	61	83	58	53	81	57
Resilience at 40°C (%)	26	62	69	49	54	61	49	52	64
Abrasion loss ($\times 10^{-6}$ m^3/1000 rev)	8·40	0·02	1·97	0·42	0·05	0·70	2·00	0·06	0·60
Compression set at 70°C for 22 h (%)	16	70	12	35	53	14	23	45	12
Heat build-up by Goodrich flexometer with a load of 10·89 kg and stroke of 4·5 mm									
ΔT^* (°C)	20	—	17	16	58	26	18	41	22
Dynamic set (%)	1·6	—	0·6	7·3	4·2	1·3	8·0	13·0	1·0
V_r	0·09	0·05	0·12	0·12	0·10	0·17	0·12	0·16	0·15

*Ambient temperature, 50°C.

the property is ascribed to the type of vulcanisate network structure.

4 Conclusions

ENR ad XNBR forms a self-vulcanisable rubber blend. This blend shows marching modulus with increasing moulding time and temperature. The poor gum strength of the blend is improved by addition of reinforcing fillers. The processability and curing characteristics of the blend depend on the type and amount of filler used. The blend vulcanisates show low compression set and high resilience when compared with conventionally cured XNBR and ENR. Silica reinforcement in self-vulcanisable blend occurs in the absence of any coupling agent.

References

1. MUKHOPADHYAY, S., CHAKI, T. K. & DE, S. K., Self vulcanisable rubber blend system based on epoxidised natural rubber and hypalon. *J. Polym. Sci., Polym. Lett. Ed.*, **28** (1990) 25.
2. MUKHOPADHYAY, S., DE, P. P. & DE, S. K., A self vulcanisable and miscible blend system based on hypalon and carboxylated nitrile rubber. *J. Appl. Polym. Sci.*, in press.
3. ALEX, R., DE, P. P. & DE, S. K., Self vulcanisable rubber–rubber blend system based on epoxidised natural rubber and neoprene. *J. Polym. Sci., Polym. Phys. Ed.*, submitted.
4. RAMESH, P. & DE, S. K., Self crosslinkable plastic–rubber blend system based on poly vinyl chloride and carboxylated nitrile rubber. *Polym. Commun.*, in press.
5. BHATTACHARYA, T. & DE, S. K., Self vulcanisable rubber blend system based on chlorobutyl rubber and carboxylated nitrile rubber. *European Polym. J.*, submitted.
6. ALEX, R., DE, P. P. & DE, S. K., Self vulcanisable rubber blend system based on epoxidised natural rubber and carboxylated nitrile rubber. *J. Polym. Sci., Polym. Lett. Ed.*, **27** (1989) 361.
7. ALEX, R., DE, P. P. & DE, S. K., Epoxidised natural rubber–carboxylated nitrile rubber blend: a self vulcanisable miscible blend system. *Polym. Commun.*, **31** (1990) 118.
8. CHAKRABORTY, S. K. & DE, S. K., Epoxy-resin cured carboxylated nitrile rubber. *J. Appl. Polym. Sci.*, **27** (1982) 4561.
9. ELLIS, B. & WELDING, G. N., Estimation from swelling, of the structural contribution of chemical reactions to the vulcanisation of natural rubber. Part II, estimation of equilibrium degree of swelling. *Rubber Chem. Technol.*, **37** (1964) 571.
10. PAYNE, A. R., In *Reinforcement of Elastomers*, ed. G. Kraus. Interscience, New York, 1965, p. 92.
11. CHAKRABORTY, S. K., BHOWMICK, A. K. & DE, S. K., Structure property relations of carboxylated nitrile rubber. *J. Appl. Polym. Sci.*, **26** (1981) 4011.
12. COLCLOUGH, T., New methods of crosslinking natural rubber, part II. The introduction of epoxide groups into natural rubber and their subsequent utilization for crosslinking. *Trans. Instn. Rubb. Ind.*, **38** (1962) 11.
13. GREENSPAN, F. P., In *Epoxidation in Chemical Reactions of Polymers*, ed. E. M. Fetters. Wiley Interscience, New York, 1964, p. 152.
14. LOO CHENG TEIK, Vulcanisation of epoxidised natural rubber with dibasic acids. In *Proc. Int. Rubber Conf. Vol. II*, Kuala Lumpur, 1985, p. 368.
15. LOO, C. T., Crosslink structures in sulphur vulcanizates of epoxidised natural rubber. In *Proc. Int. Rubber Conf.*, Columbo, Sri Lanka, 1984.
16. COTTON, C. R., The effect of carbon black surface properties and structure on rheometer cure behaviour. *Rubber Chem. Technol.*, **45** (1972) 129.
17. JUVE, A. E., In *Vulcanization of Elastomers: Principles and Practice of Vulcanization of Commercial Rubbers*, ed. G. Alliger & I. J. Sjothum. Reinhold Publishing Corporation, USA, 1964, p. 30.
18. BEHAL, M. V., Thermovulcanisation of polychloroprene rubber and its blends with poly vinyl chloride. *J. Appl. Polym. Sci.*, **35** (1983) 507.
19. ZHANG, S. W., Mechanism of rubber abrasion in unsteady state. *Rubber Chem. Technol.*, **57** (1984) 755.
20. REZNIKOISKII, M. M. & BROSKII, G. L., In *Abrasion of Rubbers*, ed. D. I. James. Maclaren, London, 1967, p. 64, 81.
21. BHOWMICK, A. K., Ridge formation during the abrasion of elastomers. *Rubber Chem. Technol.*, **55** (1982) 1055.

22. THOMAS, S., Scanning electron microscopy studies on wear properties of blends of plasticised poly(vinyl chloride) and thermoplastic copolyester elastomer. *Wear*, **116** (1987) 201.
23. MATHEW, N. M. & DE, S. K., Scanning electron microscopy studies in abrasion of NR/BR blends under different test conditions. *J. Mat. Sci.*, **18** (1983) 515.
24. GENT, A. N. & PULFORD, C. T., In *Development in Polymer Fracture — 1*, ed. E. H. Andrew. Applied Science, London, 1979, p. 155.
25. KRAUS, G., Swelling of filler reinforced vulcanizates. *Appl. Polym. Sci.*, **7** (1963) 861.
26. CHAKRABORTY, S. K. & DE, S. K., Silica and cl reinforced carboxylated nitrile rubber vulcanized by mixed cross linking system. *Rubber Chem. Technol.*, (1982) 990.
27. BAKER, C. S. L., GELLING, I. R. & SAMSURI, A. Epoxidised natural rubber. *J. Nat. Rubb. Res.*, **1** (198 135.

MASTER SET

Self-vulcanizable Rubber Blend System Based on Epoxidized Natural Rubber and Carboxylated Nitrile Rubber

R. ALEX, P. P. DE, and S. K. DE, *Rubber Technology Centre, Indian Institute of Technology, Kharagpur 721302, India*

Although carboxylated nitrile rubber (XNBR) is vulcanizable by epoxy resin,[1] it has been reported that epoxidized natural rubber (ENR) can be vulcanized by dibasic acids.[2] Accordingly, it was thought that the carboxyl groups of XNBR could be made available for vulcanizing ENR and epoxy groups of ENR could be utilized for vulcanizing XNBR in a blend of XNBR and ENR. In the present communication we report the results of our studies on physical properties of XNBR/ENR blends which are vulcanizable by the blend constituent themselves in the absence of any curatives and additives. We designate the system as a "self-vulcanizable rubber blend system."

EXPERIMENTAL

XNBR used was Krynac-221 (Polysar Limited), containing high level of carboxylated monomer and medium high bound acrylonitrile level. ENR used was ENR-50 (Malaysian Rubber Producers' Research Association, U.K.), with 50 mol% epoxidation. Both ENR and XNBR was first masticated in the 14 × 6 in. 2-roll mixing mill for 6 min each. Masticated samples were blended on the mill for a further period of 10 min. Rheographs were taken at 140°C on a Monsanto Rheometer R-100. The blends were vulcanized for 45 min at 140°C. The following physical properties of the vulcanizates were determined according to standard methods: stress-strain (Zwick UTM, ASTM D412-87), tear (Zwick UTM, ASTM D624-86), hardness (Shore A, ASTM D2240-86), resilience (Dunlop tripsometer, BS:903: Part A8:1963-method A), compression set (ASTM D395-85, method A and method B), heat build-up (Goodrich flexometer, ASTM D623-78), and abrasion resistance (Cryodon-Akron Dupon abrader, BS:903:Part A9, method C). Ageing resistance was measured by studying retention of tear and stress-strain properties of the vulcanizate. For swelling studies the vulcanizates were swollen in chloroform for 48 h and the percent increase in weight owing to solvent

TABLE I
Formulation of the Mixes

Parts by weight	Blend No.				
	A	G	H	G_c	H_c
ENR-25	100	—	—	—	—
ENR-50	—	100	100	100	100
XNBR	50	100	50	100	50
Carbon black*	—	—	—	60	45

*ISAF-type, obtained from Phillips Carbon Black Ltd., Durgapur.

Journal of Polymer Science, Part C: Polymer Letters, Vol. 27, XXX–XXX (1989)

CCC 0360-6384/89/000000-00$04.00

ALEX, DE, AND DE

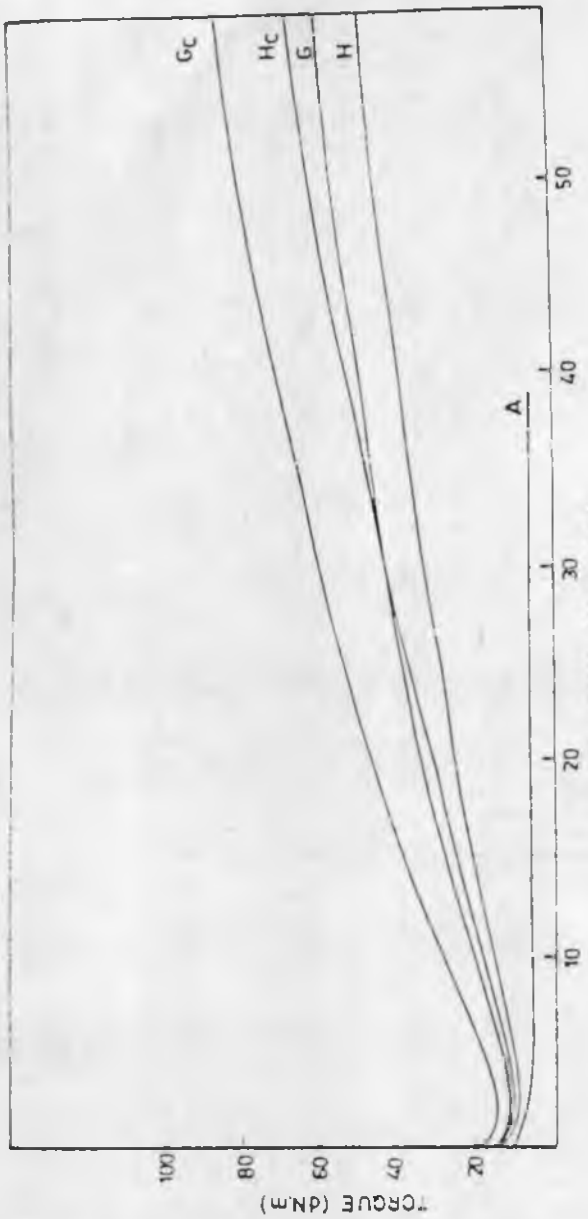

Fig. 1. Rheographs at 140°C.

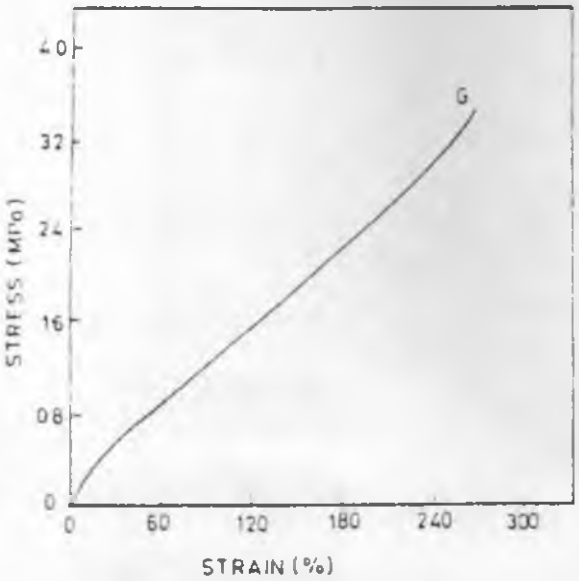

Fig. 3. Stress-strain plot for blend G.

system as measured by the maximum torque is higher in the case of formulation G(ENR/XNBR 100/100) as compared with H(ENR/XNBR 100/50). Mix G contains a higher quantity of XNBR, and the proportion of carboxyl groups available for crosslinking is also higher in case of mix G as compared with mix H. Accordingly, the extent of crosslinking and the resultant torque in the rheographs is higher in mix G. Teik,[4] while studying vulcanization of ENR by dibasic acids, observed that rheometric torque depends on the concentration of the acid. Matching increase in modulus with cure time as shown in the rheographs implies that the cure reversion is absent and the vulcanizate network is thermally stable (Fig. 2). Reinforcing carbon black owing to

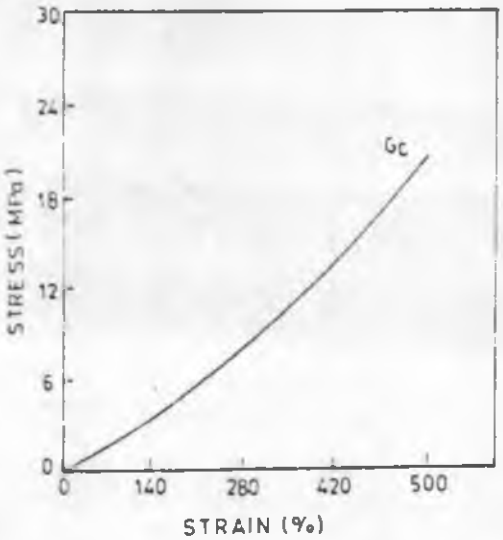

Fig. 4. Stress-strain plot for blend G_c.

swelling was noted. The hysteresis behavior of the blend vulcanizates was determined from the ratio of the retraction energy to the ratio of input energy of deformation up to the point of strain reversal, recorded by the electronic integrator attached to the Instron Universal Testing machine model 1193. The samples were pulled to the desired extension (200% or 400%) and retracted at a crosshead speed of 100 mm/min.

RESULTS AND DISCUSSION

Blend compositions are shown in Table 1. Blends C and H contain two different proportions of ENR and XNBR and no other additives. Blends G_r and H_r are the corresponding blends containing the reinforcing ISAF carbon black filler. Rheographs of different blends are shown in Figure 1. Preliminary experiments with ENR-25 showed that an epoxidation level of 25 mol% is not sufficient to cause crosslinking of XNBR, as evident from the rheographs of XNBR/ENR-25 blend (Fig. 1). There is no increase in modulus with cure time. Chakraborty and De,[1] while studying vulcanization of XNBR by epoxy resins, observed dependence of crosslink density and the resultant rheometric torque on the loading of epoxy resin. However, where epoxidation level was increased to 50 mol%, as in ENR-50, crosslinking occurred and the rheographs show gradual increase in modulus with cure time. Teik[2] has also observed that vulcanization of epoxidized natural rubber by dibasic acids depends very much on epoxidation level. It is apparent that the extent of vulcanization in the XNBR/ENR-50

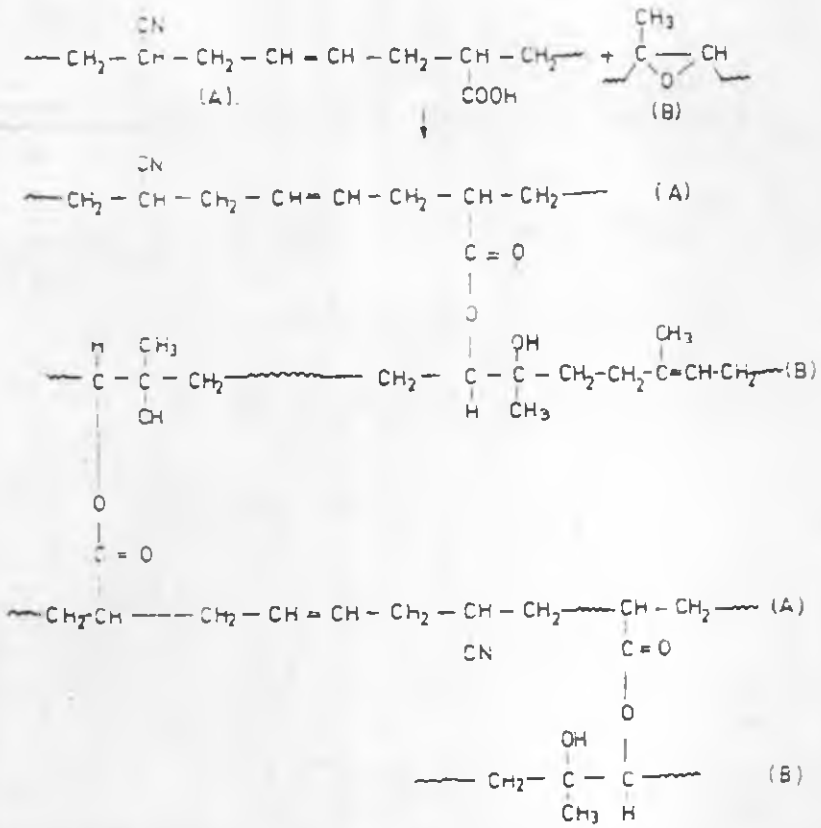

Fig. 2. Epoxidized natural rubber (B) crosslinked by carboxylated nitrile rubber (A) and vice versa in the self-vulcanizable rubber blend system.

TABLE II
Physical Properties of Self-Vulcanizable Rubber Blends

	Blend No.			
	G	H	G_c	H_c
100% Modulus (MPa)	1.28	1.18	2.40	1.25
Tensile strength (MPa)	3.62	3.01	19.46	22.30
Elongation at break (%)	273	327	535	634
Tear strength (N/m)	12.6	11.1	41.9	38.5
Abrasion loss (cm^3/h)	2.88	24.23	0.48	2.65
Compression set, constant stress (%)	0.6	5.2	1.8	6.8
Compression set, constant strain (%)	8.5	9.9	8.6	22.0
Heat build-up (ΔT), above 50°C (°C)	12.5	17.0	32.0	27.5
Resilience (%)	62	55	49	41
Hardness (Shore A)	40	32	54	54
Swelling in chloroform, increase in weight (%)	833	1192	532	581

strong polymer-filler interaction causes an increase in torque values in rheographs. Results of physical properties and swelling studies, as discussed below, further substantiates these observations. Typical stress-strain curves are shown in Figures 3 and 4, for blend G and blend G_c. Blends H and H_c also show similar behavior. Physical properties of different systems are summarized in Table II. It is evident that the gum systems show poor strength which, however, increases 6 to 7 times in the presence of reinforcing carbon black filler. Analysis of the results for mixes G and H (Table I) shows that blend G shows higher tensile value, tear resistance, hardness, and resilience and lower values of compression set. This is indicative of a greater extent of crosslinking in blend

TABLE III
Hysteresis Behavior of Different Blends

Blend No.	Cycle No.	Hysteresis loss (%)	Set (arbitrary units, Instron chart)
G	1	15	4.5
	2	7	1
	3	6.5	0.6
H	1	31	3
	2	9.5	0.9
	3	9	0.6
G_c*	1	25.5 (43)	7 (16)
	2	18 (23)	1.5 (3)
	3	16 (18)	0.8 (2)
H_c	1	35	8
	2	19	2
	3	20	1

*Values in parentheses are the values where the extension was increased to 400%.

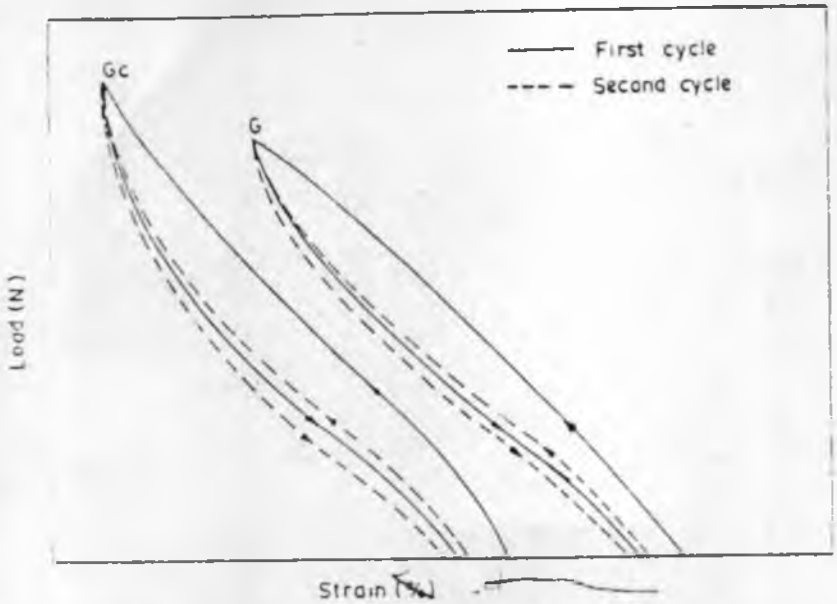

Fig. 5. Hysteresis curves for blend G and G_c at 200% extension.

G as compared with blend H. That heat build-up and abrasion loss for blend G is less than blend H also points out tighter crosslinking in the case of blend G. Solvent swelling studies show that blend G offers greater restriction to solvent penetration owing to higher crosslinking density. The proportion of carboxyl group available for crosslinking and for being crosslinked is more in blend G than blend H. This is true for both gum and filled systems. Rheographs also substantiate these observations. Blend G shows higher torque value than blend H. Similarly, blend G_c registers higher torque than blend H_c. Teik[2] has also observed that the tensile strength of ENR vulcanizates depends on the concentration of dibasic acid crosslinking agent.

Addition of carbon black reinforces both blend G and H. Both tensile and tear properties improve several fold owing to higher dissipation of energy in the filled system, which is manifested in higher heat build-up and set properties. Hysteresis studies (Fig. 5) showed that both energy dissipation and set are higher in blend G_c as compared with G owing to the additional energy dissipation mechanisms, such as motion of filler particles, chain slippage, and dewetting at high strains.[4] That abrasion loss, resilience, and solvent swelling decrease and hardness increases in filled systems also points out a high degree of polymer-filler interaction. When the hysteresis experiment was repeated after the first cycle is over, both hysteresis loss and set in the second and third cycles were less as compared with the first cycle. This is due to stress-softening or Mullin's effect. Where the extension was increased to 400% from

TABLE IV
Percent retention of Properties after Ageing at 100°C for 48 h

	Blend No.			
	G	H	G_c	H_c
Tensile strength (MPa)	75	76	78	64
Tear resistance	73	70	49	60
Elongation at break (%)	55	62	33	30

200%, as was done in the case of G_c, higher energy input caused a higher dissipation of energy. This results in higher hysteresis and set.

Retention of properties after ageing for 48 h at 100°C (Table IV) indicates that the vulcanizates are quite stable under the ageing conditions owing to carbon-carbon and carbon-oxygen covalent bonds in the crosslinks (Fig. 2). Expectedly, carbon black catalyzes the degradation reactions during ageing, and the retention of properties worsens in filled systems, as is the case with normal rubber vulcanizates vulcanized by a sulfur curative system.[4]

In summary, we conclude that a novel self-vulcanizable rubber blend system has been studied wherein one constituent vulcanizes the other in the absence of any curatives. Further work on such systems is in progress.

Thanks are due to Sri S. Mushtaq, K. L. Saha, A. Talukdar, R. K. Banerjee, and J. Mitra of this center for assistance in experimental work.

References

1. S. K. Chakraborty and S. K. De, *J. Appl. Polym. Sci.*, 27, 4561 (1982).
2. L. C. Teik, Proceedings of the International Rubber Conference, 1985, Kuala Lumpur.
3. N. M. Mathew and S. K. De, *Polymer*, 24, 1042 (1983).
4. S. S. Bhagawan, D. K. Tripathy, and S. K. De, *J. Appl. Polym. Sci.*, 34, 1581 (1987).

Received January 6, 1989
Accepted February 9, 1989